WATERFLOOD AND ENHANCED OIL RECOVERY STUDIES USING SALINE WATER AND DILUTE SURFACTANTS IN CARBONATE RESERVOIRS

A Dissertation

by

MOHAMMED BADRI S. ALOTAIBI

Submitted to the Office of Graduate Studies of
Texas A&M University
in partial fulfillment of the requirements for the degree of

DOCTOR OF PHILOSOPHY

December 2011

Major Subject: Petroleum Engineering

Waterflood and Enhanced Oil Recovery Studies Using Saline Water and Dilute Surfactants in Carbonate Reservoirs

WATERFLOOD AND ENHANCED OIL RECOVERY STUDIES USING SALINE WATER AND DILUTE SURFACTANTS IN CARBONATE RESERVOIRS

A Dissertation

by

MOHAMMED BADRI S. ALOTAIBI

Submitted to the Office of Graduate Studies of
Texas A&M University
in partial fulfillment of the requirements for the degree of

DOCTOR OF PHILOSOPHY

Approved by:

Chair of Committee,	Hisham A. Nasr-El-Din
Committee Members,	Alfred Daniel Hill
	David Schechter
	Mahmoud El-Halwagi
Head of Department,	Stephen A. Holditch

December 2011

Major Subject: Petroleum Engineering

ABSTRACT

Waterflood and Enhanced Oil Recovery Studies Using Saline Water and Dilute Surfactants in Carbonate Reservoirs.

(December 2011)

Mohammed Badri S. Alotaibi, B.S., King Fahd University of Petroleum & Minerals;

M.S., Texas A&M University

Chair of Advisory Committee: Dr. Hisham A. Nasr-El-Din

Water injection has been practiced to displace the hydrocarbons towards adjacent wells and to support the reservoir pressure at or above the bubble point. Recently, waterflooding in sandstone reservoirs, as secondary and tertiary modes, proved to decrease the residual oil saturation. In calcareous rocks, water from various resources (deep formation, seawater, shallow beds, lakes and rivers) is generally injected in different oil fields. The ions interactions between water molecules, salts ions, oil components, and carbonate minerals are still ambiguous. Various substances are usually added before or during water injection to enhance oil recovery such as dilute surfactant.

Various methods were used, including surface charge (zeta potential), static and dynamic contact angle, core flooding, inductively coupled plasma spectrometry, CAT scan, and geochemical simulation. Limestone and dolomite particles were prepared at different wettability conditions to mimic the actual carbonate reservoirs. In addition to seawater and dilute seawater (50, 20, 10, and 1 vol%), formation brine, shallow aquifer

water, deionized water and different crude oil samples were used throughout this study. The crude oil/water/carbonates interactions were also investigated using short and long (50 cm) limestone and dolomite rocks at different wettability and temperature conditions. The aqueous ion interactions were extensively monitored via measuring their concentrations using advanced analytical techniques. The activity of the free ions, complexes, and ion pairs in aqueous solutions were simulated at high temperatures and pressures using OLI electrolyte simulation software.

Dilute seawater decreased the residual oil saturation in some of the coreflood tests. Hydration and dehydration processes, through decreasing and increasing salinity, showed no impact on calcite wettability. Effect of individual ions (Ca, Mg, and Na) and dilute seawater injection on oil recovery was insignificant in comparison to the dilute surfactant solutions (0.1 wt%). The reaction mechanisms were confirmed to be adsorption of hydroxide ions, complexes and ion pairs at the interface which subsequently altered the surface potential from positive to negative. Results in this study indicate multistage waterflooding can enhance oil recovery in the field under certain conditions. Mixed streams simulation results suggest unexpected ions interactions ($NaCO_3^{-1}$, HSO_4^{-1}, $NaSO_4^{-1}$ and SO_4^{-2}) with various activities trends especially at high temperatures.

.

DEDICATION

To my parents, wife and children (Raghad, Muhand, and Yazan)

ACKNOWLEDGEMENTS

First and foremost, I owe deepest gratitude to Saudi Aramco Company for sponsoring my Ph.D. degree. I would like also to thank my advisor and committee chair Dr. Hisham A. Nasr-El-Din, for his constructive comments and support throughout the course of this research. Special thanks to him for giving me the freedom to think and work independently.

It is a pleasure to thank the members of the supervisory committee: Dr. Dan Hill, Dr. David Schechter, and Dr. Mahmoud El-Halwagi for their guidance, insightful comments and questions. I am particularly grateful to Dr. Richard H. Loeppert, Department of Soil and Crop Sciences, for his willingness to listen and discuss my research subject and his steady interest in my work. It was an honor for me to audit a very important course “Soil Chemistry” with him which added a major contribution to Chapter V.

I would like to thank Dr. Hisahm’s group for their valuable assistance and friendship. I reserve my special thanks to the undergraduate students: M. Ali, J. Fletcher, H. Ramirez, J. Martinez, and S. Crews, for their help in fluids preparation and atomic absorption/ICP measurements. The facilities and resources provided by the Harold Vance Department of Petroleum Engineering and Evans Library in Texas A&M University are gratefully acknowledged. I am thankful to OLI and MIPAV Companies who graciously offered their licenses free to us.

Last but not the least, I would like to thank my family, especially my parents, my wife, and my children for their unconditional love, patience, and understanding.

NOMENCLATURE

$\Delta\rho$	Difference in density between fluids at interface
a_i	Effective diameter of the ion
AQW	Aquifer water
C	Concentration
cP	Centipoise
DIW	Deionized water
DSA	Drop shape analysis
EDL	Electrical double layer
G	Gravitational constant
GC/MS	Gas chromatography/mass spectrometry
HTHP	High temperature high pressure
I	Ionic strength
K_{iap}	Ion activity product
K_{sp}	Solubility product constant
L	Length
N_B	Bond number
pals	Phase analysis light scattering
R_0	Radius of drop curvature at apex
S	Saturation

SI	Saturation index
ST	Scaling tendency
z_i	Charge of ionic species i
B	Shape factor
Z	Zeta potential
Γ	Interfacial tension (IFT)
α	Chemical activity
γ_ι	Activity coefficient of ionic species i

TABLE OF CONTENTS

CHAPTER Page

CHAPTER Page

CHAPTER Page

CHAPTER Page

Page

LIST OF FIGURES

Page

Page

Page

Page

Page

Page

Page

LIST OF TABLES

CHAPTER I

INTRODUCTION

Primary Production

Some oil fields have sufficient forces to displace their oil out of the oil-bearing rock and into the producing wells. This process is called primary production as the natural water beneath the rock or the dissolved gases expand and force the hydrocarbons out of the rock. Such natural forces are quickly depleted and the oil production will drop significantly if secondary oil recovery techniques are not applied, for example water or gas flooding. An additional of 30 to 40% of the original oil in the reservoir is usually recovered after the secondary recovery methods (Schumacher 1978).

Waterflooding

In waterflooding, either treated water (seawater, reservoir water) or fresh water (lakes and rivers water, shallow beds water) are injected into the oil-bearing rocks to displace the oil to the adjacent production wells. Water, because of its high density and incompressibility nature, has relatively efficient displacement characteristics which can raise the reservoir pressure in a short time period.

Injection water, in general, has two major problems that hinder its efficiency (Schumacher 1978). First, it does not flush all of the oil from the pore spaces as it moves

---

This dissertation follows the style of *SPE Reservoir Evaluation & Engineering Journal*.

through the reservoir rock because of the fluids' immiscibility or the rock wettability condition. Therefore, 25 to 50% of the oil is left unrecovered in the form of small droplets detained within the large pores. Second, the water front can bypass part of the reservoir due to the well placement and rock heterogeneity (fractures and vugs). Overall, 50 to 70% of the oil in place remained unrecovered after waterflooding (Schumacher 1978).

The physical treatments of the injection water, such as presence of suspensions and dissolved gases, are given more attention than the chemical properties (ion concentrations, ion-ion interactions within the water molecules or between water ions and rock minerals). In addition, precipitation of insoluble salts and fluids compatibility were thoroughly studies to avoid waterflooding failure.

Tertiary Recovery Methods

Tertiary recovery methods are usually applied to recover a third crop of oil after the successful waterflooding processes. Various substances are usually added before or during fluid injection to enhance the oil recovery such as surfactants, polymers, gas flooding, steam injection, in-situ combustion….etc.

Research Objectives

The main objective of this study is to determine the role of the injection water salinity on oil recovery as secondary and tertiary modes. In addition, comparison studies were conducted between conventional chemical flooding (dilute surfactant and polymer) and

saline water technology. More emphasis in this work is given to the carbonate reservoirs (limestone and dolomite), because the residual oil saturation in carbonates after waterflooding is typically higher than that of sandstone.

Dissertation Outline

The approaches for each chapter to accomplish the objectives of this dissertation are stated as follows:

In Chapter II, the charge of the limestone and dolomite particles were studied at different temperatures and atmospheric pressure. Saline and fresh water were tested without crude oil. The aim in this chapter was to understand the water-rock interactions in terms of the surface charge.

Chapter III presents zeta potential of limestone particles at different wettability conditions. In addition, reservoir conditions were simulated very closely by sonicating crude oil droplets in aqueous water phase (emulsion) with and without limestone particles. Formation brine (230K ppm), seawater (54K ppm), shallow aquifer water (5K ppm), and fresh water were used at different ionic strength. Cations (Na^{+}, Ca^{2+}, Mg^{2+}) and anions (SO_4^{2-}) concentrations were tuned individually in seawater as well.

Next, in Chapter IV, interfacial tension of crude oil/brine systems were presented as a function of temperatures, pressures, aqueous solution salinity, and different crude oil compositions. In addition, static contact angle was evaluated at different calcite surfaces (Iceland spar crystals and outcrop limestone rock).

Then, in Chapter V, concentrated brine, fresh water and dilute amphoteric surfactants were thoroughly studied using dynamic contact angle technique. Salinity and surfactant concentrations were for the first time adjusted at high temperature and pressure conditions.

In Chapter VI, adsorption tests are presented for dolomite and limestone cores using seawater and chemical tracer fluids. Fluids were injected using coreflood instrument and fresh cores to overcome the interference with the connate brine and better understand the ions interactions with carbonate minerals. Crude oil was excluded for the same reason. Ion concentrations were determined using different analytical techniques (atomic absorption, spectrophotometer, and ion-selective electrode).

Coreflood tests were also presented in Chapter VII using dolomite cores only. The aim of this chapter was to investigate the effect of injection water salinity on oil recovery as secondary and tertiary modes.

Then, in Chapter VIII, salinity and dilute amphoteric surfactants were injected in dolomite cores (L= 50.8 cm). The impact of the residence time was investigated via using longer cores. An iodide dopant was mixed with the aqueous solution to track the fluids movement in vugular dolomite cores.

Dolomite rock was more heterogeneous than the limestone cores. In Chapter IX, besides the homogenous limestone cores, seawater, fresh water, formation brine and crude oil were used. The importance of individual metal ions, anions, and dilute seawater were all reported at reservoir conditions. Dilute surfactants were injected in some limestone tests for two reasons: 1) to recover more oil, and 2) to show how the

amphoteric surfactant was affecting the capillary forces more than electrolyte solutions. Analytical techniques were utilized to determine the concentration of effluent samples and perhaps the water ions interactions. Visualization technique, using CAT scan, was applied to monitor the fluids distribution within the core.

In Chapter X, the chemical activity of free ions, complexes and ion-pairs in the injection water are presented using OLI geochemical simulation software. More focus in Chapter X was given to role of ionic strength on the chemical activities of individual ions at wide temperature and pressure range. Presence of calcite was also included at various salinity conditions. Determining such activities helps in understanding the electrostatic interactions.

Finally, main conclusions from the experimental and simulation results are presented in Chapter XI. Six appendices, at the end, list additional details. Appendix A contains glossary terms that were previously used in zeta potential chapters. The crude oil compositions were also displayed in Appendix B. The preparation procedure for the rock substrates in contact angle tests was presented in Appendix C. In addition, Appendix D shows more images of contact angle tests at different temperatures and contact times. Tri-planar view (x-y, y-z. x-z) and slices images of the CAT scan results (IL–5) are displayed in Appendix E. The last Appendix (G) illustrates the chemical activities of salt compounds in injection water as a function of temperature and divalent ions concentration.

CHAPTER II

ELECTROKINETICS OF LIMESTONE AND DOLOMITE ROCK PARTICLES

Summary

High salinity water such as seawater, or formation brines, is frequently injected in carbonate reservoirs. Ions interaction between injection water, reservoir fluids and rock surface are quite complex. It is recently believed that the chemistry of injection water can significantly enhance oil recovery. Several reaction mechanisms were suggested, including: rock dissolution, change of surface charge, and/or sulfate precipitation.

This study attempts to characterize the electrokinetics of limestone and dolomite suspensions at 25 and 50ºC. In addition, reaction mechanisms at the water/rock interface were established. Synthetic formation brine, seawater, and aquifer water were chosen from Middle East reservoirs. Carbonate particles were soaked in high and low–salinity water. Phase analysis light scattering technique was used to determine the zeta potential (surface charge) of carbonate particles over a wide range of pH, ionic strength, and temperature.

Zeta potential of limestone particles were significantly affected by calcium ion. Low–salinity water created more negative charges on limestone and dolomite particles by expanding the thickness of the diffuse double layer. Individual divalent cations decreased the zeta potential of limestone particles in sodium chloride solutions, while sulfate ions showed a negligible effect. Limestone particles in high–salinity water decreased zeta potential. The solubility of calcium ions increased as temperature was

increased and thus created additional negative charges. The absence of sulfate in aquifer water strongly influenced the dolomite surface charge. In summary, surface charge adjustment from positive to negative can alter the wettability of carbonate rock from preferentially oil to water–wet. As a result, residual oil saturation should be decreased.

Introduction

Interfacial phenomena at carbonate/water interfaces are controlled by the electrical double layer (EDL) forces. Therefore, it is necessary to understand the behavior of the ions interactions with the rock surface. Charged species are only transferred across any solid/liquid interface until reaching equilibrium. It can be visualized as a semi-membrane that allows the common charged species between solid and solution to pass through. These species are called potential determining ions**.** As a result of the relative motion between the charged dispersed phase and the bulk liquid, the electrical double layer is sheared. The potential, at this shear plane, is commonly called electrokinetic or zeta potential (ζ). Different methods are applied to measure the potential at the shear plane. However, the most commonly used technique is the electrophoresis method (Pierre *et al.* 1990).

Adjusting the ionic strength has been recently reported to enhance oil recovery (Austad and Standnes 2003). The expected mechanism behind that is still uncertain. Zhang *et al.* (2007) proved that sulfate adsorption on the chalk rock changed the surface charge to negative. Other researchers stated the reaction mechanisms to be one of the following: a) chemical dissolution of calcite, b) change of the rock surface charge

(Zhang and Austad, 2006; Strand *et al.* 2006), and/or c) precipitation (Hiorth *et al.* 2010).

The aim of this work is to establish the role of different ionic strength solutions in charging mechanisms of limestone and dolomite particles. A second objective is to investigate the influence of temperature and pH on electrokinetic behavior. Explanations of terms and abbreviations used in this chapter are given in the Appendix A.

Literature Review

Formation brine and seawater (high–salinity) cause carbonate dissolution and mineralogical changes over certain temperature range. Hence, rock strength gave different hydrostatic yield point. In general, brines have chemical reactions either with the bulk solution or the rock surface. Ions that normally exist in aquifer, seawater, or formation brines are: H^+, Ca^{2+}, HCO_3^-, H_2O, Na^+, Mg^{2+}, Cl^-, and SO_4^{2-}. Complexes are formed either in the bulk aqueous phase or at the rock surface (van Cappelen *et al.* 1993; Pokrovsky *et al.* 2000), **Figure II-1**.

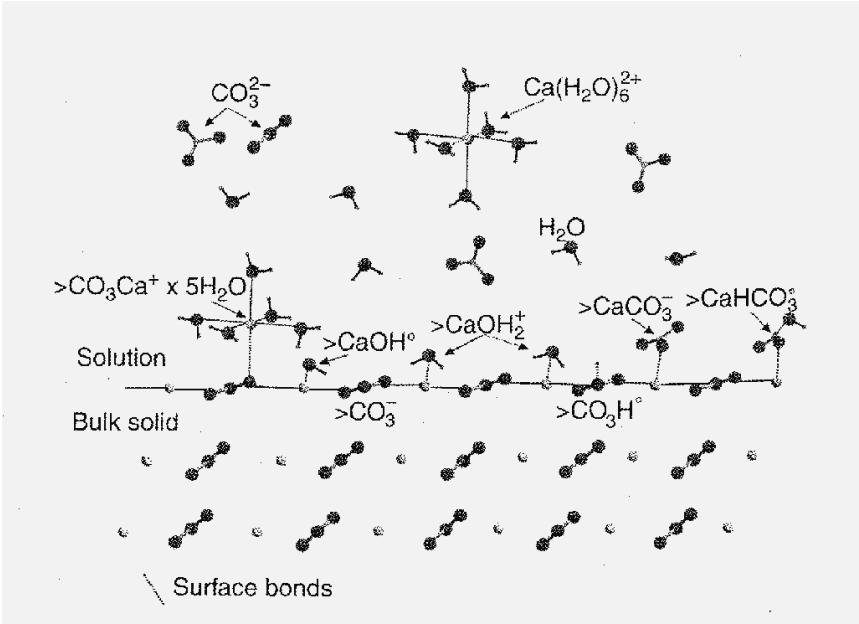

Figure II-1. Complex ions present at the calcite/water interface (Pokrovsky *et al.* 2000).

Aqueous solutions

Several ions will be formed in the aqueous phase. They are mainly combination of the previous set (Hiorth *et al.*, 2010):

$$CO_3^{2-} \Leftrightarrow HCO_3^- - H^+ \quad \text{(1)}$$

$$H_2CO_3 \Leftrightarrow HCO_3^- + H^+ \quad \text{(2)}$$

$$CaSO_4^o \Leftrightarrow Ca^{2+} + SO_4^{2-} \quad \text{(3)}$$

$$MgSO_4^o \Leftrightarrow Mg^{2+} + SO_4^{2-} \quad \text{(4)}$$

$$CaHCO_3^+ \Leftrightarrow Ca^{2+} - HCO_3^- \quad \text{(5)}$$

These reactions are controlled by chemical processes taking place at the interface between the mineral lattice and bulk solution. Ions can make complexes at the rock surface as well.

Zeta potential

Hydrolysis reaction of carbonate rocks in water generates the surface charge. In general, H^+ and OH^- are potential determining ions for many solids. Therefore, the surface charge is pH dependent and can be either negative or positive. High pH will favor an excess concentration of negative species (HCO_3^- and CO_3^{2-}), while positive species (Ca_2^+, $CaHCO_3^+$, and $CaOH^+$) will be favored at low pH. Isoelectric point or point of zero charge represents zero ζ potential at certain pH value. Carbonate particles carry positive charges in high−salinity brines. In literature, some scientists reported negative charges for calcite (Douglas and Walker 1950; Smani *et al.* 1975), whereas other investigators found that calcite had positive charges (Yarar and Kitchener 1970; Siffert and Fimbel 1984). Calcite displays complex behavior in aqueous media mainly due to its solubility, which is governed by surface electrical charge and chemical equilibrium (Rodríguez and Araujo 2006). Three factors affect ζ potential of the carbonate particles: 1) ionic strength, 2) pH, and 3) surfactant concentration. Only the first two factors were investigated in more detail in this study.

Experimental Studies

Materials

Limestone and dolomite samples were dried in an oven at 120.6°C until constant weight was achieved. A ceramic mortar and pestle were then used to crush the rocks into fine

powders. Both Winterset limestone and Silurian dolomite are outcrop rocks in USA. To avoid contamination from sieve analysis, the powders were used without sorting.

Fluids

Synthetic brines were chosen to represent Middle East reservoirs as listed in **Table II-1**. Aquifer water (AQW) was diluted in 1:1 volume ratio to determine the impact of low–salinity water on carbonates' surface charge. The water used to prepare all brine solutions was deionized water resistivity of 18.2 MΩ·cm at room temperature**.**

Apparatus and procedure

Zeta potential (ζ). Phase analysis light scattering technique (pals) was used to determine zeta potential of the suspensions. The instrument's electrodes were coated by palladium, and He–Ne laser was used as a light source. It determined the electrophoretic mobility of charged, colloidal suspensions. Polystyrene cuvette was used to hold 1.5 cm^3 of the sample. The mobility range for this instrument was 10^{-11} to 10^{-7} $m^2/V.s$, Figure II-2. Temperature was varied from 6 to 70°C. Suspensions were prepared by mixing 0.2 g powdered particles of limestone or dolomite with 50 cm^3 of aqueous solutions for two days. Samples were centrifuged to separate the supernatant into small tubes. Particles were then extracted and transferred to the supernatant solution. pH was adjusted using either HCl or NaOH solutions. A parallel plate electrode was inserted into the cuvette. This instrument measured electrophoretic mobility and calculated ζ potential. An average of 5 runs was selected using at least 30 cycles of measurement for each run. The instrument had an accuracy of ±2%.

Table II-1. Formulation of aquifer water, seawater, and formation brine.

Salt	Aquifer water	Seawater	Formation brine
	mg/L		
NaCl	2,781.0	38,386.3	127,523.3
$CaCl_2.2H_2O$	1,437.9	2,435.6	109,162.6
$MgCl_2.6H_2O$	551.9	19,058.1	35,657.7
$SrCl_2.6H_2O$	15.2	–	3,149.4
$BaCl_2$	–	–	15.2
Na_2SO_4	1,035.0	5,263.8	159.7
$NaHCO_3$	264.4	265.7	483.3
TDS, mg/L	5,436	54,680	230,000

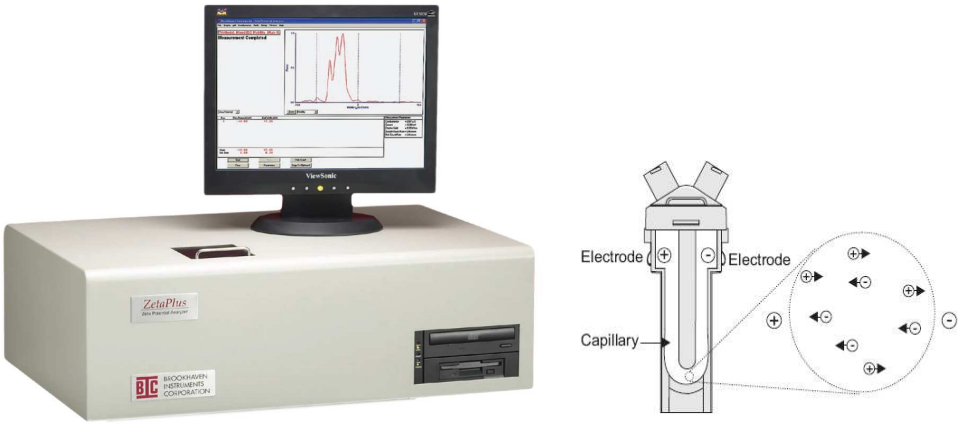

pH Range: 1 to 13
Temperature Control: 6°C to 100°C, ±0.1°C

Figure II-2. Zeta pals (phase analysis light scattering) machine.

Results and Discussion

Reaction mechanisms

High–salinity brines (formation brine and seawater) have more ions and different chemistry than low–salinity water (aquifer, lakes and river water). Therefore, chemical reactions with carbonate particles are also expected to be completely different. In sandstone reservoirs, clays control the interaction, especially with low–salinity level of water (Zhang and Morrow 2006; Alotaibi *et al.* 2010). But, in carbonate reservoirs, the effect of salinity is more pronounced. Seawater, for example, might cause more dissolution to carbonate rocks than low–salinity water. Ions form complexes in the aqueous phase and rearrange as a result of any change in the ionic strength.

Zeta potential

Zeta potential, in general, decreases as salinity increases. The water film around carbonate particles affects the zeta potential. Since there are no universally accepted ζ potential standards, a reference manual from the equipment manufacturer was used to calibrate the instrument.

Set of experiments were carried out to determine the multiple ions interaction with dolomite and limestone particles. Carbonate particles were tested at 25 and 50°C. Most carbonate reservoirs have pH value of 7-9. Hence, the solution pH was adjusted using HCl or NaOH solutions. Then, the samples were left at least 15 minutes to reach equilibrium. Alkaline/Surfactant/Polymer (ASP) and CO_2 flooding either increase or decrease the reservoir fluids' pH to certain levels. For this reason, the surface charge of the carbonate particles was evaluated over a wide pH range, from 3 to 12.

Limestone particles

Aquifer and seawater. Aquifer and seawater were tested at two temperature conditions, 25 and 50°C. The ionic strength of AQW was adjusted by excluding certain ions according to Table II-1. The results suggested a negative ζ potential from pH 3 to 9, Figure II-3. Despite changing the ionic strength, the zeta potential was positive at pH 12. This might be due to discrete ion effect at the particle surface and high NaOH concentration (Levine et al. 1967). These tests were conducted at 25°C and atmospheric pressure.

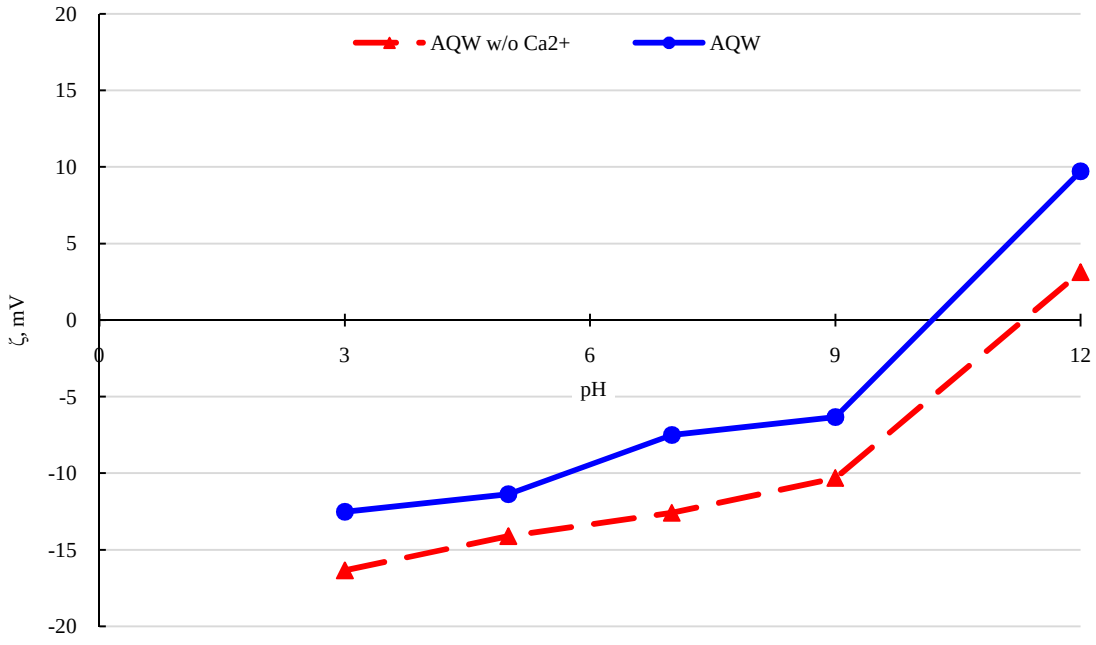

Figure II-3. ζ potential of limestone particles dispersed in aquifer water as a function of pH at 25°C.

Zeta potential depends strongly on pH and ionic strength. Excluding the calcium ion from AQW produced a significant change in ζ potential. Magnesium and sodium

ions, surprisingly, reduced the negative charges only at low pH. Our results agree with those obtained by Pierre *et al.* (1990), where low concentrations of divalent ions shifted the ζ potential from positive to negative. Monovalent ion (Na^+) showed no significant effect on the surface charge. Studies by Nyström *et al.* (2001), also, indicated that Na^+ had minor impact on the surface charge compared to calcium, barium and lanthanum ions.

Aquifer water is considered the reference case to compare with other tests. Lacking of Na^+ and other cations in AQW decreased the ζ potential at pH 12. The isoelectric point varied between pH 9.75 to 11.9 as described in **Table II-2**. Aquifer water without sulfate created less negative charges only at high pH values (9 and 12). Limestone particles suspended in deionized water at neutral pH created negative charges (-11.2 mV). Smani *et al.* (1975) reported ζ potential of -15 mV for calcite in deionized water. In brief, low–salinity water created negatively charged limestone particles. Zeta potential has ascending trend with pH. Aquifer water without calcium showed the lowest zeta potential. **Figure II-4** shows the effect of ionic strength on ζ potential at pH 7.

Table II-2. Isoelectric point for aquifer water solution at 25°C.

Aqueous solution	Excluded ion	Isoelectric point (ISP)	
Aquifer water (AQW)	SO_4^{2-}	9.75	Increasing
	–	10.2	
	Ca^{2+}	10.6	
	Na^+	11.3	
	Mg^{2+}	11.9	

Low–salinity water. Seawater (54,680 mg/L) represents the highest brine concentration used for zeta potential measurements, Table II-1. Limestone particles in seawater showed a positive surface charge (6.8 mV) at pH 7 and 25°C. The electrical double layer is usually compressed at higher salt concentrations. This perhaps causes a weaker electrostatic repulsion and a stronger flocculation (Möller and Werr 1972). It, also, explains the instability in the ζ potential measurements at high ionic strength level after using formation brine.

Aquifer water created negatively charged limestone particles as mentioned earlier. Aquifer water was diluted with deionized water in 1:1 ratio (50%). Results in **Figure II-5** suggested that 50% diluted AQW increased the magnitude of the zeta potential.

Effect of temperature. Reservoir's temperature condition was simulated by conducting several tests at 50ºC. Selective samples were tested at 25 and 50°C. Zeta potential of limestone in AQW was -7.5 mV at 25°C and pH 7, Table II-3. Increasing the temperature to 50°C decreased the ζ potential to -13.4 mV. Solubility of calcium ions increased as the temperature increases to 50°C. Hence, the calcium preferentially left the calcite lattice, and that created more negative charges. Somasundaran and Agar (1967) suggested the hydrolysis of the surface Ca^{2+} and CO_3^{2-} ions or the dissolved ions influenced the ζ potential result. Ion complexes, also, could strongly impact the fluid/particles interactions.

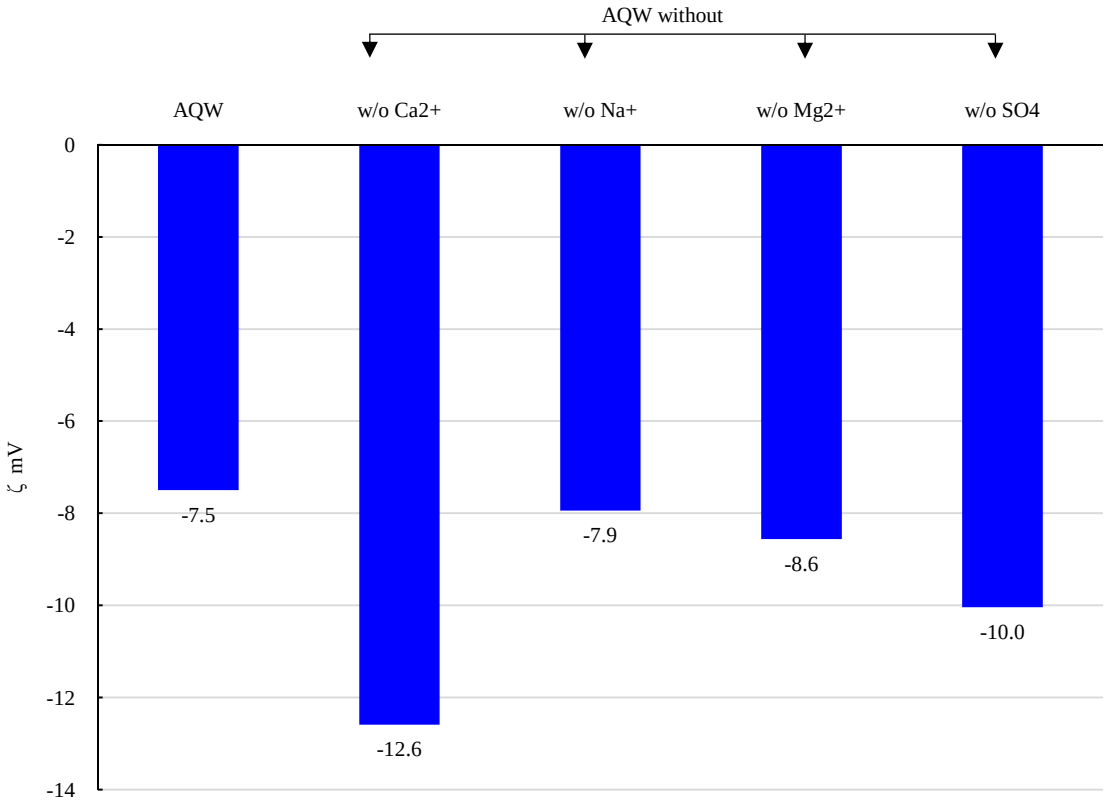

Figure II-4.ζ potential of limestone particles at different salts, 25°C and pH 7.

Table II-3. Zeta potential of seawater at different pH and 25°C.

pH	5	7	9
Zeta potential, mV	10.6	6.8	4.4

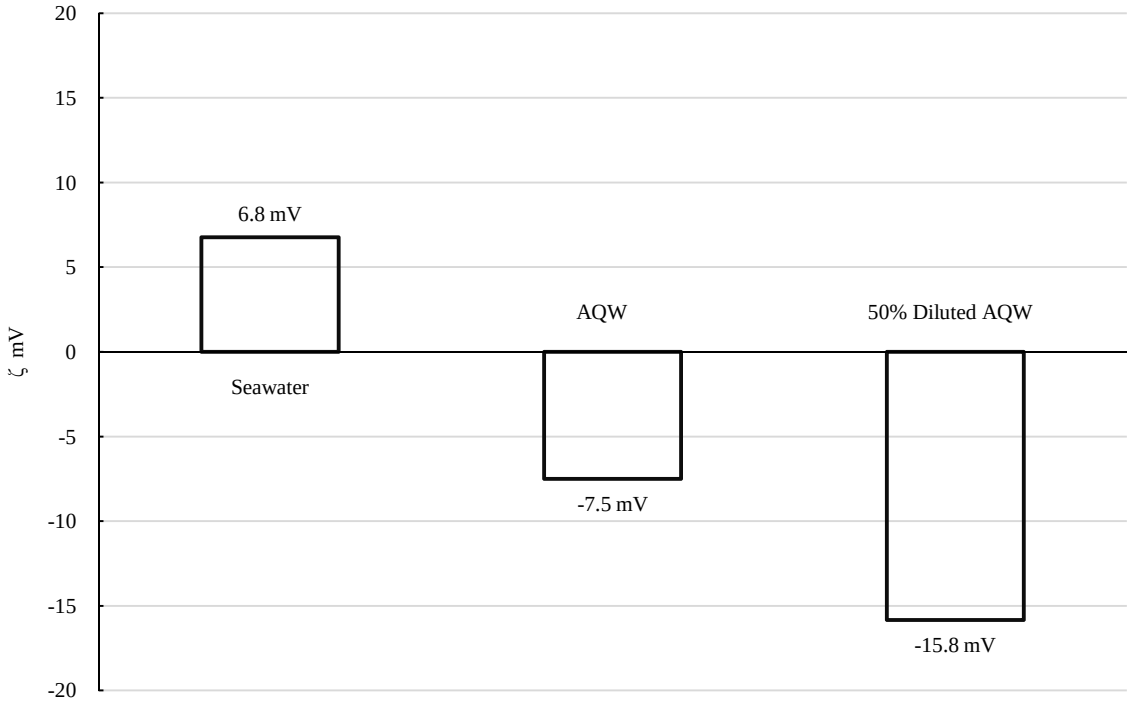

Figure II-5. Effect of seawater and low salinity water on ζ potential of limestone particles at 25°C and pH 7.

Temperature effect on ζ potential over a wide pH range is described in **Figure II-6**. A similar descending trend was reported as increasing the temperature from 25 to 50°C. Zeta potential magnitude, in general, increased as temperature was increased from 25 to 50°C. Moreover, aquifer water without Mg^{2+} ion created more negative charges at 50°C and pH of 3, 5, and 7 as shown in **Figure II-7**.

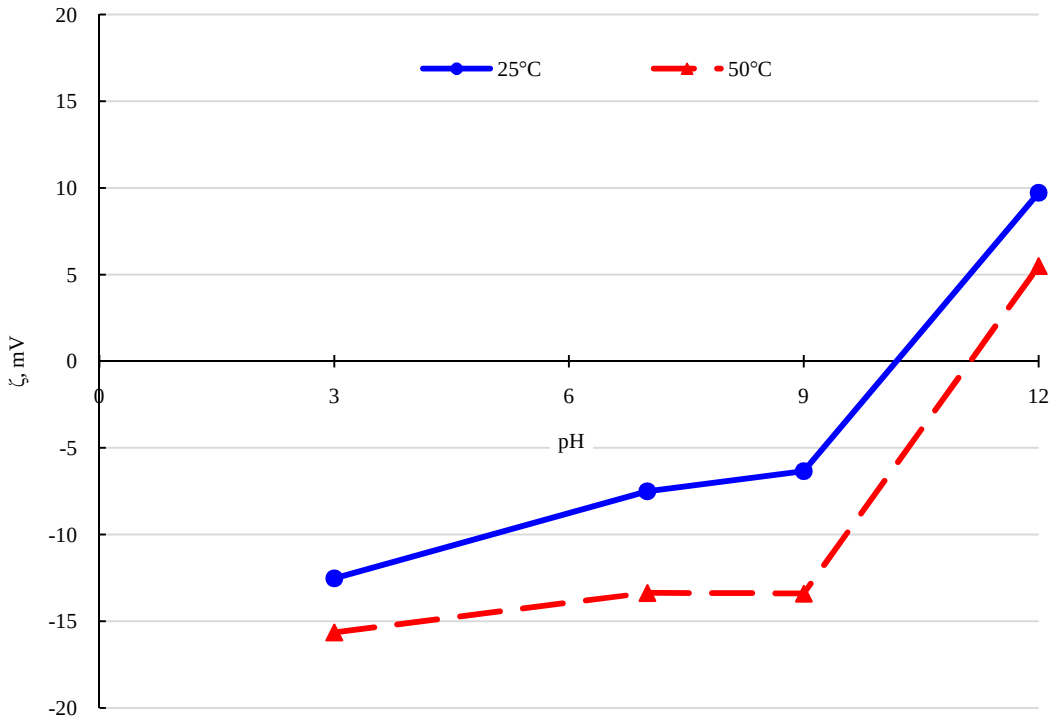

Figure II-6. Effect of temperature on ζ potential of limestone particles/aquifer water at different pH.

Aquifer water samples (AQW, 50% diluted AQW, 10% diluted AQW, AQW without NaCl, and AQW without $MgCl_2.6H_2O$) were all tested at 50°C and pH 7, **Figure II-8**. Temperature effect was more pronounced of limestone particles suspended in AQW, 10% diluted AQW, and AQW without $MgCl_2.6H_2O$. In summary, limestone particles' surface charge, at different pH, and ionic strength, decreased as temperature was increased.

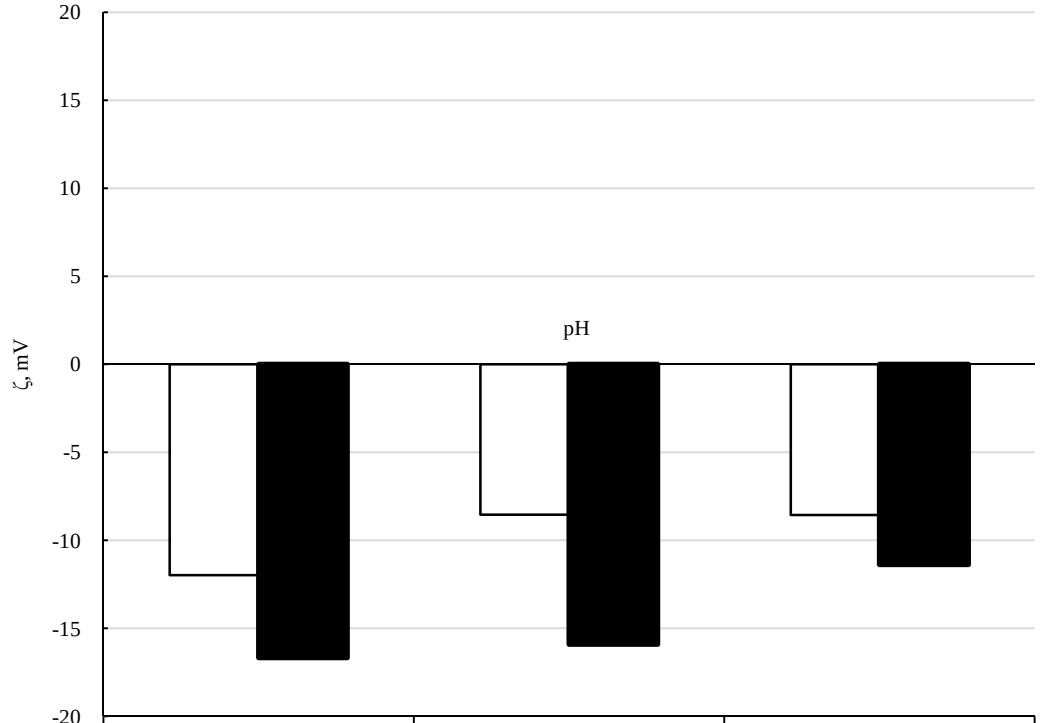

	3	5	7
T=25°C	-11.98	-8.54	-8.56
T=50°C	-16.66	-15.90	-11.37

Figure II-7. Effect of temperature on ζ potential of limestone particles dispersed in aquifer water without $MgCl_2.6H_2O$ at different pH.

NaCl solutions. To avoid multiple ions interactions, NaCl solution was prepared and individual ions were tested according to Table II-1. The ions concentration was identical to AQW. The test temperature was 25°C, while the samples pH was maintained at 7. The limestone particles were negatively charged in sodium chloride solutions, as shown in Figure II-9. Adding sodium sulfate (Na_2SO_4) to NaCl solution slightly decreased the zeta potential. Magnesium chloride ($MgCl_2$) significantly dropped the ζ potential to -11.5 mV. In addition, calcium chloride showed similar results as those obtained with $MgCl_2$.

In brief, divalent cations decreased the magnitude of the ζ potential, while sulfate ions showed no significant effect.

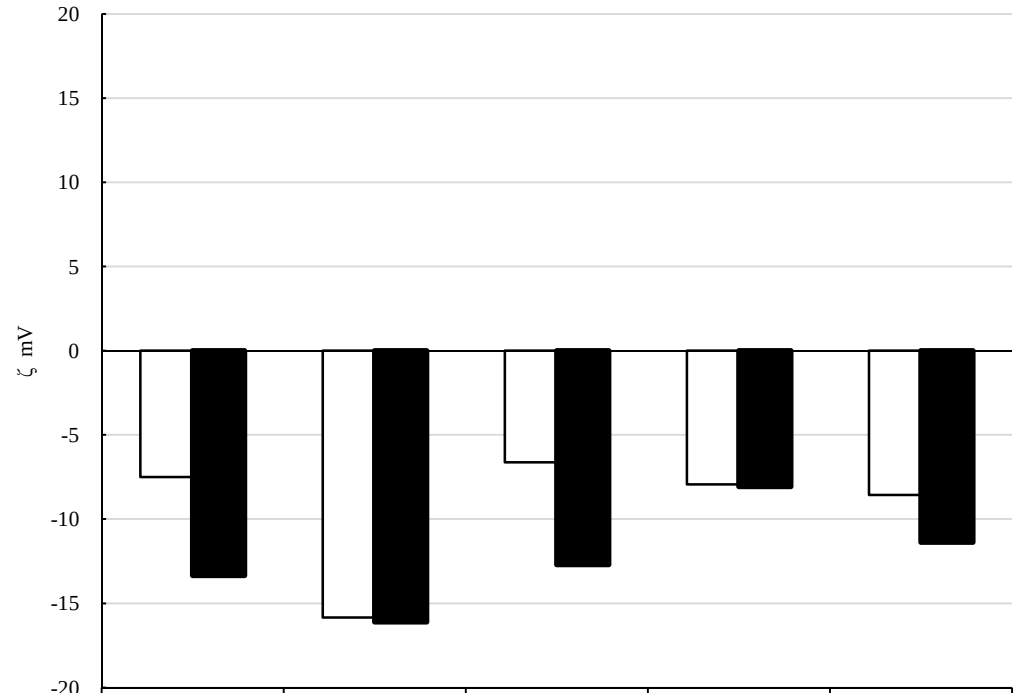

	AQW	50% Diluted AQW	10% Diluted AQW	AQW w/o NaCl	AQW w/o MgCl2.6H2O
□T=25°C	-7.5	-15.84	-6.63	-7.94	-8.56
■T=50°C	-13.36	-16.11	-12.7	-8.08	-11.37

Figure II-8. Effect of temperature and salinity on ζ potential of limestone particles at pH 7.

Formation brine. A thin layer of formation brine covers the reservoir rock surface. In order to mimic that, limestone particles were soaked in high–salinity formation brine for 2 days, TableII-1. After that, the particles were filtered and re–soaked in low–salinity brine for another 2 days. The objective from this step was to determine the dilution effect on the surface charge. No previous study has investigated the surface charge of pre-soaked solids, especially in such high–salinity brine.

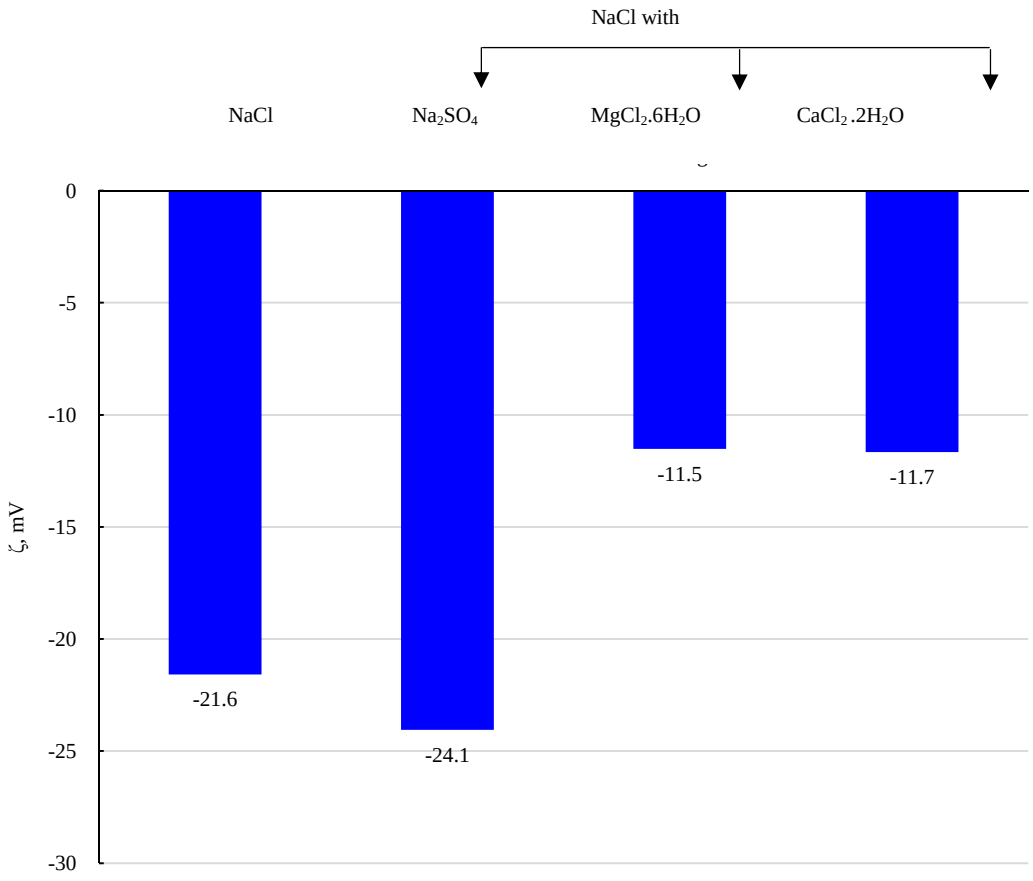

Figure II-9. Effect of salts on ζ potential of limestone particles at 25°C and pH 7.

Aquifer water, 50% diluted AQW, and deionized water were all tested at pH 7 and 25°C. Decreasing the water salinity was found to decrease ζ potential values. The deionized water, also, decreased the ζ potential of the particles to -18.5 mV, **Figure II-10**. The aquifer water increased the surface charge to 0.9 mV, while 50% diluted AQW decreased it to -3.1 mV. In comparison to the previous tests, the isoelectric point apparently decreased to be less than 7.

It indicates that ions surrounded the limestone particles were diluted with the low–salinity water. Hence, the particles were closer to isoelectric point than previous test. For example, ζ potential of limestone particles was -15.8 mV in 50% diluted AQW. Using pre-soaked particles in formation brine increased the ζ potential to -3.1 mV in 50% diluted AQW.

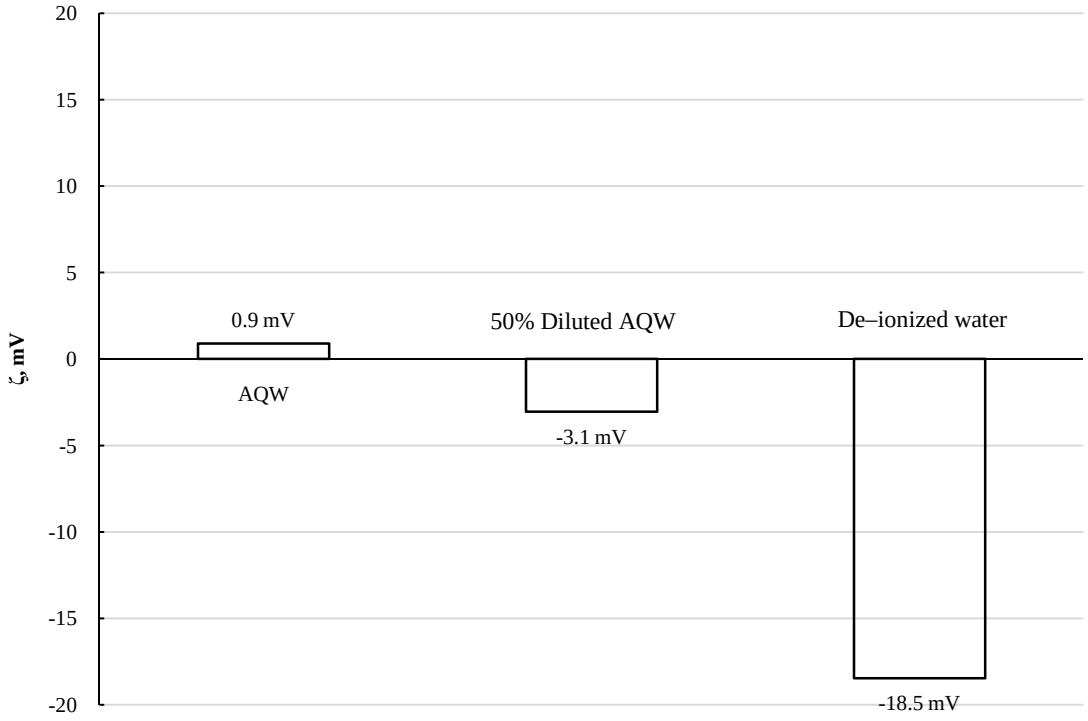

Figure II-10. Effect of low salinity water on ζ potential of limestone particles soaked in formation brine at 25°C and pH 7.

Two mechanisms are possible when calcite surface comes in contact with water or any electrolyte solution (Douglas and Walker 1950):

- Either Ca^{2+} or CO_3^{2-} might preferentially leave the rock surface into the solution and as a result, the surface charge will be opposite to the original one,

- The calcite surface might preferentially adsorb H^+, OH^-, or other ions present in aqueous solution, and so acquire a net charge, which will lead to the formation of a diffuse double layer.

The tendencies of Ca^{2+} or CO_3^{2-} to leave the lattice are determined by two factors:

- The required energy to remove a Ca^{2+} or CO_3^{2-} from the surface against the rock forces,
- The hydration energies of Ca^{2+} and CO_3^{2-} ions.

Dolomite particles

Aquifer water. The presence of magnesium in dolomite lattice structure creates different interactions with aqueous solutions. Selected cations (Ca^{2+}, Mg^{2+}), and sulfate anion (SO_4^{2-}) in AQW were tested at pH 7 and 25°C. Aquifer water created a negative surface charge on dolomite particles (-8.3 mV). Like limestone particles, dolomite solids showed a negative ζ potential in AQW. Lack of SO_4^{2-} in AQW significantly decreased ζ potential (-17.4 mV). Lack of calcium in AQW composition produced a negligible effect on the surface charge, Figure II-11. Moreover, the absence of Mg^{2+} decreased ζ potential to -13.7 mV. A 10% diluted seawater produced a very close zeta potential value (-8.3 mV) to the AQW test. They had similar ionic strength as well (AQW = 5,436 mg/L, 10% diluted seawater = 5,468 mg/L, Table II-1).

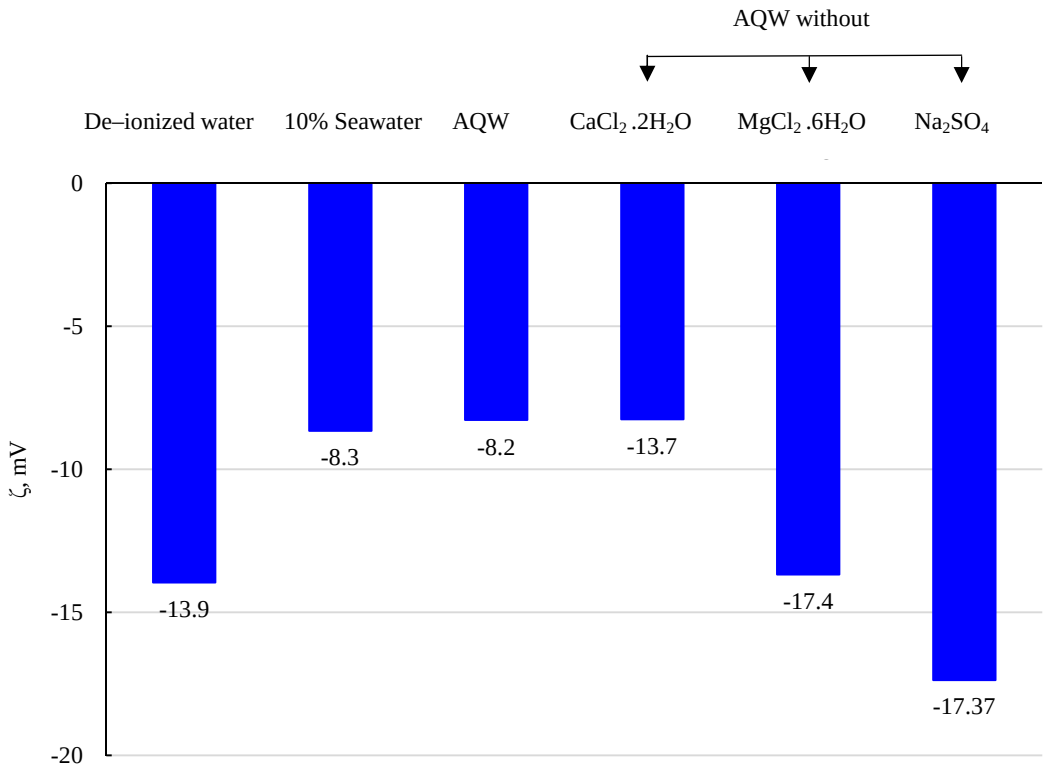

Figure II-11. Effect of salts on ζ potential of dolomite particles at pH 7 and 25°C.

Figure II-12 describes the pH effect on the dispersed dolomite particles in AQW at 25°C. The particles were negatively charged below pH 9. A direct relationship between ζ potential and pH was noticed. The isoelectric point of dolomite is lower than that of limestone.

Three major mechanisms are expected to influence the surface charge of dolomite particles: 1) ions interactions, 2) adsorption of ions complexes, and 3) hydrolysis of rock surface components (Ca^{2+}, Mg^{2+}).

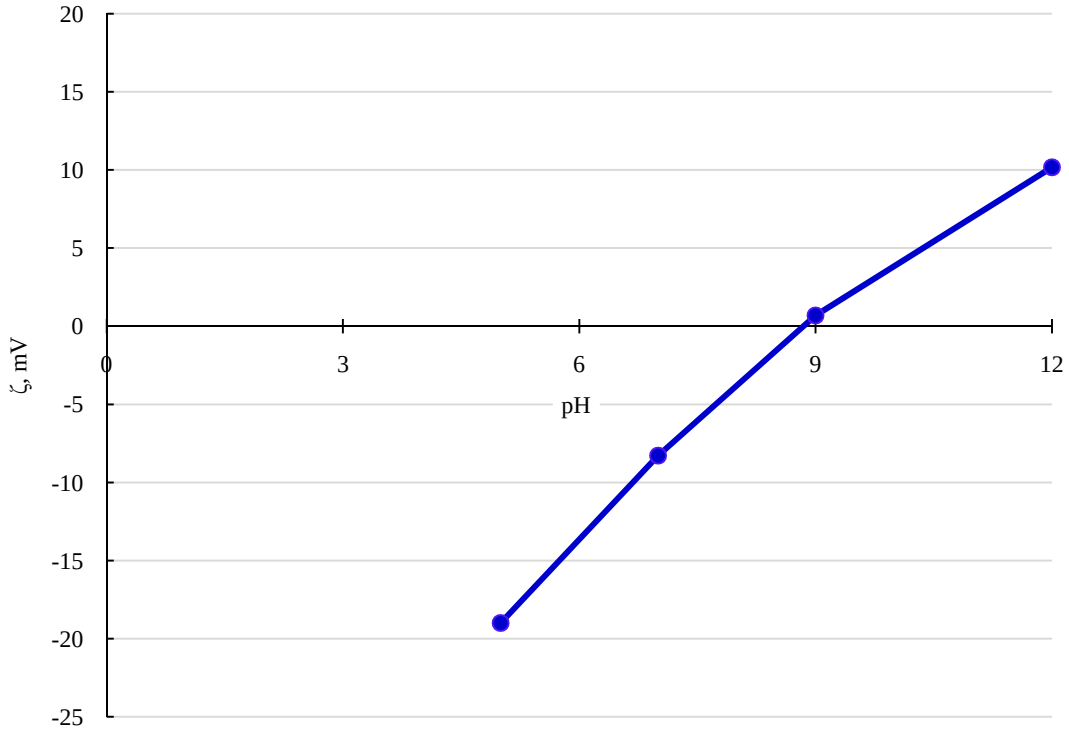

Figure II-12. ζ potential of dolomite particles dispersed in aquifer water as a function of pH at 25°C.

Low–salinity water. Deionized water decreased the ζ potential of the dolomite particles to -14 mV at temperature and pH of 25°C and 7, respectively.

Effect of temperature. Aquifer water without Na_2SO_4 was tested at two different temperature conditions over a wide pH range. The temperature effect on dolomite suspension was more significant at pH 3, Figure II-13. Solubility of Ca and Mg increased at high temperatures. Hence, the surface charge decreased as a result of the hydrolysis interaction.

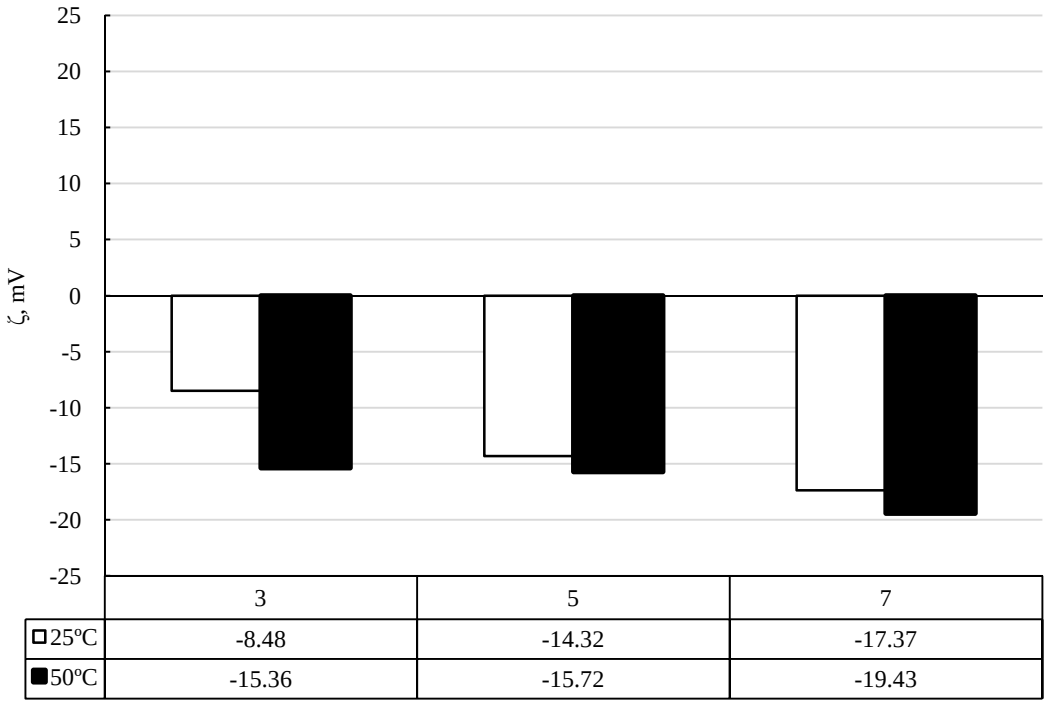

	3	5	7
25ºC	-8.48	-14.32	-17.37
50ºC	-15.36	-15.72	-19.43

Figure II-13. Effect of temperature and pH on ζ potential of dolomite particles dispersed in aquifer water without Na_2SO_4.

Wettability of most carbonate reservoirs is classified as a neutral or oil–wet. Altering the rock wettability considers one if not the most challenging problem. Adjusting water chemistry proves to change the carbonate surface charge from positive to negative. Therefore, optimizing the water composition is extremely essential for a successful waterflooding process. Applying such technology in the field should enhance the oil recovery by modifying the rock surface charge. Rock wettability will be modified toward water–wet condition accordingly. In this study, more focus was given to the original carbonate rocks interactions with different saline solutions. Oil-wet particles and emulsion (oil droplet in water) are expected to produce negative surface charge due to

the carboxylates groups present in the crude oil. Oil-wet particles and droplets in saline brines are thoroughly investigated in Chapter III.

Surface charge is also important in other EOR applications such as surfactant and ASP (Alkaline/Surfactant/Polymer) flooding. Injecting low–salinity water into a carbonate reservoir can reduce the surfactant adsorption risk at rock/liquid interface. Determining the rock surface charge may help in selecting the right surfactant system.

Conclusions

The main conclusions from this study are:

1. The interactions between injection water, reservoir fluids, and carbonate surface are complex.
2. Decreasing the salinity creates more negative charges on limestone and dolomite particles by expanding the thickness of the electrical double layer.
3. Zeta potential of limestone was strongly affected by the concentration of calcium ion in aquifer water.
4. Divalent cations decreased the zeta potential magnitude of limestone in sodium chloride solutions, while sulfate ion showed a negligible effect.
5. Increasing temperature significantly reduced zeta potential results.
6. Limestone particles in high–salinity water decreased the zeta potential magnitude.
7. Aquifer water without sulfate ion strongly influenced the surface charge of dolomite particles.

CHAPTER III

ELECTROKINETICS OF LIMESTONE PARTICLES AND CRUDE OIL DROPLETS IN SALINE SOLUTIONS

Summary

Salinity adjustment of waterflooding has recently been applied as an EOR technique in sandstone and carbonate reservoirs. Reaction mechanisms were different due to the variation in rock mineralogy and reservoir characteristics. Interactions between injection water, crude oil and limestone particles are still ambiguous. Anions in seawater believed to alter carbonate surface potential to negative and thus created repulsion forces between crude oil droplets (negatively charged) and connate water layer. As a result, rock wettability was altered toward water-wet.

In this chapter, the surface potential of crude oil and limestone particles were studied at 50ºC. Ionic strength was varied using formation brine (230K ppm), seawater (54K ppm), shallow aquifer water (5K ppm), and fresh water. Cations (Na^+, Ca^{2+}, Mg^{2+}) and anions (SO_4^{2-}) concentrations were tuned individually in seawater as well. The influence of H^+ and OH^- ions on the suspensions' surface potential was investigated by diluting seawater and aquifer water with deionized water at different volume ratios. Two phases (crude oil in water, limestone particles in water) and three phases tests (crude oil, and limestone particles in water) were performed at pH 8.

The surface potential of oil droplets were strongly affected by 10 vol.% diluted seawater, seawater without divalent ions (Ca^{2+} and Mg^{2+}), and de-ionized water due to

the adsorption of OH^- ions at the oil/water (O/W) interface. Sodium sulphate solutions (7,120 ppm) also increased the zeta potential absolute value of oil droplets. The effect of ionic strength on zeta potential was more pronounced in the oil-wet limestone particles than the intermediate-wet samples. An aqueous layer around crude oil droplets played a key role in determining droplet charges. Results from this study provide some insights on electrokinetics of limestone particles and oil droplets in different saline solutions. Wettability of the rock and oil recovery are directly affected by the zeta potential of oil droplets and suspensions.

Introduction

Suspensions, that include solid particles and oil droplets, can create surface charges in saline solutions. Different reaction mechanisms occur at the colloid surfaces such as: 1) adsorption of charged species from the surrounding solution, 2) differential loss of ions from the crystal lattice due to the rupture of ionic or covalent bonds, and 3) ionization of chemical groups on the surface (Garrison 2004; Sjöblom 2006). Therefore, the nature of surface charge depends on the different physico-chemical properties of various components in the system (Erbil 2006). Electrical double layer thickness (EDL) is affected by pH, ionic strength, and surfactant concentration. Understanding the nature of the surface charge in the oil displacement process can contribute significantly to waterflooding, and EOR performance. Also, determining the surface charge of carbonate particles can facilitate in the selection process of the proper surfactants that can propagate in carbonate formation with minimum loss due to adsorption.

Most carbonate reservoirs are classified as either oil–wet or intermediate–wet conditions (Chilingarian and Yen 1983). In addition, movement of crude oil droplets in the presence of reservoir fluids (connate formation brine and injection water) and rock particles was simulated by running two and three-phase tests, **Figure III-1**. In literature, water–wet limestone particles were commonly used to examine the effect of ionic strength on the particles' zeta potential (Zhang *et al.* 2007; Strand and Austad 2008). To mimic the actual reservoir wettability conditions, the carbonate rock particles should be at oil or intermediate–wet state. Formation wettability, in particular, is considered an important factor that controls fluids distribution in carbonate reservoirs, **Figure III-2**. Electrical properties at oil/water and water/rock interfaces can affect the flow behavior of emulsions, reservoir wettability, and indeed oil recovery.

The objectives of this study are to: 1) determine the effect of ionic strength on the surface potential of limestone particles at 50ºC, 2) study the impact of rock wettability on limestone particle's zeta potential and 3) evaluate the zeta (ζ) potential of crude oil droplets as a function of ionic strength. Three-phase tests (crude oil/brine/limestone particles) were also considered in this study.

Emulsion (oil droplets in seawater)

Oil-wet limestone particles in seawater

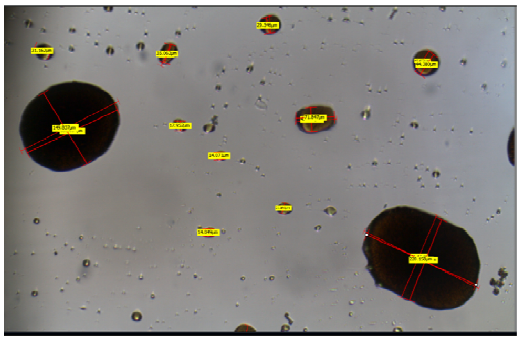

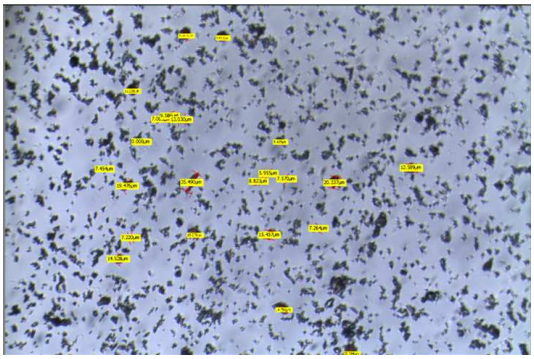

Microscopic images

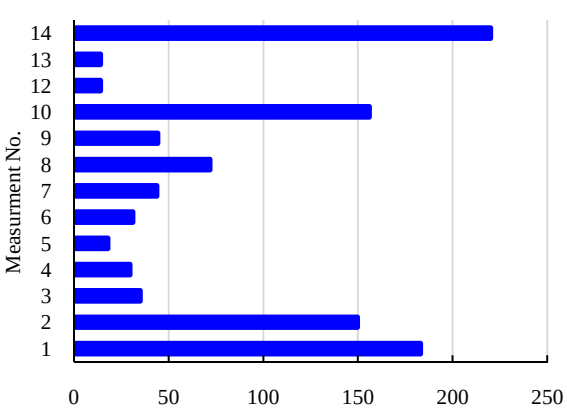

Crude oil droplet length, µm

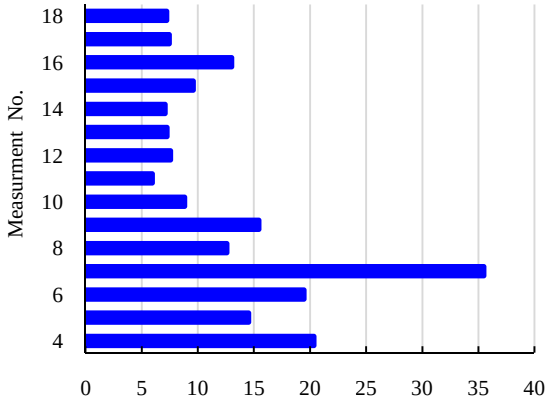

Limestone particle length, µm

Particle and droplet size distribution

Figure III-1. Macroscopic and microscopic images of oil-wet limestone particles and crude oil droplets in seawater and their size distribution.

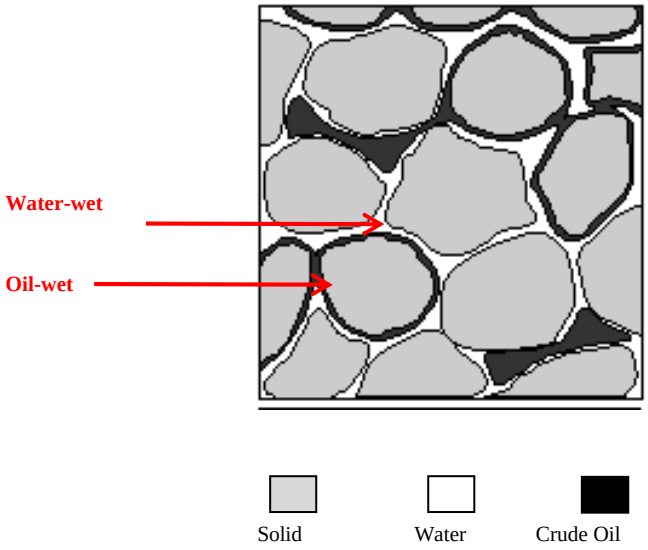

Figure III-2. Fluids distribution in carbonate reservoir (Abriola and Bradford 1998).

The differences between this study and other research work that had been published on limestone particles and oil droplets are:

1. Bitumen and heavy crude oils were previously studied. But, in this study, the author used a conventional crude oil.
2. In the literature, wettability of the used carbonate particles was water-wet. Various wettability conditions were investigated in this work.
3. Temperature conditions significantly affect the surface potential of suspensions. Therefore, all tests were conducted at 50ºC. Most of the previous work was done at atmospheric conditions.

4. It is the first time to conduct three-phase tests (limestone particle/crude oil/water). In the literature, either carbonate particles/water or crude oil/water systems was examined.

Literature Review

The disjoining pressure between crude oil and carbonate surfaces depends on three types of interactions. They are London-van der Waals attractive force, electrical double layer (EDL) force, and short-range repulsive forces. In this study, more attention was given to EDL force by measuring ζ potential of limestone particles, oil droplets, and mixture of both.

The EDL force is a function of water chemistry (ionic strength, pH), temperature, and the charge characteristic of oil/water and mineral/water interfaces. The interfacial charge depends on the type of the molecules in the crude oil that can adsorb at these interfaces (Toulhoat and Lecourtier 1991). These materials can also leave the oil/water interface and alter the charge characteristics of the mineral/connate water interface. Asphaltene adsorption can decrease the crude oil's surface charge. The responsible polar groups for asphaltene adsorption are oxygen-containing functional groups such as carboxylic acid and phenolic acid groups (Hall *et al.* 1983).

Dickinson (1941) reported negative ζ potential at the hydrocarbon/water interface due to the adsorption of hydroxide ions (OH^-). Zeta potential decreased with increasing the solution pH and decreasing NaCl concentrations. In addition, the affinity of the OH^- ions to adsorb at the hydrocarbon/water interface depends on the type of hydrocarbons

(Douglas 1943). The surface potential of three different crude oils, in NaCl solutions, changed from negative to positive at pH less than 4 (Buckley *et al.* 1989).

Issacs *et al.* (1998) showed that crude oil/water interfaces (10^{-2} M NaCl) were electronegative at neutral and high pH. This was attributed to the dissociation of moieties belonging to surfactants naturally present in the bitumen such as carboxylate groups ($RCOOH \rightarrow RCOO^{-}+H^{+}$). Moreover, the acid components in the crude oil diffused easily to the oil/water interface than the basic components (Rodríguez-Valverde *et al.* 2003). Zeta potential of bitumen particles varied with the ionic strength of NaCl solutions and pH (Takamura and Chow 1985). The functional groups that contain nitrogen and oxygen in crude oil may give amphoteric or zwitterionic character to the oil/water interface (Buckley 1994). The ionic strength effect on water-wet and dry carbonate particles was thoroughly investigated in Chapter II (Alotaibi *et al.* 2011). In this study, more attention was given to crude oil/water interactions.

Chow and Takamura (1988) studied the ζ potential of two crude oil samples that had different values of acid number and asphaltene content. Multivalent ions (Ca^{2+}, Mg^{2+}) were evaluated in the presence and absence of NaCl solutions. Zeta potential of bitumen in water emulsion was almost identical in the presence and absence of 10^{-2}M NaCl except at low Ca^{2+} concentrations (10^{-4}M). This result indicated that Ca^{2+} interacted with $RCOO^{-}$ on bitumen surface and caused a smaller degree of electrophoretic relaxation effect. The authors also reported an inverse relationship between the pH and ζ potential of bitumen droplets in $CaCl_2$ solutions. Similar results were noticed for the conventional crude oils in water emulsion samples.

Sulphate is believed to be a very strong potential determining ion towards calcium carbonate particles (Pierre *et al.* 1990; Strand *et al.* 2003; Strand and Austad 2008). In addition, adsorption of SO_4^{2-} changed the carbonate surface potential to negative and thus created more repulsion forces with the acid carboxylic groups in crude oil. Wettability might be altered towards water-wet accordingly.

Experimental Studies

Materials

Outcrop limestone rock from USA was used for ζ potential experiments. A ceramic mortar and pestle were then employed to crush the rock into fine powders. The sieve analysis step was skipped to eliminate any solids contamination from the sieves' columns.

Fluids

Synthetic brines (formation brine, seawater, shallow aquifer water) were tested simulating a field case in the Middle East, **Table II-1**. All brines were prepared using deionized water and then passed through 1 µm filter paper. Stock tank crude oil A (sweet) was collected from one well in Alaska field. The crude oil was filtered through a core sample to remove any solid particles. Afterwards, the oil was centrifuged for 5 minutes at 2,000 rpm. Crude oil composition was determined using gas chromatography and mass spectrometry system (GC/MS), Appendix B. Thirty five compounds were identified in the crude oil sample, 17.6% aromatics, 13.7% naphthenes, and 67.7% paraffins. Densities and viscosities of crude oil and aqueous solutions were measured at

50ºC using high temperature density meter DMA 4100 and a capillary viscometer, respectively (**Table III-1**). In addition, standard test method D-664 and D-974 were used to determine acid and base numbers (0.18 mg KOH/g, less than 0.01 mg HCl/g). A shallow aquifer water and seawater were diluted with deionized water at different volume ratios to determine the role of the ionic strength on the ζ potential of suspensions.

Table III-1. Properties of crude oil and brines.

Fluid Description	Density*	Viscosity*	Acid number	Base number
	g/cm^3	cP	mg KOH/g	mg HCl/g
Crude oil	0.8687	7.1615	0.18	<0.01
Formation brine	1.1391	1.0331		
Seawater	1.025	0.737		
Shallow aquifer water	0.9893	0.6203		

*Density and viscosity were measured at 50°C.

Apparatus and procedure

Zeta potential (ζ). Phase analysis light scattering technique (pals) was applied to determine the ζ potential of limestone particles and crude oil droplets. The instrument determined the electrophoretic mobility of charged, colloidal suspensions. The maximum temperature limitation for the electrode to be used was 50ºC. More information about the instrument was reported in Chapter II. The emulsion and suspensions preparation procedures are shown next.

Emulsion. Various brines were prepared and then NaOH and HCl solutions were used to adjust pH accordingly. Emulsions samples were created by sonicating 10 droplets of crude oil vigorously in 40 cm^3 aqueous solution for 10 min. at ambient condition. A tuberculin syringe (1 cm^3) was used to transfer aliquot emulsion into electrode's cuvette (2 cm^3). The preparation procedure is critical because it can cause measurements errors if not prepared properly. A small hole was drilled in the upper side of the polystyrene cuvette slightly above the electrode's hole. A syringe needle was then inserted at a 45º angle and placed all the way in the bottom corner of the cuvette. After that, the sample was injected slowly until filling the hole, keeping the needle submerged at all the time. Placing the needle half way or not fully submerged can result in air bubbles.

Water-wet limestone particles. Suspensions, on the other hand, were prepared by mixing 0.2 g powdered particles of limestone with 40 cm^3 of aqueous solutions for two days using a magnetic stirrer. Samples were centrifuged to separate the concentrated and supernatant into different tubes. A few droplets of the concentrated solution (limestone particles and aqueous solution) were transferred to the 2 cm^3 of the supernatant solution (aqueous solution). A syringe was then used to load the suspensions in the electrode cuvette as described earlier. Injection water often has different chemistry and salinity than formation brine. Hence, some tests were conducted by mixing formation brine with different brines to mimic waterflooding and EOR processes in the field.

Oil-wet limestone particles. Oil-wet limestone particles were prepared since most carbonate reservoirs are either at oil or intermediate wet condition. Carbonate formations were originally water-wet, and for that reason, water film layers usually surround the

carbonate rock. To mimic the actual reservoir condition, limestone particles were first soaked in formation brine for two weeks to make sure the equilibrium condition was reached. Then, the particles were filtered and soaked in crude oil sample at 90ºC overnight. The oil-wet particles were re-filtered and dried in the oven before being dispersed in various brine solutions as done earlier.

Zeta potential tests for all samples were conducted at 50ºC and atmospheric pressure. Special electrode was particularly designed for high ionic strength fluids such as formation brine and seawater. Various sets of two and three phases' tests were conducted as follows:

1) Crude oil in water.
2) Oil-wet limestone particles in water.
3) Intermediate-wet limestone particles in water (by mixing oil and water wet particles).
4) Water-wet particles in water.
5) Crude oil, water-wet limestone particles in water.

The crude oil droplets and limestone particles were sonicated first in various brines. The aliquot was then dispersed either in the same brine or different ones, **Figure III-3**.

Results and Discussion

Injection water ions interact with the rock minerals, reservoir fluids, and with other ions in the same injection fluid. Hence, it is a complicated process especially not all the ions are free; some of them are expected to be complex as will be described in Chapter X.

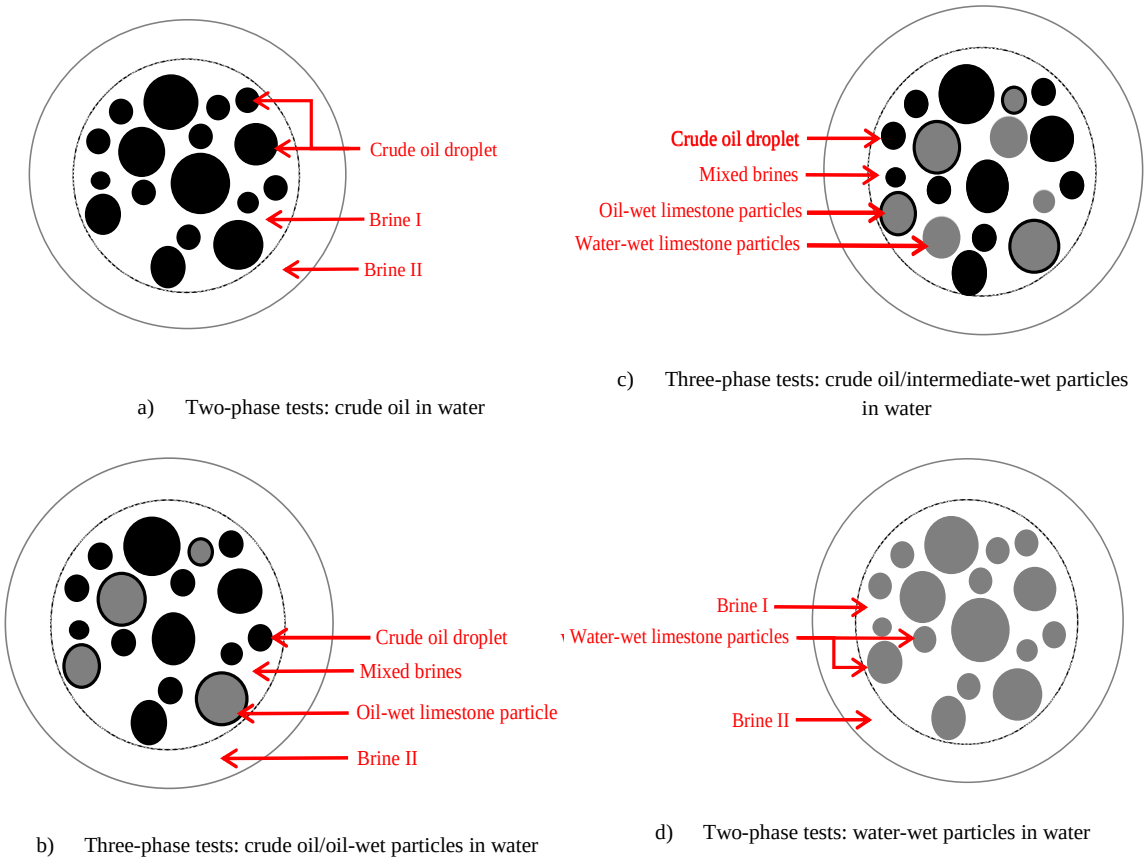

Figure III-3. Emulsion and suspensions in saline solutions.

Since some of the carbonate reservoirs are classified as intermediate-wet, particles were soaked in formation brine and then mixed with oil-wet particles in aqueous solutions. Microscopic images of suspensions in seawater showed limestone particles had uniform size distribution than crude oil droplets, **Figure III-1**. Fluids in carbonate reservoirs are usually noticed to be more basic (pH>7). For that reason, most of the surface potential tests were carried out at pH 8 and temperature of 50ºC, except

two set of tests were conducted over a wide pH range. In general, absolute value of ζ potential increases with temperature (Rodríguez and Araujo 2006).

Two-phase tests

Crude oil/seawater. Crude oil samples were dispersed in seawater solutions using a sonicator mixer. Seawater composition is shown in Table II-1. Seawater was considered the base case for comparisons with other solutions. All other factors such as temperature, pH, and soaking time were similar. Zeta potential of oil droplets in seawater was - 10.45 mV, Figure III-4. Crude oil samples were prepared and dispersed in the same brine. Diluted seawater at 50 and 10 vol% reduced the ζ potential of crude oil. The absolute value of ζ potential significantly decreased after using 10% diluted seawater. Adsorption of the OH^- ions suggested the significant increase in the absolute value of crude oil ζ potential.

Calcium and magnesium in water are commonly called “hardness”. These ions can form hard films and scales when deposited in pipes or adsorbed at rock surfaces. Removal of these ions from the water is called “softening”. Softening the seawater decreased the surface potential to - 17.7 mV because the divalent ions were tightly bonded to carboxylate group at the interface. The absence of Ca^{2+} only in seawater increased the ζ potential slightly to - 8.1 mV because calcium concentration was low (664 mg/L, **Table II-1**). Seawater without a monovalent Na^+ ion also produced similar trend because the sodium was weakly bonded to the interface in comparison with

divalent ions. Increasing Ca^{2+} and decreasing Mg^{2+} concentration showed almost no impact on the surface potential of oil droplets.

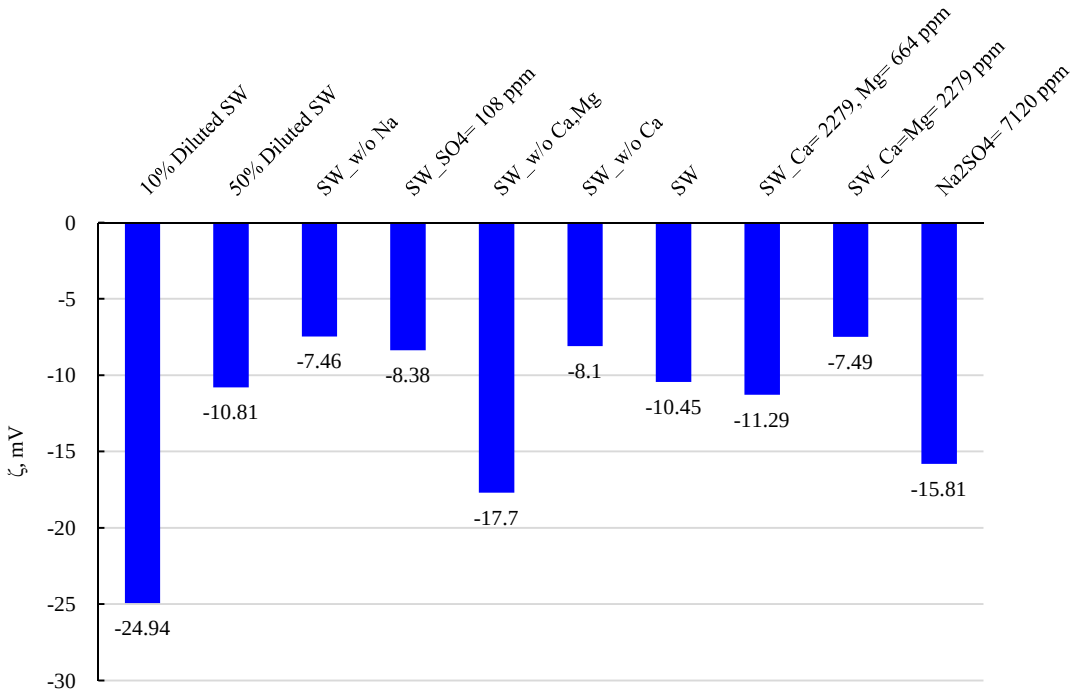

Figure III-4. ζ potential of crude oil droplets dispersed in different saline solutions at pH 8 and 50°C.

Using low SO_4^{2-} concentration (108 mg/L) in seawater had insignificant impact on the surface potential of crude oil as well. Sodium sulphate solution was prepared in deionized water at a concentration of 7,120 ppm (two times SO_4^{2-} level in seawater). The objective was to determine if SO_4^{2-} ions have any influence on the crude oil surface potential in presence of Na^+ ions only. As shown in **Figure III-4**, SO_4^{2-} ions decreased the ζ potential of crude oil to - 15.8 mV.

In short, 10% diluted seawater, seawater without divalent ions, and 7,120 ppm Na_2SO_4 solution produced the lowest surface potential at the oil/water interface. Our results matched similar observations by Chow and Takamura (1988). Reducing the injection water salinity using deionized water confirmed the decrease in the ζ potential of oil droplets further to - 26.37 mV because of OH^- adsorption at oil/water interface. Mixing 5 crude oil droplets in a supersaturated formation brine sample (1 cm^3) increased their ζ potential to 5.38 mV. This was expected as formation brine had noticeable amount of Ca^{2+} ions and believed to strongly attach to COO^- groups at oil/water interface.

The surface charge at any fluid/fluid or fluid/rock interfaces is affected by the solution pH. Hence, oil droplets were sonciated in seawater and deionized water. The ζ potential of crude oil in seawater at low pH was not stable because of neutralizing the COO^- group and ions' interactions. For that reason, the zero point of charge (1.4 mV) was determined from the linear relationship between the pH and surface potential as depicted in **Figure III-5**. De-ionized water, on the other hand, had a higher slope than seawater system. In addition, the zero point of charge for crude oil/deionized water system was 4.3 mV.

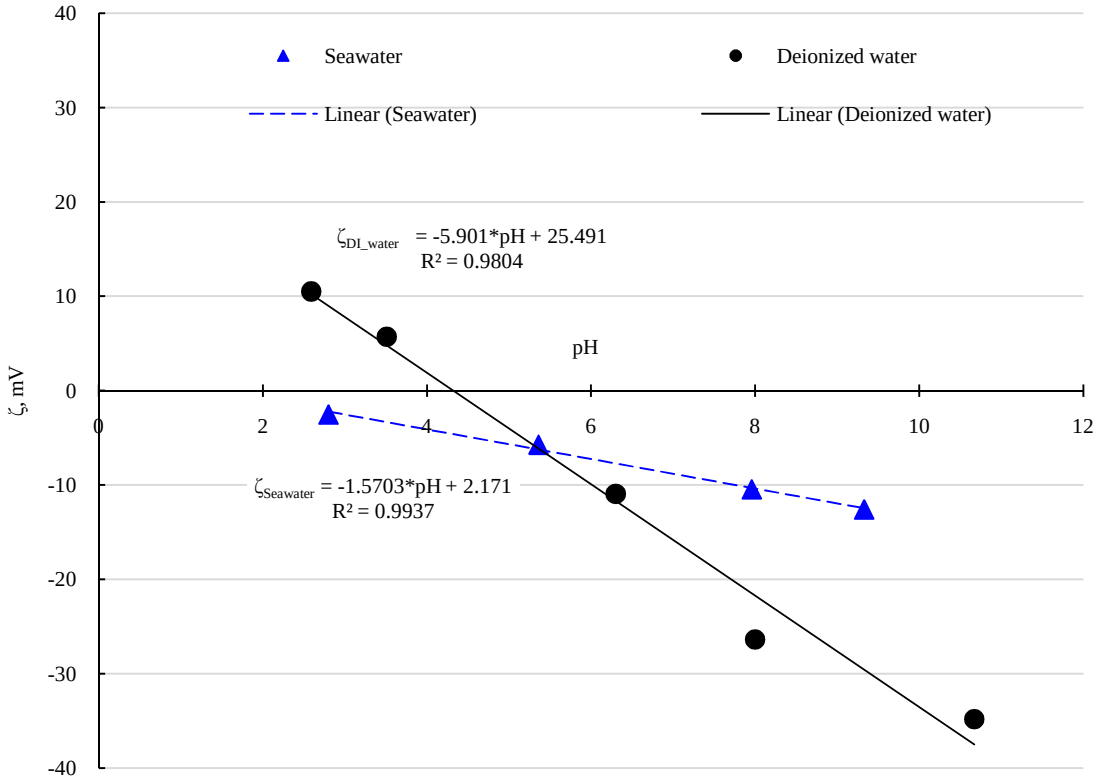

Figure III-5. ζ potential of crude oil droplets dispersed seawater and deionized water at 50°C., ZPC=1.4, 4.3.

Crude oil/shallow aquifer water. The same procedure was followed to prepare emulsion sample of crude oil in shallow aquifer water. In general, the absolute value of surface potential decreased at the 50% diluted aquifer water/crude oil interface. The proton (H^+) and hydroxide ion (OH^-) had a clear impact on the rock/fluids interactions. Zeta potential of crude oil in the presence of aquifer water was - 15.22 mV. As expected, 50% diluted aquifer water decreased the crude oil surface potential further to - 16.40 mV due to decreasing the ionic strength.

Oil-wet limestone particles. Limestone particles (0.2 g) were soaked in 50 cm^3 formation brine for two days. The particles were filtered afterward through 2 μm filter paper and were soaked in crude oil sample overnight at 90ºC. The limestone particles were also re-filtered through 2 μm filter paper. Oil-wet limestone particles were dispersed in seawater and deionized water at pH 8 and ambient temperature afterward. The ζ potential of limestone particles in seawater was - 12.72 mV. Reducing the salinity using deionized water decreased the ζ potential to - 34.12 mV. In comparison to crude oil in seawater in the previous test, ζ potential of the limestone particles in seawater decreased by 2 units. This was due to the difference in the electrophoretic mobility of liquid droplets compared to rigid particles.

Intermediate-wet limestone particles. Dry limestone particles were soaked in formation brine to mimic the water-wet part of carbonate rocks, Figure III-2. As described earlier, some carbonate reservoirs have intermediate wettability. The oil-wet particles were surrounded with seawater while the water-wet ones were suspended in formation brine. Five droplets of oil and water-wet particles were mixed in seawater and deionized water. The salinity effect was minimal where the ζ potential of the particles in seawater and deionized water were - 4.65 and - 6.53 mV, respectively. Results suggested that mixed wet limestone particles showed a different behavior than the oil-wet ones. The ζ potential of the particles decreased toward the isoelectric point (point of zero net charge) due to the presence of cloud of ions from formation brine around the particles.

Water-wet limestone particles. Connate formation water was tested in the presence of limestone particles that were soaked earlier with the same brine. High ionic strength, for sure, increased ζ potential of limestone particles toward positive numbers. The surface potential of limestone particles in formation brine was 6 mV at 50ºC. To the best of my knowledge, this is the first time to study surface potential of limestone particles in a supersaturated brine solution at such high ionic strength. It is a common assumption that most of the carbonate reservoirs are positively charged (Schramm et al. 1991; Schramm 2000).

Three-phase tests

Crude oil/limestone particles/water. Dispersed crude oil in seawater and deionized water were mixed with water-wet limestone particles in formation brine individually. Crude oil and limestone particles showed very close ζ potential results and were not affected by the salinity of the third aqueous phase (seawater or deionized water). The ζ potential of suspension in seawater and deionized water were - 4.12 and - 6.67 mV, respectively. Table III-2 gives the results for all tests.

Table III-2. Summary of electrokinetics results of limestone particles and crude oil droplets.

Suspension Type	Original Aqueous Phase	Second Aqueous Phase	Zeta Potential, mV
Crude oil droplets	10% SW		- 24.94
	50% SW		- 10.81
	SW without Na^+		- 7.46
	SW (SO_4^{2-} = 108 ppm)		- 8.38
	SW without Ca^{2+} and Mg^{2+}		- 17.70
	SW without Ca^{2+}		- 8.10
	SW		- 10.45
	SW (Ca^{2+} = 2,279 ppm, Mg^{2+} = 664 ppm)		- 11.29
	SW (Ca^{2+} =Mg^{2+} = 2,279 ppm)		- 7.49
	Na_2SO_4 solution (SO_4^{2-} = 7,120 ppm)		- 15.81
	SW	Formation brine	5.38
	SW	De-ionized water	- 26.37
	Aquifer water		- 15.22
	50% aquifer water		- 16.4
Oil-wet particles	SW		- 12.72
	Deionized water		- 34.12
Oil-wet particles	SW	SW	- 4.65
Water-wet particles	Formation brine		
Oil-wet particles	SW	Deionized water	- 6.53
Water-wet particles	Formation brine		
Water-wet particles	Formation brine	Formation brine	6
Crude oil droplets	SW	SW	- 4.12
Water-wet particles	Formation brine		
Crude oil droplets	SW	Deionized water	- 6.67
Water-wet particles	Formation brine		
Crude oil droplets		Formation brine	7.45
Water-wet particles			
Crude oil droplets		SW	Not stable
Water-wet particles			
Crude oil droplets		Deionized water	- 2.87
Water-wet particles			

Crude oil/limestone particles/formation brine. Formation brine, seawater and deionized water were all tested in the presence of crude oil and water-wet limestone particles. The difference between this and the previous tests was the ionic strength of the dispersion media. In this test, crude oil was sonicated in formation brine. Whereas in the previous three phase tests, crude oil was dispersed in seawater and deionized water. Formation brine definitely produced the highest ζ potential for limestone particles and crude oil droplets (7.45 mV). This was the highest surface potential result in this study. Deionized water decreased the ζ potential of the suspensions to - 2.87 mV. Seawater test was not stable although it was repeated several times. Seawater was expected to produce a surface potential between deionized water and formation brine results.

Conclusions

The following conclusions are drawn from the electrokinetics study of crude oil droplets and limestone particles:

1. The surface potential of crude oil droplets were affected by 10% diluted seawater (- 24.94 mV), seawater without Ca^{2+} and Mg^{2+} ions (- 17.7 mV), and deionized water (- 26.37 mV) because of hydroxide ions adsorption at the oil/water (O/W) interface.
2. Sodium sulphate solution (7,120 ppm) increased the zeta potential absolute value of the crude oil droplets by 5 mV. The zeta potential values in seawater and sodium sulphate solution were - 10.45 and - 15.81 mV, respectively.

3. Oil-wet limestone particles behaved differently in water than the intermediate or water-wet particles.
4. The effect of ionic strength was more pronounced in the oil-wet limestone particles than others.
5. The aqueous layer around oil droplets such as formation brine and seawater played a key role in the generated zeta potential. In addition to hydroxide ions, cations and anions in saline solutions can either increase or decrease the crude oil droplets' surface potential.

CHAPTER IV

INTERFACIAL PROPERTIES AND STATIC CONTACT ANGLE OF CRUDE OIL/BRINES/CALCITE ROCK

Summary

Injection of water for pressure maintenance and waterflooding applications is becoming an increasingly important issue. Historically, the total suspended solids of the water were given more consideration rather than the total dissolved solids. The water from injection wells physically sweeps the displaced oil to adjacent production wells. Displacement of the oil is highly affected by many interacting variables. Wettability has been recognized as one of the controlling parameters of the remaining oil-in-place. Brine salinity, oil chemistry, and rock lithology play a key role on altering rock wettability. Recent studies showed that low–salinity water can decrease the residual oil saturation in carbonate reservoirs.

This chapter highlights extensive interfacial tension (IFT) and wettability studies to determine the optimum brine salinity, which expects to result in higher oil recovery. Contact angle is considered one of the most common methods to measure the preferential affinity to the reservoir rocks. Crude oil, carbonate rocks, and synthetic brines (formation, aquifer, and seawater) were used in this study. All experiments were conducted at high pressure (up to 2,000 psi), and elevated temperature (up to 130°C).

Fluids' interfacial tension and surface wettability in carbonate reservoirs depends on salinity, temperature, and crude oil compositions. Currently, there is confusion

concerning the optimum brine salinity for secondary and tertiary recovery. Using aquifer solution, deionized water, and sodium sulfate (1780 mg/L) adjusted the rock wettability towards water-wet condition. Contact angle results were clearly independent on the pressure. The result of this study gives a new insight on the optimum salinity and provides better understanding of some wettability challenges in carbonate reservoirs.

Introduction

Carbonate rocks (limestone and dolomite) account for more than half of the world's hydrocarbon reserves. Understanding the important mechanisms which control recovery and retention in a given reservoir is essential for successful oil production. The wettability preference, towards oil or water–wet, influences many aspects of reservoir performance. Making incorrect assumption about reservoir wettability might result in unexpected formation damage. Reservoir rocks are complex structures of a variety of minerals. For this reason, it is extremely difficult to describe the wetting character of reservoir rocks. Most petrophysical properties such as capillary pressure, relative permeability, electrical properties, and waterflood behavior are directly affected by the wettability.

Carbonate reservoirs, in general, are believed to have mixed wettability or oil–wet. It is also recognized that recovery factors are higher for sandstone reservoirs than for carbonates. Carbonate reservoirs present a number of specific characteristics posing complex challenges in reservoir characterization, production and management.

Adjusting the injection water ions can impact rock wettability and thus could enhance oil recovery (Høgnesen *et al.* 2005). Høgnesen *et al.* focused an imbibition study at high temperatures using reservoir limestone, outcrop chalk cores, seawater and formation water. Increasing sulphate ion concentration at high temperatures proved to be a major factor in recovering additional oil. Possibility of scale and sour problems is expected as increasing the sulphate concentration. Moreover, this strategy has limitations with regard to the initial brine salinity and temperature (Webb *et al.* 2005).

Literature Review

Interfacial tension

Interfacial and flow properties of any fluids in porous media are highly affected by the film properties at the interface. This film has different properties than the bulk fluids. Xu (2005) studied the effect of the brine composition on the IFT of live crude oil as a function of time. Five systems were examined: deionized water, NaCl, $CaCl_2$, formation brine, and 50% formation brine. $CaCl_2$ solution had the highest equilibrium IFT value in comparison to the other solutions. In addition, 50% formation brine showed higher IFT than that of the original formation brine sample.

Okasha and Al-Shiwaish (2009) recently studied the effect of salinity level on crude oil/water IFT measurements. Both dead and live oil samples were tested. Synthetic formation brine solutions were prepared at TDS: 52,346, 107,906, and 214,943 ppm. Results for low, medium and high salinity solutions were varied between 17.7 and 34.4 dyne/cm. The IFT in presence of dead oil decreased as increasing temperature and

pressure conditions. On the other hand, presence of gases in crude oil decreased the IFT in compare to dead oil.

Wettability alteration mechanism

Wettability alteration is the main challenge for enhancing oil recovery in carbonate reservoir. Strand *et al.* (2008) showed the effect of injection water ions (Ca^{2+}, Mg^{2+} and SO_4^{2-}) on oil recovery. The activation energy for chemical reactions is important and required for any wettability improvement. In general, the bonding energy between polar components in oil and divalent ions in carbonates is usually high. Carbonate rock is neutral to preferentially oil–wet, because of the carboxylate components adsorption. Sulphate is believed to be a very strong potential determining ion towards calcium carbonate (Pierre *et al.* 1990; Strand *et al.* 2003; Strand and Austad 2008).

Adsorption of sulphate ions decreased the positive charge on the rock surface and that affected the electrostatic repulsion forces (Strand *et al.* 2006; Strand *et al.* 2008). Such interactions facilitates the desorption process of the negatively charged carboxylic materials from the chalk surface (Strand *et al.* 2003).

Lichaa *et al.* (1992) investigated the wettability changes in carbonate reservoir rocks using USBM, Amott, and contact angle methods. In brine/crude oil/rock system, the salinity and pH were strongly affecting the surface charges at the interfaces, which in turn can affect the wettability. In addition to the polar compounds in the crude oil, multivalent ions (Ca^{+2}, Mg^{+2}, and Sr^{+2}) in the injection seawater and formation brines were significantly altering the wettability condition.

Contact angle method

Contact angle is a function of the IFT at the solid/liquid and liquid/liquid interfaces. Wettability of a reservoir rock is a manifestation of the thermodynamic equilibrium between fluids within the pores and the mineral surfaces of the pore walls. Therefore, temperature, pressure, and fluids characteristics are strongly believed to have an effect on wettability. Roughness and heterogeneity of the solid surface will affect the contact angle and contribute to what is commonly known by hysteries. A contact angle of 180º implies complete oil-wet characteristics, while 0º means complete water-wet. Wettability classifications, in terms of contact angle, was well classified by Anderson (1986) as water-wet (0–75º), intermediate (75–115º), and oil-wet (115–180º). Weakly water-wet and oil-wet conditions can be also represented by (55–75º) and (115–135º), respectively.

Hjelmeland and Larondo (1986) studied the effect of pressure, temperature, and oil composition on the wettability of calcium carbonate rocks. At low temperatures (22.2°C), the solid phase exhibited oil-wet behavior, whereas at high temperatures (≥ 60°C), it produced water-wet behavior. Moreover, the rock surface suggested an intermediate state of wettability at 40°C. Calcium carbonate wettability, on the other hand, was not affected by the light fraction of the oil.

Contact angle at ambient condition decreased from 61° to 42° as increasing the salinity from 20 to 200K ppm (Saner *et al.* 1991). Yet under elevated temperature conditions, low salinity did not demonstrate any significant variation in the contact angle (32° versus 28°). Pressure was varied from 20 to 2,800 psi at constant temperature (70°C). Results clearly indicated that pressure did not affect the wettability.

Saudi Arabian carbonate reservoir wettability was evaluated and compared by Lichaa *et al.* (1992) using USBM, Amott, and contact angle techniques. Calcite, marble, and formation rocks were used in the receding contact angle measurements, as well as synthetic formation brine, seawater, and dead crude oil. A wide temperature range was examined in all experiments between 25 to 90°C. The test pressure was varied from ambient to 50 psi. Calcite surface tests became preferentially more water–wet at higher temperatures. Formation rock tests, on the other hand, showed an intermediate wettability or preferentially, slightly oil–wet at room temperature and became preferentially less oil–wet at higher temperatures.

Wang and Gupta (1995) investigated the influence of temperature and pressure on reservoir rocks wettability. They used stock-tank crude oil and reservoir brine from a carbonate reservoir. Contact angle of calcite system was not sensitive to pressure. Wettability of calcite surfaces changed toward weakly water-wet as temperature increased from 22 to 79°C. This change in wettability with temperature might due to changing the fluids chemistry at the interface.

The effect of salinity on the contact angle was investigated by Almehaideb *et al.* (2004). Limestone rock, crude oil, NaCl solutions were all used in their study. Four runs were examined using distilled water, 1,000, 10,000, and 50,000 ppm. All experiments were conducted at room temperature. A significant reduction of oil/water contact angle was observed at 10,000 ppm.

Wettability alteration of chalk rocks by sulphate containing water were determined by Yu *et al.* (2007). They reported contact angle measurements on both

calcite crystal and chalk slices at high temperatures (up to 130°C). Increasing the temperature up to 90°C changed the calcite crystal wettability toward water-wet due to the desorption of stearic acid from the calcite surface. The authors concluded a decrease in the contact angle after replacing distilled water with sulphate containing water. Similar study was conducted on vuggy limestone rock by Yang *et al.* (2008).

Hamouda and Karoussi (2008) measured the advancing and receding contact angles as a function of temperature for modified calcite surfaces with 0.005 M stearic acid dissolved in decane. Contact angle decreased with increasing the temperature; indicating that the calcite surface is becoming more water-wet at high temperatures. The authors stated that this phenomenon is based on the total interaction potential, which consists of van der Waals attractive and short-range Born repulsive and double layer electrostatic forces. The fluid/rock interaction was shown to be dominated by the repulsive forces above 80°C.

The objectives of this chapter are to:

1) Determine the salinity effect on the IFT of crude oil/water systems.
2) Study the wettability of carbonate rocks over a wide range of salinity using contact angle method.

All tests were conducted at high-temperature/high-pressure conditions (HTHP) using two different crude oil samples, calcite crystals, and outcrop limestone rocks.

Experimental Studies

Porous media

Calcite crystals and outcrop limestone samples were utilized for contact angle tests. Iceland spar calcite crystals were ordered from WARD's Natural Science in small specimens. The outcrop limestone sample (Laurda) was very tight and obtained from a quarry in Dallas, Texas, USA.

Fluids

Synthetic brines were used in this study: 230K ppm formation brine, 54K ppm seawater, 4K ppm aquifer water, and de–ionized water, **Table II-1**. In addition, IFT and contact angle tests were conducted using sweet (no H_2S) and sour stock tank crude oil samples. Crude oil A (sweet) was sampled all from one well in Alaska, USA. Its density was determined at high temperature (90ºC) which equal to 0.87 g/cm^3. The sour crude oil B was received from West Texas field, USA, and has a density of 0.79 g/cm^3 at 90ºC. Capillary viscometer was used to determine oil viscosity at ambient temperature. The viscosities of the sour and sweet crude oil were 3.35 and 7.2 cP, respectively. The two crude oil samples were filtered through 1 µm filter paper, and then re-filtered through a short core to remove solid particles that may cause plugging problems. The filtered oil was centrifuged afterward at high rpm to ensure no heavy residue was still present. The oil compositions were determined using GC/MS instrument, Appendix B.

Apparatus and procedure

Drop Shape Analysis System (DSA). The Pendant drop method is well known to determine interfacial property from the drop shape that generated inside a view chamber (Andreas *et al.* 1938). The results were subjected to fairly high errors due to analogous photographing images and an empirical evaluation method. Electronic data processing is developed lately to digitalize drop images and solve the theoretical equation of a drop profile. Drop Shape Analysis System (DSA) is a technique to determine liquid-fluid interfacial tensions and contact angles from the shape of axisymmetric menisci, i.e., from sessile as well as pendent drops (Li *et al.* 1992), **Figure IV-1**.

Contact angle. The application of 'Drop Shape Analysis' to sessile and captive drop contact angles requires the solid surface to be smooth and homogenous to ensure the drop is axisymmetric. The preparation procedure is described in appendix C. The angle between the baseline and the tangent at the drop boundary is measured using Young's equation.

A very important step before any experiment is a thorough cleaning of the apparatus, because trace amounts of contamination can alter the results. Flow line was cleaned several times with hexane. Acetone was then used to flush the lines. The line was dried afterward by flowing dry air and flushed with copious amounts of deionized water. The system was tested for leakage with deionized water before each experiment. The prepared rock substrate was placed inside the chamber with its holder. Brine solution was introduced into the cell until completely cover the rock substrate. Nitrogen gas was slowly injected into the brine to pressurize the system. Temperature controller

was then used to adjust the temperature manually to the set point (50, 90, and 130°C). The rock substrate usually equilibrated with brines for at least 20 h. Captive drop of crude oil was formed on the rock substrate surface. To an extent, the quality of the measurements relies very much on the skill of the experimentalist and the heterogeneity of the rock substrates.

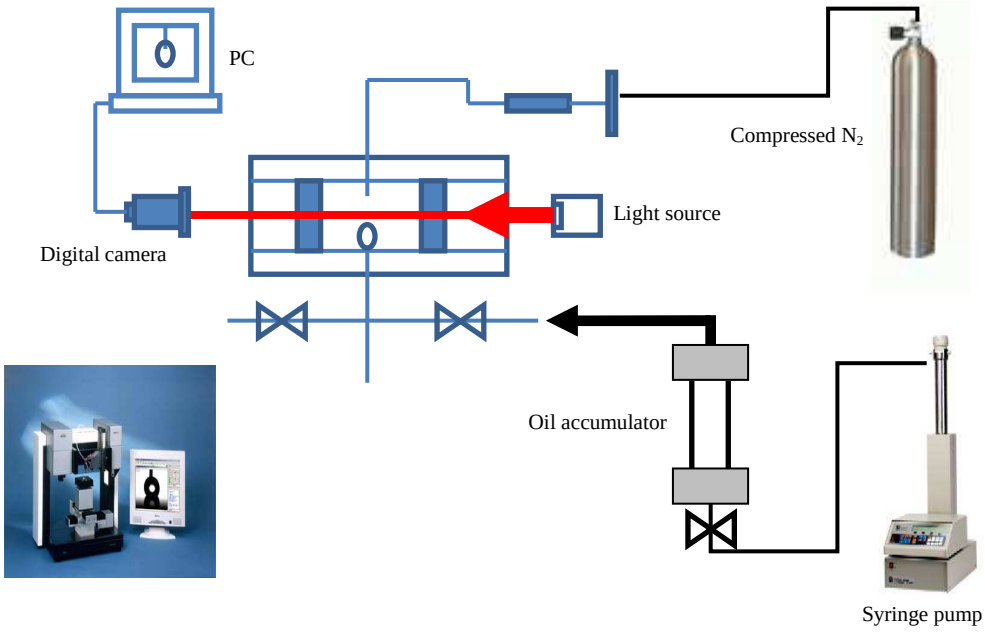

Figure IV-1. Axisymmetric Drop Shape Analysis Instrument.

Results and Discussion

Interfacial tension of sour crude oil

The interfacial tension of water/oil and oil/water systems was determined at HTHP conditions. In the first case, the brine droplet was injected from the top of the chamber to overcome the density difference. For that reason, the shape of the droplet was pendant, but in the second system it was more spherical since the oil droplet was injected from the bottom. Gravity plays a major role on the equatorial or maximum horizontal diameter as well as the drop shape factor.

$\gamma = \Delta\rho.g.R_0^2/\beta$ (Attension Company 1990).

where

γ = interfacial tension

$\Delta\rho$ = difference in density between fluids at interface

g = gravitational constant

R_0 = radius of drop curvature at apex

β = shape factor

In brine/oil system, a small glass cuvette was filled with crude oil and then pressurized using inert nitrogen (N_2) at 50°C. Few seawater droplets were released through 0.79 mm capillary to avoid any trapped air bubbles in the tubing. Seawater droplet was suspended in the oil phase up to 30 min.

Figure IV-2 shows the IFT behavior of seawater/crude oil as a function of pressure and time. The equilibrium IFT value was observed after approximately 15 min.

Results also suggest a direct relationship between IFT and pressure condition. Increasing the temperature to 90°C at 200 psi reduced the IFT from 23.0 to 16.3 mN/m.

The IFT of sour crude oil/formation brine decreased as increasing the temperature from 25 to 90°C, **Figure IV-3**. Moreover, a steep decrease in the IFT was noticed at the beginning of the ambient temperature test. This observation was not reported at high temperature condition because of the variation in the fluids' density and kinetic energy.

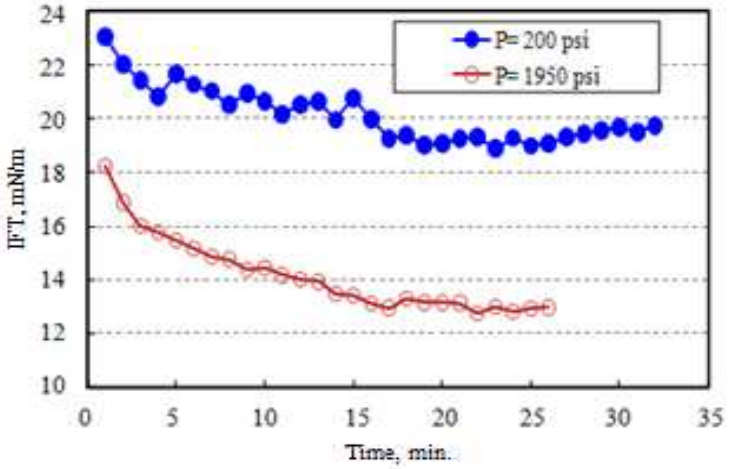

Figure IV-2. IFT of seawater droplet in sour crude oil as a function of pressure and time, (T= 50°C, time interval= 1 min.).

Figure IV-4 described the IFT of low salinity water with time at 90°C and 2,000 psi. Indeed, the IFT stabilized at 12 and 9 mN/m for DIW and aquifer water, respectively. This was an abnormal behavior because IFT is directly affected by the density difference. It could be also due to adsorption of the ions at the interface and their way of orientation. The required time to reach equilibrium in DIW was three times

higher than that of the aquifer water, **Figure IV-4**. In the literature, there was some cases where decreasing the salinity increased the oil/water interfacial tension (Xu *et al.* 2006).

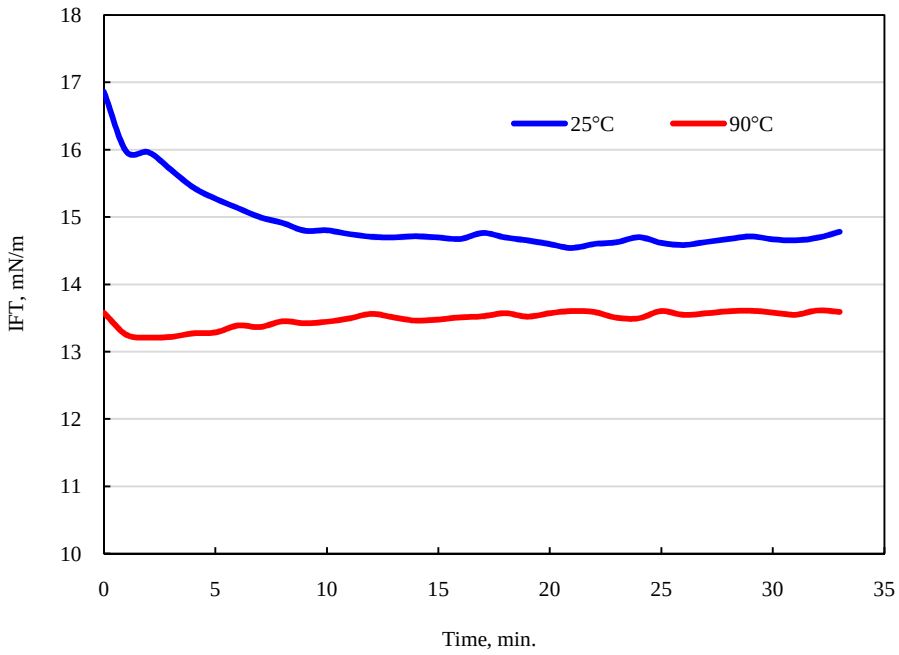

Figure IV-3. IFT of sour crude oil droplet in formation brine as a function of temperature and time, (P= 2,000 psi, time interval= 1 min.).

Interfacial tension of sweet crude oil

A wide salinity range was considered in this study including: formation brine, seawater, aquifer water, and deionized water, **Table II-1**. Moreover, the IFT tests were conducted at 90ºC and various pressures (500, 1,000, and 2,000 psi).

Contaminations from drilling fluids and oilfield chemicals in oil samples can mobilize to the oil/water interface and affect the IFT result. For that reason, the molecules at the interface should reach equilibrium to obtain the right IFT value. For

example, IFT of formation brine/oil system decreased at the beginning and then stabilized with time, **Figure IV-5**. The IFT behavior was almost independent on the pressure conditions.

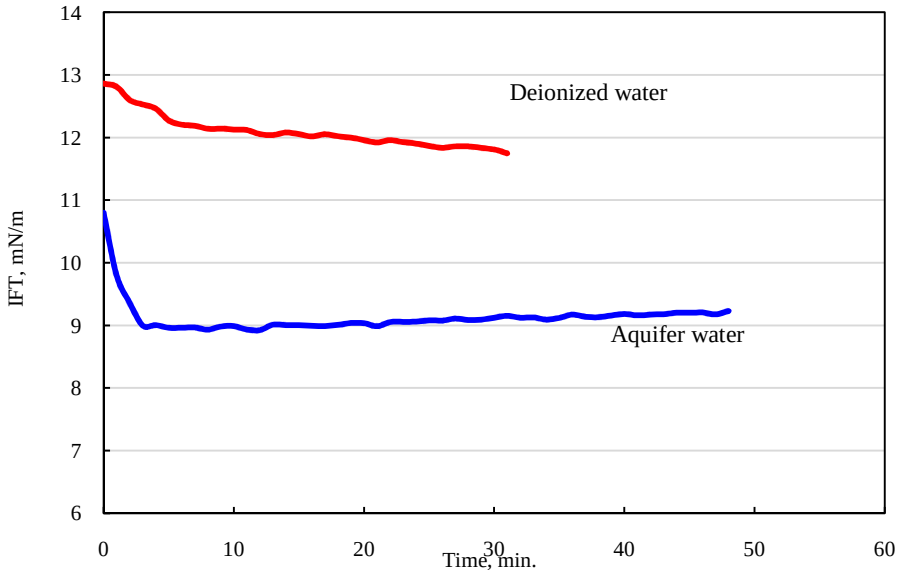

Figure IV-4. IFT of sour crude oil droplet in deionized water and aquifer water as a function of time, (P= 2000 psi, T= 90°C, time interval= 1 min.).

The highest salinity in this study (240K mg/L) increased the oil/water IFT by 12 units in comparison to DIW, **Figure IV-6**. On the other hand, aquifer and seawater produced comparable IFT results (~19 mN/m). Different crude oil composition apparently was affecting the interfacial properties at similar temperature, salinity, and pressure conditions.

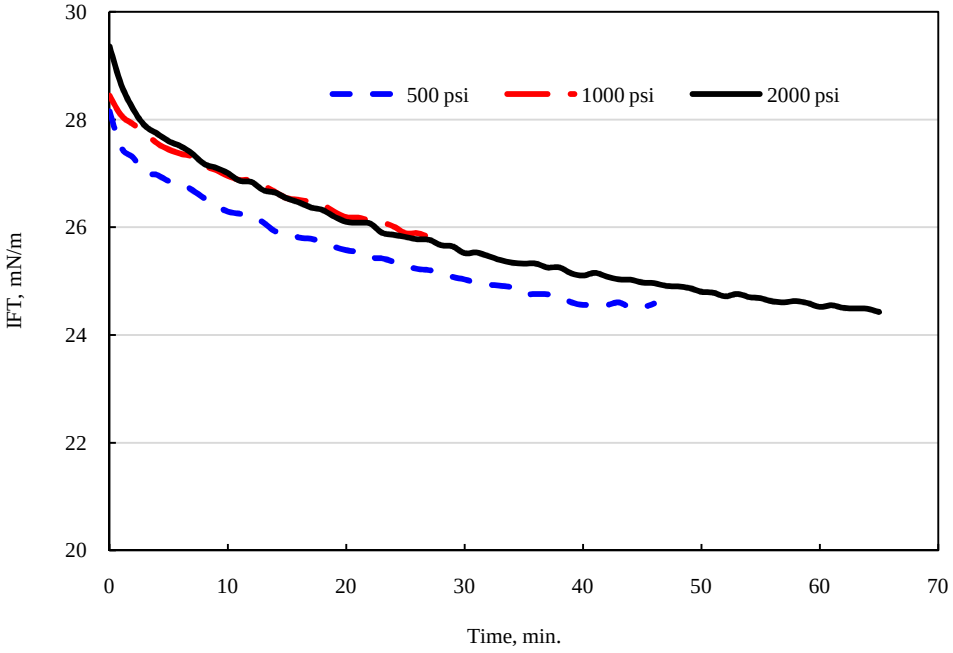

Figure IV-5. IFT of sour crude oil and formation brine as a function of pressure at 90ºC.

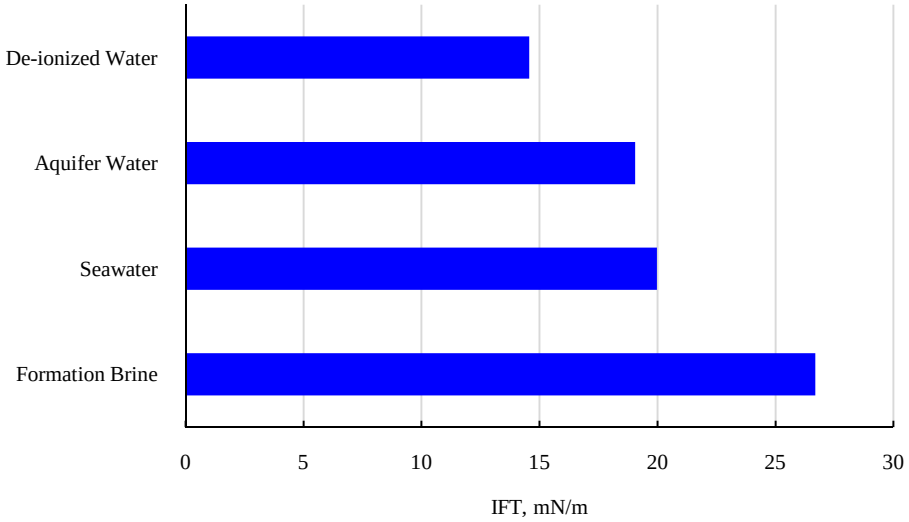

Figure IV-6. IFT of sweet crude oil as a function of salinity at 90ºC and 2000 psi.

Contact angle

Sour crude oil/calcite crystal. Rock substrates were soaked in formation brine at 50°C and 2000 psi overnight for equilibration. Contact angle, aging time, and fitting errors were recorded subsequently with time. In the first test, a fresh calcite model was used without any aging process. Formation brine (240K mg/L) at 50 and 90°C produced an intermediate-wet surface with contact angles less than 100°, Figure IV-7. To mimic the actual reservoir condition, crystal substrates were soaked in crude oil for 24 h at 90°C. Heavy end components in crude oil significantly affect reservoir wettability. The contact angle advanced as expected toward oil-wet condition. In general, the divalent cations in the connate water created more positive charges on calcite surface. These positive charges acted as attractive sites for the negative ends of polar components in crude oil (Xu et al. 2006). Such interaction mechanism explained the oil-wet characteristics of calcite surface with formation brine. The aging time was maintained constant at 24 h for all other tests.

Salinity effect on wettability. All conditions such as temperature, pressure and aging time were maintained identical except salinity. A wide salinity range was examined including: formation brine, seawater, aquifer water, deionized water, and three sodium sulfate solutions at different concentrations (3,560, 1780, and 890 mg/L), Table II-1.

Ions interactions at the oil/water/rock interface might affect wettability. The rock surface charge is definitely affected by the heavy components in crude oil. The optimum salinity, that changed the wettability condition toward more water-wet, was 1,780 mg/L

Na_2SO_4 and deionized water. Cations in the water film reacted with the sulfate anion, and hence the contact angle decreased below 50º. The calcite surface was negatively charged in presence of sulfate or hydroxide ions (Chapters II and III). This was attributed to different anions adsorption at the rock/water interface.

The salinity of the seawater is different from one place to another. Its concentration varied between 30 to 54K mg/L. Synthetic Gulf seawater at 54K mg/L was only used in this study along with formation brine and other electrolyte solutions. Wettability results indicate that seawater altered the calcite wettability to an intermediate-wet condition, **Figure IV-7**. There is a good match between contact angle and zeta potential result of calcite minerals (Chapter II). The positively rock surface charge in presence of seawater strongly attracted carboxylate groups in crude oil. Hence, the surface wettability would be expected to be either intermediate or oil-wet.

The contact angle of aquifer water/calcite/oil system was 72.5°. This was ascribed to the electrostatic interactions between aquifer water and calcite surface. Aquifer, sulfate solution, and deionized water changed the zeta potential of calcite surface toward negative. The electrostatic interactions were the main mechanism that reduced the contact angle results.

The calcite wettability in presence of seawater was examined at different pressures (2,000 to 500 psi), **Figure IV-8**. Decreasing the pressure slightly increased the contact angle without any significant effect on the surface wettability. For that reason, all upcoming tests were conducted at 2,000 psi.

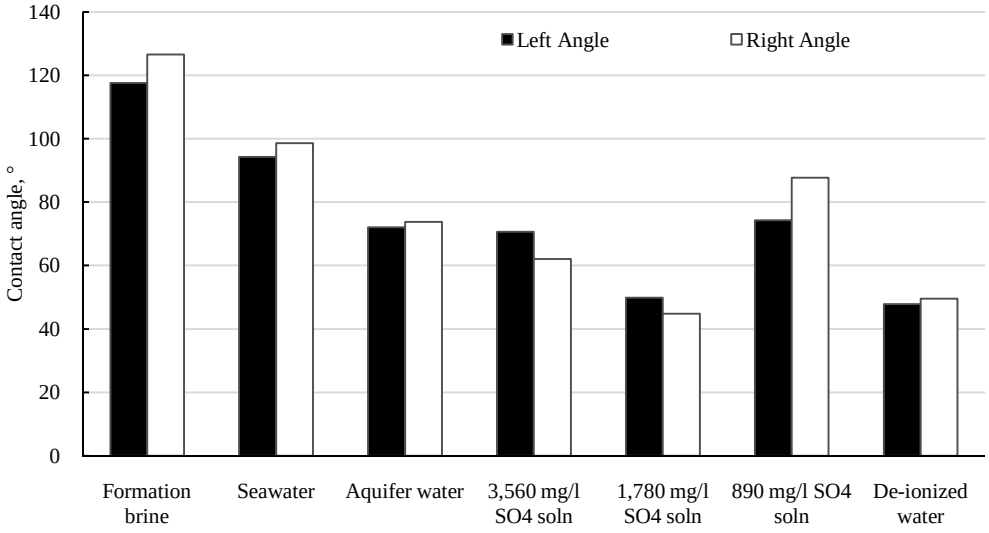

Figure IV-7. Contact angle of sour calcite/sour crude oil/water as a function of salinity at 90ºC and 2000 psi.

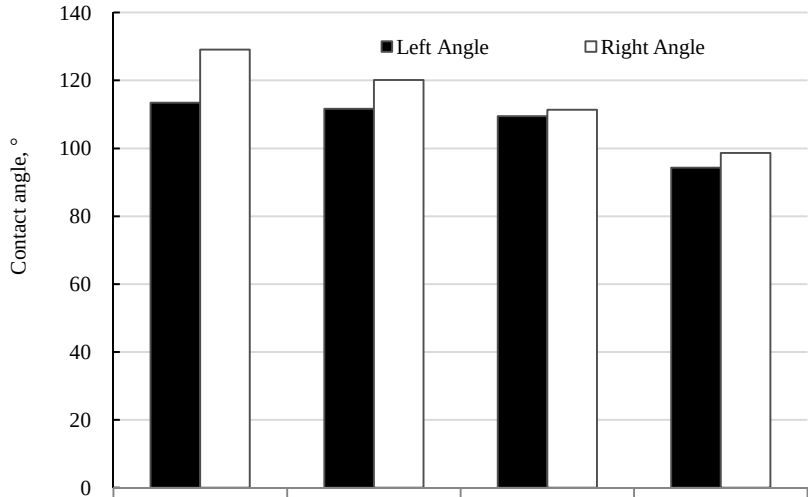

	500	1,000	1,500	2,000
Left Angle	113.4	111.6	109.5	94.3
Right Angle	129.1	120.1	111.4	98.6

Figure IV-8. Contact angle of calcite/sour crude oil/seawater system as a function of pressure at 90ºC.

To determine the role of temperature on fluids/rock interactions, series of tests were carried out at 50, 90, and 130°C, accordingly. Mixed results were obtained but

most of contact angle increased with increasing the temperatures from 50 to 90°C, **Figures IV-9 and IV-10**. Insignificant change on wettability was observed at 130°C. The effect of temperature was more pronounced at 90°C.

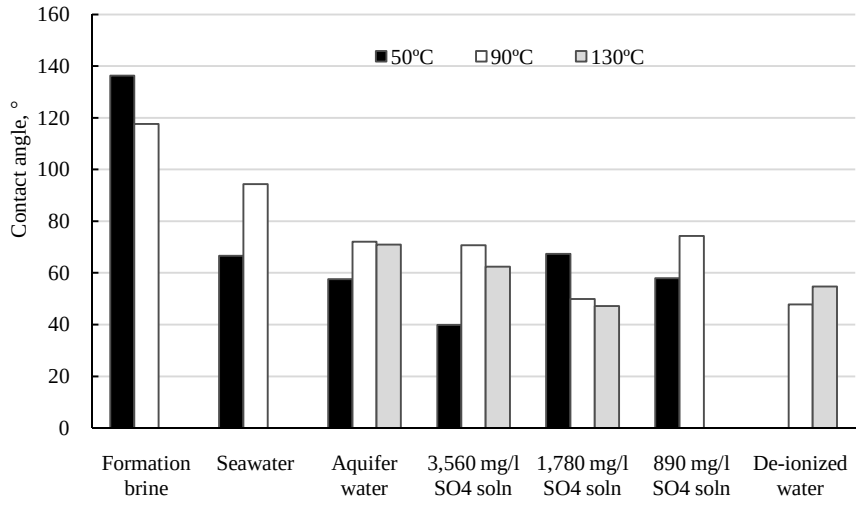

Figure IV-9. Left contact angle of calcite/sour crude oil/water as a function of temperature and salinity.

All in all, calcite wettability showed intermediate-wet surface in formation brine without aging. Divalent ions can form strong binding forces with the carboxylate group in the oil-phase. Hence, most carbonate reservoirs are at either intermediate or oil-wet condition. The effect of temperature on wettability was more significant at 90ºC. Sulfate solutions, aquifer water and DIW modified the rock wettability within water-wet state. The interaction mechanisms between calcite minerals and aqueous solution were through the anions adsorption at the interface. Appendix D shows crude oil/aqueous solution/calcite images at different conditions.

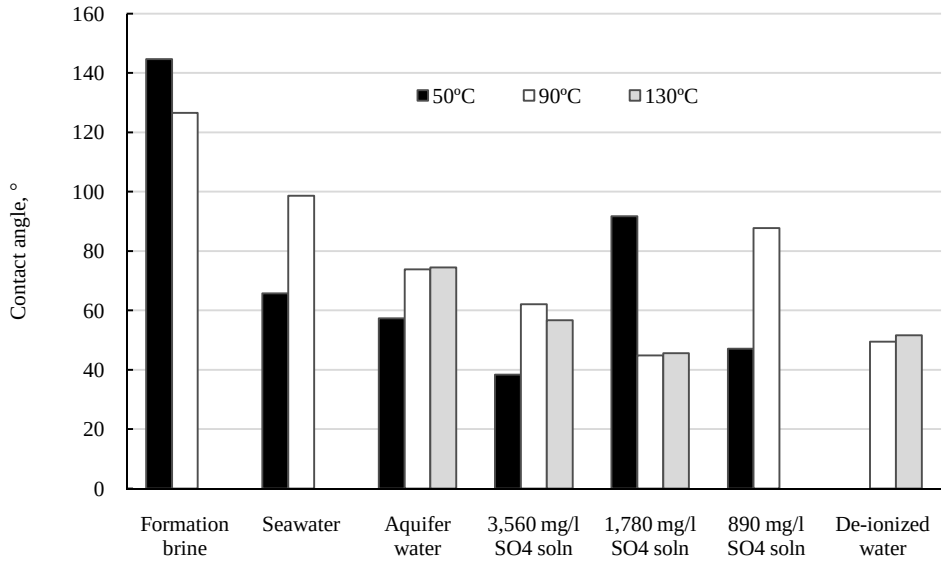

Figure IV-10. Right contact angle of calcite/sour crude oil/water as a function of temperature and salinity.

Sweet crude oil/calcite crystal. Oil components are playing a major role in the rock/brines interactions. Therefore, the main objective of the next tests was to determine the salinity impact on wettability behavior at 90°C and 2000 psi, but with different crude oil composition.

The contact angle results, in general, were within water-wet state, **Figure IV-11**. Seawater and DIW displayed a strong water-wet surface compared to the other fluids. Excluding divalent and monovalent ions showed negligible impact on wettability.

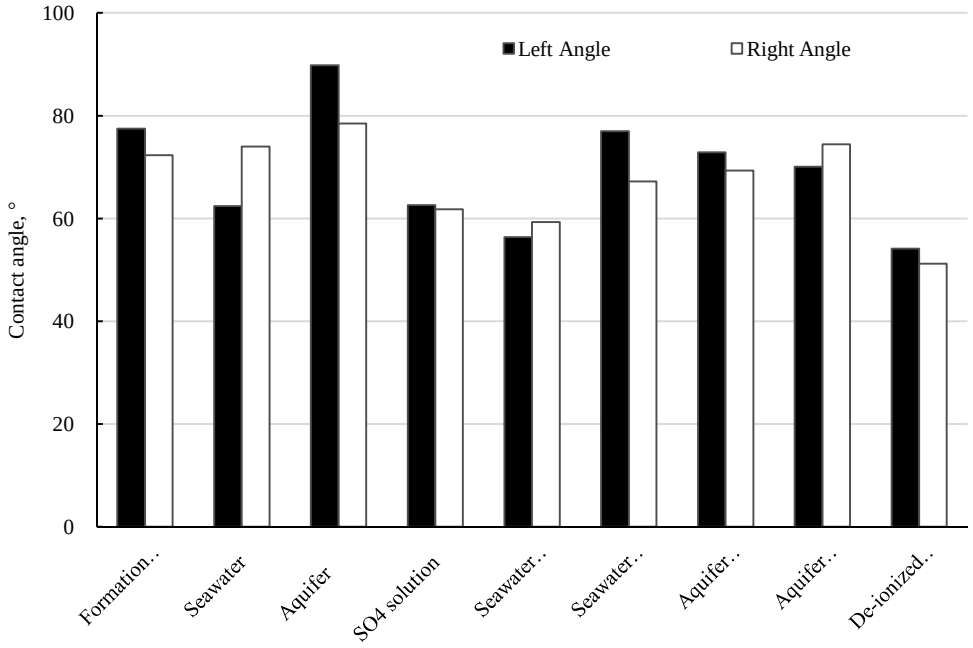

Figure IV-11. Contact angle of calcite/sweet crude oil/water as a function of salinity at 90°C and 2000 psi.

Sweet crude oil/limestone outcrop rock. Limestone outcrop rock was used for two reasons: 1) to mimic the actual reservoir rock, and 2) to determine the impact of minerals' impurities on surface wettability. The rock specimens were smoothed using various sizes of sand papers to minimize the roughness effect on wettability. The preparation procedures and the aging time for the outcrop and calcite specimens tests were similar.

The next major aqueous solutions were tested: formation brine, seawater, aquifer water, and DIW. In addition, the tests were conducted at 90°C and 2000 psi. The aqueous solutions, in general, showed contact angle results less than 90°, **Figure IV-12**. Formation brine has the highest concentrations of divalent ions, which is strongly linked

to the calcite surface and adsorbed carboxylate ions. Hence, the contact angle results was closer to intermediate-wet condition (>84º). Seawater, on the other hand, showed the lowest contact angle in compare to the other solutions. Likewise, aquifer water and DIW showed similar water wetting preference to the rock substrates.

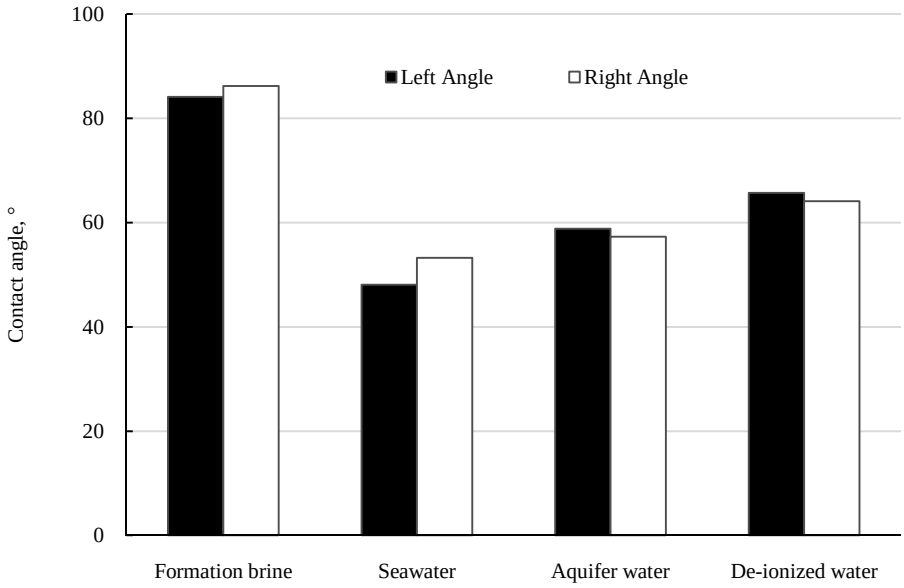

Figure IV-12. Contact angle of limestone/sweet crude oil/water as a function of salinity.

Conclusions

The effect of salinity on contact angles of calcite and limestone outcrop substrates was examined over a wide range of parameters (temperature, pressure, salinity, and oil composition). Based on the contact angle results, the following conclusions were drawn:

1. The oil composition and the temperature conditions are significantly affecting water/rock interactions and wettability states.

2. Formation brine and seawater changed calcite wettability toward intermediate-wet, only when sour crude oil was used. High divalent ions concentrations form strong bonds with the negatively charged carboxylate group in the crude oil.
3. Excluding mono and divalent ions from brine solution showed a negligible effect on contact angle results. This observation was reported for sweet crude oil tests.
4. Deionized water altered calcite wettability toward water-wet because of the hydroxide ions adsorption at the rock surface.
5. The effect of pressure on wettability was not significant.

CHAPTER V

IMPACT OF SALINITY AND DILUTE SURFACTANT ON CARBONATE WETTABILITY

Summary

Different trends in oil recovery are often observed in clastic versus calcareous reservoirs. These different trends are attributed to the different mechanisms of ion interactions, wettability conditions and rock heterogeneity such as fractures and vugs in carbonate reservoirs. Injection of low salinity water in clastic reservoirs results in significant reductions in residual oil saturation due to ion interactions with the clay minerals. Also dilute surfactant technology has been shown to enhance oil recovery by minimizing interfacial tension to ultra-low values (10^{-3} mN/m). The aqueous solution/rock/crude oil interactions in terms of surface chemistry and wettability need further investigation, especially in harsh salinity environments and high temperature/high pressure (HTHP) conditions. The emphasis in the current study is with carbonate minerals.

Salinity and dilute surfactant technology were thoroughly investigated at 90ºC and 500 psi using an advanced macroscopic wettability technique. Synthetic formation brine, seawater, deionized water, crude oil, and a new class of amphoteric surfactant were used in contact angle tests. To minimize hysteresis issues in the porous rocks, the tests were carried out on calcite (Iceland spar) specimens. Aqueous aliquots were collected after every stage of salinity adjustment using the same specimen and were analyzed for dissolved Ca, Mg, and sulfate concentrations.

Hydration and dehydration processes through decreasing and increasing salinity showed no impact on calcite wettability. The attraction of ions with calcite was either by ion exchange or surface complex formation. However, these forces were not strong enough to alter the surface wettability condition upon change of salinity. This conclusion was confirmed in various tests using high salinity formation brine and seawater as original solutions. Dilute surfactant altered rock wettability towards an oil-wet condition. The spreading of the crude oil droplet on the calcite surface was due to the van der Waals attraction forces between the oil and either the calcite surface or the hydrophobic parts of the surfactant tails. Results from this study provide new insights on the influence of salinity and dilute amphoteric surfactant on surface chemistry and wettability.

Introduction

Most carbonate reservoirs are classified as either oil or intermediate wet (Chilingarian and Yen 1983; Plank and Bassioni 2007). The exact condition depends heavily on salinity and crude oil properties such as carboxylate concentration and asphaltene/resin fractions. Pendular rings of water film around the rock are commonly believed to affect fluid/rock interactions (Salathiel 1973; Dawe and Egbogah 1978; Francisca *et al.* 2003). The water film thickness is reported to be 100 nm or less, and is considered to be dependent on salinity and diffuse double layer interactions and stability (Kaminsky and Radke 1997). But there is uncertainty about the water film presence, as some researchers have reported a rupture of the water film followed by direct deposition of asphaltenic material at the rock surface (Fogden 2009).

Interfacial tension (IFT) of crude oil with either high or low salinity water usually ranges from 10 to 40 mN/m. Fluid density and impurities in crude oil from drilling or chemical treatments can influence IFT results (Hirasaki and Zhang 2003). Salinity can slightly influence interfacial properties, but it is still unlikely to overcome the capillary forces that control carbonate wettability (Chapter IV). The situation and mechanisms in sandstone reservoirs are different and thoroughly investigated by other researchers (Lebedeca *et al.* 2009; Alagic and Skauge 2010). The addition of a surface active agent to the injection water is necessary to reduce the IFT to ultra-low values ($<10^{-3}$ mN/m). However, surfactant solutions do not always have a positive impact on wettability (Pope and Bavière 1991). Surfactant adsorption and orientation on the rock surface complicate the interaction mechanisms. In addition to temperature, high divalent ion concentrations are considered the most challenging issue in enhanced oil recovery (EOR) (Zhang *et al.* 2006; Hirasaki *et al.* 2008).

Contact angle or Amott cell techniques are often applied for wettability studies. In the current work, the contact angle technique was modified to inject and collect aqueous samples at high temperature, high pressure (HTHP) conditions. Contact angles are usually determined on macroscopic, smooth, nonporous, and planar substrates (Kwok and Neumann 1999).

The objectives of this study were to: 1) determine the impact of salinity on the wettability of calcite crystals at 90ºC and 500 psi, and 2) investigate the effect of an amphoteric surfactant at various concentrations (0.01 to 0.1 wt%) on calcite wettability. This study is different from other work in the literature because the salinity and

surfactant concentrations were adjusted on the same calcite substrate at HTHP conditions. The salinity was gradually increased or decreased with time, and contact angles were subsequently determined at almost identical temperatures and on the same calcite surface.

Ion interactions

The adsorption of surface-active agents at solid/liquid interfaces is controlled by the nature of the hydrophilic and hydrophobic groups and the characteristics of the solid surface. The surfactant adsorption can be due to either the specific chemical interactions or the electrostatic bonding.

The main parameters to be considered for enhanced oil recovery by surfactant flooding are: 1) interfacial tension, 2) interfacial viscosity, 3) interfacial charge, and 4) contact angle (Bansal and Shah 1978). Interfacial tension for different surfactants has been extensively studied at ambient and high temperature conditions (Aoudia *et al.* 2010a). IFT of crude oil/water systems should be decreased to ultra-low values to enhance oil recovery. The solution viscosity is only slightly affected by the surfactant because the required concentration to achieve the IFT target is usually low. The nature of the surfactant head group (e.g., anionic, cationic, or amphoteric) plays a key role in the electrostatic and adsorption interactions. Generation of ultra-low IFT is often important, but will not by itself ensure success (Hammond and Unsal 2009).

Mohanty *et al.* studied different anionic surfactants (aryl-alkyl sulfonates and propoxylated sulfates) at a concentration of 0.05 wt% using the contact angle technique

(Seethepalli *et al.* 2004; Gupta and Mohanty 2008). They found that some surfactants were able to alter the rock wettability from oil to intermediate-wet condition. Only the sulfonates surfactants changed the wettability towards a water-wet state.

Hirasaki and Zhang (2003) evaluated different anionic sulfate surfactants in the presence of alkali sodium carbonate. The surfactant systems altered calcite wettability towards intermediate and water-wet conditions as a result of the IFT reduction. The authors correlated detachment of the crude oil droplet with the bond number ($N_B = \Delta\rho g L^2/\gamma$), which is normally used to account for the influence of gravity in vertical flow regimes.

Interaction mechanisms of anionic and cationic surfactants with crude oil are completely different. Cationic surfactants can form ion pairs between the cationic head group and the negatively charged carboxylate groups of the crude oil. Anionic surfactant molecules can form complexes with surface-structural or adsorbed Ca^{2+} on the rock surface. Ion-pair or surface-complex interactions are believed to be much stronger than hydrophobic interactions (Milter and Austad 1996; Austad *et al.* 1998; Standnes and Austad 2000; Salehi *et al.* 2008; Hammond and Unsal 2011).

Specific and nonspecific adsorption

Specific adsorption of anions can involve either inner-sphere adsorption, i.e., direct coordination to surface structural cations, or outer-sphere complexation via a water bridge. Specifically adsorbed anions might include the conjugate bases of weak acids, e.g., carbonate, phosphate and organic anions, or those of strong acids, e.g., sulfate.

Specific adsorption might also be impacted by short-range electrostatic interactions, especially hydrogen bonding, as is often the case with outer-sphere complexation (Mott 1981).

Nonspecific anionic interactions are physical and are totally impacted by the charge of the interacting species, in which each maintains its electronic configuration, as opposed to specific chemical interactions in which there is some redistribution of electrons as a result of the interaction. Nonspecific anionic interactions include repulsion (negative adsorption) and electrostatic attraction of anions to positively charged sites. Various factors impact anion repulsion, including 1) ionic strength, 2) anion charge, 3) species of counter-ion (cation), 4) pH, 5) the presence and speciation of competing anions, and 6) the characteristics and charge of the colloid surface (Parfitt 1978). Anion repulsion generally increases with any increase in anion or surface negative charge or both, which can each be influenced by pH. Anion repulsion also increases with increasing negative charge character of the colloid that is caused by the specific adsorption of anions (Hingston *et al.* 1967).

Nonspecific and specific surface adsorption reactions might occur in carbonate reservoirs. The interaction is also influenced by diffusion processes and reaction kinetics, van der Waals attractions, and the steric availability of charged sites for the reaction. Ions have higher energy at high temperature, which therefore affects ion transport, reaction kinetics, and the achievement of equilibrium.

Experimental Studies

Materials

Calcite rhombohedral crystals (Iceland spar) were obtained from Ward's Natural Science Company **(**Rochester**,** New York, USA**)**. Synthetic formation brine and seawater were prepared according to their compositions in **Table II-1**. More information about the sweet crude oil and brine systems were reported in Chapter III. Aqueous formation brine, seawater and deionized water were only used in this chapter.

A new class of amphoteric surfactant I (alkyl dimethyl betaine) was supplied by Oil Chem Company (Houston, TX, USA) and used at concentrations of 0.1 wt% (Berger and Berger 2009). The surfactant preparation also includes a short chain polymer (lignin) that is added to the surfactant by the manufacturer to reduce the adsorption on carbonate rock. The molecular weight range for this surfactant family was 300-500 g/mol. The screening test results for this surfactant are described in Chapter VIII along with coreflood studies.

Apparatus and procedure

Drop Shape Analysis System (DSA). This instrument was similar to the DSA system in Chapter IV, but was slightly modified to inject crude oil and aqueous solution simultaenously. This instrument was manufactured by KRÜSS GmbH Company (Hamburg, Germany) under model number PA3210, **Figure V-1**.

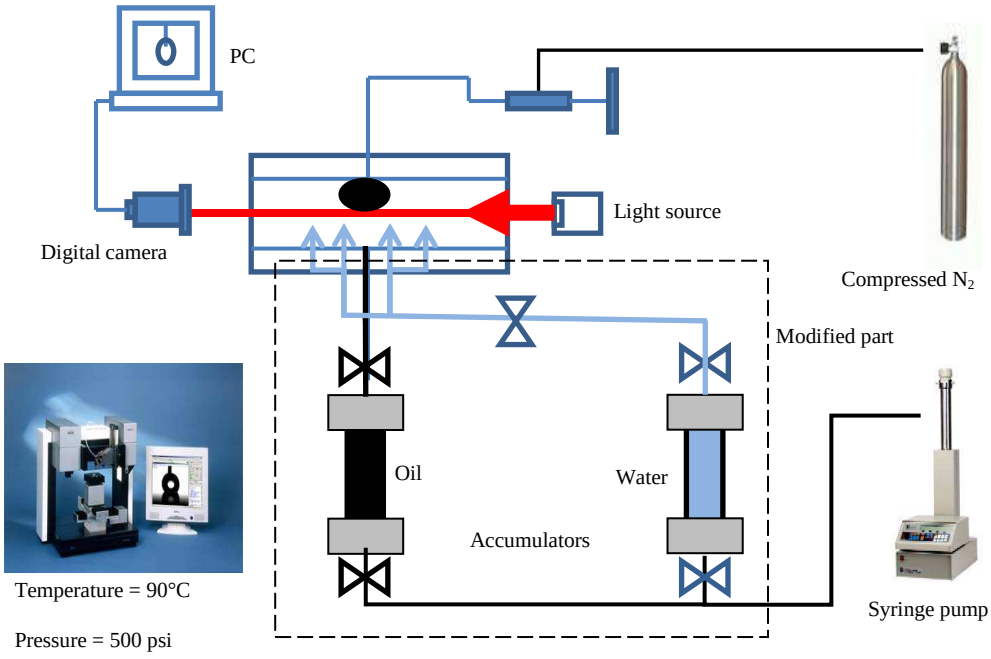

Figure V-1. Axisymmetric drop shape analysis instrument and fluid accumulators which were connected to a syringe pump.

Procedure. A diamond saw was used to cut calcite crystals into approximately 1.6x1.8x0.6 cm mineral fragments. Samples were soaked in deionized water for a few minutes and then dried in an oven at 100ºC for 24 h. A fresh calcite sample was used for each contact angle test. The sample was loaded in the rock holder and aligned properly with the camera source. The chamber was then filled with the brine solution (~22 cm^3) through 0.317 cm tubing. The temperature and pressure conditions were set at 90ºC and 500-1000 psi, respectively.

Crude oil droplets were pumped gently through 0.158 cm capillary tubing and attached to the calcite surface. The DSA software was activated to capture images and

analyze contact angle using the Young-Laplace equation. Aqueous samples (2-3 cm^3) were frequently collected from the chamber through 0.317 cm tubing for two reasons: 1) to measure dissolved Ca, Mg, and sulfate concentrations, and 2) to make room for the new injection fluid above the calcite surface. In addition, 2-3 cm^3 of solution were injected in every stage through a three-way ball valve. As a result, the pressure in the chamber was slightly disturbed, though it did not affect the contact angle results.

Results and Discussion

Formation brine/calcite/crude oil

The calcite surface in the presence of formation brine was oil-wet, **Figure V-2** (Anderson 1986), with contact angles between 140 and 142° during the 10 h contact time. The surface charge of calcite is reported to be positive because of the high Ca^{2+} concentration in the formation brine (Somasundaran and Agar 1967; Siffert and Fimbel 1984; Pierre *et al.* 1990). Due to the attraction forces between the carboxylic groups in crude oil and the Ca^{2+}, wettability of the calcite was either intermediate or oil-wet (Schramm *et al.* 1991; Schramm 2000). Slight fluctuations at the left and right sides, < 2º, were noticed, but that change is considered to be insignificant.

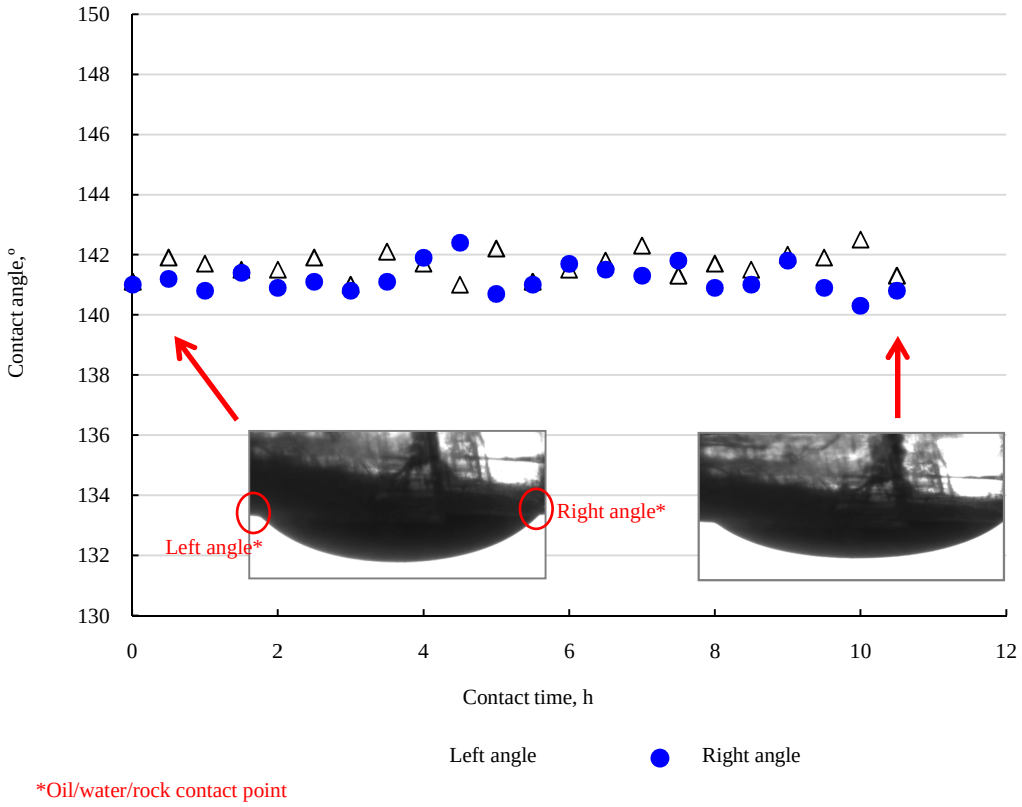

Figure V-2. Contact angle results and images of calcite/formation brine/crude oil system following crude oil injection, (T= 90ºC, P= 500 psi).

Seven stages of deionized water were subsequently injected during 67 h, and aliquots were collected accordingly as shown in **Figure V-3**. The diffusion of water and any change in hydration state of the calcite surface in this system were apparently very slow processes, and the calcite wettability remained oil-wet even after 67 h of interaction (Francisca *et al.* 2003). Calcite wettability was oil-wet in the presence of formation brine and even after seven dilution steps. In addition to the water molecules, interactions between divalent cations and anions with calcite minerals are very complex.

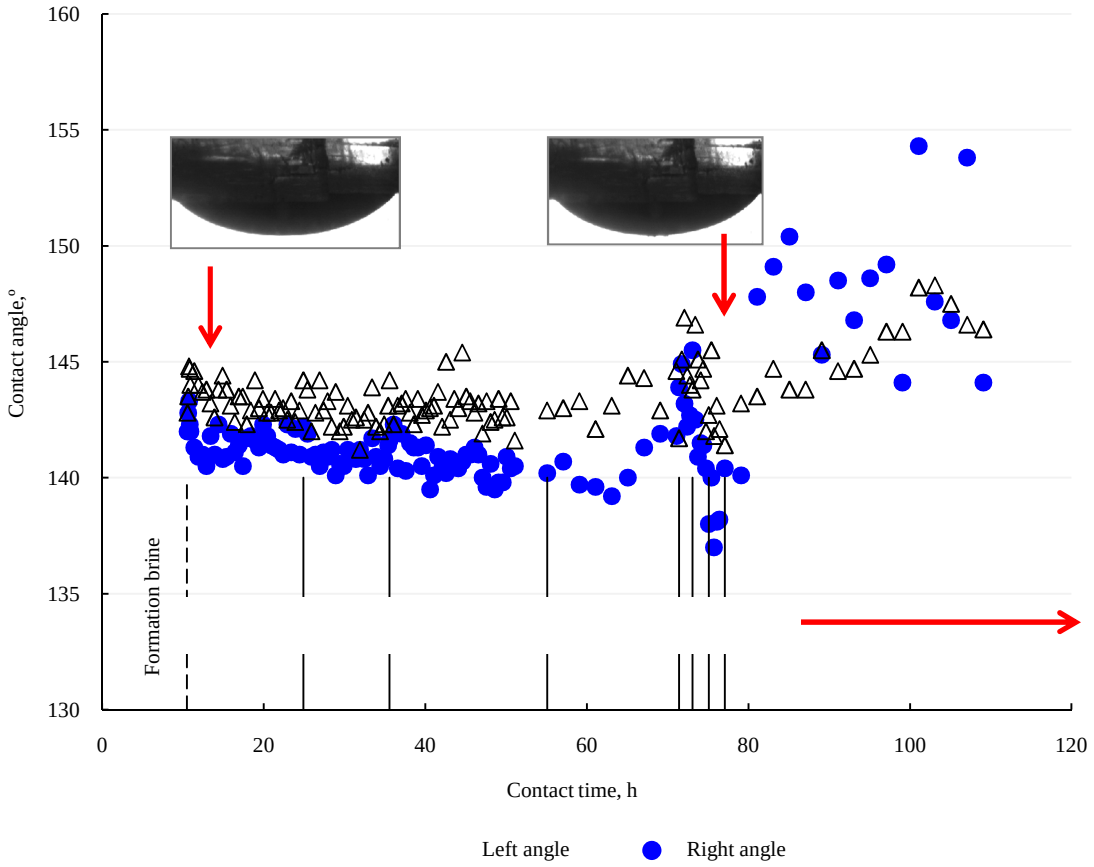

* The dashed line indicates the start of deionized water injection, while the solid lines indicates the individual stages of deionized water injection to decrease the electrolyte concentrations.

Figure V-3. Contact angle results and images of the calcite/formation brine and deionized water/crude oil system following crude oil injection (T= 90ºC, P= 500 psi).

To determine the effect of dissolved sulfate concentration on contact angle, four stages of 0.5 wt% Na_2SO_4 were subsequently injected into the brine solution, and aqueous samples were collected accordingly **(Figure V-4)**. Contact angle and wettability were not affected by sulfate concentration during the 37 h of contact time with Na_2SO_4. The contact angle was slightly different at the left versus the right side of the oil droplet,

possibly due to fluid dynamics during the injection process. The potential determining ions for calcite are Ca^{2+}, CO_3^{2-}, H^+ and OH^- (Madsen 2006). Sulfate is generally considered to impact neither the surface potential nor the surface charge of calcite and does not affect divalent ion exchange at calcite surfaces (Möller and Werr 1972). The negligible impact of dissolved sulfate concentration on contact angle and surface wettability in the current study, further substantiates the negligible role of sulfate on the surface hydration properties of calcite.

In final stage of the Na_2SO_4 injection sequence, sulfate concentration was increased to 5 wt%. As a result, $CaSO_4$ precipitated (likely as gypsum, $CaSO_4 \cdot 2H_2O$), due to the presence of Ca in the solution **(Figure V-4)**. The solubility product constant of the $CaSO_4$, mineral phase was exceeded, and the test was discontinued for that reason. The $CaSO_4$ scale tendency was confirmed by using OLI simulation software (OLI Systems Incorporated 2011a) for electrolyte solutions. The scale tendencies (OLI Systems Incorporated 2011b) before and after the addition of 5 wt% Na_2SO_4 solution to the formation brine were 0.2 and 38, respectively.

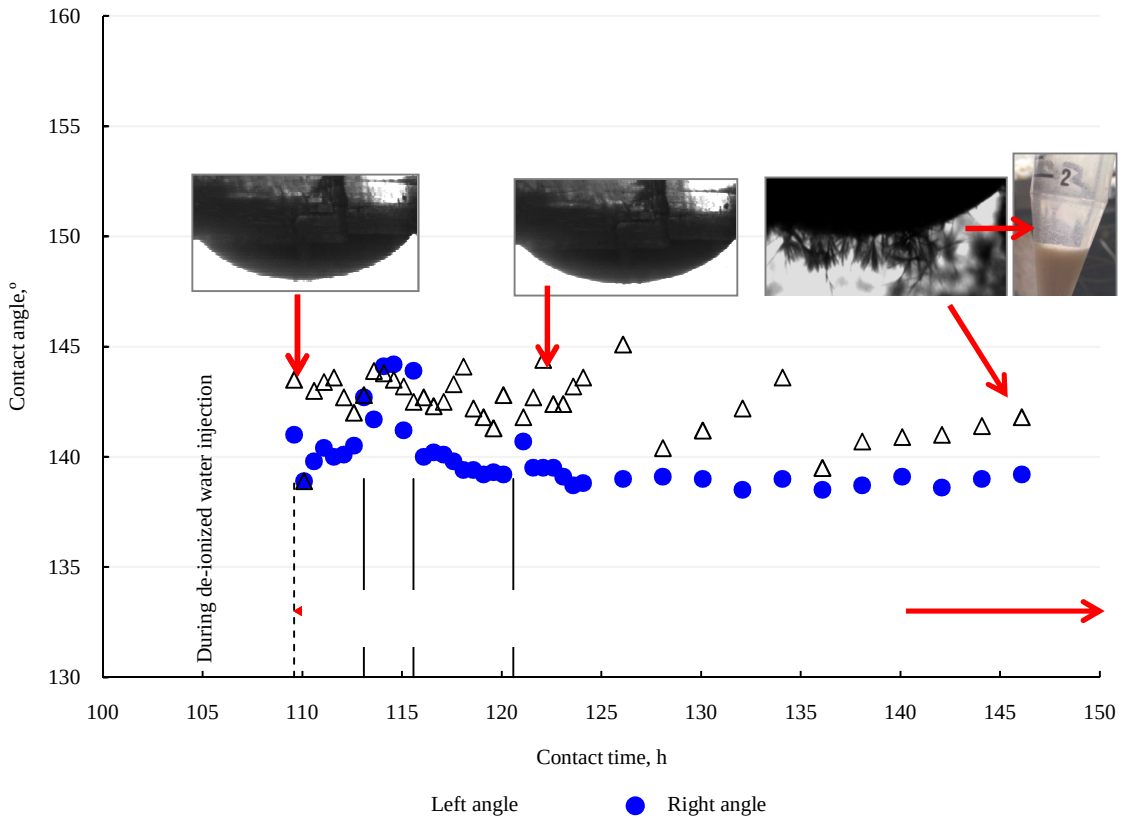

Figure V-4. Contact angle results and images of calcite/ mixed brines and 0.5wt% Na_2SO_4/crude oil following crude oil injection at 90ºC and P= 500 psi.

Dissolved elemental concentrations in the original and collected samples from the chamber are summarized in **Figure V-5**. Ca, Mg, and sulfate concentrations at the end of the deionized water injection stage were 9523, 1294, and 32 mg/L, respectively. The sulfate concentration in the aqueous phase was 10,833 mg/L after injecting 5 wt% Na_2SO_4, indicating that the formation brine in the chamber was diluted three times without any noticeable effect on wettability.

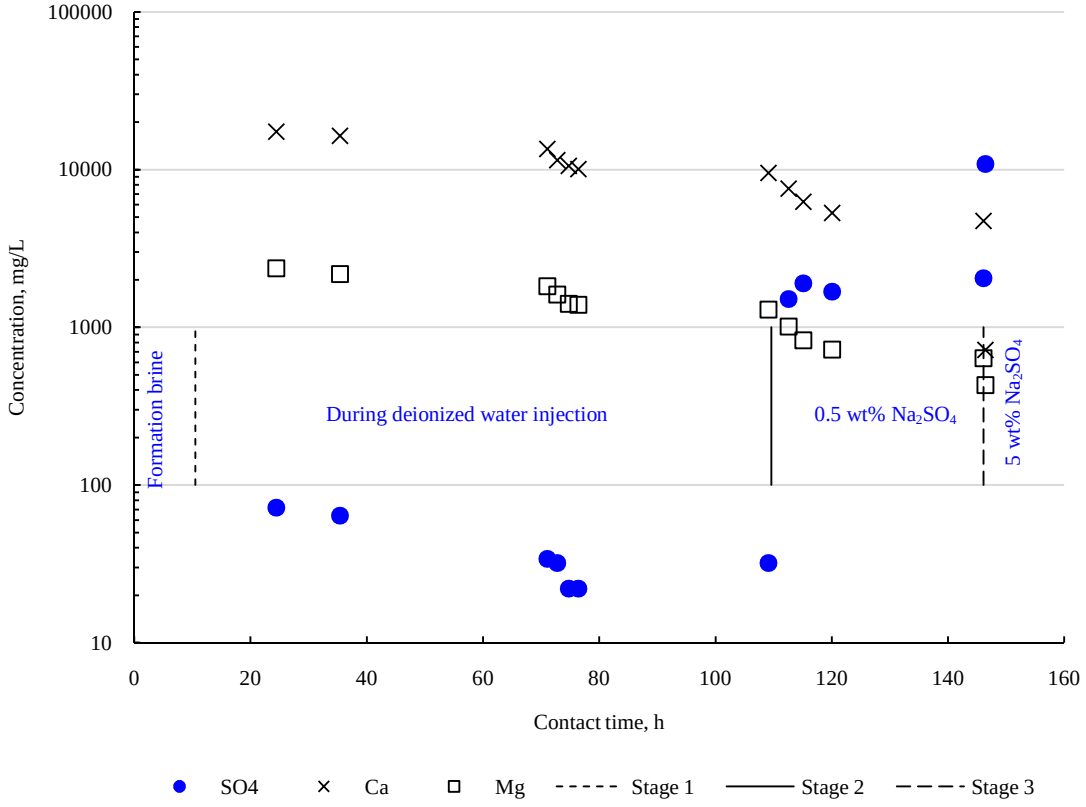

Figure V-5. Ion concentrations of the calcite/formation brine, deionized water, Na_2SO_4/crude oil system at 90ºC and P= 500 psi.

Deionized water/calcite/crude oil

The chamber cell was filled at the beginning with deionized water. Then, the calcite surface was partially dehydrated by injecting formation brine in successive stages. The crude oil/water interface is negatively charged because of the carboxylate groups (Marinova *et al.* 1996; Franks *et al.* 2005). The surface potential of calcite in the presence of deionized water has been reported to be negative (Cicerone *et al.* 1992), thus

resulting in repulsion of carboxyl groups of the crude oil and contributing to an intermediate-wet calcite surface **(Figure V-6)**. In deionized water and various NaCl solutions, OH^- ion interaction with Ca^{2+} at the calcite surface was reported to be greater than that of H^+ with CO_3^{2-} (Eriksson *et al.* 2007). This phenomenon was also observed on Ca^{2+}-rich positively charged surfaces and was confirmed by zeta potential measurements (Eriksson *et al.* 2007).

a. After 30 sec b. After 8 h

Figure V-6. Calcite/deionized water/crude oil system at 90ºC and 1000 psi.

Formation brine was injected in 8 separate stages over 24 h, while recording the contact angle **(Figure V-7)**. An intermediate-wet condition was observed because the partial hydration of the calcite surface had no effect on wettability. This result confirms that neither increase nor decrease the water salinity due to change in brine concentration impacted calcite wettability. The original water film composition on the calcite apparently played a key role in determining the surface wettability.

The 0.1 wt% surfactant was prepared in deionized water instead of seawater to avoid $CaSO_4$ precipitation. The amphoteric betaine carries both a constant positive

charge and a pH dependent negative charge, hence net charge is pH dependent (Domingo 1996). The contact angle decreased slightly at very low surfactant concentration (~0.01 wt%). The second injection stage of surfactant surprisingly altered calcite wettability to oil-wet **(Figure V-8)**. The oil droplet then flowed over the calcite surface after 10 min. of contact time. pH measurements were not conducted due to the limitation of the sample volume; however, the pH of the solution in the chamber was expected to be more than 7 based on that of the original brine.

Surfactant adsorption depends on many factors including the charge properties of the surfactant and the solid surface, the pH of the system, and the structure of the surfactant (Schramm 2000; Schramm and Kutay 2000). The betaine surfactants are zwitterionic at pH values at and above their isoelectric points (neutral and alkaline pH), and cationic below their isoelectric points (acid pH). Such amphoteric surfactants show no net anionic properties (Rosen 1978). The spread of the crude oil droplet on the calcite surface was likely due to van der Waals attraction forces between the hydrophobic tails of the calcite-adsorbed surfactant and the crude oil. Further discussion of the expected reaction mechanisms is presented for the next test.

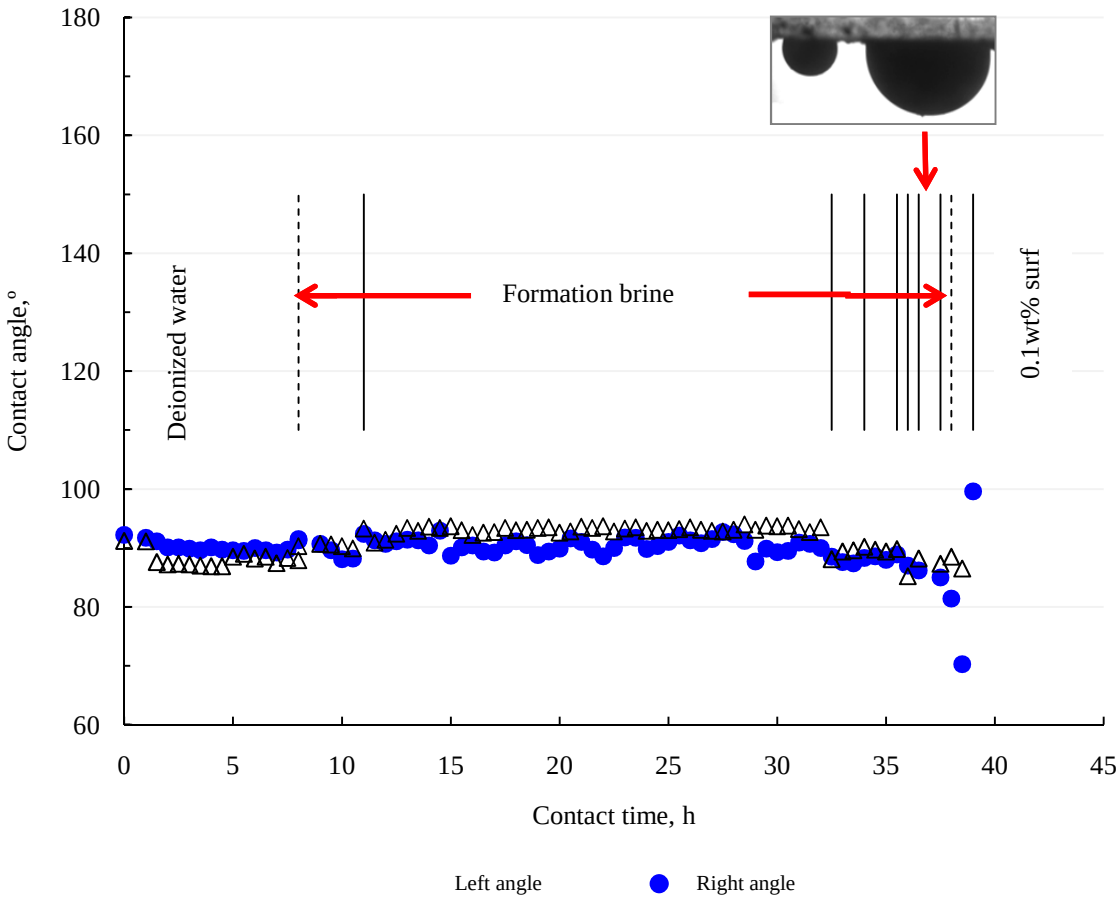

Figure V-7. Contact angle of calcite/mixed brines and 0.1wt% Surfactant/crude oil following crude oil injection at 90ºC and 1000 psi.

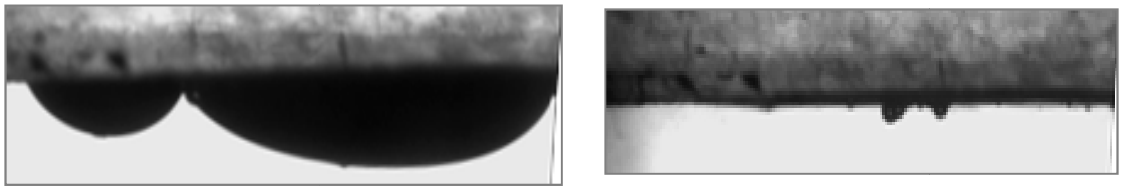

a. After 5 min. b. After 10 min.

Figure V-8. Calcite/mixed brine and 0.1 wt% betaine surfactant solution/crude oil at 90ºC and 1000 psi.

The adsorption behavior of amphoteric surfactant on the calcite surface is quite complicated (Mannhardt *et al.* 1992). Divalent cations in formation brine or at the calcite mineral surface can form complexes with the carboxylate group in the surfactant (Mannhardt *et al.* 1992). In the current study, with increasing surfactant concentration there was an apparent decrease in IFT at the crude oil/formation brine interface. Hence, the oil droplets detached from the rock surface due to gravity segregation and buoyancy effects (Hirasaki and Zhang 2003). Decreased the interfacial tension also results in increased electrophoretic mobility of the oil droplets, as has been observed in various surfactant systems (Shah *et al.* 1977; Bansal and Shah 1978; Yunan *et al.* 1995).

The chemistry of the solution in the chamber at various injection stages is summarized in **Figure V- 9**. The calcite surface was partially hydrated at the beginning. Upon addition of brine the surface hydration of the calcite was likely altered; however, no impact on water quality was apparent. After the third stage of brine injection, the system was equilibrated for more than 20 h, because the chemical interactions were expected to be slow. The extended equilibration with brine did not impact the surface wettability, which remained at an intermediate-wet condition. The dissolved salt concentration almost matched that of the formation water after 37.5 h. Thereafter, it decreased due to the injection of surfactant solution that was originally prepared in deionized water.

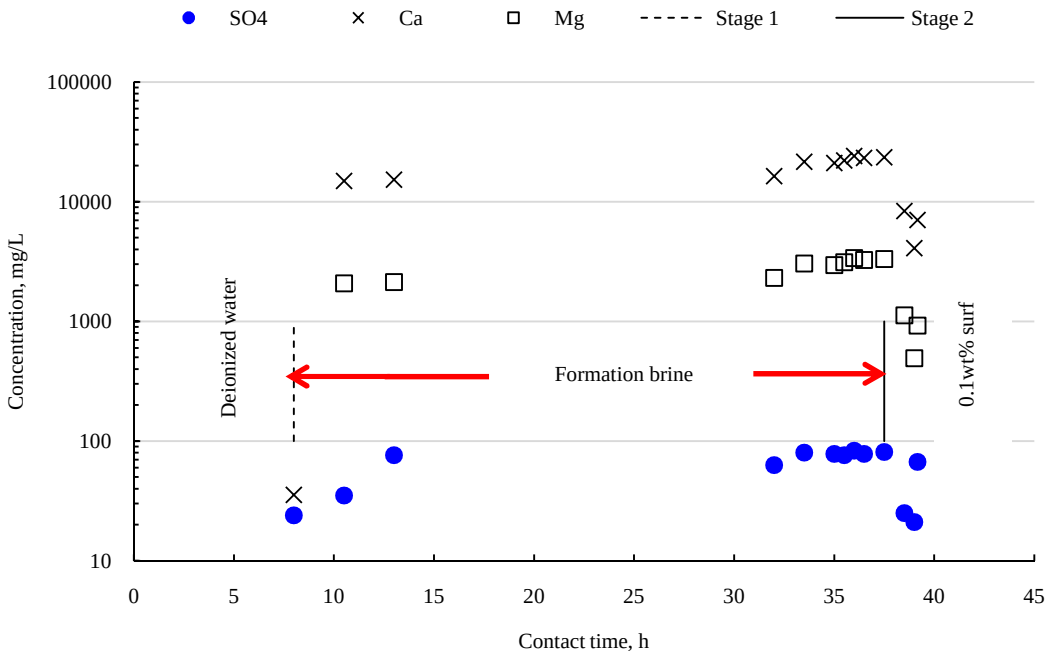

Figure V-9. Ion concentrations of the calcite/deionized water, formation water, 0.1wt% surfactant/crude oil system at 90ºC and 1000 psi.

Seawater/calcite/crude oil

Sulfate concentration in seawater is often higher in comparison with formation brine or shallow aquifer water **(Table II-1)**. It has been suggested that seawater might decrease residual oil saturation due to the interactions between sulfate ions and carbonate minerals (Zhang *et al.* 2007). In the current study, seawater was diluted several times with deionized water to evaluate a possible effect of dilution on wettability.

Seawater produced a water-wet calcite surface, as depicted in **Figure V-10**. The contact angle changed slightly between 60 and 48º during 7 h of contact time. Ten stages of deionized water were sequentially injected into the chamber. The hydration processes slightly increased the contact angle, but the calcite surface was still in a water-wet

condition. The hydroxide ion might adsorb at Ca^{2+} sites on the mineral lattice and could have contributed to repulsion forces with the crude oil droplet (Chapters II and III). This mechanism was reported based on the surface charge behavior of calcite particles in 10 vol% dilute seawater and deionized water.

Dilute surfactant in seawater (0.1 wt%) was then injected and equilibrated for 8 h **(Figure V-10)**. Since the injection volume was roughly equal to only 10% of the total chamber volume, the low final concentration of surfactant did not impact wettability. For that reason, seven stages of surfactant solution were subsequently injected. The contact angle decreased slightly after the second and third stages. The slight drop in the contact angle was due to the reduction in the IFT value, as observed at the oil/water/calcite contact point **(Figure V-10)**.

Oil droplet coalescence occurred after increasing the surfactant concentration in the solution. In the 5^{th} injection stage, wettability was surprisingly altered towards an oil-wet condition as shown in **Figure V-10**. Contact angle increased to over 120º. This unexpected behavior could be due to van der Waals attraction forces between the hydrophobic tail of calcite-adsorbed surfactant and the crude oil, and deserves further investigation. Surfactant likely accumulated at the interface, with the hydrophilic head in contact with surface-structural Ca^{2+} at the calcite surface and the hydrophobic tails oriented away from the interface towards the crude oil (Francisca *et al.* 2003).

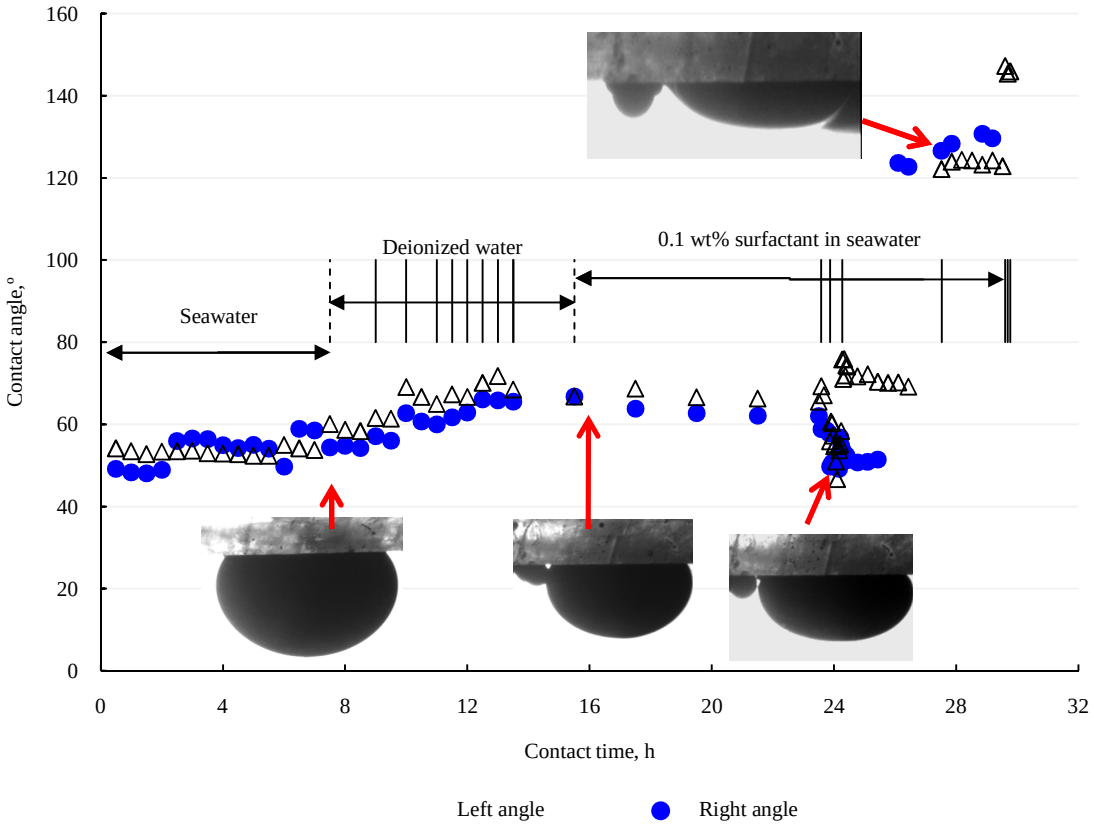

Figure V-10. Contact angle of calcite/mixed brines and 0.1wt% Surfactant/crude oil after 30 h of crude oil injection at 90ºC and 500 psi.

Oil droplets were detached from the calcite substrate after 40 min. of the 7th injection stage. Adhesion forces between the calcite and crude oil droplets were apparently decreased. In summary, with increasing concentration of the betaine amphoteric surfactant, the calcite system changed from water-wet to oil-wet to water-wet. These results indicate the complex behavior of the amphoteric surfactant that is very highly dependent on surfactant concentration and equilibration time. These systems deserve further study.

Conclusions

1. The partial hydration and dehydration of calcite surface showed no impact on calcite wettability.
2. Contact angle results were not affected by sulfate ions. At high sulfate concentration, $CaSO_4$ precipitation was observed when exceeding the solubility product limitation.
3. Formation brine altered calcite wettability towards oil-wet; however, a subsequent adjustment in salinity did not impact the contact angle.
4. Dilute amphoteric surfactant altered the rock wettability to water-wet at certain concentrations.

CHAPTER VI

BRINE/CARBONATE ROCK INTERACTIONS

Summary

Ions interactions between injection fluid, formation brine and rock mineral are quite complex. Water chemistry recently showed a significant impact on the desorption of oil components from the mineral surfaces. Several mechanisms were suggested including: rock dissolution, surface charge change, and sulfate precipitation.

To better mimic rock/brine interaction in carbonate reservoirs, short (10.2–15.2 cm) and long (50.8 cm) limestone and dolomite cores were used. Synthetic seawater was investigated in more detail. High-temperature condition believes to influence ions adsorption and interactions with rock minerals. Hence, moderate and high-temperature conditions were tested (90 and 130°C). To understand the reaction mechanisms, core aqueous effluent samples were frequently collected for further geochemical analysis.

Ions analysis clearly suggested insignificant chemical interactions in the short and long cores during the first pore volume of fluids displacement. There was no indication of sulfate precipitation as the pressure drop along the core was steady with time. Dedolomitization process was observed where magnesium was replaced by calcium ion. The current study gives new insights on the interactions between seawater, and carbonate minerals at high temperatures.

Introduction

The interfacial phenomena at carbonate/water interfaces are controlled by the electrical double layer (EDL) forces. Charged species are transferred across any interface until equilibration is reached. These species are called potential determining ions and were previously discussed in Chapters II and III.

Adjusting the salinity of injection water was lately reported an effective EOR technique. The expected mechanisms behind it are still unknown. Sulfate adsorption on the chalk rock changed the surface charge from positive to negative (Zhang *et al.* 2007). Calcium and magnesium ions afterward replaced the sulfate ions at high temperature conditions. Such adsorptions weaken the electrostatic repulsion forces and consequently released the carboxylic groups from the rock surface. Other scientists (Hiorth *et al.* 2010) stated the reaction mechanisms to be one of the following: a) chemical dissolution of calcite, b) change the rock surface charge, or c) precipitation.

The objective of this work is to study the interactions between seawater (5.5% TDS) and KI solution (2-3% TDS) in presence of carbonate rock. In addition, we did not use crude oil because the major interactions are expected between water ions and rock minerals. Nevertheless, water/oil/rock interactions were comprehensively studied in Chapters VII, VIII, and IX.

The reaction kinetics between injection brines and carbonate rock is dependent on temperature. In addition, mineralogical changes and rock dissolution are usually expected. Brines, in general, have chemical reactions either with the rock surface or the bulk solution. The major ions that normally exist in seawater, aquifer, or formation

brines are: H^+, Na^+, Ca^{2+}, Mg^{2+}, HCO^{3-}, Cl^-, and SO_4^{2-}. Complexes are formed either in the bulk aqueous phase or at the rock surface. Chapter X has more data about the complex ions and ions activity in injection water. These reactions are controlled by chemical processes taking place at mineral lattice and bulk solution interface (van Cappelen *et al.* 1993).

The concentrations of Ca^{2+}, Mg^{2+}, and SO_4^{2-} ions in seawater can affect the spontaneous imbibition process in the chalk reservoirs (Zhang *et al.* 2007). At high temperatures, Mg^{2+} substitutes Ca^{2+} at the chalk surface and the degree of substitution increases with temperature due to dehydration. The reaction rate of the chalk surface toward potential determining ions is higher than limestone simply because of the difference in the rock surface area (Austad and Standnes 2003; Strand *et al.* 2006; Zhang and Austad 2006).

Webb *et al.* (2005) studied the effect of SO_4^{2-} ions in seawater and formation brine on oil recovery. They observed an increase in the water wetting characteristics due to seawater injection. Strand and Austad (2008) conducted another study using spontaneous imbibition and coreflooding apparatus. Wettability improvement was noticed toward water–wet state at high temperatures (>90°C). Høgnesen *et al.* (2005) varied the sulfate concentration in seawater and reported similar findings on oil recovery as well. In general, the activity of the sulfate increased at higher temperatures.

Sulfate concentration is usually high in seawater; whereas formation brines are supersaturated with calcium ions. As a result, mixing the last two brines can cause

calcium sulfate precipitation if it is not within the solubility product limitation. More details on the scale tendency and precipitation issues are discussed in Chapter X.

In terms of rock mechanics, chalk rocks compaction was noticed in North Sea field after seawater injection for a long time. The slow dissolution process and chemical reaction were expected to impact the rock's mechanical strength. In addition to temperature, rock and fluids properties are considered key factors in controlling the interactions and compaction process (Korsnes *et al.* 2006).

Möller and Werr (1972) studied the influence of anions and cations exchange on calcite. They found that Na^{+}, Cl^{-}, and SO_4^{2-} at seawater concentration do not have any impact on the ions exchange at the calcite surface. Sulfate at higher concentrations formed a $CaSO_4$ layer adsorbed on the calcite. Other ions can form strong complexes with Ca^{2+} and lead to inhibition of ion exchange process (Ca^{2+}/Mg^{2+}).

Experimental Studies

Materials

Limestone and dolomite cores were dried in the oven at 120°C until constant weight was reached. Both Winterset limestone and Silurian dolomite are outcrop rocks in the USA. Dolomite cores are more heterogeneous where scattered vugs were observed on the rock surface. A wide permeability range, between 120 and 1,349 md, was reported for the dolomite cores. Porosity range varied between 15 to 18 wt%. Winterset limestone had a porosity and permeability of 24.5% and 28 md, respectively. Dolomite cores were tested at 90 and 130°C.

Fluids

A synthetic seawater was chosen from Middle East reservoirs, **Table II-1**. Deionized water was doped with 2–3 wt% potassium iodide (KI) as a chemical tracer. The densities of seawater and KI solutions at 25°C were 1.036 and 1.019 g/cm^3, respectively. The solutions viscosities were determined using a capillary viscometer technique at 25°C. The viscosities of seawater and 3 wt.% KI solutions were 1.074 and 0.872 cP. The used water in all experiments was purified in a water purification system with a resistivity of 18.2 MΩ·cm at room temperature**.**

Coreflood setup

Coreflood equipment consists of three major parts: core holder, accumulators, and two pumps, as depicted in **Figure VI-1**. Fluids displacement was achieved by operating the syringe pump at a constant injection rate. Brines were stored in stainless steel accumulators (2 L) at room temperature. A hydraulic pump was utilized to apply 1,000 psi of overburden pressure. Two back pressure regulators were installed to regulate the overburden pressure and core outlet flow at 1,000 and 500 psi, respectively. Differential pressure transducer (300 psi) was used to monitor the pressure drop along the core. The experiments were run inside an oven to control the temperature condition uniformly.

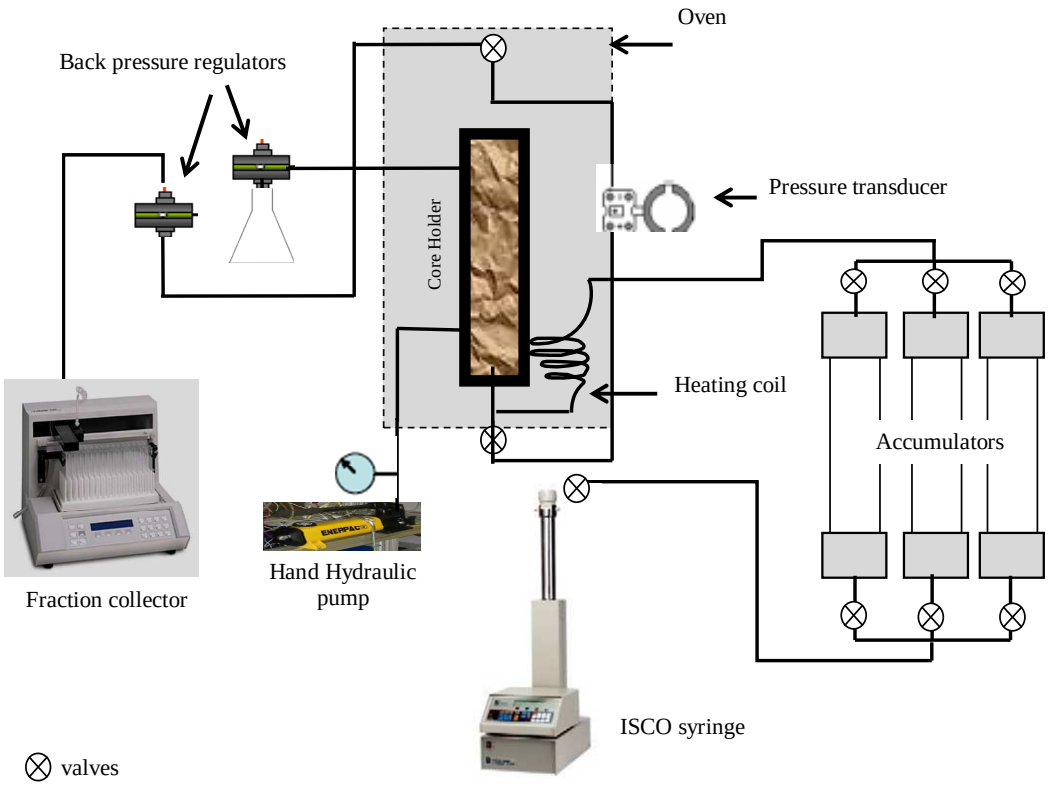

Figure VI-1. A schematic diagram of core flood apparatus.

Measurement errors

The measurements are subject to error and that has a major contribution to the results accuracy. Therefore, it is necessary to quantify and understand the measurement errors. There are possible sources of errors in the concentration measurements as follow:

- Dilution error of the samples and standard solutions. To minimize the error, class A volumetric flasks (100 ml) were used with accuracy of ±0.1%.
- High performance pipettors were used with an accuracy of ±0.5%. Also, the pipettors were calibrated on a regular basis.

- Standard samples for cations (Ca^{2+}, Mg^{2+}) were prepared from pure standards (1,000 mg/L) to yield reliable, accurate results. It was ordered directly from the manufacture (PerkinElmer). During measurements, standard samples were rechecked every 5 measurements to avoid any deviation in the calibration curve.
- Turbidity method was applied to measure SO_4^{2-} concentration. The spectrophotometer instrument accuracy was ±5%.
- Iodide concentration was measured using ion-selective electrode technique. The error range for this method was 2-3%, **Table VI-2**.

Table VI-1. Measurement errors in cations and anions measurements.

Method / Ions	Atomic Absorption	Inductively Coupled Plasma – Emission Spectrometry	Spectrophotometer	Ion Selective Electrode
	Error, %			
Ca^{2+}	3	1	–	–
Mg^{2+}	3	1	–	–
SO_4^{2-}	–	–	5	–
I^-	–	–	–	2-3

Results and Discussion

The chemistry of seawater (5.5 wt% TDS) is totally different than that of other injection water (shallow aquifer and formation brine). In sandstone reservoirs, clays control rock/fluid interactions, especially at low salinity water level (Zhang and Morrow 2006;

Alotaibi *et al.* 2010). Saline water might cause more chemical dissolution to carbonate rocks than deionized water. Complexes in the aqueous phase can be formed and rearranged as a result of any changes in the ionic strength.

Limestone coreflood–1

To better understand the interactions between carbonate rock and the injection water, dry cores were used in the next set of experiments. Seawater was injected at a constant injection rate of 0.5 cm^3/min. and 90ºC. The pressure drop was recorded every minute via using lab view software. The core permeability and other properties are reported in **Table VI-2**. 6 PV of seawater was injected to make sure the core/brine system reached equilibration. Core effluent samples were collected every 5 cm^3 using an automatic fraction collector. A 3 wt% potassium iodide (KI) was blended with deionized water to track the movement of the fluids inside the core.

The pressure drop throughout seawater injection was stable between 7 to 7.5 psi, **Figure VI-2**. A slight decrease in the pressure drop was observed after switching to KI brine. The pressure profile was stable which indicates no chemical precipitations occurred. Any chemical interactions between injection water and carbonate minerals should reflect on the pH values. **Figure VI-3** suggests a slight decrease in the pH of the seawater samples at the first 3 PV. The effluent tracer solution showed a higher pH result than that of the original sample (pH=7), with maximum and minimum values of 8.2 and 7.6, respectively. Enough pore volumes of KI brine were injected to overcome the dilution effect at the flood front.

Table VI-2. Properties of dolomite and limestone cores.

Core ID.	Mineralogy	Diameter	Length	Bulk Volume	Pore Volume	Porosity	Base Permeability
		inch		cm^3		%	md
1	Limestone $CaCO_3$	3.78	14.02	157.8	38.6	24.5	28.2
12	Dolomite $CaMg(CO_3)_2$	3.78	14.96	167.4	31.2	18.6	655.3
15		3.76	14.96	167.1	26.1	15.6	379.0
16		3.78	50.67	570.0	86.9	15.2	1348.8

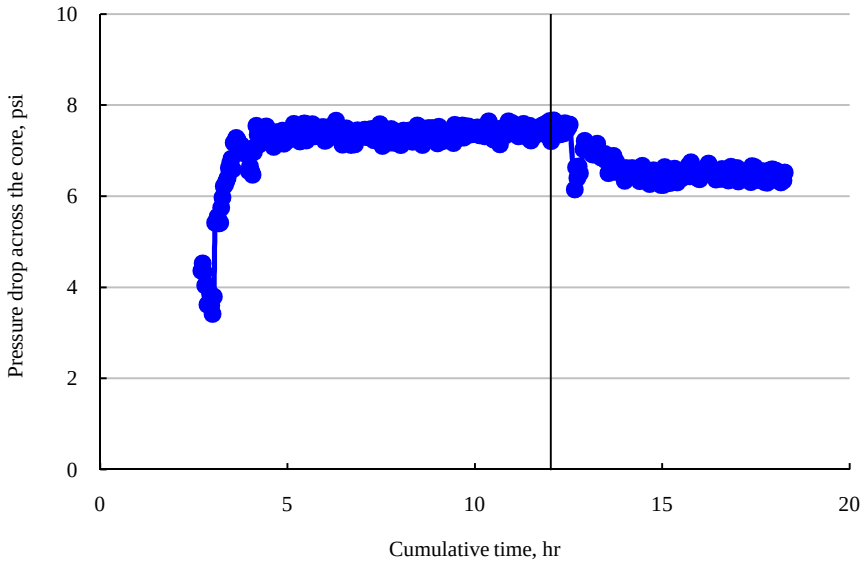

Figure VI-2. Pressure drop of limestone core test at temperature 90°C.

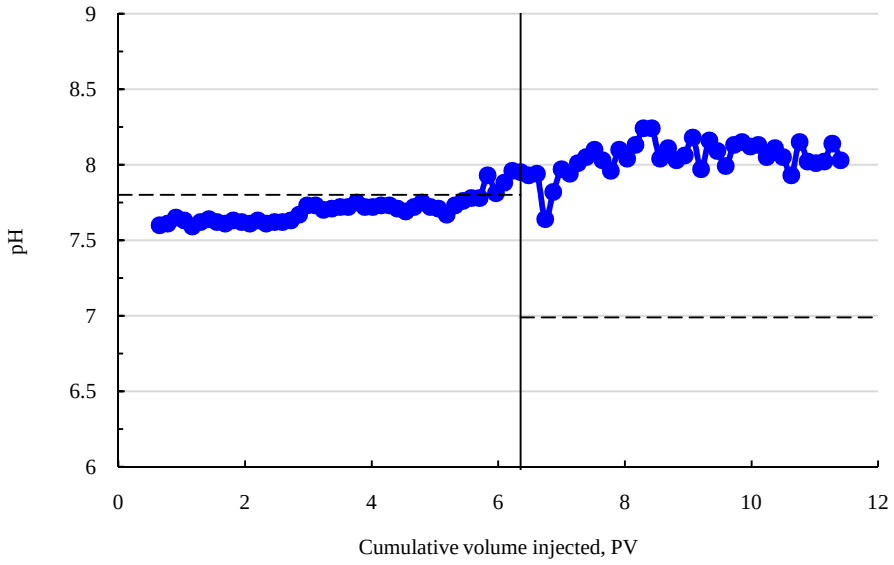

Figure VI-3. pH measurements of core effluent samples in limestone core test, core–1.

Sulfate concentration in seawater is very high in comparison to others divalent cations and anions; for that reason, calcium sulfate might be precipitated depending on the solubility product at the target temperature. Insignificant change was noticed on sulfate behavior during the first PV, **Figure VI-4**. Results subsequently matched the original sulfate level in seawater (3,572 mg/L). There was a sudden decrease in sulfate ion concentration, which observed after converting the fluid injection to KI solution. It took about 1.5 PV to displace the seawater from the core. Later, sulfate and iodide concentrations stabilized at their original concentrations.

It is very important to monitor the behavior of other divalent cations at high temperatures. Calcium and magnesium ions matched the seawater level after almost half pore volume. As expected, an abrupt decrease in the divalent cations' concentrations was subsequently reported. During KI injection, the concentrations of Ca^{2+}, Mg^{2+} and SO_4^{2-}

ions were consistent. The main objective of using KI tracer was to determine the required pore volumes to displace the original fluid from the core. No tracer breakthrough was noticed, which indicates the limestone core was homogenous **(Figure VI-4)**.

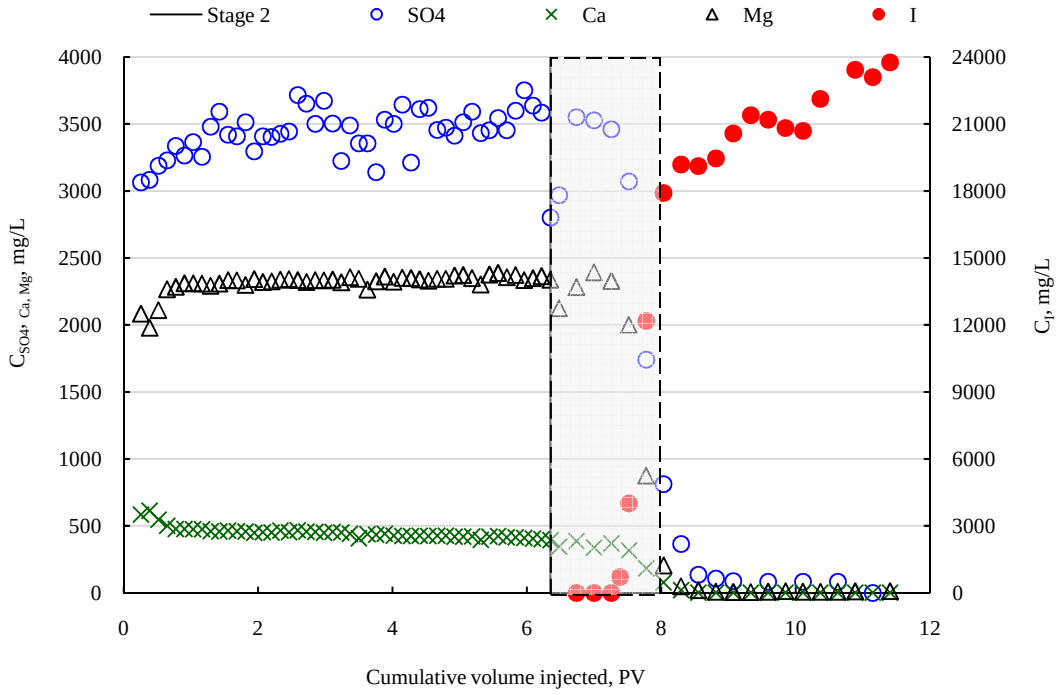

Figure VI-4. Effluent ions concentration of limestone test, core–1.

In summary, there was a slight decrease in the Ca^{2+}, Mg^{2+} and SO_4^{2-} concentrations at the first half pore volume. Sulfate ions in solution usually form a complex with the positively charged ions in the solution such as Na^+, Ca^{2+}, Mg^{2+}…etc. As a result, the concentration of free sulfate ions that was expected to react with

limestone rock might be low. The complexes can also inhibit any reaction between the sulfate and the rock surface.

Cations generally create an ion binding with CO_3 mineral. Injection of Mg enriched fluids such as seawater (Mg/Ca=3.4) usually alter the limestone mineralogy and transform it into dolomite which is known as dolomitization process (Machel 2004). But, these are weak reactions and need longer period of time to observe any significant change in the ions' concentrations (Hanshaw *et al.* 1971). This confirmed the slight decrease in Mg level at the beginning, which is not conclusive.

Dolomite coreflood–2

Temperature is strongly impacting the water/rock interactions from different perspectives (Strand *et al.* 2006). Therefore, dolomite rocks were tested at moderate and high temperatures. Other parameters were kept unchanged. In this test, the temperature condition was maintained at 90°C. At the beginning, seawater was injected (9 PV) and then followed with 3 wt% KI solution (8 PV).

A stable pressure drop was observed with the injection time. Darcy's law was applied to calculate the base permeability as shown in **Table VI-3**. Decreased injection water salinity increased the alkalinity of the core effluent samples, **Figure VI-5**. In addition, the free sulfate ions showed chemical interactions at the first PV, **Figure VI-6**. Magnesium and calcium results matched their original concentration in seawater.

Iodide measurements were consistent in comparison to the behavior of the other ions (Ca^{2+}, Mg^{2+}, SO_4^{2-}). As previously reported, the chemical tracer displaced the

seawater after 1.5 PV. The slight fluctuation in the ion's concentration was within the measurement errors range.

Dolomite coreflood–3

This test was conducted at 130°C. A total of 14 PV of seawater and 3 wt% KI solutions were injected at a constant injection rate (0.5 cm^3/min). Pressure data were stable with time. As a result, the possibility of sulfate precipitation was very minimal. The pH of the original seawater was 7.8, whereas a slight drop up to 0.5 was observed in the aqueous effluent samples. The alkalinity increased after shifting the injection solution to KI fluid, this behavior was repeated in several displacement tests, **Figure VI-7**. Therefore, there might be either a deprotonation reaction (removal of H^+ protons from the water molecules) or CO_3^{2-} dissolution. In addition, the CO_2 concentration in the air can dissolve in the samples and within minutes decrease the fluid's pH.

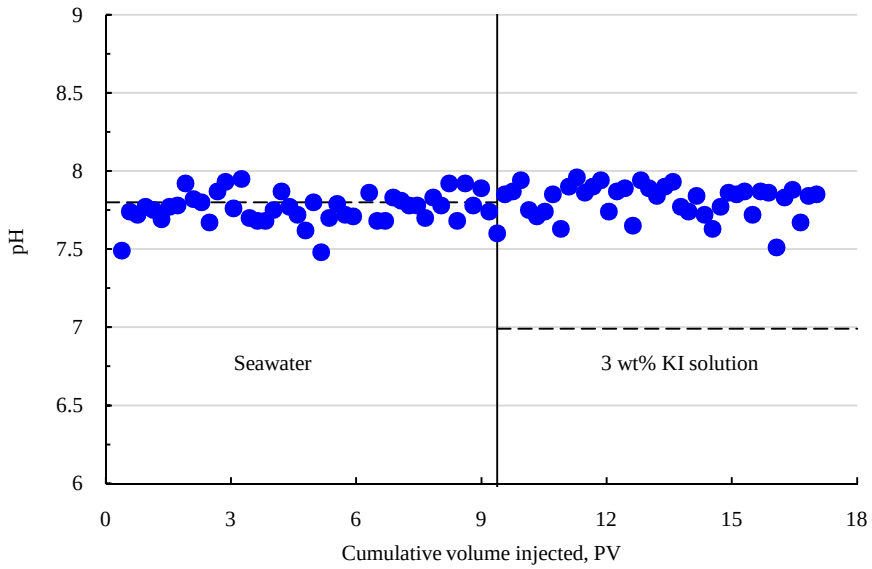

Figure VI-5. pH measurements of core effluent samples in dolomite core–2.

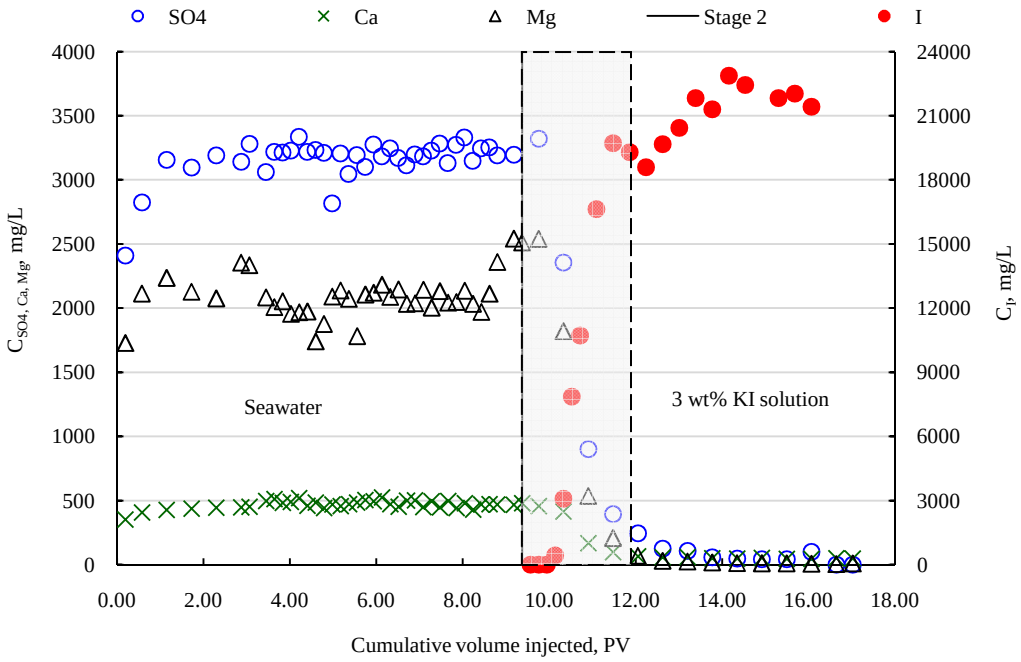

Figure VI-6. Effluent ions concentration of dolomite core–2.

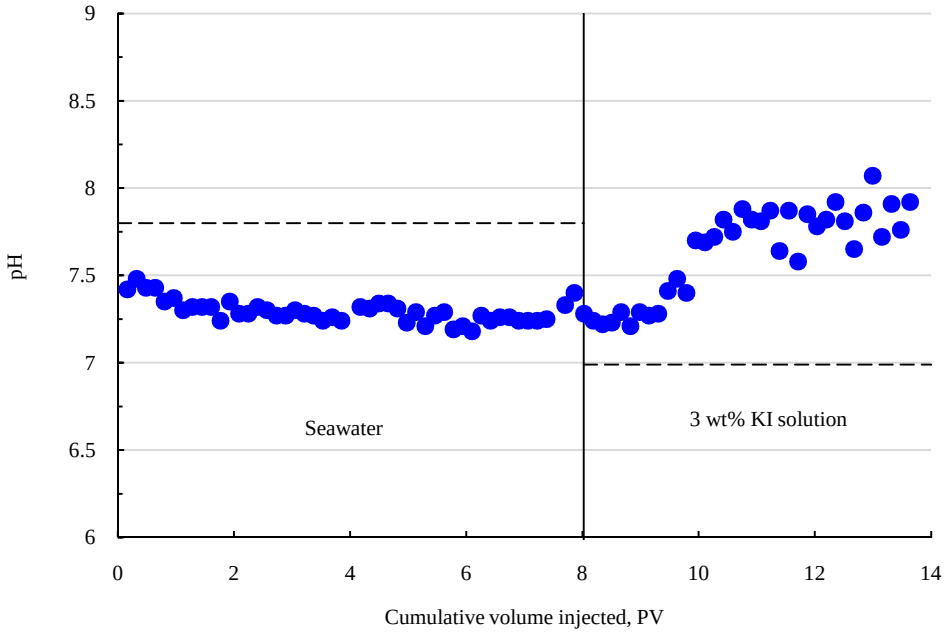

Figure VI-7. pH measurements of effluent samples in dolomite core–3.

Analysis of sulfate ions showed a good match between the injected and collected water samples, as depicted in **Figure VI-8**. Results implied that sulfate did not adsorb on the dolomite surface at 130°C. The results of divalent cation concentration, also, confirmed no ionic exchanged occurred between calcium and magnesium. After 1.3 PV, KI solution displaced all seawater from the core. In addition, Ca^{2+}, Mg^{2+}, and SO_4^{2-} ions abruptly decreased during one pore volume of fluid injection. In brief, no interactions were noticed between seawater and dolomite rock at 130ºC.

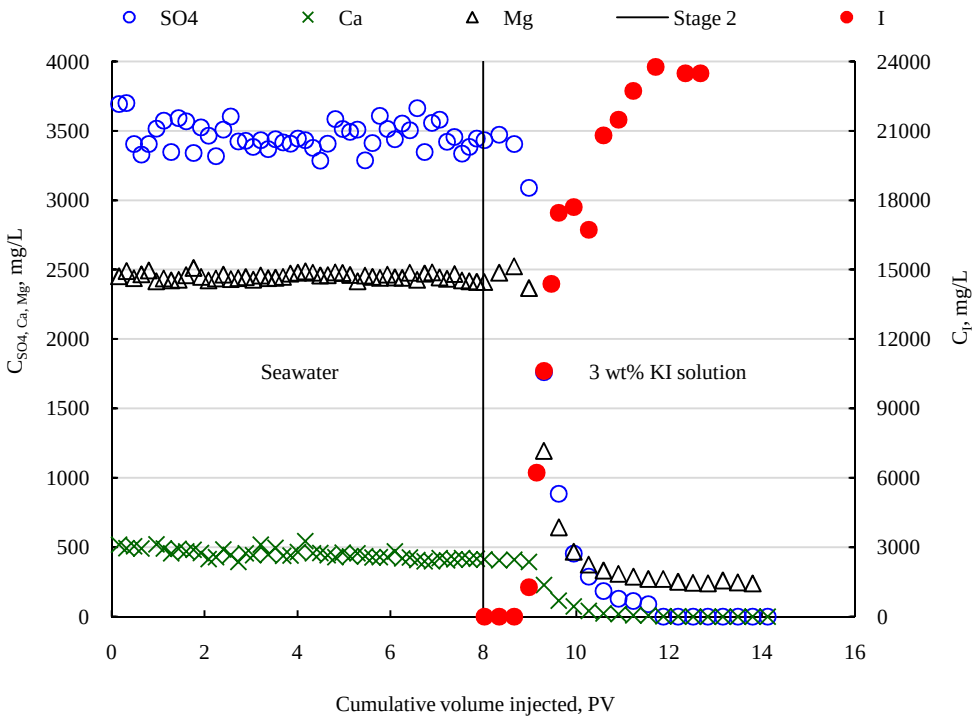

Figure VI-8. Effluent ions concentration of dolomite core–3.

Dolomite coreflood–4

The fluid/rock interactions were investigated in a long dolomite core (50.8 cm) to support the previous findings in the short ones. The temperature condition in this test was maintained constant at 130°C; seven PV of seawater was injected. The pH behavior tends to be more neutral compared to the original seawater (7.8), **Figure VI-9**. This was attributed to the hydroxide ion adsorption on the rock surface which subsequently decreased the pH result. On the other hand, the pH increased slightly to 7.5 after switching the injection to KI solution.

Sulfate ions showed insignificant decrease after seawater injection, as depicted in **Figure VI-10**. The secondary axis in **Figure VI-10** shows an increase in iodide concentration up to 13,300 mg/L which matches the original iodide concentration (13,260 mg/L). The anions (sulfate and iodide) concentrations were steady after 8 PV. No breakthrough was noticed during the tracer injection which indicates the core was homogenous.

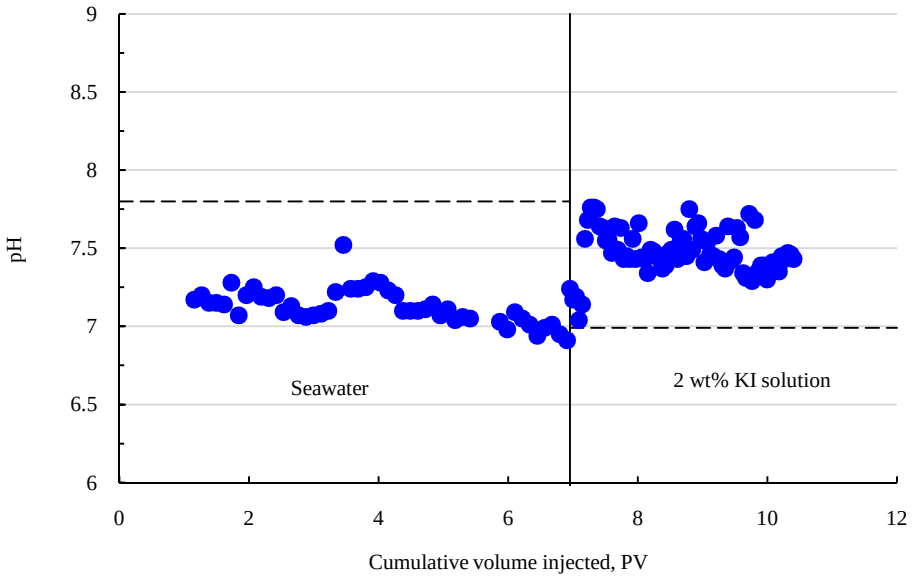

Figure VI-9. pH measurements of effluent samples in dolomite core–4.

In addition, calcium concentration decreased to 300 mg/L while the original concentration was 533 mg/L, **Figure VI-10**. In the same graph, magnesium level in the collected samples was higher than the injected ones. Another analysis technique was utilized to determine Ca^{2+} ion concentration. The objective of this was to confirm the measurements accuracy through using various analytical techniques. The most chemical

activities were observed at the first pore volume, for this reason, we analyzed the core effluent samples only during that period (1st PV). **Figure VI-11** depicted Ca^{2+} concentration results after using atomic absorption and inductively coupled plasma analytical methods. The highest difference in Ca^{2+} measurements was observed at 0.69 PV (59.2 mg/L). In general, the trend behavior was decreasing from ~600 to ~300 mg/L. Results suggested dedolomitization might occurred where calcium replaced magnesium in the mineral lattice structure (Sanz-Rubio *et al.* 2001).

$$CaMg(CO_3)_2 + Ca^{2+} \xrightarrow{Dedolomitization} 2CaCO_3 + Mg^{2+}$$

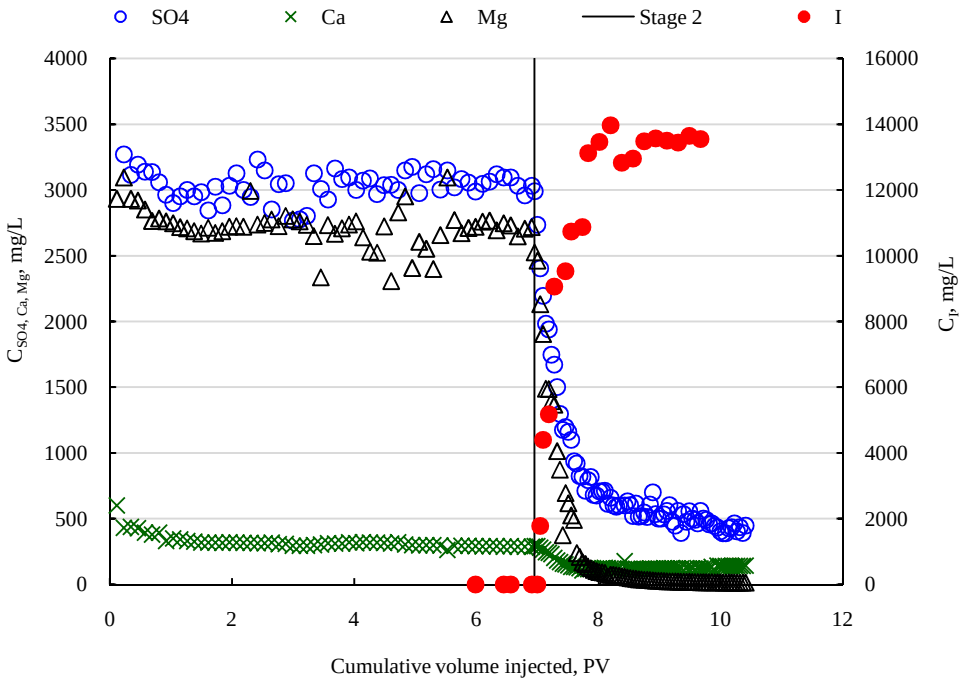

Figure VI-10. Effluent ions concentration of dolomite core–4.

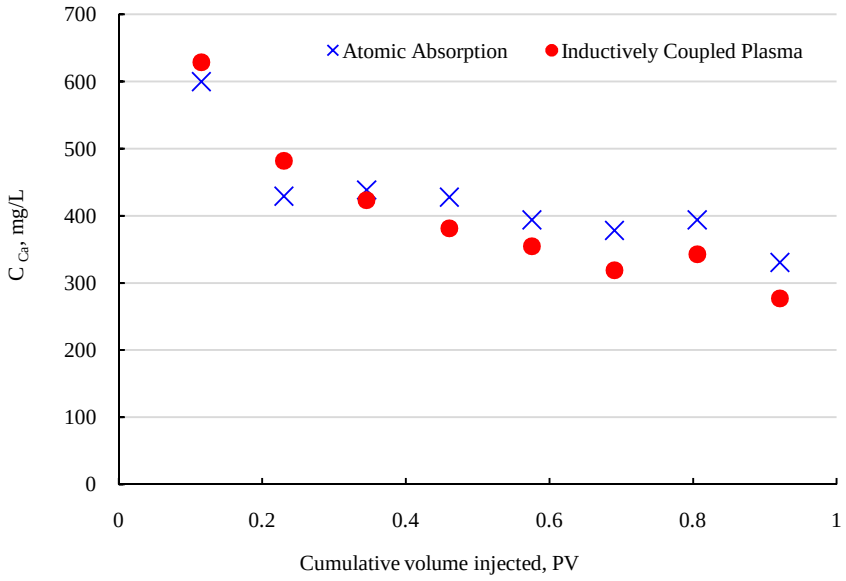

Figure VI-11. Calcium analysis in effluent samples of dolomite core–4 using different analysis techniques.

In summary, the sulfate ions showed some interactions with the rock at the first pore volume of water injection. In addition, ionic exchange was noticed between Ca^{2+} and Mg^{2+} ions in the long core. All results are summarized in **Table VI-4** to compare the ions behavior easily.

Conclusions

The main conclusions that can be drawn from this study are:

1. Decreasing the salinity produced alkali solution because of either H^{+} removal or CO_3^{2-} dissolution.
2. Ionic exchange was observed between dolomite rock and seawater.
3. Results indicate no sulfate adsorption in the short dolomite cores.

4. Dedolomitization process, where calcium replaced magnesium ion in dolomite lattice, was observed in the long dolomite core.
5. Sulfate adsorption on dolomite core was insignificant.
6. Different analytical techniques were used to confirm calcium concentration results in the long dolomite core.

Table VI-3. Results summary of pH, sulfate, calcium, and magnesium concentrations for all displacement tests.

Core ID	Injection fluid	T	pH	SO_4^{2-}	Ca^{2+}	Mg^{2+}	I^-
1	Seawater	90ºC	↓ during first 3 PV	↓ during first PV	↓ slightly after 4 PV	↓	–
	3 wt% KI solution		↑ one unit	↓			↑
2	Seawater		No change		↓ during first 3 PV	No change	–
	3 wt% KI solution		↑ by one unit	↓			↑
3	Seawater	130ºC	↓ 0.5	No change			–
	3 wt% KI solution		↑ up to one unit	↓			↑
4	Seawater		↓ 0.8	↓	↓	↑	–
	2 wt% KI solution		↑ 0.5	↓			↑

CHAPTER VII

WATERFLOODING AS SECONDARY AND TERTIARY RECOVERY MODES IN DOLOMITE RESERVOIRS

Summary

Fluids/rock interactions are affected by aqueous phase salinity, crude oil composition, and rock lithology. Over the last decade, low salinity water clearly reduced residual oil saturation in sandstone reservoirs. Clays in sandstone limit the injection water salinity to a certain ionic strength. Reaction mechanisms are quite different in carbonate than that of sandstone. However, the divalent anions are believed to reverse the carbonate surface charge from positive to negative. In short, the chemistry of the aqueous solution might influence the carbonate wettability and residual oil saturation.

A coreflood study was conducted using up to 12.7 cm outcrop dolomite core plugs. Various injection fluids were used including: synthetic formation brine, seawater, shallow aquifer water, sulfate solution, chemical tracer, and deionized water. Fluids properties, such as density and viscosity, of the injection brines and crude oil were determined at 90ºC. CAT scan technique was applied to determine the rock characteristics. In addition, chemical analysis of the divalent cations (Ca^{2+}, Mg^{2+}) and anions (SO_4^{2-}) of the core effluent was conducted using atomic absorption technique.

Injection of formation brine showed higher oil recovery in the secondary mode. Seawater and aquifer water flooding increased the oil recovery when applied as tertiary modes. No ions interactions were reported between the dolomite mineral lattice and

injection water molecules. Mixed results were reported for deionized water tests throughout the multistage water injection.

Introduction

The microscopic displacement in carbonate reservoirs is affected by various physical and chemical properties including: 1) geometry of pore network, 2) fluid-fluid properties, such as IFT, density, and phase behavior, 3) fluid-rock interactions (wettability, ion exchange, and adsorption); and 4) pressure gradient and gravity (Shah and Schechter 1977). Carbonate reservoirs account for more than half of the world's hydrocarbon reserves. Identifying and understanding the important mechanisms, which control recovery and retention in a given reservoir is essential for successful oil production.

Formation wettability controls the location, flow, and fluids distribution in the reservoir. Most carbonate reservoirs are classified as either oil or intermediate wet (Saner *et al.* 1991). Wettability and heterogeneity of carbonate reservoirs are by far the most common reasons behind the high oil saturation after waterflooding (Chilingar *et al.* 1992).

Waterflooding in carbonate reservoirs mainly depends on the availability of the water resources. The chemistry of the injection water varied from high salinity water (formation water and seawater) to moderate and low salinity water (shallow aquifer, lake water, and even fresh water). More focus was generally given to the total suspended solids than the total dissolved solids (TDS). Formation brines, in general, have more divalent cations (Ca, Mg) than anions (SO_4, CO_3). In comparison to formation and

shallow aquifer brines, SO_4 concentration in seawater is usually higher. Fluid/fluid and fluid/rock interactions should be affected by water chemistry, especially the presence of divalent ions (Ca, Mg) in connate water, injection fluid and carbonate minerals' lattice.

The main objectives of this study are to determine the effect of salinity on waterflooding performance at different injection modes (secondary and tertiary). In this chapter, new findings were discussed about the effect of water salinity on oil recovery at 90ºC.

Literature Review

The salinity of the injection water was investigated by adjusting divalent cations and anions of seawater and brines' composition (Bagci *et al.* 2001; Strand *et al.* 2003; Webb *et al.* 2005; Zhang *et al.* 2007). Increasing the sulfate concentration in North Sea water decreased the residual oil saturation in the laboratory coreflooding tests (Høgnesen *et al.* 2005; Strand *et al.* 2008). Divalent cations are necessary for SO_4 to adsorb at the mineral surface and subsequently altered its surface charge from positive to negative (Pierre *et al.* 1990; Strand *et al.* 2006; Strand and Austad 2008). Such adsorption weakens the electrostatic repulsion forces and changed the rock wettability toward water-wet.

In addition to crude oil droplets, the surface charges of limestone and dolomite particles were recently investigated as a function of brine's salinity (Chapters II and III). Three different wettability modes were tested: water-wet, intermediate-wet and oil-wet. Carbonate rocks' surface charge was commonly assumed to be positive despite the connate water composition and wettability conditions (Schramm *et al.* 1991; Schramm

2000). In general, seawater and formation brine can modify the carbonate surface charge to positive for only the water-wet particles. But, crude oil and oil-wet particles were negatively charged because of the acid carboxylate groups. Therefore, the mechanism of the sulfate adsorption might be true in the water-wet carbonate surfaces, but further investigations are required about the oil and intermediate wet cases.

Experimental Studies

Materials

Outcrop Silurian dolomite rock was utilized for the coreflood experiments in this chapter. Thornton in Chicago (USA) is the main source for the dolomite block. To avoid any ions interactions and/or adsorption on the rock surface, deionized water was used to drill the core plugs.

Synthetic brines were used simulating a field case in the Middle East. The preparation procedure of the brines and crude oil compositions were previously discussed in Chapter II. Sweet crude oil was only used in the core flood tests.

The densities of the injection water and crude oil were measured at 90ºC using high temperature density meter DMA4100. Moreover, capillary viscometers were used to measure brines' viscosities at 90ºC, **Table VII-1**.

Apparatus and procedure

The coreflood set up was previously reported in Chapter VI. Fluids displacement was achieved by operating the syringe pump at different injection rates 0.1–1 cm^3/min. The

overburden and back pressure regulators were set, for all tests, at 1,000 and 500 psi, respectively.

The dolomite cores were dried overnight at 120ºC until a constant weight was reached. A vacuum pump was then operated for 6 hrs to remove trapped air from the cores. A PVC pipe was used to vacuum and saturate the cores in a vertical position to avoid the negative effects of gravity and density differences (air and formation brine). To reach ionic equilibrium, we left the cores in the formation brine for 3 days. The base permeability was, then, determined by measuring the differential pressure at different flow rates (0.1, 0.5, and 1 cm^3/min.). The conventional weight method was utilized to measure the rocks' porosity, **Table VII-2**. The cores were oil flooded at a flow rate of 0.5 cm^3/min. until the irreducible water saturation was achieved. The core samples were aged in crude oil for 30 days at 90ºC.

Table VII-1. Crude oil and brines' properties at 90ºC.

Fluid Description	**Density, g/cm^3**	**Viscosity, cP**
Crude oil	0.792	6.540
Formation brine	1.119	0.821
Seawater	1.00	0.534
Shallow aquifer water	0.969	0.506

Table VII-2. Dolomite cores' properties at atmospheric conditions.

Core ID	Diameter, cm	Length, cm	Porosity, %	Permeability, md	S_{wi}, %
1	3.81	10.18	16.94	108.20	32.17
2		10.92	13.04	99.18	28.92
3	3.76	12.55	12.98	180.80	28.40
4		12.70	12.39	177.88	31.60
5			13.60	176.00	27.68

Results and Discussion

Core–1

This core was flooded first with seawater, 2 wt% potassium iodide brine, and aquifer water. The flow rate was maintained constant at 0.5 cm^3/min. and enough pore volumes were injected until reaching the plateau level. The first injection stage suggested an oil recovery of 69.9% OOIP, **Figure VII-1**. The water breakthrough (WBT) was observed at 2.0 PV and 54.1% OOIP. Core effluent analyses were conducted to determine pH, sulfate (SO_4), calcium (Ca), magnesium (Mg), and iodide (I) concentrations accordingly. Major variations in oil recovery and ions' analysis took place during the first 3 PV. A stable pressure drop was reported after 2 PV of injection. Any chemical interactions are expected to influence the solution's pH. Therefore, pH measurements were conducted for seawater (7.7), aquifer water (7.6), and KI solution (7.4) **(Figure VII-1)**. The CO_2 in the air obviously is affecting the pH measurements. For that reasons, all collected

aqueous samples were stored in a sealed plastic tubes, and opened for few seconds to either measure the pH or take aliquot for ion analysis.

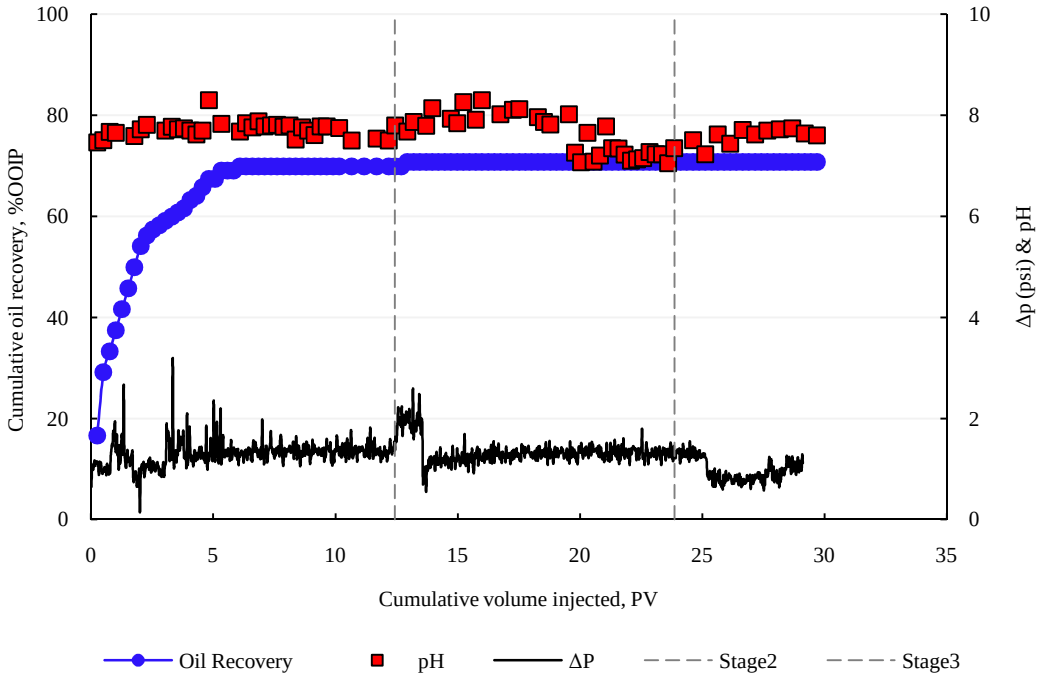

Figure VII-1. Cumulative oil recovery, pressure drop and pH of core−1 (seawater-KI-aquifer).

The original SO_4 concentration in seawater is 3,560 mg/L, **Table II-1**. The geochemical ion analysis shows a decrease in SO_4 concentration up to 2,850 mg/L, **Figure VII-2**. This might be attributed to the dilution effect from the connate formation brine in the core (SO_4 = 108 mg/L). Sulfate adsorption and precipitations were also proposed by others (Zhang *et al.* 2007). To confirm the right reaction mechanisms, the cations' concentrations were determined consequently. Atomic absorption was utilized to measure Ca and Mg concentrations in the collected samples. Samples were collected every 6 cm^3 in conical graduated tubes. A sudden drop in Ca was observed from 3,954 to

807 mg/L during the first 3 PV. This result confirms the dilution effect as the Ca concentration in the connate brine was higher than that in seawater.

Magnesium concentration, on the other hand, increased to 2,970 mg/L, while the original Mg in seawater was 2,455 mg/L. Formation brine has higher Ca and Mg concentrations than seawater **(Table II-1)**. Seawater might also dissolve dolomite minerals (Ca and Mg). In short, there was no evidence of any dissolution or precipitation. In addition, the drop in the ions' concentrations at the beginning was apparently due to mixing the injection water with connate brine.

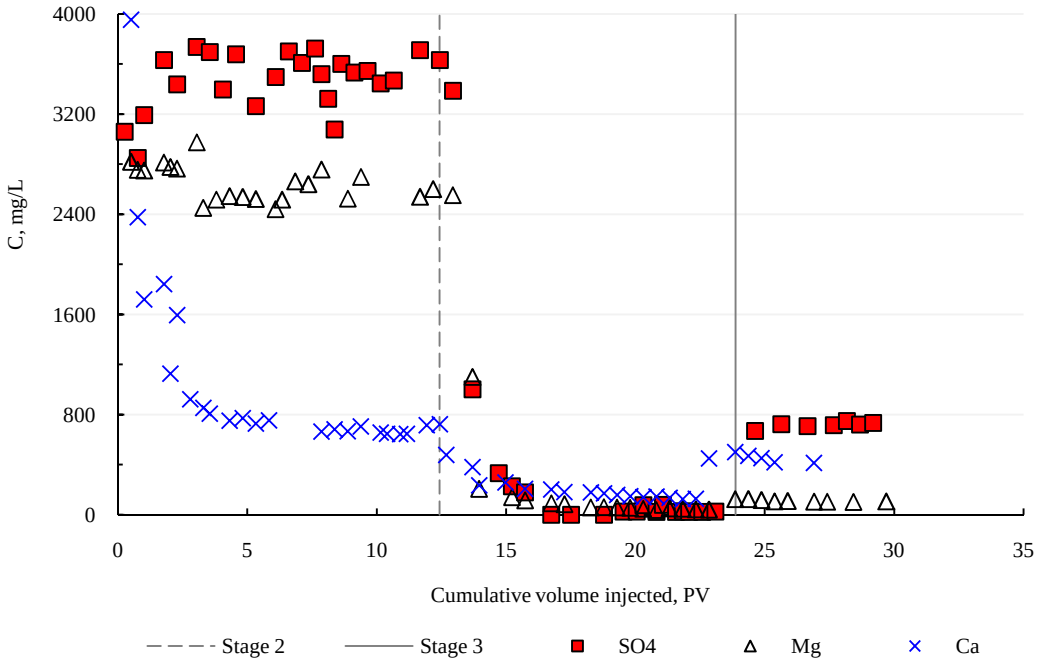

Figure VII-2. Ions analysis of core−1 effluent samples.

Samples of dolomite rocks were visualized using CAT scan technique, **Figure VII-3**. Vugs and fractures were observed in two different cores samples. For that reason, a chemical tracer (2 wt% potassium iodide, KI) was utilized in some of the tests to detect any fluids breakthrough. The KI injection was started at 12.4 PV. Pressure drop data increased slightly during the first PV injection as a result of shifting the fluids' accumulators. Oil recovery increased by 1% at 12.9 PV. The seawater was displaced from the core after almost one PV and that was confirmed by cations and anions concentrations **(Figure VII-4)**. This result confirms the fractures were not connected as indicated by the upcoming tracer analysis result. The iodide concentration was steady with time until the third stage of injection was initiated. Moreover, no breakthrough was observed during the chemical tracer injection stage. Aquifer water injection did not in fact affect the residual oil saturation. In terms of the cations and anions, the concentration of the effluent and original aquifer samples had a good match.

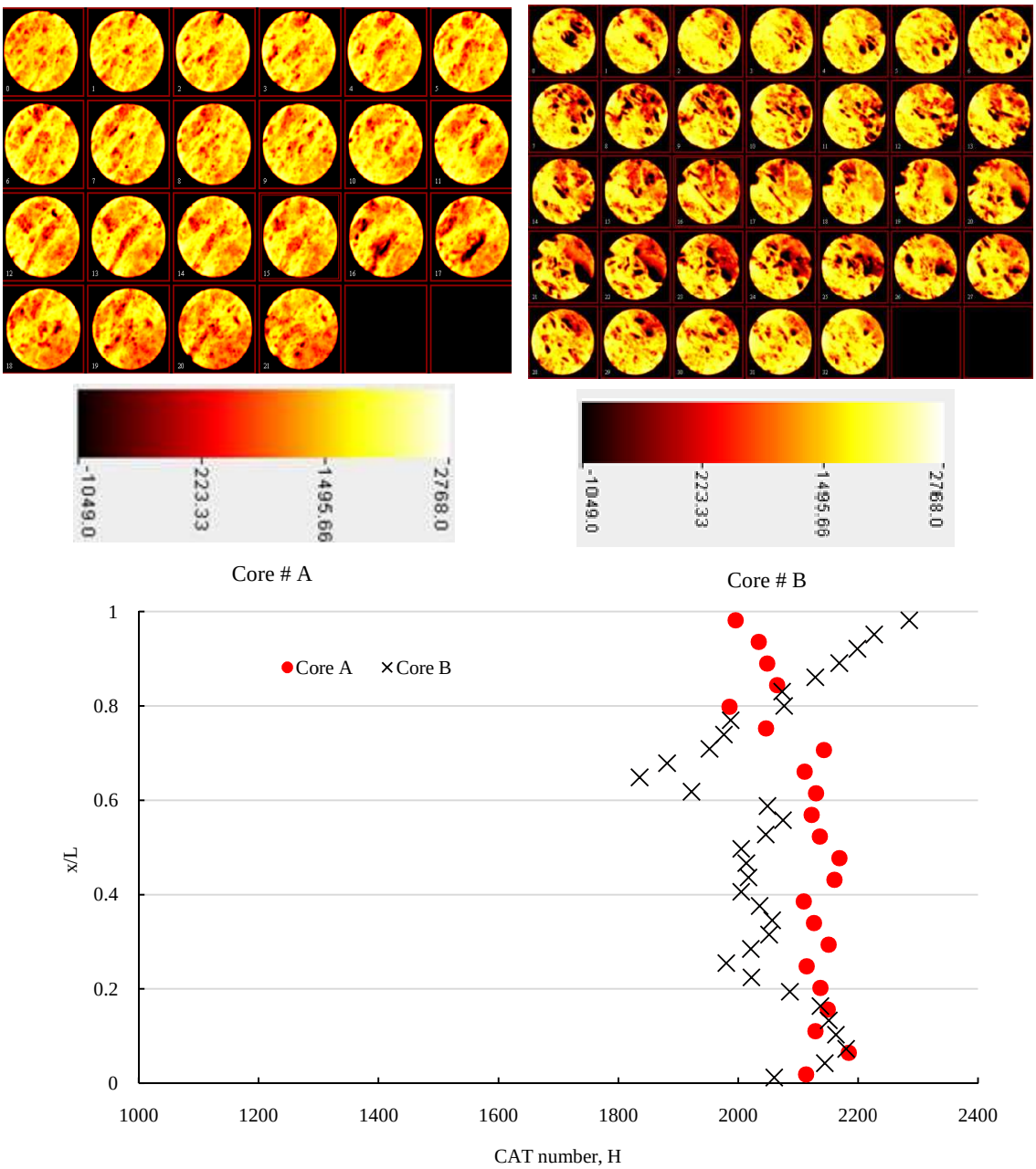

Figure VII-3. CAT scan analysis of two dry dolomite cores.

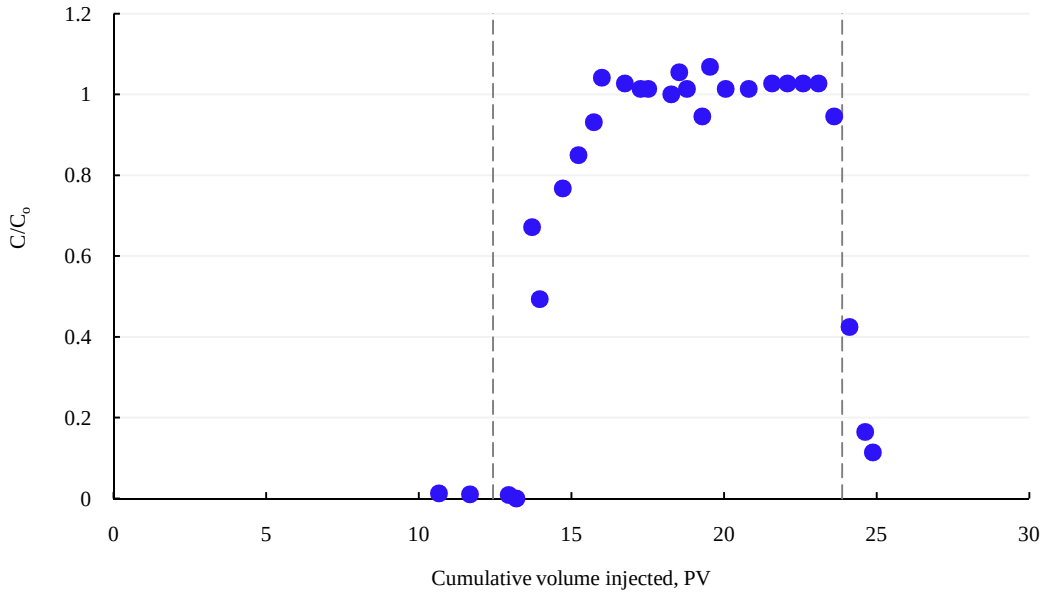

Figure VII-4. Iodide concentration of core effluent after the second injection stage (core−1).

Core–2

The same injection fluids in core–1 were used in this test (core–2) but with different order. The injection sequence was as follow: potassium iodide, seawater, and aquifer water, while the injection rate was 0.5 cm^3/min. The first stage of KI fluid injection produced 66.5% OOIP, **Figure VII-5**. The water breakthrough (WBT) was noticed after 3.7 PV. In addition, the oil recovery at WBT point was 50.5% OOIP. Pressure drop data was almost steady at 4 psi after 0.5 PV of injection.

In the second injection stage, seawater increased the oil recovery to 71.6% OOIP, **Figure VII-6**. Pressure drop decreased slightly as switching from one accumulator to another. The last injection stage of shallow aquifer water increased the oil recovery to 74.7% OOIP accordingly.

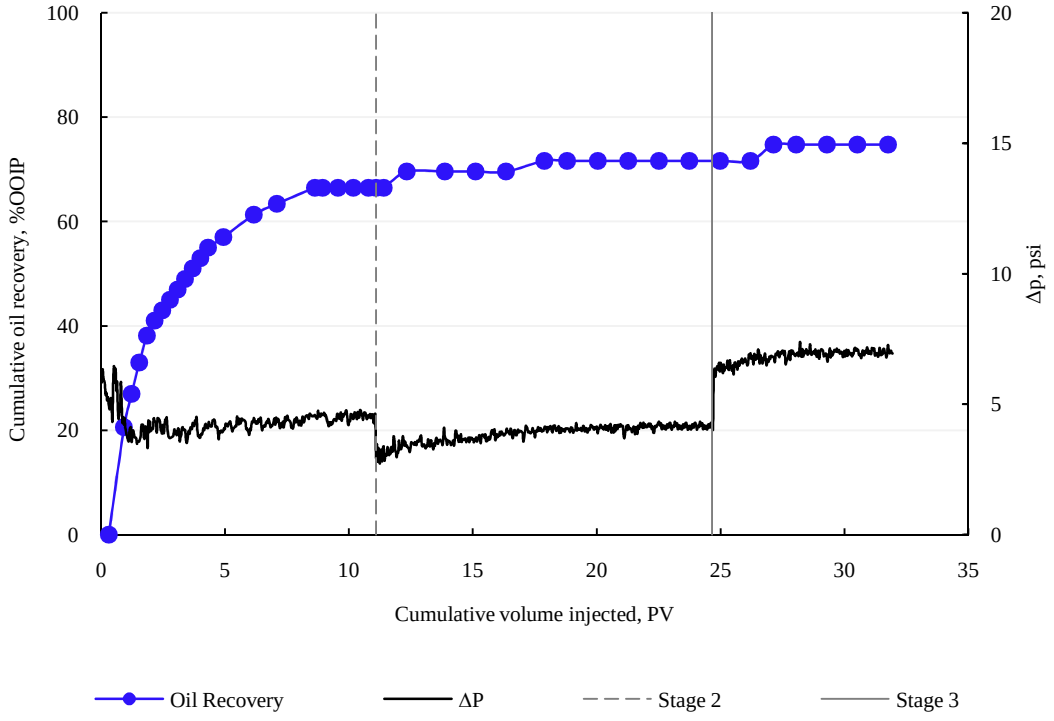

Figure VII-5. Cumulative oil recovery, pressure drop and pH of core−2 (KI-seawater-aquifer water).

Potassium iodide injection physically displaced the crude oil from the core. The second injection stage of seawater increased the recovery by almost 5%, and that was attributed to the interactions between the water ions, crude oil and dolomite minerals. Reduced the salinity to aquifer water (~4K mg/L) also enhanced the recovery by approximately 3%. It was proved in Chapter II that low salinity and aquifer water altered the dolomite surface potential into negative. Adsorbed carboxylate group in crude oil is also negatively charged, and as a result, repulsion forces were created with the mineral surface. This could change the wettability toward water-wet condition.

Iodide concentration was monitored for the first 14 PV, **Figure VII-7**. Results suggested a sudden increase in iodide concentration after 1.2 PV. The iodide ion did not interfere with other ions. For that reason, iodide concentration was reported as a ratio to the original sample. A sudden drop in the iodide concentration was observed at 11.1 PV after seawater injection was started.

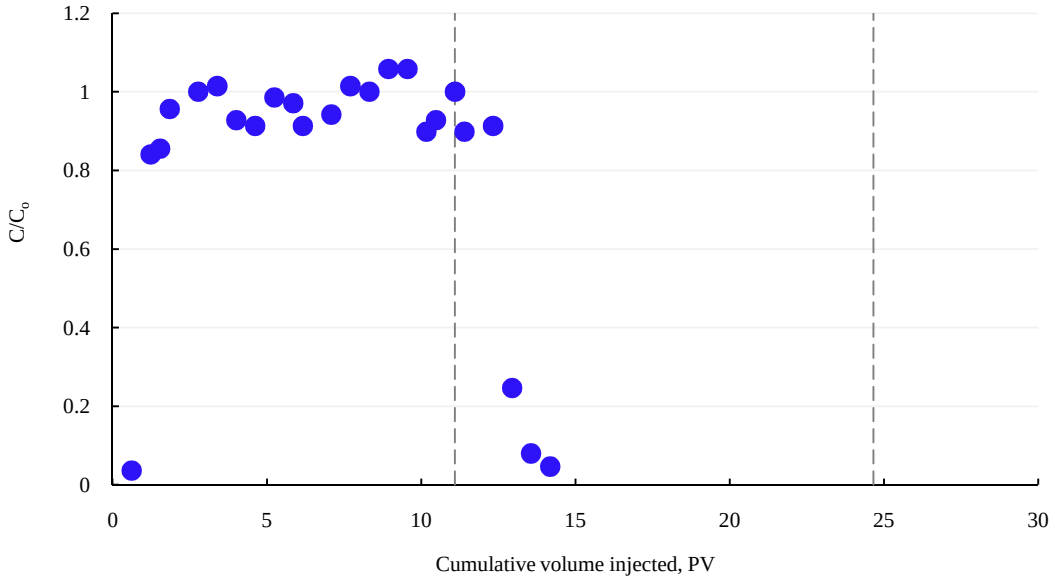

Figure VII-6. Iodide concentration during the first injection stage of core−2.

Core–3

Various solutions were injected as follow: seawater, aquifer water, deionized water, and sodium sulfate solution (7,120 mg/L). Seawater injection as a secondary mode produced 43.6% OOIP **(Figure VII-7)**. Despite using the same injection fluids and test conditions, the oil recovery results from core–3 and core–1 were different. Therefore, the core

heterogeneity and fluids distribution were significantly affecting the final oil recovery results.

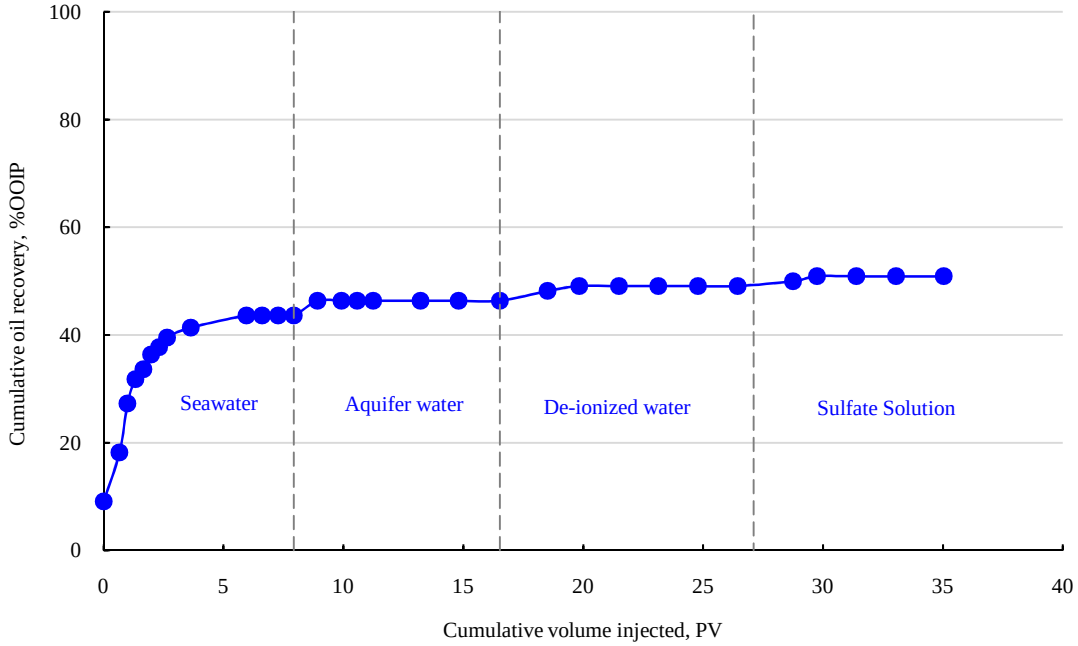

Figure VII-7. Cumulative oil of core−3 (seawater-aquifer-deionized water-sulfate solution).

Aquifer water was injected as a second stage at 0.5 and 1 cm^3/min. to ensure reaching the residual oil saturation. Enough pore volumes of aquifer water were injected (8 PV). The oil recovery increased to 46.4% OOIP confirming the previous findings in core–2. Reversing the dolomite surface charge from positive to negative was the expected reaction mechanism. Recently, deionized water changed the surface charge of carbonate particles toward negative and thus might alter the wettability condition (Chapter II). Results suggested an increase in the oil recovery to 49.1 and 50.9% after

the fresh water and sulfate solutions were injected, respectively. We think the sulfate is not a potential determining ion; therefore it is not affecting the surface charge of the dolomite. It might form a non-specific adsorption, but though the recovery was insignificantly affected. More about specific and nonspecific adsorption phenomena are thoroughly reported in Chapter V.

In general, the trend of the ion analysis matched the original concentration in the injection water. Analysis results suggested no interactions between injection water ions and dolomite rock minerals as depicted in **Figure VII-8**.

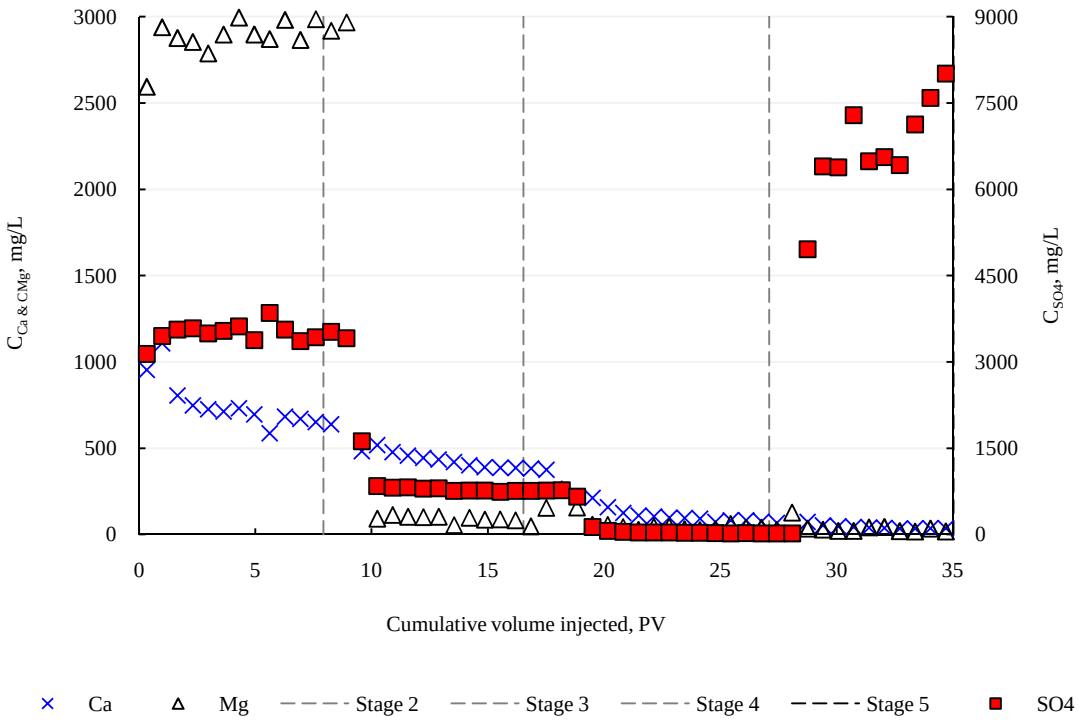

Figure VII-8. Ions analysis of core−3 effluent samples.

Core–4

Formation brine, deionized water, and seawater were injected at a constant injection rate (0.5 cm^3/min.). Enough pore volumes of formation brine were injected (9.4 PV), and recovered 77.1% OOIP, **Figure VII-9**. Compared to the other tests, the oil recovery was higher during the secondary mode injection stage. The injection fluid and connate water had similar salinity and that might be the main reason for getting higher recovery than others. Deionized water was subsequently injected to determine the effect of reducing the salinity on oil recovery. Results suggested no additional oil recovery through the deionized water injection stage. It can be concluded that the electrostatic forces did not affect the residual oil saturation in this test. Increasing the salinity to seawater level increased the oil recovery to 81.4% OOIP. No chemical interactions were observed between the injection water and dolomite rock minerals as depicted in **Figure VI-10**.

Core–5

This test was carried out to confirm the previous finding in Test–4 where formation brine injection produced the highest recovery as a secondary mode. The next fluids were injected at 0.5 cm^3/min.: formation brine, shallow aquifer water, and seawater. Most of the crude oil was recovered (67%) during the first 2 PV.

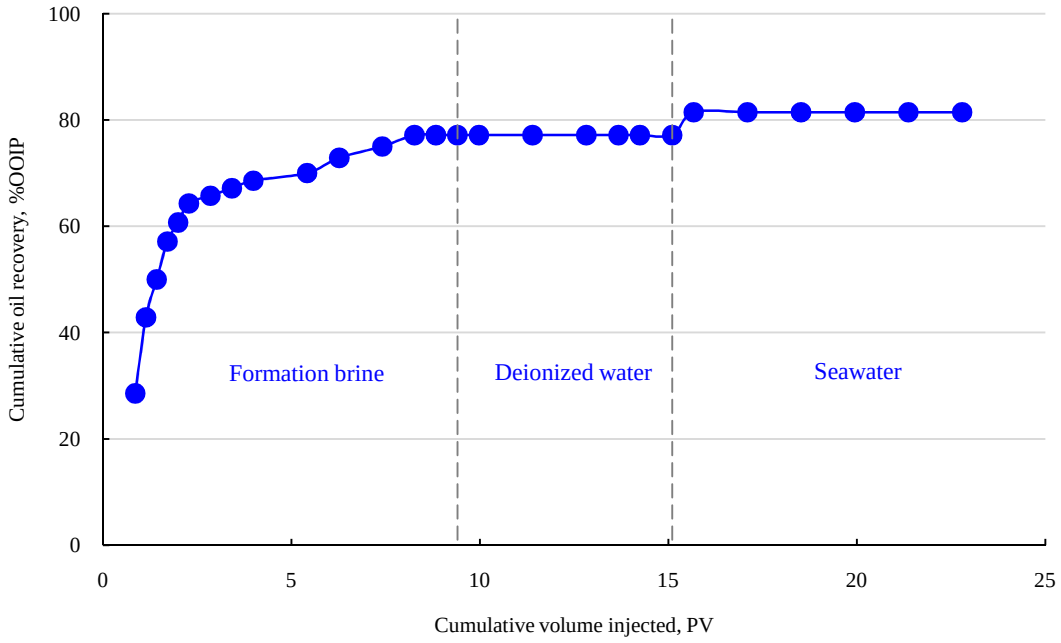

Figure VII-9. Oil recovery of core−4 (formation brine, deionized water, seawater).

After that, the oil production ceased at 71.5% OOIP and 3.9 PV (**Figure VII-11**). Shallow aquifer water was injected at 0.5 cm^3/min for 7 PV without any improvement in oil recovery. Seawater was injected as a third stage for 6.5 PV. As a result, incremental recovery of 1.5% was observed at 15 and 17.3 PV. The cumulative oil recovery, at the end of the seawater injection, was 75% OOIP. No ions interactions were noticed as depicted in **Figure VII-12**.

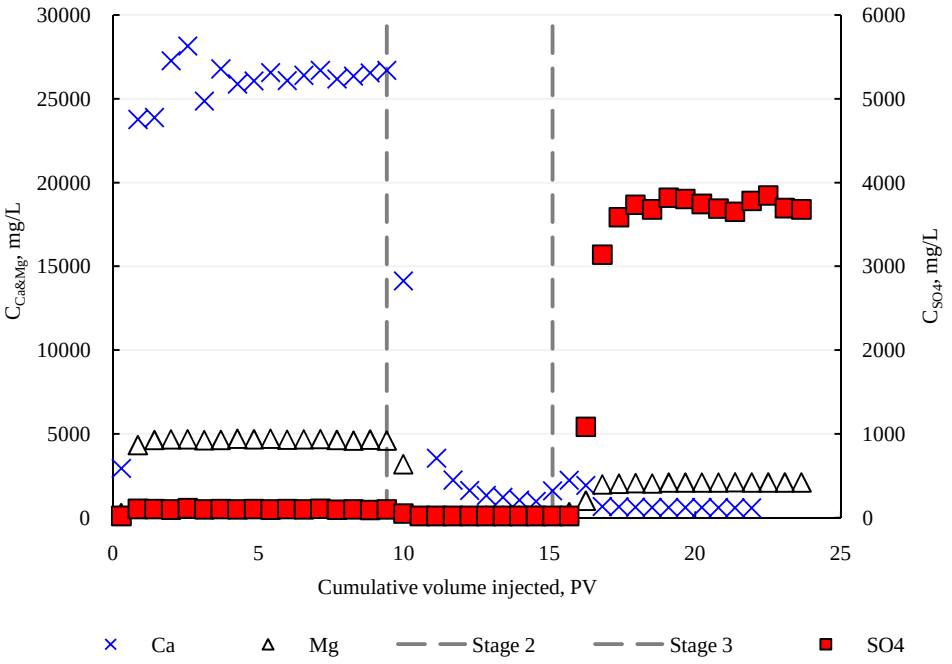

Figure VII-10. Ions analysis of core−4 effluent samples.

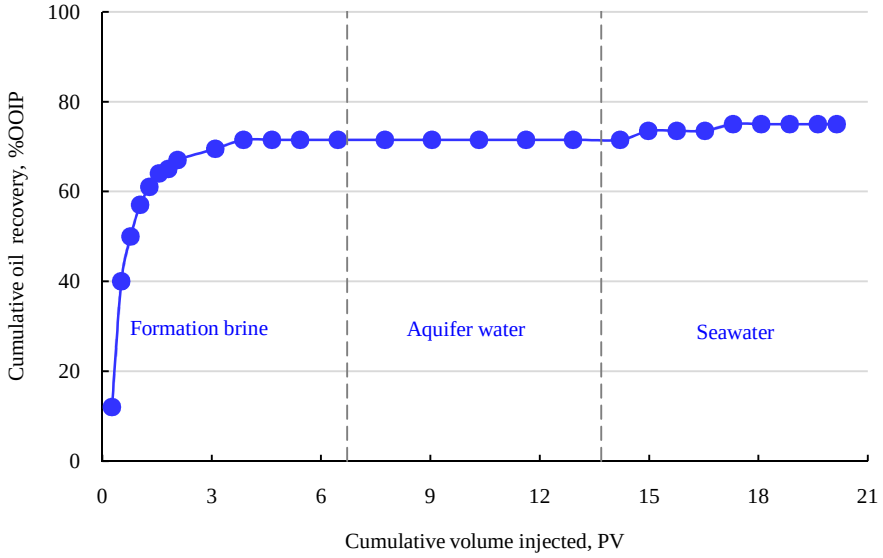

Figure VII-11. Cumulative oil recovery of core−5 (formation brine-aquifer-seawater).

Conclusions

The following conclusions were drawn from this study:

1. Injection of formation brine showed the highest oil recovery in secondary mode tests.
2. Injection of aquifer and seawater also slightly increased the tertiary oil recovery.
3. No ions interactions were observed between dolomite minerals and saline water ions.
4. Deionized water showed mixed results throughout multistage water injection.

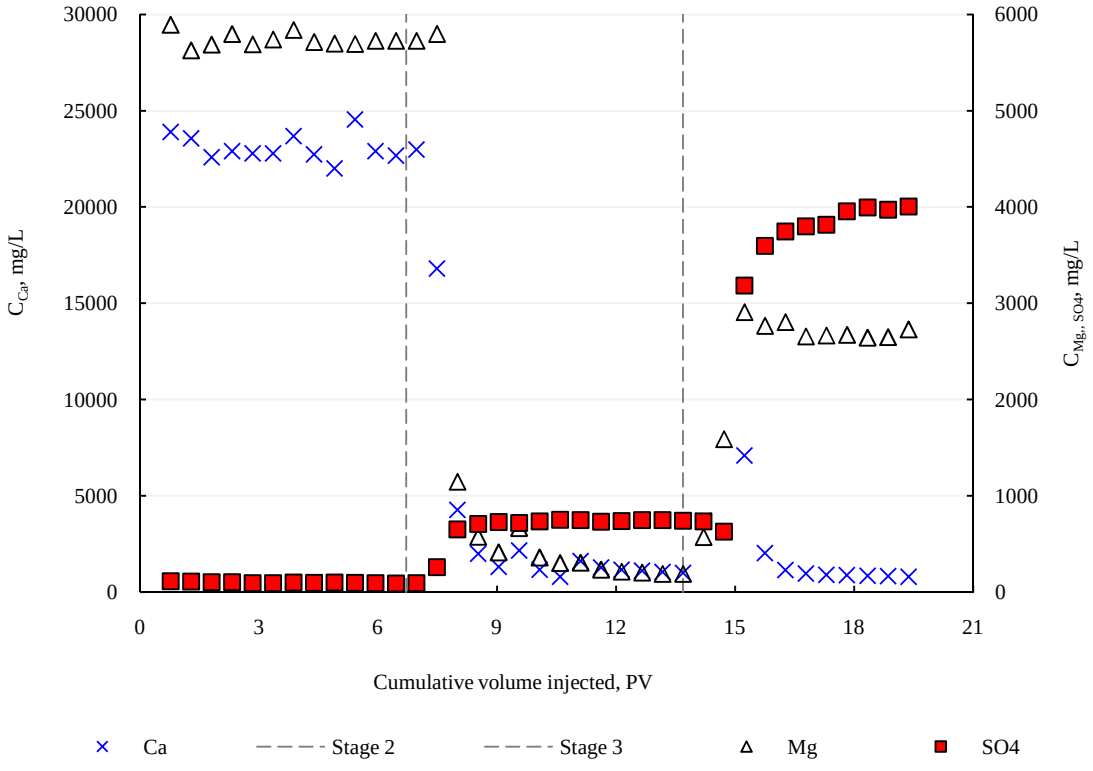

Figure VII-12. Ions analysis of core−5 effluent samples.

CHAPTER VIII

MULTISTAGE INJECTION OF BRINE AND DILUTE SURFACTANT IN VUGULAR DOLOMITE RESERVOIRS

Summary

Salinity of the injection water in carbonate reservoirs is not limited to certain level. Produced water, seawater, shallow aquifer and fresh lake water have been injected in different oil fields. Ions interaction with dolomite minerals, in general, is not investigated in literature especially in heterogeneous reservoirs.

A coreflood study was conducted using up to 50 cm vugular dolomite cores (outcrop samples). A wide range of salinity was tested including: synthetic formation brine, seawater, shallow aquifer water, chemical tracer, and deionized water. In addition, the effect of low salinity water (10 and 50 vol% seawater), cyclic salinity, and various ions (Na, Ca, Mg, SO_4) on the fluids interactions and oil recovery were also studied at 90ºC. After several stages of water injection, the cores were flooded with dilute beatine amphoteric surfactant (0.1 wt%) in presence and absence of HPAM polymer. CAT scan technique was used to monitor fluids propagation inside the core. Water/rock interaction was also examined using rotating disk apparatus at high temperature and pressure condition.

Injection of high salinity formation brine as a secondary mode showed the highest oil recovery. Dilute seawater at 10 and 50 vol% increased the oil production up to 4.7% OOIP. Insignificant change on recovery was reported due to the cyclic salinity

and absence of sulfate in seawater. Insignificant chemical interactions were reported between dolomite minerals and injection brines. Amphoteric betaine surfactant with HPAM polymer enhanced oil recovery up to 21.3%. This study gives new insight on the importance of salinity on oil recovery at high temperatures. Wettability of dolomite cores was apparently altered toward water-wet condition after using dilute surfactant system with and without mobility control fluid.

Introduction

Water injection in carbonate reservoirs essentially depends on the available water resources. Seawater, aquifer, produced water, and even lake water have been injected in different oil fields worldwide. Salinity and ionic strength lately caught scientists' attention, and still questionable especially in terms of chemical interactions between ions, rock minerals, and crude oil components. Temperature, for sure, can affect the kinetic energy and chemical reactions (precipitations, adsorption, ionic exchange…etc).

Rock wettability and heterogenty of the most carbonate reservoirs are strongly affecting the oil production during the primary and secondary recovery process (Chilingarian and Yen 1983). In addition, the fluid variables (viscosity, density, and interfacial tension) and rock petrophysical properties are major factors controlling oil recovery processes in carbonate reservoir (Hobson 1989; Wardlaw 1996). The ionic strength, in general, is slightly affecting the IFT properties of crude oil/water system (Chapter IV).

The specific objectives of this chapter are to: 1) determine the effect of individual ions (Na^+, Mg^{2+}, Ca^{2+}, SO_4^{2-}) in seawater on oil recovery using long vugular dolomite cores, 2) study the impact of salinity (high-low-high) and dilute seawater (10 and 50 vol%) on oil production at 90ºC, and 3) investigate a new betaine amphoteric surfactant at low concentrations (0.1 wt%) with and without HPAM polymer in high salinity environments. Surfactant and polymer concentrations were identical in two tests to determine the influence of the rock heterogeneity on the recovery performance. The core length might eventually affect other important factors such as: 1) the errors of the capillary end effects which are common in the short core tests, and 2) the residence time of the fluids inside the core and perhaps the chemical interactions.

This work adds new findings on the role of salinity, dilute surfactant and surfactant/polymer solutions on oil recovery. The new findings were also supported with full chemical analysis of the major ions (Ca, Mg, SO_4) in the core effluent. Computerized axial tomography and visualization technique was also applied to understand the displacements characteristics of the fluids inside the dolomite cores.

Literature Review

Vugular dolomite rock

Dolomitization of limestone rocks develops a secondary network of fractures and vugs, in addition to the primary pore system (Ehrlich 1971). The flow properties in the secondary pore system are quite different than the primary ones. Vugs can be either connected to the major fracture system or isolated in the matrix rock (Kossack and

Gurpinar 2001; Zhan-guo and Jun 2009). The vugs that are located in the matrix vary in size, shape, orientation, and connectivity (Domingo 1996). Capillary forces have no effect on the oil flow from the vugs, because the vugs have zero capillary pressure. Viscous and gravity forces will act to displace the oil from the vugs (Kossack and Gurpinar 2001). In addition, various factors are affecting the displacement mechanisms such as the density difference between the fluids, the vertical height of the vugs and the matrix permeability.

Water salinity

Water salinity was extremely investigated in sandstone reservoirs at different percent of clays content and reservoir conditions (Lebedeca *et al.* 2009; Alagic and Skauge 2010). In carbonate reservoirs, some researchers investigated the influence of SO_4, Ca, and Mg ions in seawater on oil recovery (Strand *et al.* 2003; Webb *et al.* 2005; Strand *et al.* 2006; Zhang *et al.* 2007). These investigations were conducted in short limestone and chalk cores (length up to 7.5 cm). Salinity adjustment can impact the attraction and repulsion forces (van deer Waals, diffuse double layer, and Boron forces) with rock mineral (Schembre and Kovscek 2005). Other forces such as hydration, hydrodynamic and structure forces are usually considered negligible (Khilar and Fogler 1984).

In chalk formations, it was previously believed that SO_4^{2-} ions altered the surface charge from positive to negative (Zhang *et al.* 2007). But, this mainly depends on the connate water composition especially the concentration of the divalent ions. Most crude oil/water interfaces are negatively charged because of the carboxylate group (Chapter

III). Therefore, repulsive forces are dominant between SO_4 ion and crude oil layer in the oil-wet carbonate system. In the absence of crude oil, adsorption ratio of Mg/Ca on dolomite from seawater was 3 times larger than calcite at atmospheric condition (Mucci and Morse 1985). In short, the interactions mechanisms between injection water and carbonate minerals are still ambiguous. The surface charge of dolomite is different than limestone simply because of Mg ions incorporation in the structure (Farooq *et al.* 2011). Therefore, the fluid/rock interactions are expected to be different (Vdović 2001).

Spontaneous imbibition tests on Middle Eastern limestone cores were reported using three different molar ratios of SO_4/Ca (2.73, 8.2, 27.3) prepared in fresh aquifer water (Ligthelm *et al.* 2010). The last two solutions were spontaneously imbibed after formation brine, and as a result the oil recovery increased up to 5% OOIP at 60ºC. Calcium content was reduced to avoid exceeding the solubility constant of $CaSO_4$. The ultimate oil recovery, from three different Amott tests, was lower than 20% OOIP. It indicates the limestone wettability was still within either intermediate or oil-wet condition.

Amphoteric surfactant/polymer

Divalent ions and reservoir temperatures are the most challenging issues in EOR process (Jamaloei and Rafiee 2008). Divalent ions can also associate with the surfactant and cause precipitation or partition to the oil phase (Green and Willhite 1998). Researchers designed various amphoteric surfactants that can work in harsh environments (Maddox

and Tate 1977; Kumar *et al.* 1984; Kalpakci and Chan 1985; Berger and Lee 2002; Berger and Berger 2009).

In fractured carbonate reservoirs, dilute amphoteric surfactants were tested as secondary and tertiary recovery using limestone cores at high temperature and salinity conditions (Aoudia *et al.* 2010b). Aoudia and his coworkers presented various IFT screening tests and short limestone coreflood studies (L= 7.6 cm).

Wang *et al.* (2010) evaluated various surfactants including betaine amphoteric. Betaine surfactant/polymer system surprisingly matched ASP performance in terms of oil recovery. Indeed, ASP flooding depends on the crude oil properties especially the acid number. Moreover, excluding the alkali metals can reduce scale and corrosion issues that are commonly associated with ASP flooding (Jirui *et al.* 2001). Adsorption studies were also conducted using anionic and amphoteric surfactants and different rock minerals (Mannhardt *et al.* 1992; Weifeng *et al.* 2011).

Polymer is usually mixed with surfactant solution to provide mobility control and reduce water fingering issues especially in the field (Schumacher 1978). Polysaccharide and polyacrylamide polymers are commonly used in EOR process such as xanthan gum, and partially hydrolyzed polyacrylamide (HPAM), **Figure VIII-1** (Littmann 1988; Sorbie 1991). The later is negatively charged while xanthan gum is anionic (Shupe 1981). Due to the high cost of xanthan gum polymer, HPAM has been used in about 95% of the field polymer flooding (Lake 2010).

The hydrolysis process of the HPAM causes the anionic carboxyle groups ($-COO^-$) to be scattered along the backbone chain (Lake 2010). For that reason, the

polymers are called HPAM. The degree of hydrolysis (DOH) range is between 30 and 35% of the acrylamide monomers, which eventually affect the polymer physical properties. Optimizing certain properties such as water solubility, retention, and solution viscosity can be performed through the DOH factor. If the DOH is too large, the properties of the polymer solution will be sensitive to salinity and hardness (Shupe 1981). On the other hand, the polymer will not be water soluble if the DOH is too small.

The high molecular weight and the created repulsion between polymer molecules and the segments causes elongation to the polymer structure which definitely affect the viscosity results (Lake 2010). The polymer molecules will coil up if the brine salinity is high and that also decreases the repulsion forces between molecules through ionic shielding. The ionic shielding can cause precipitation and thus reduces the effectiveness of the polymer.

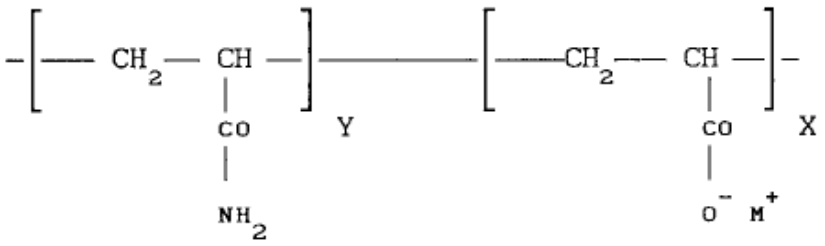

Figure VIII-1. Molecular structure of HPAM, M^+ denotes K^+ or Na^+ while X and Y are the number of the carboxylate and amide groups (from Nasr-El-Din *et al.* 1991).

Experimental Studies

Materials

X-ray diffraction analysis test showed identical d-spacings to the original dolomite mineral, **Figure VIII-2**. Long dolomite cores (L~ 39 to 50 cm) were used to avoid capillary end effects that are usually common in the short length cores. Description of dolomite core was previously reported in Chapter VII.

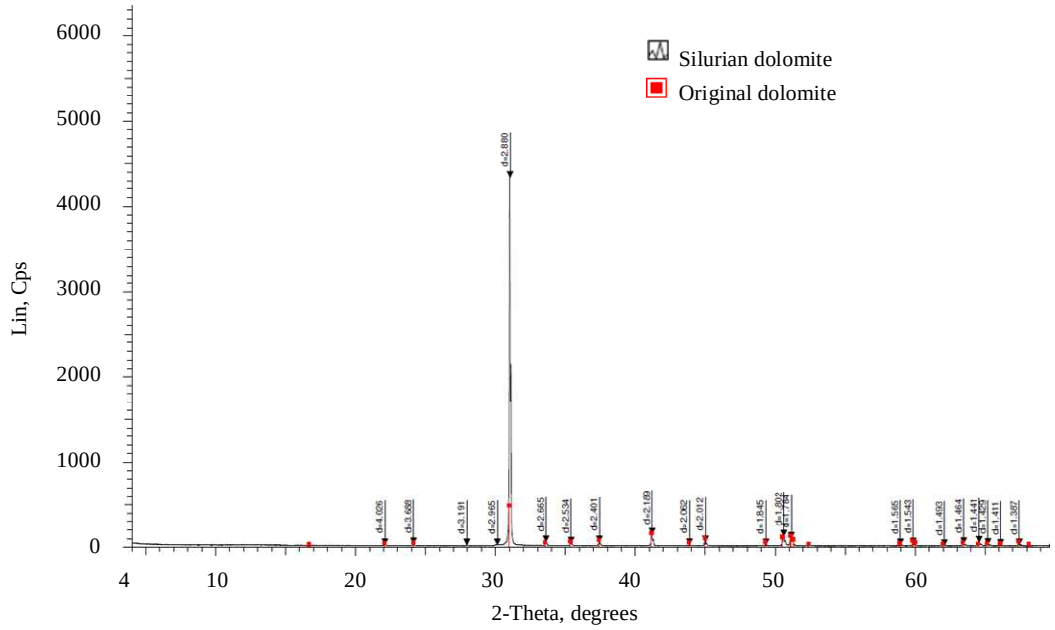

Figure VIII-2. X-ray diffraction of Silurian dolomite sample.

Fluids

Table II-1 shows the brine compositions that were used throughout this study. Seawater composition was tuned via excluding individual ion (Na, Ca, Mg, and SO_4) to determine its impact on fluids/rock interactions and oil recovery. In addition, seawater was diluted

at two ratios (50 and 10 vol%) using deionized water. A dopant (KI) was mixed with deionized water at 5, 7 and 10 wt% to track fluids movement in the core.

A new class of amphoteric surfactant (alkyl dimethyl betaine: $RN^{+}(CH_3)_2 CH_2 COO^{-}$) was at a low concentration of 0.1 wt% (Berger and Berger 2009). More detail about this surfactant was previously reported in Chapter V.

Partially hydrolyzed polyacrylamide (HPAM) polymer is commonly used in EOR processes (Delshad *et al.* 2008). This polymer was mixed with and without surfactant at 0.3 wt% to improve fluids' mobility. The molecular weight and degree of hydrolysis of the HPAM polymer are 20 million Daltons and 30%, respectively.

Apparatus and procedure

Core flood. The setup consists of 50.8 cm stainless steel core holder, accumulators, syringe and hand pumps, and various gauges and regulators to observe and control the pressure with time. It was exactly similar to the short core setup that was described earlier in Chapter VI, but with longer core holder and bigger oven size. Dolomite cores were air vacuumed for at least 12 hrs; then they were saturated in formation brine, Table II-1. The base permeability was determined at ambient temperature and injection rates 0.5, 1, and 2 cm^3/min. Crude oil was injected at various rates 0.25, 0.5, 1 and 2 cm^3/min until the irreducible water saturation was reached. Then, the cores were aged for 30 days in a steel pipe (ID= 10 cm, L= 61 cm) filled with crude oil. The aging temperature was 90ºC simulating a Middle East reservoir condition, while the pressure was at

atmospheric condition. The petrophysical properties of the core plugs are shown in Table VIII-1.

Table VIII-1. Petrophysical properties of long dolomite cores.

Core ID	Diameter	Length	Porosity	Base Permeability	Irreducible water saturation
	cm	cm	%	md	%
Dol–1	3.8	43.2	22.7	1308.6	31.4
Dol–2		39.4	16.3	202.1	31.6
Dol–3		50	18.8	721.4	34.3

CAT-scan. The used CAT-scan is a fourth generation universal HD 200 system. It uses X-Ray technology and computerized mathematical algorithms to reconstruct an object from a series of plane cross-sectional images made along an axis (Akin and Kovscek 2003). The CAT number is usually calculated from the intensities of the incident and detected X-Ray beams (Wellington and Vinegar 1978). The cores were CAT scanned after the oil saturation step and at the end of chemical flooding as will be shown in the results section. Potassium iodide was used as a dopant to improve the attenuation coefficients contrast between crude oil and brine solutions. The propagation of the fluids in the core was analyzed based on the CAT numbers.

Due to some limitations in the used CAT machine, the scanning process was conducted immediately after completing the saturation and chemical flooding stages. Cross sectional scans were made at regular intervals (slice thickness = 2 mm, index = 5 mm). Medical image process and visualization (MIPAV) software was utilized to process the core images at different axis.

Rotating disk reactor. This reactor was used to determine the reaction kinetics at elevated temperatures and high pressures conditions (Fredd and Fogler 1998). It consists of reactors and reservoir vessels, rotation system, and various switches and valves to control rotation speed, temperature and pressure conditions, Figure VIII-3. A dry dolomite disk sample (ID = 3.8 cm, h = 2.5 cm) was first attached to the core holder using shrinkable Teflon tube and then screwed to the rotator assembly. A seawater solution was poured in the reservoir and then transferred to the reactor at temperature and pressure of 130ºC and 700 psi, respectively. The temperature was higher than that in coreflood tests simply because most carbonate/seawater interactions were reported to occur above 100ºC (Strand et al. 2006). The rotation speed of the core sample was maintained constant at 500 rpm. Core effluents were collected every 2 min. for 30 min. to determine ions concentration with time.

1. Reactor vessel
2. Reservoir vessel
3. Reactor stirring system
4. Rotation speed controller
5. Temperature controller
6. Pressure regulator system
7. Fraction collector
8. Core holder
9. Rock sample

Figure VIII-3. Rotating disk reactor setup.

Results and Discussion

Interfacial tension

The interfacial tension of two alkyl dimethyl betaine surfactants (0.1 wt% in seawater) were determined using spinning drop tensiometer model 500 (University of Texas at Austin, Texas) at different temperatures (Gardner and Hayes 1981). The first surfactant (I)/crude oil system showed ultralow IFT beyond the detection limit of the spinning drop tensiometer. Ultralow IFT was observed at the oil/water interface, which subsequently formed microemulsions, **Figure VIII-4**. Several trials were conducted to confirm this up-normal behavior. The crude oil droplet breaks up was one of the difficulties in using the spinning drop technique (Cayias *et al.* 1975). Similar IFT behavior was also observed by Aoudia *et al.* (2010a).

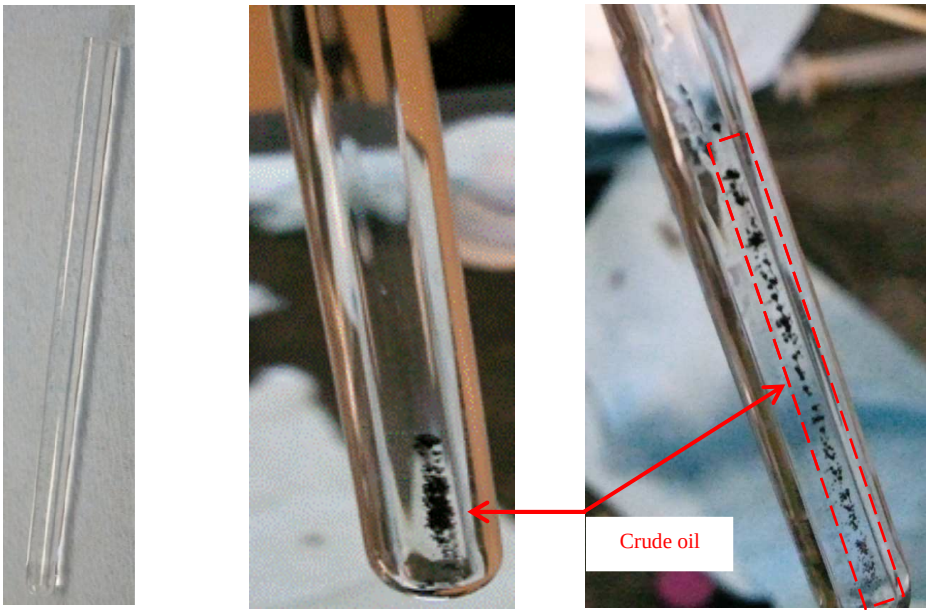

a) Surfactant I in seawater solution b) Oil droplet at the beginning c) Oil droplet after 30 sec.

Figure VIII-4. Images of amphoteric surfactant I in a glass tube at atmospheric condition.

Interfacial tension between crude oil and surfactant II in seawater was determined at a constant concentration (0.1 wt%) and different temperatures (28, 61.6, and 80ºC). An abrupt IFT decrease was reported at 28ºC from 0.009 to 0.0022 mN/m, **Figure VIII-5**. The systems reached equilibration almost after 42 min. at 0.0002 mN/m. Raising the temperature condition to 61.6 and 80ºC increased the IFT values to 0.0016 and 0.0025 mN/m accordingly. The increasing trend in the IFT values of crude oil/surfactant II with temperature was also reported by Aoudia *et al.* (2010b).

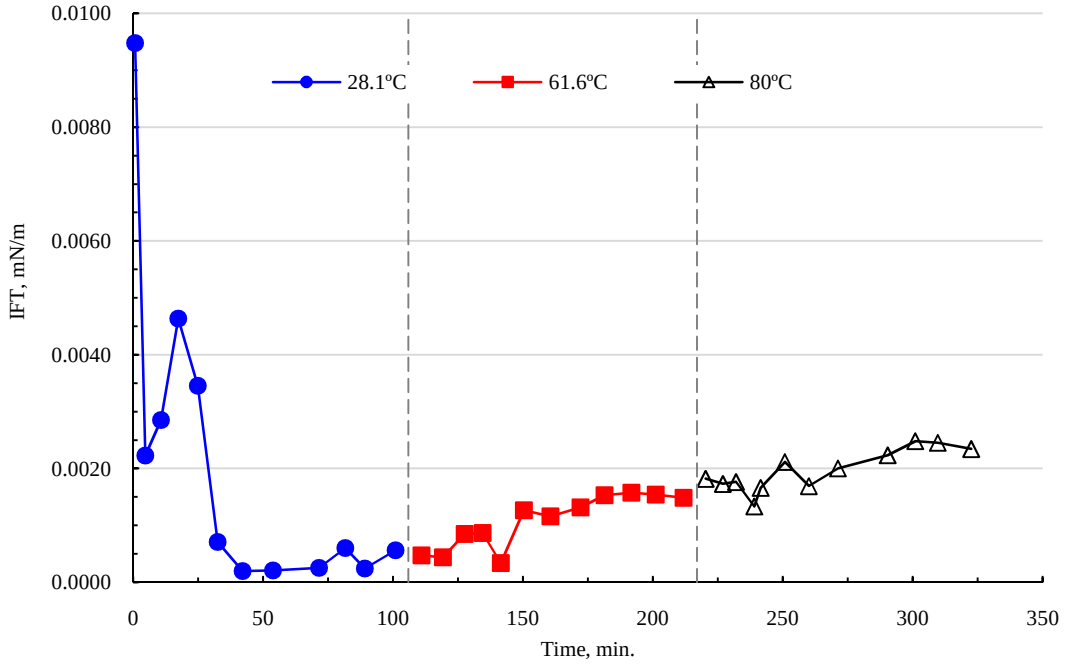

Figure VIII-5. IFT measurements of crude oil/surfactant II (0.1 wt%) in seawater with time at temperatures 28.1, 61.6 and 80ºC.

Dolomite–1

The objective of this test was to investigate the effect of individual ions in seawater such as Na, Ca, Mg, and SO_4 on oil recovery. Seawater was injected as a secondary mode until the oil recovery stabilized at 42.6% and 3.2 PV, **Figure VIII-6**. The injection rate was maintained constant at 0.5 cm^3/min. Excluding Na, Ca, and Mg ions from seawater did not affect the interactions and perhaps the oil recovery. Sodium is a monovalent ion and can be weakly bonded at the mineral/water interface (Möller and Werr 1972). For that reason, Na is expected to have a negligible effect on the fluids/rock interactions. But, Ca and Mg consider potential determining ions to dolomite and even though no change on recovery was reported. It might be due to two reasons: 1) strong capillary

forces, 2) divalent ions concentration in seawater was not enough to cause interactions and eventually decrease the residual oil saturation (< 0.3%). Insignificant increase in the oil production was observed after excluding the SO_4 ions from seawater and after injecting 10 vol% seawater. Increasing the concentration of the water molecules altered the dolomite surface charge towards negative (Chapter II). As a result, repulsive forces were created between the carboxylate group in crude oil and dolomite minerals and thus slightly increased oil production. In short, the effect of salinity on solution viscosity and IFT is considered insignificant. For that reason, more than 50% of the oil was unrecovered in this test.

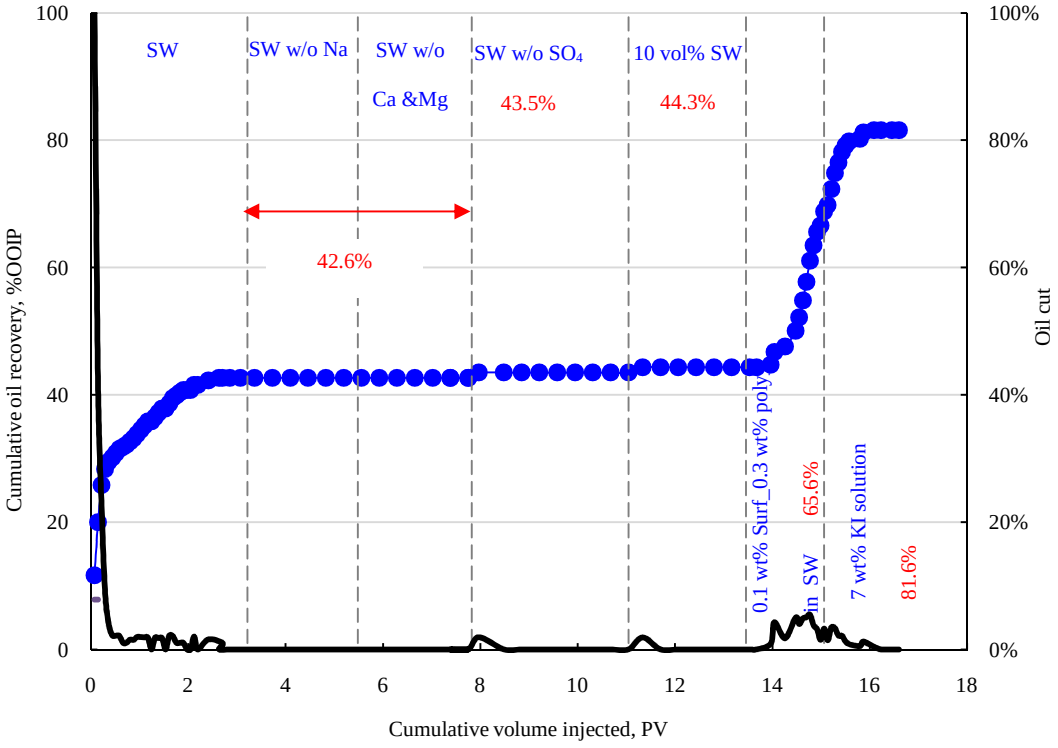

Figure VIII-6. Oil recovery during multistage water injection and dilute surfactant in seawater (dolomite–1).

Chemical flooding using 0.1 wt% surfactant and 0.3 wt% polymer in seawater was performed at 0.18 cm^3/min. A continuous oil bank was reported throughout 1.6 PV. In addition, the oil recovery increased linearly from 44.3 to 65.6% OOIP which essentially attributed to the increase in the capillary number. KI solution (7 wt%) was injected in the last stage to displace all mobile oil at higher rates (0.5 and 1 cm^3/min). The oil recovery increased accordingly to 81.6% OOIP, **Figure VIII-6**. The core was then CAT scanned but unfortunately there was no enough intensity difference between the images followed oil and chemical/tracer flooding stages. For that reason, the tracer concentration was increased further to 10 wt% in the next test.

Cation and anion analyses of the aqueous core effluents were conducted as shown in **Figure VIII-7**. Results suggest a good match between the concentrations of the ions in the core effluents and that of the original solutions. Likewise, the concentration of cations in the chemical slug stage stabilized at seawater level. It implied no divalent ions were precipitated or partitioned to the oil phase. In summary, the chemical interactions between electrolyte solution ions and dolomite minerals were not observed.

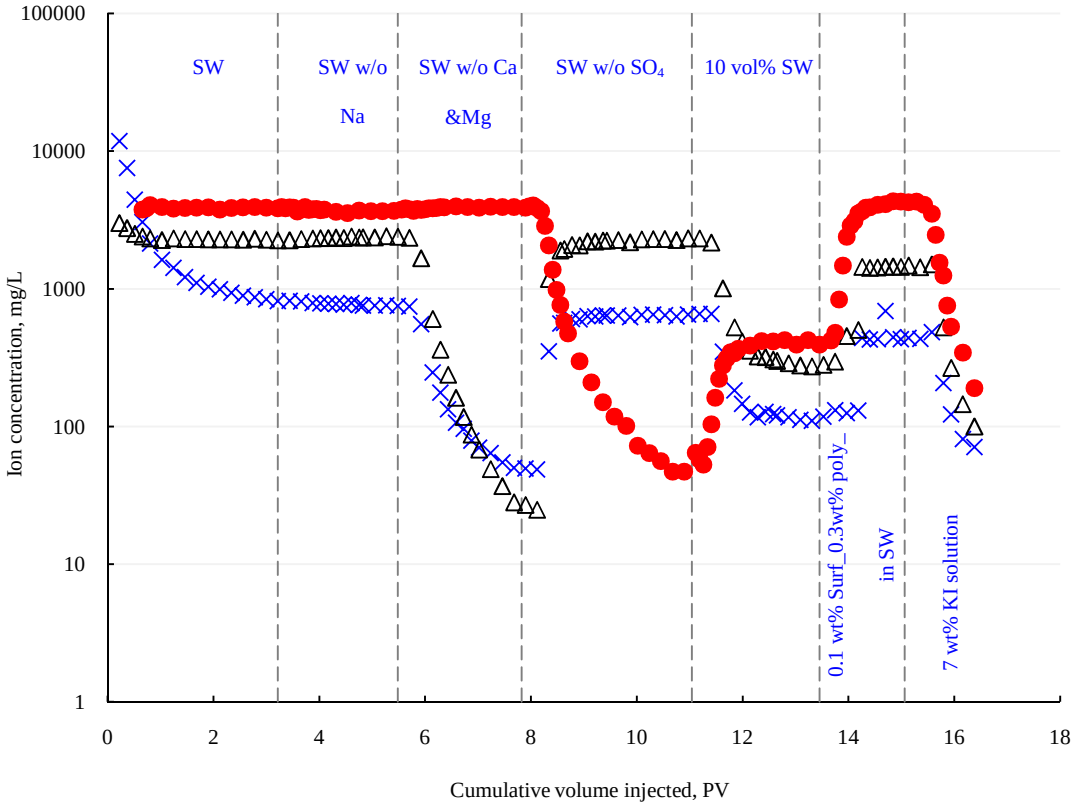

Figure VIII-7. Ions analysis of core effluent during multi saline water and surfactant/polymer flooding (dolomite–1).

Waterflooding using various saline solutions showed a maximum differential pressure of 5 psi, **Figure VIII-8**. During the chemical flooding stages, the pressure drop increased gradually to 15.9 psi at 0.18 cm^3/min. This was attributed to the macromolecule size of the HPAM polymer in the chemical slug. The last injection stage of KI brine decreased the pressure drop to 2.6 psi at injection rate of 0.5 cm^3/min.

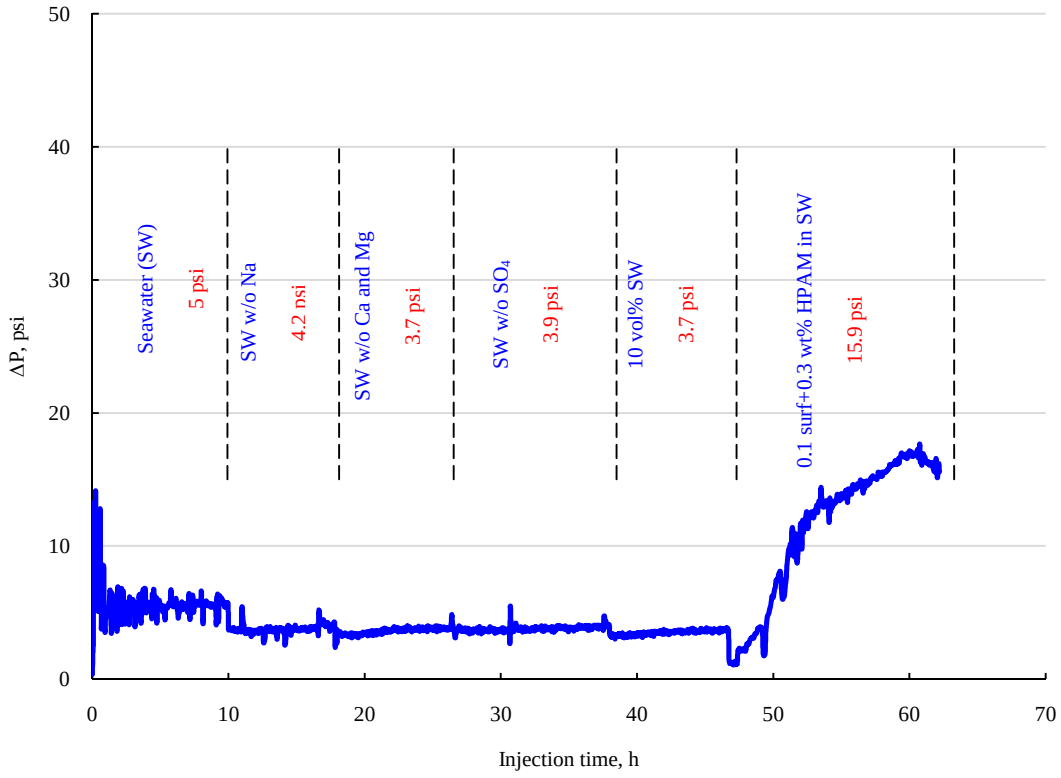

Figure VIII-8. Pressure profile during water and dilute surfactant flooding (dolomite–1).

Dolomite–2

Various saline solutions were injected as follow: seawater, 50 vol% seawater, 10 vol% seawater, shallow aquifer water, and formation brine. The goal of this test was to determine the influence of cyclic salinity injection on oil recovery. In addition, seawater salinity was gradually decreased to 50 and 10 vol%. Lowering the salinity level can affect the ions interactions and perhaps expand the diffuse layer thickness. Also, it increases the concentration of water molecules and decreases the level of ions which proved previously to alter the carbonate surface charge from positive to negative (Farooq

et al. 2011). Seawater injection as a secondary mode showed 54% of OOIP during 3.8 PV, **Figure VIII-9**. The injection rate was increased from 0.5 to 1 cm^3/min. at PV 2.9 to ensure the residual oil saturation stage was achieved. Dilute seawater (50%) was injected at 0.5, 1 and 2 cm^3/min, and PV 7.6 and 8.5 for the last two injection rates. The oil recovery increased to 56 and 58.5% at PV 4.37 and 8.8, respectively. Hydration the rock surface and oil/water interactions produced additional 3.5% of the OOIP. Increasing the hydroxide ions in the solution apparently increased the electrostatic interactions with dolomite surface and altered its surface charge toward negative.

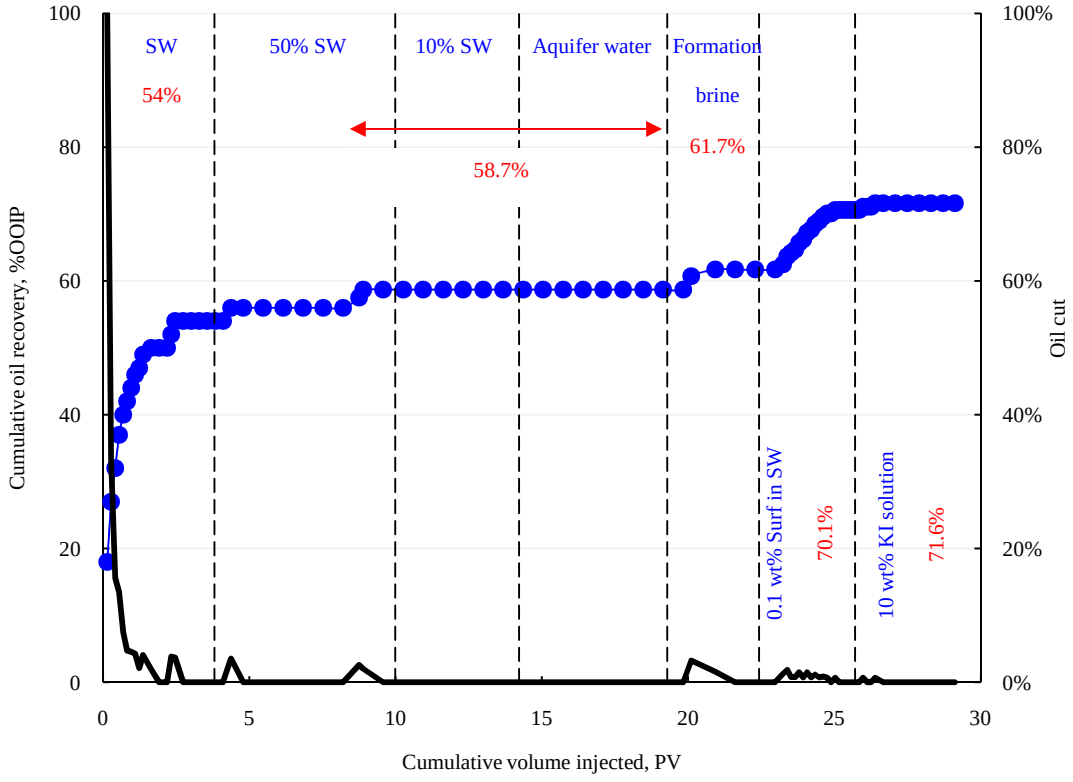

Figure VIII-9. Oil recovery of multistage waterflooding and dilute surfactant in seawater (dolomite–2).

Reducing the salinity to 5,400 mg/L (10 vol% seawater and aquifer water) in the third and fourth injection stages did not affect the residual oil saturation. Moreover, cyclic salinity (high-low-high) was tested by injecting formation brine afterward at 0.5 and 1 cm^3/min. As a result, the oil recovery increased by 2 % but the exact mechanism is still unknown and deserve further investigations. In carbonate rocks, it is believed the surface charge is positive due to the specific adsorption of Ca ions from formation brine on the rock surface (Huang *et al.* 1991). Microscopic studies using contact angle at high temperature showed that increasing the salinity from deionized water to formation brine (230K mg/L) did not alter the wettability condition of the rock substrate (Chapter V).

Dilute surfactant (0.1 wt% in seawater) was then injected without HPAM polymer. In this test, the polymer was excluded to determine the role of ultra-low IFT (capillary forces) on recovery and avoid any interference between the surfactant micelles and polymer molecules. The dilute surfactant solution was injected at low flow rates (0.25 and 0.5 cm^3/min.) for 3 PV. The injection rate was increased to 0.5 cm^3/min at PV 25.3. As a result, the oil recovery increased linearly to 70.1% OOIP and formed a continuous oil bank as shown in **Figure VIII-9**. This implied that capillary forces are more important than the viscous forces in displacing the trapped oil (Patel and Greaves 1987). The chase brine (10 wt% KI solution) was then injected at 0.5 and 1 cm^3/min to displace all mobile oil (71.6% OOIP).

Core effluent analysis of Ca, Mg, and SO_4 ions are displayed in **Figure VIII-10**. Overall, no chemical interactions were observed between injection water ions, connate water ions, and rock minerals. The first collected samples showed a higher cation

concentration than that of the injection solution. This was expected because seawater first displaced the connate formation brine. The concentrations of the ions were leveling out, accordingly. During dilute surfactant flooding stage, the divalent ions concentrations in the aqueous effluent samples matched the original ion concentrations in seawater. Hence, this result confirmed no divalent ions precipitation was observed.

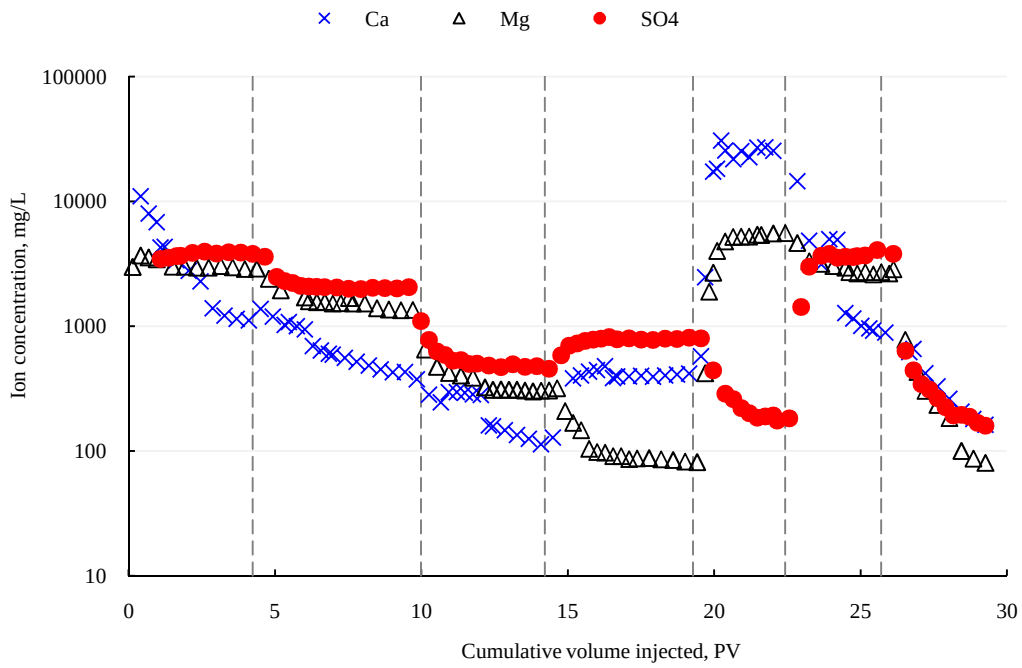

Figure VIII-10. Ions analysis of core effluent during multi saline water and dilute surfactant flooding (dolomite–2).

Computerized axial tomography (CAT) scans were conducted followed oil saturation and surfactant flooding stages to find out the swept areas in the core. In Chapter VI, the images of dry dolomite cores showed to be vugular and heterogeneous. Due to some limitations in the CAT scan apparatus, the scanning process was performed after completing the oil saturation and the surfactant flooding stages. This core had

scattered vugs, but they were not connected unless through microfractures which cannot be detected unless using micro CAT scan technique, **Figure VIII-11**.

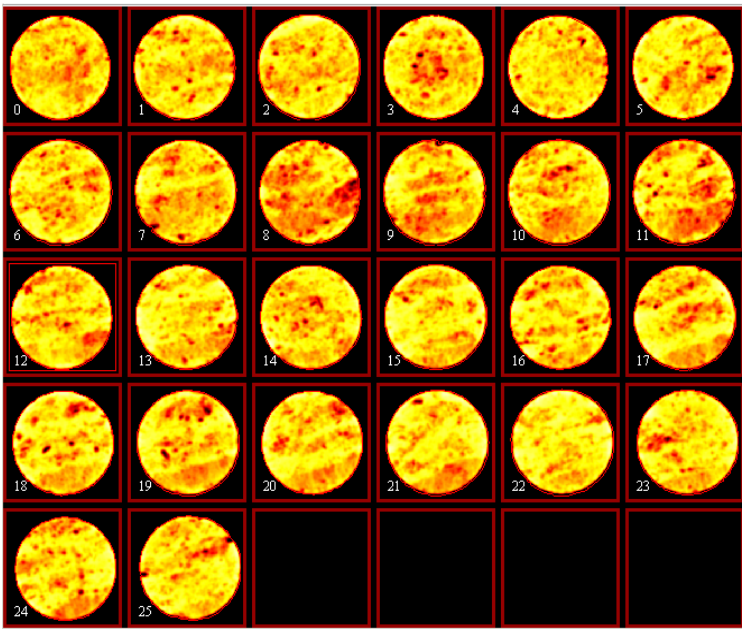

a. Image slices

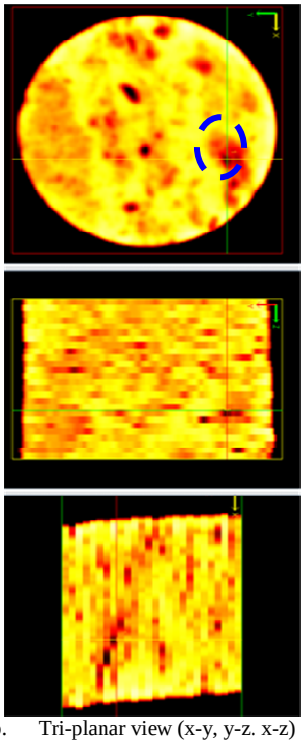

b. Tri-planar view (x-y, y-z. x-z)

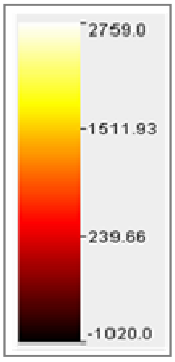

c. Intensity range

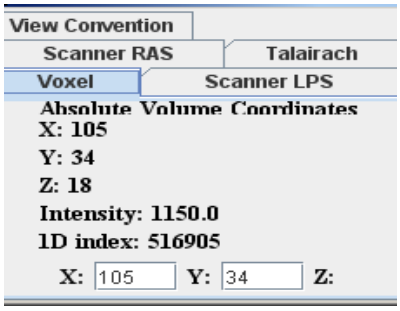

d. Volume coordinates and intensity of slice no. 18 (8.7 cm)

e. CAT scan setup

Figure VIII-11. CAT scan images of core slices along with tri-planar view, dolomite–2 after oil saturation stage.

To confirm if the vugs were connected through fractures or not, a small area around an individual vug in slice no. 18 was selected and extended along the core. After that, the average CAT number was determined as depicted in **Figure VIII-12**. The vugs were continuous for only a short distance in slice 18 and 19 (< 4 cm). The CAT numbers of the injection fluids and dolomite rock are shown in **Table VIII-2**.

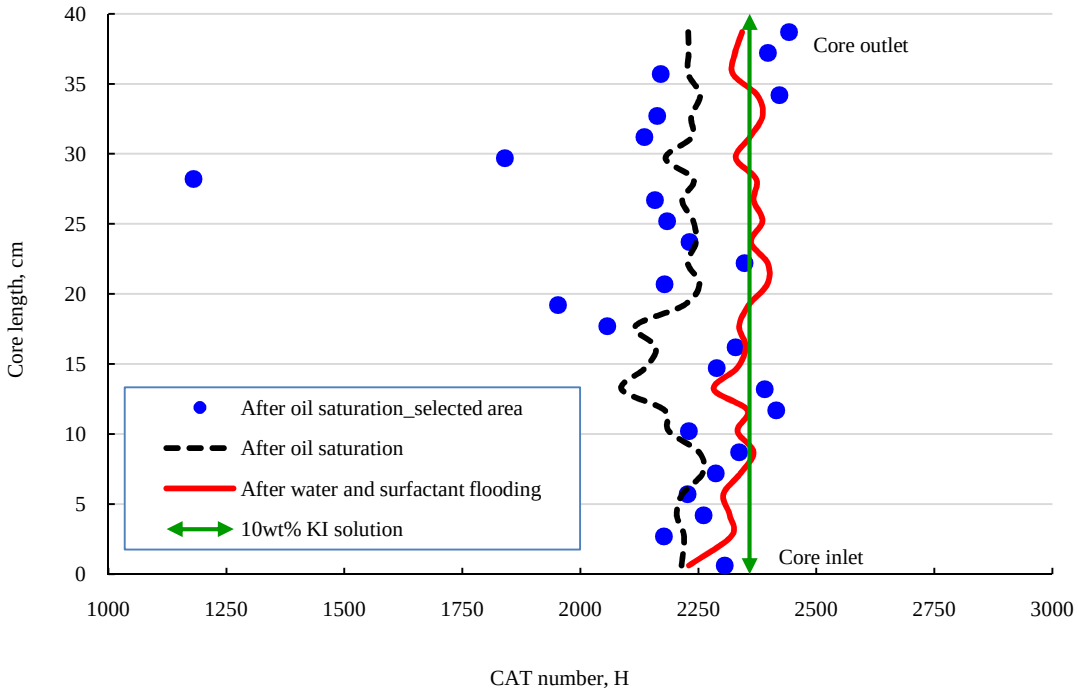

Figure VIII-12. CAT scan images of core–2 following oil saturation and dilute surfactant flooding.

Figure VIII-12 also describes the average CAT number profiles after the crude oil flooding and water/dilute surfactant injection stages. The analysis of CAT images shows the first 7 cm of the core had lower CAT number lower than that of KI tracer fluid. Some areas were not completely swept after the water and surfactant flooding, and

that justified the noticeable drop in the CAT number near to the core inlet. The iodide analysis in **Figures VIII-13 and VIII-14** shows no breakthrough of the tracer solution which indicates that most of the vugs in the core were isolated and not connected.

Table VIII-2. CAT numbers of dolomite rock and various fluids.

Fluid	Dolomite rock	Formation brine	Crude oil	10 wt% KI solution
CAT number, Hounsfield	2332	435	-135	2358

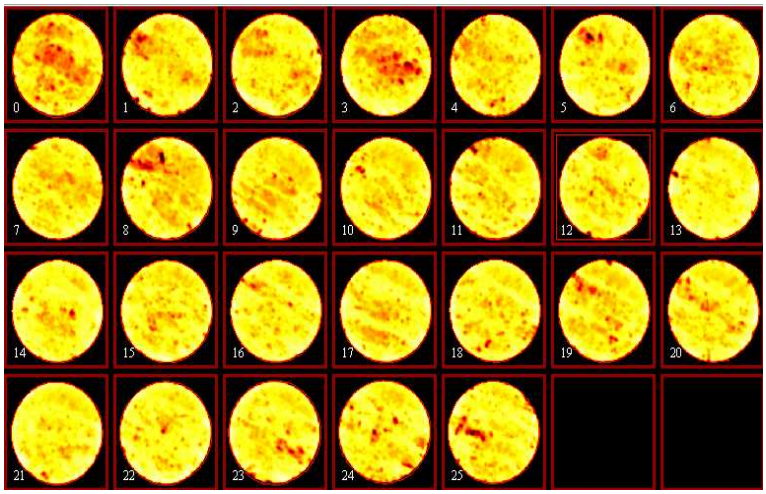

a. Image slices

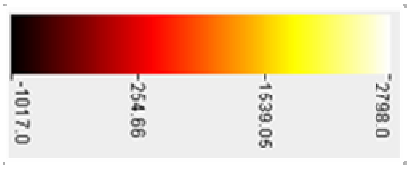

b. Intensity range

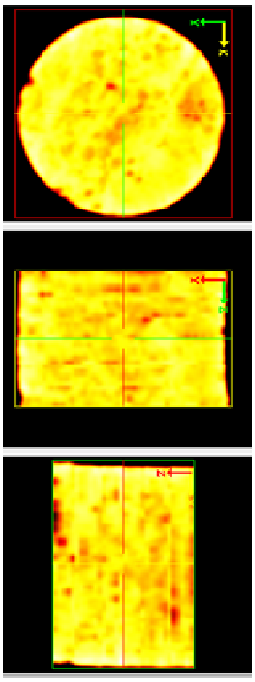

c. Tri-planar view (x-y, y-z. x-z)

Figure VIII-13. CAT scan images for core slices along with tri-planar view, test D–2 after water and surfactant flooding.

Additional analysis was conducted to determine the length of the vugs in slice no. 18 (L = 28.2 cm) and also to confirm the previous CAT number results, **Figure VIII-14**. It is worth noting the calculated CAT number was the average for the each slice which included fluids (oil, water, and chemicals), rock matrix and scattered vugs.

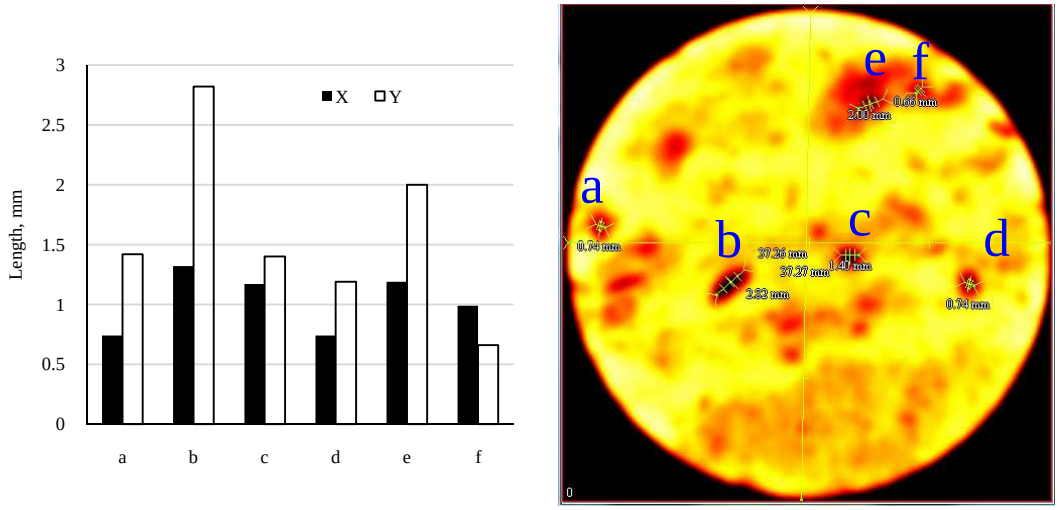

a. More details on vugs length at core length 28.2 cm (slice no. 18), dolomite–2

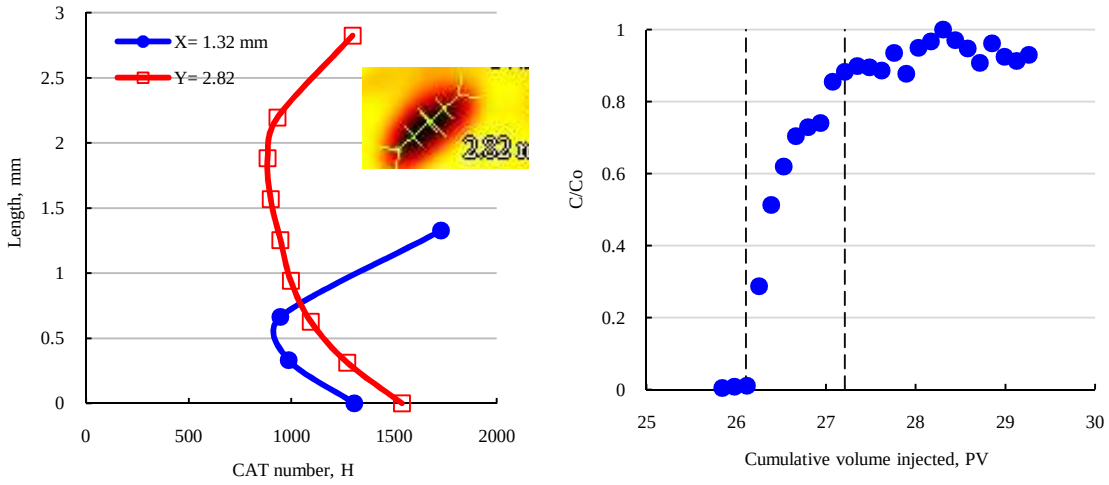

b. CAT number for vug (b) at different dimensions

c. Concnetration ratio of potassium iodide in core effluent (dolomite–2)

Figure VIII-14. Vugs dimensions (slice no. 18) and KI tracer concentration ratio of effluent samples.

The length of the vugs in the x-y dimension was observed between 0.66 to 2.82 mm. Also, the CAT numbers decreased as moving towards the rock matrix from the center of the vugs. This was expected because the dolomite rock had higher CAT number than that of the reservoir fluids in the scattered vugs (Akin and Kovscek 2003). Based on the CAT analysis, the dolomite rock is classified as a vuggy-no filling (Walschmidt *et al.* 1956).

Dolomite –3

The following brines were injected in this test: formation brine, seawater 1 (SO_4= 108 mg/L), regular seawater, seawater 2 (Ca= 2279 mg/L, Mg= 664 mg/L), and seawater 3 (Ca=Mg= 2279 mg/L). The ions in the parentheses were adjusted from the original seawater composition to determine their effect on the interactions. Oil recovery after formation brine flooding reached 57.7% OOIP at 2.6 PV, **Figure VIII-15**.

In addition, the water breakthrough was noticed after 1.3 PV. The connate water film and injection brine had similar chemistry, and this could be the reason for having higher oil recovery. The calcium concentration in formation brine was very high (29,760 mg/L). Therefore, the flood front between formation brine and seawater can form $CaSO_4$ scale. For that reason, the sulfate concentration in seawater was decreased to 108 mg/L which matched also the SO_4 level in formation brine. More than 2 PV of seawater 1 was injected at 0.5 and 1 cm^3/min.; though the residual oil saturation did not change even after reducing the sulfate level to low concentration.

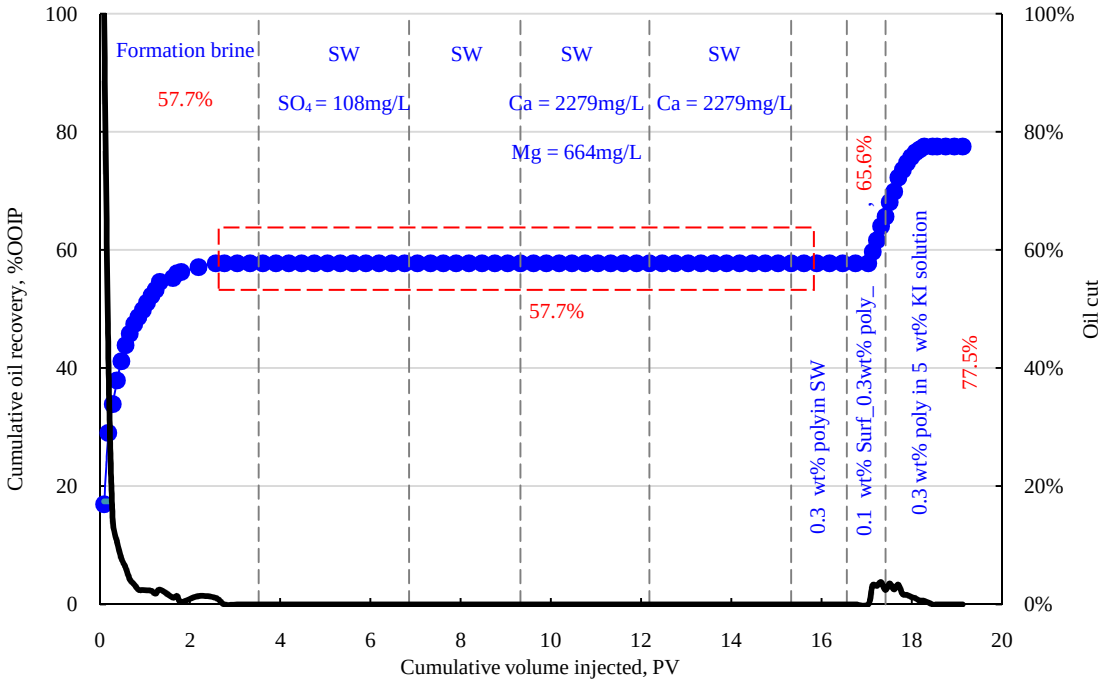

Figure VIII-15. Oil recovery followed multistage of waterflooding and dilute surfactant injection (dolomite–3).

Despite changing the Ca and Mg ratio in seawater 2 and seawater 3, the oil recovery was independent on the water composition. To determine the effect of mobility control on oil recovery, 0.3 wt% polymer in seawater was subsequently injected for more than one PV. As a result, the differential pressure increased to 44 psi at an injection rate of 0.25 cm^3/min. **(Figure VIII-16)**. The oil recovery was not affected after the viscous forces were increased via using 0.3 wt% HAPM polymer in seawater. To determine the role of the capillary forces on oil recovery, 0.1 wt% surfactant/0.3wt% polymer in seawater was injected at 0.5 and 0.1 cm^3/min. The pressure drop at 0.5 cm^3/min was high (68 psi), and for that reason the injection rate was decreased to 0.1 cm^3/min. The differential pressure stabilized with time at 8 psi accordingly. The objective of this step was to overcome the capillary forces by decreasing the fluids' IFT

to ultralow value. Hence, the oil recovery increased to 65.6% OOIP and formed a continuous oil bank. To displace the mobile crude oil from the core, 0.3 wt% polymer in 5 wt% KI solution was injected at 0.5 cm^3/min. Potassium iodide was used just to mimic the salt composition as had been done in the previous tests. The final oil recovery stabilized at 77.5% OOIP with continuous oil banking. In summary, the capillary forces were influencing significantly the oil production. The macromolecule size of the HPAM polymer rapidly increased the pressure drop to 164.7 psi. Core effluent analysis in **Figure VIII-17** confirmed no interactions were observed between the injection fluids, connate water and rock minerals.

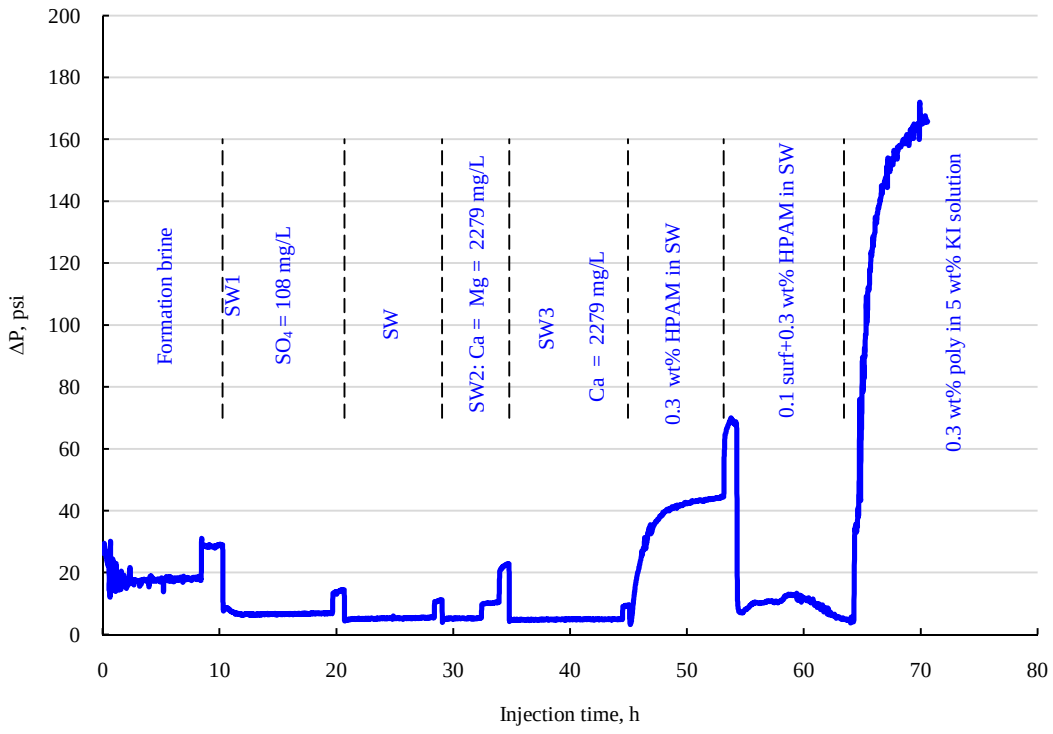

Figure VIII-16. Pressure drop data in test dolomite–3.

The chemicals injection in the first and last core tests showed a significant improvement in oil recovery despite the differences in the rock heterogeneity and properties. Presence of HPAM polymer in the surfactant solution significantly increased oil recovery in comparison to surfactant solution without polymer. Therefore, displacement efficiency was much higher in presence of polymer due to the effect of mobility control.

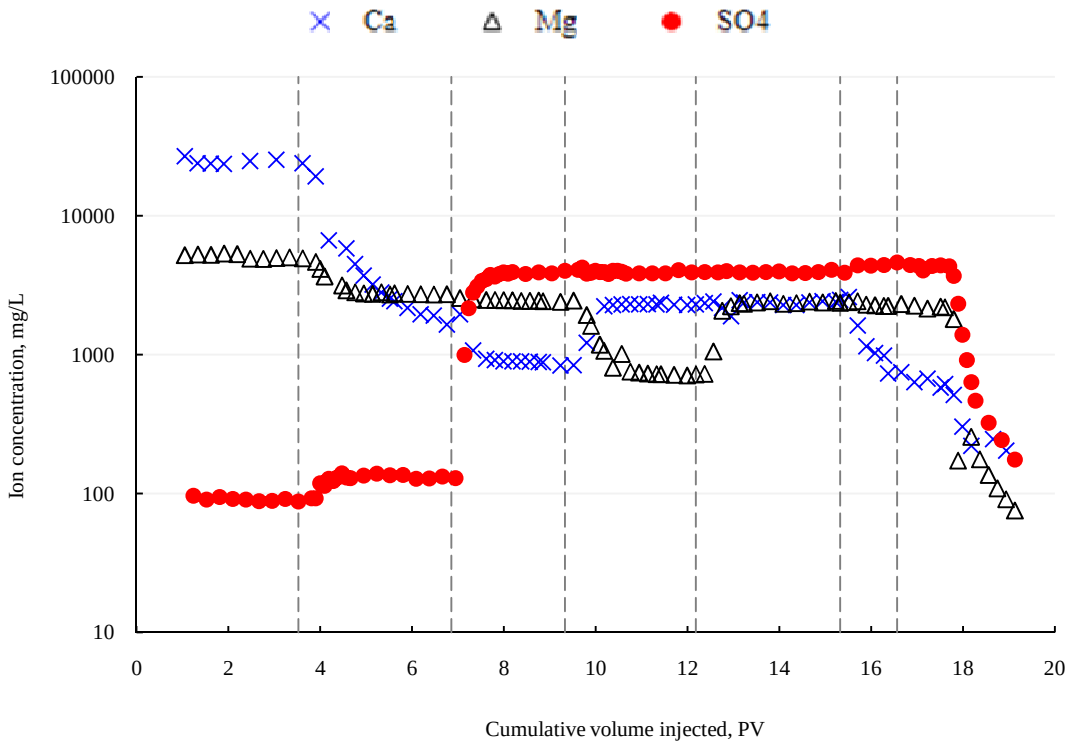

Figure VIII-17. Ions analysis of dolomite core–3 effluent samples.

Rotating disk test

The objective of this test was to determine the seawater interactions directly with dolomite minerals. The reaction rate between water and carbonate rocks is known to be

very slow (Pesret 1972). It also depends on the surface area and solution's pH. On the other hand, the rate of dissolution is affected by the mass transfer and the surface reaction between seawater and dolomite minerals (Fredd and Fogler 1998). Ca, Mg, and SO_4 results show negligible interactions as illustrated in **Figure VIII-18**. In summary, the interactions between dolomite and seawater were very minimal at 130ºC. Ions analysis confirmed the previous conclusion from coreflood analysis results although the temperature conditions were different.

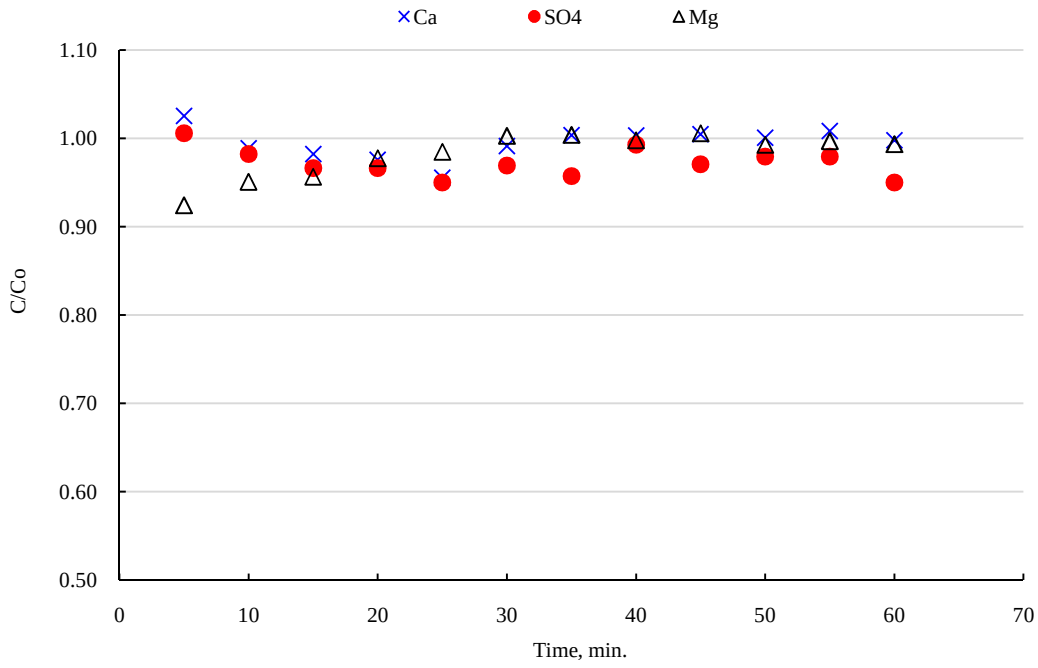

Figure VIII-18. Ions analysis of aqueous effluent samples during rotating disk experiment at 130ºC and 700 psi.

Conclusions

The coreflood and kinetic studies of vugular dolomite cores at high temperatures showed the following:

1. Insignificant change in oil recovery was observed as a result of modifying the chemistry of the injection water.
2. Injection of formation brine as a secondary mode showed the highest recovery (57.7%). The similarity in the injection water and connate brine compositions produced higher oil recovery.
3. Cyclic salinity and dilute seawater injection increased oil recovery by 2 and 4.7% OOIP, respectively. Adsorption of the hydroxide ion at the interface altered the surface charge of the dolomite to negative. As a result, more repulsion forces were created between the carboxylate group in crude oil and the OH^- ions in the water.
4. Dilute amphoteric surfactant with and without HPAM polymer showed significant enhancement in oil production (up to 21.3%) in comparisons to various stages of waterflooding.
5. HPAM polymer flooding did not reduce the residual oil saturation, which indicates the capillary forces are more important than the viscous forces.
6. Rotating disk test confirmed no interactions took place between seawater ions and dolomite minerals at 130ºC for 60 min.

CHAPTER IX

SALINE WATER AND SURFACTANT/POLYMER INJECTION IN LIMESTONE RESERVOIRS

Summary

Injection water has been frequently used as a secondary oil recovery method in carbonate reservoirs. Recently, the salinity adjustment in sandstone reservoirs shows a significant improvement in oil recovery. Modified seawater was injected in the chalk carbonate reservoirs as a tertiary mode, and as a result, the residual oil saturation was reduced. The interaction mechanisms in calcareous (carbonate) and clastic (sandstone) reservoirs are different because of the rock mineralogy. Surfactant and polymer injection afterwards in high-temperature and saline reservoirs consider a challenging issue in EOR industry.

In this chapter, coreflood studies were carried out to determine the effect of salinity on secondary and tertiary oil recovery. Various saline solutions were injected, such as seawater, shallow aquifer water, low salinity water and combination of mono and divalent ions, at an elevated temperature condition. In addition, new class of amphoteric surfactants and sulfonated acrylamide polymer were subsequently injected at such harsh conditions. Analytical techniques including computerized axial tomography (CAT) and inductively coupled plasma optical emission spectroscopy were utilized to visualize and determine fluids-rock interactions.

Seawater injection as a tertiary recovery showed the highest increment in oil recovery (4.4%). The residual oil saturation was substantially reduced by adding equivalent concentrations of magnesium and sulfate ions. In addition, any steep increase or decrease in the salinity slightly increases the oil production (up to 1.7%). Surfactants/polymer benefits in four coreflood tests ranged from 7.3 to 17.1% OOIP. The concentrations of Ca, Mg, and SO_4 ions in the effluent samples and original solutions were similar after almost one pore volume of injection. The CAT scan analysis confirmed scattered residual oil near the inlet and along the core. Results from this study indicated the multistage waterflooding can be applied in the field under certain conditions. Low concentration of surfactant and polymer flooding produced more oil than that of the combined multistage waterflooding.

Introduction

Carbonate reservoirs have been flooded with saline water to maintain reservoir pressure and displace the residual oil towards adjacent production wells. Wettability and reservoir heterogeneity are major factors affecting residual oil saturation. For that reason, two thirds of the original oil in place (OOIP) is left unrecovered after waterflooding.

In sandstone reservoirs, low salinity and shallow aquifer water had been recently proved to enhance oil recovery at different conditions (Boussour *et al.* 2009; Ashraf *et al.* 2010; Alotaibi *et al.* 2010; Morrow and Buckley 2011). On the other hand, laboratory experiments were only reported on low permeability chalk carbonate rocks using modified seawater solutions (SO_4, Ca, and Mg). In general, the wettability of the

carbonate reservoirs is classified as either intermediate or oil-wet. For that reasons, chemical EOR technology (surfactants and polymers) was invented to overcome the capillary forces and control fluids mobility.

Several chemical and physical interactions occur between the displacing and displaced fluids which lead to efficient microscopic displacement (Green and Willhite 1998). These include miscibility between fluids, lowering IFT, oil volume expansion, reducing oil viscosity, and maintain favorable mobility ratio.

The specific objectives of this work are to: 1) assess the significant of salinity on oil recovery as secondary and tertiary modes, 2) compare the multistage water injection to the conventional chemical EOR methods (surfactant and polymer flooding) at 90ºC.

This study addresses many unknown questions about the role of salinity on oil production. Moreover, different EOR techniques were applied using saline water and amphoteric surfactant flooding with copolymers of acrylamide and sodium 2-acrylamido-2-methylepropane sulfonate (AMPS). An analytical technique was utilized to monitor ions interactions with limestone minerals. The core characteristic and fluids distribution were visualized using computerized axial tomography (CAT) technique. It is worth to mention that this chapter discusses only the fluids/rock interactions in the limestone rocks.

Literature Review

Saline water

Over the last decade, low salinity water technology was applied in various sandstone reservoirs. The rock mineralogy in sandstone is different than carbonate, and hence the reaction mechanisms are not similar. In this study, more attention is given to carbonate rock and saline water interactions at high temperatures.

Scientists suggested a relationship between the level of SO_4, Ca, and Mg ions in seawater and the oil recovery at high temperatures (Strand *et al.* 2003; Webb *et al.* 2005; Strand *et al.* 2006; Zhang *et al.* 2007). Seawater composition is different from one place to another. Therefore, most laboratory studies in petroleum literature were conducted using only North Sea water (34-35K mg/L). But, most of the gigantic fields in the Middle East are flooded with seawater that has higher salinity ~50K mg/L.

In general, the concentration of the major divalent ions (Ca and Mg) in the formation brines is usually high. As a result, the carbonate rock surface charge is assumed to be positive. SO_4 adsorption is believed to alter the zeta potential of chalk particles from positive to negative. The reaction mechanisms are quiet complicated especially at the interfaces (water/oil, oil/connate water, connate water/rock, oil/rock), **Figure IX-1**. In addition, the stability of the connate water film affects the rock/fluids interaction and perhaps the rock wettability (Kussakov and Mekenitskaya 1955; Hall *et al.* 1983; Buckley and Liu 1998; Kaminsky and Radke 1997). Rupture cases were reported to the water film and in such cases only two interfaces are existed (water/oil and oil/rock). Crude oil/water interface is negatively charged because of the hydroxyl ions

adsorption at the interface (Omotoso *et al.* 2002; Knecht *et al.* 2007). In short, the interactions mechanisms between injection water and carbonates in presence of crude oil are still ambiguous. In the previous chapters, saline water injection in dolomite reservoirs was thoroughly studied.

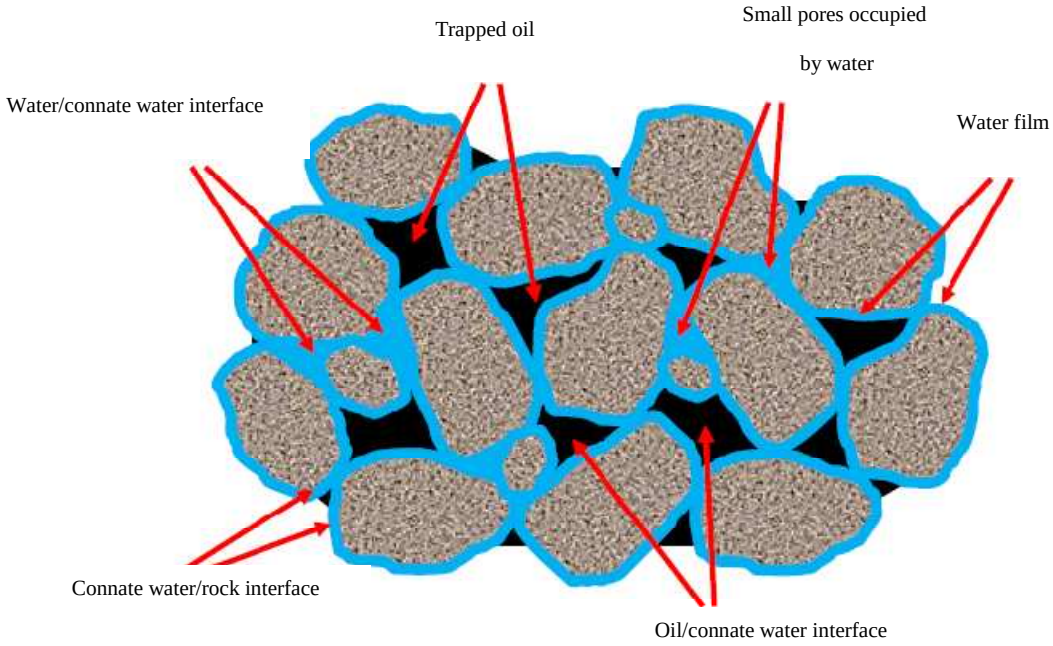

Figure IX-1. Fluids distribution in a carbonate reservoir (Aksulu 2010).

Surfactant/polymer flooding

Salinity and reservoir temperatures are the most challenging issues in EOR process (Sanz *et al.* 1995; Jamaloei and Rafiee 2008). Divalent ions can associate with the surfactant and cause precipitation or partition to the oil phase (Green and Willhite 1998). Researchers designed various amphoteric surfactants which can work in harsh

environments (Maddox and Tate 1977; Stournas 1984; Kalpakci and Chan 1985; Berger and Berger 2009).

The literature review of the amphoteric surfactant application was summarized in Chapters V and VII. Polymer is usually mixed with or without surfactant solution to provide mobility control and reduce water fingering issues in the field (Schumacher 1978). General review about the polymer also was previously mentioned in Chapter VIII. Presence of divalent ions in the aqueous solution can form precipitation with HPAM polymers. For that reason, different acrylamide copolymers with higher thermal and salt stability were lately introduced in polymers industry such as AMPS (Rashidi *et al.* 2010; Zaitoun *et al.* 2011). The viscosity and elasticity properties of AMPS polymer were thoroughly studied by Magbagbeola (2008). The effect of high salinity, hardness and temperature on the adsorption, retention and viscosity was also determined by Rashidi (2010).

Experimental Studies

Materials

Indiana and Winterset limestone samples were obtained from Kocurek Industries Company (Houston, Texas, USA). The limestone cores were then drilled from that block in one direction at diameter and length of 3.8 and 50.8 cm, respectively. The rock mineralogy was confirmed with XRD analysis. Based on the CAT scan visualization results, the core was homogenous with no fractures or vugs. More discussion on CAT scan is presented next in the results section.

Fluids

The saline water used in this study represents a Middle East field case as shown in **Table II-1**. Ions (Na, Ca, Mg, SO_4) were excluded from seawater to determine their impact on fluids/rock interactions and ultimate oil recovery. Seawater was also diluted at three ratios (50, 20, and 10 vol%) using deionized water. Likewise, 10 wt% KI solution was prepared to track fluids movement in the limestone core.

A new class of amphoteric surfactant (alkyl dimethyl betaine) was used at concentrations less than 0.5 wt% (Berger and Berger 2009). A short chain polymer (lignin) was added to the surfactant to reduce the adsorption issue on the rock. In this study, two surfactants were used with different molecular weight 353 (I) and 381 (II).

AMPS polymer (AN-125) was obtained from SNF Floerger Company (Riceboro**,** Georgia, USA) and used at a concentration range of 0.1 to 0.3 wt% to improve the fluids' mobility ratio. The polymer's molecular weight and degree of hydrolysis are 8 million Daltons and 20-30%, respectively.

Apparatus and procedure

Core flood. **(**The coreflood setup was previously covered in Chapter VI). All equipment and apparatus used throughout this study were listed in Appendix F. Limestone cores were air vacuumed for at least 12 hrs and then were saturated in formation brine. The overburden and back pressures were maintained constant for all Indiana limestone tests at 1,000 and 500 psi, respectively. Winterset limestone had very low permeability, and for that reason, the back pressure regulator was decreased to low pressure (~200 psi).

The base permeability was determined at ambient temperature and various injection rates 0.25, 0.5, and 1 cm^3/min. To ensure ionic equilibrium was achieved, the cores were left in formation brine for one week. Crude oil was injected at various rates 0.1, 0.2 and 0.4 cm^3/min. until the irreducible water saturation was achieved. The Indiana limestone cores were then aged for 20 days in a sealed steel pipe (ID = 10 cm, L = 61 cm) filled with crude oil. The aging temperature was 90ºC, while the pressure was at atmospheric. The Winterset limestone sample was used without aging, and the injection rate during saturation and flooding stages was 0.3 cm^3/min. The petrophysical properties of the core plugs are shown in Table IX-1.

Table IX-1. Petrophysical properties of Indiana and Winterset limestone cores.

Source	Core ID	Diameter	Length	Porosity	Base Permeability	Irreducible water saturation
		cm	cm	%	md	%
Indiana (IL)	10	3.7	50.8	19.1	170.7	30
	8			19.4	168.1	35.2
	9			20.1	159.5	27.9
	6			18.6	154.7	32.8
	11			19	200.6	22.1
	12			18.7	169.9	24.1
	5			18.5	169.4	27
Winterset (W)	1			25.9	4.2	17

CAT-scan. (More details about the CAT instrument specifications were reported earlier in Chapter VIII). Because of the limitations in the used CAT machine, the scanning process was conducted immediately after completing the core saturation and chemical flooding. Cross sectional scans of the core were made at regular intervals (slice thickness

= 2 mm, index = 5 mm). Medical image process and visualization (MIPAV) software was utilized to process the core images as shown in the Appendix E.

Results and Discussion

The main objective of the coreflood is to determine the effect of salinity on oil recovery as secondary and tertiary modes. Amphoteric surfactants and polymers were subsequently injected at high temperatures and over a wide salinity range. The results and discussion were organized as follow: multistage waterflooding, surfactant/polymer injection, pressure behavior, effluent ions analysis, and CAT scan results.

Multistage waterflooding (Indiana limestone)

Core IL–10 was flooded with 4 PV of seawater, which resulted in oil recovery of 31.3% OOIP, **Figure IX-2**. In Chapters II and III, we know the limestone rocks are positively charged in presence of seawater or formation brine. Increasing the ionic strength results in a compression of the diffuse double layer thickness and that decreases the rock/fluids interactions due to counter ions adsorption at the rock surface (Shaw 1966). Instant salinity reduction to deionized water level improved the oil production to 32.9%. The carbonate surface potential at low salinity water was reported by many scientists to be negative (Hiorth *et al.* 2010; Farooq *et al.* 2011). Therefore, the electrostatic interactions might affect the residual oil through creating repulsion forces with Ca^{2+} ions in the rock surface. Varying the salinity again to 50 vol% seawater had no effect on oil production. The intent from this step was to simulate the flood front where the salinity is commonly diluted to certain extent.

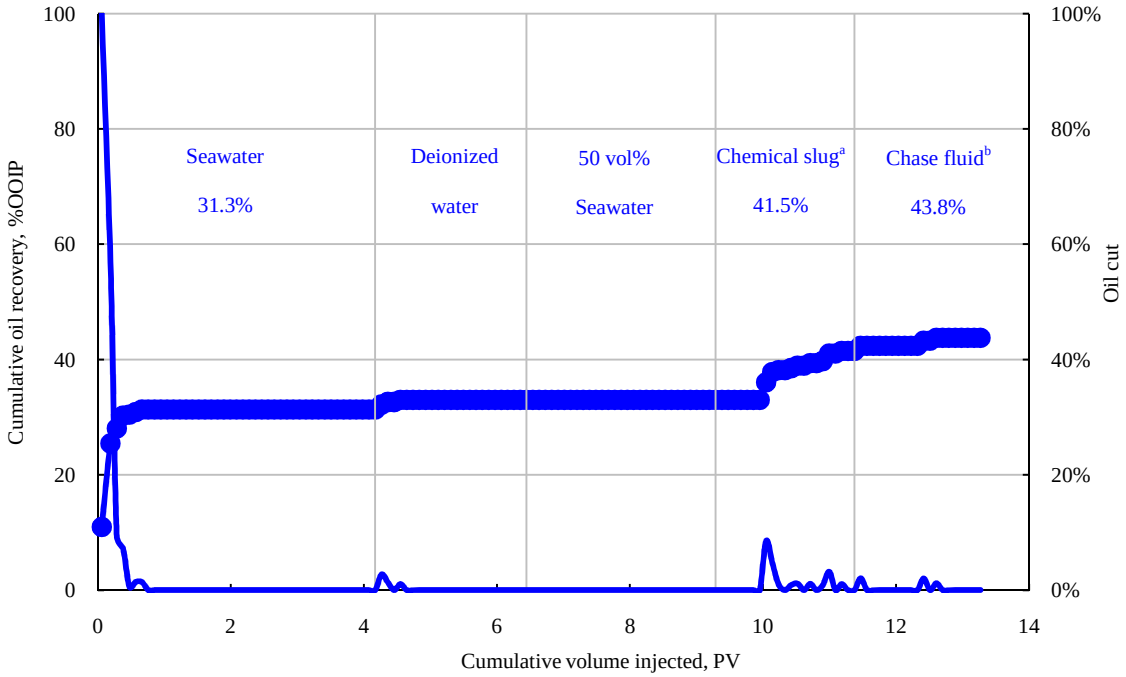

a) Chemical slug: 0.1 wt% surfI+ 0.2 wt% AMPS in 50vol% seawater
b) Chase fluid: 0.3 wt% AMPS in 50 vol% seawater

Figure IX-2. Oil recovery during multistage waterflooding and surfactant I/polymer injection (IL–10).

The oil recovery value stabilized at 53.2% OOIP during 3.5 PV of seawater injection in Core IL–8, **Figure IX-3**. The objective of this test was to determine the role of individual ions on oil recovery as a tertiary mode. Despite the similarities in the core and fluid characteristics, the final secondary oil recovery results were not essentially the same as observed in tests IL–8 and IL–10. Insignificant increase (1.1%) in oil production was reported during 0.5 wt% $CaCl_2.2H_2O$ injection. Potential determining ions (Ca^{2+}, H^+, OH^-, CO_3^{2-}) can specifically adsorb at the carbonate sites and subsequently affect the electrostatic interactions (Madsen 2006). Injection of 0.5 wt% $MgCl_2.6H_2O$ solution

afterward unexpectedly showed the highest increment in oil recovery (2.5%). Magnesium ions reduced the calcite surface charge more than calcium ions (Smallwood 1977). This was mainly attributed to the specific adsorption of Ca^{2+} ions onto the calcite surface.

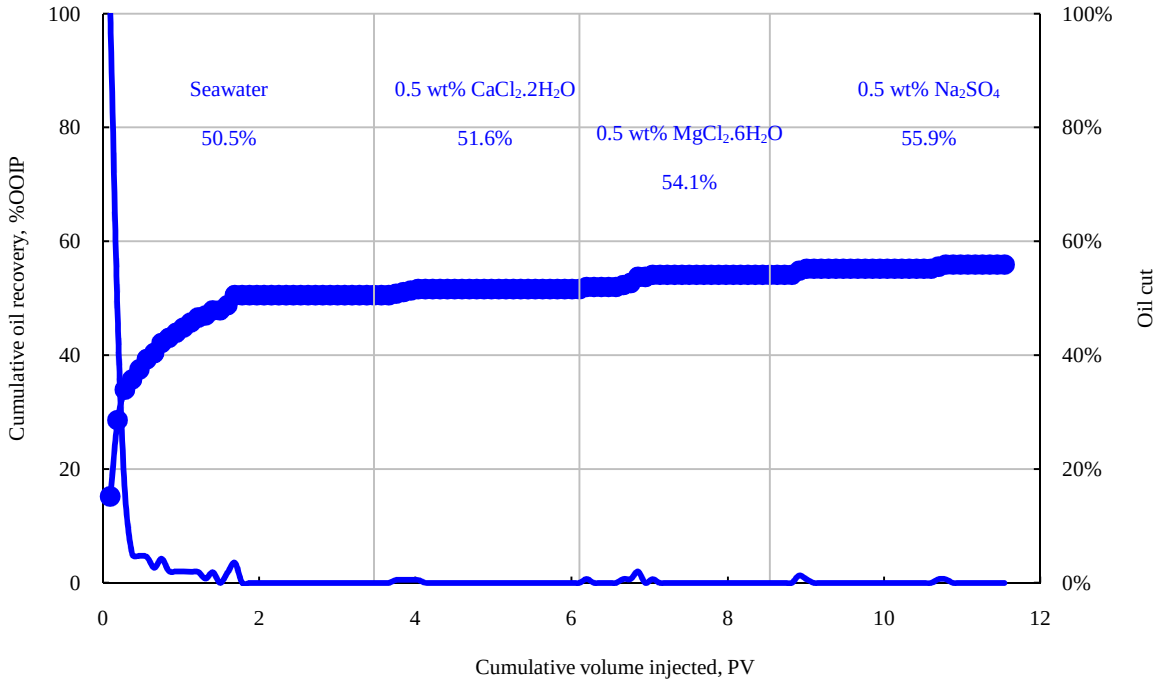

Figure IX-3. Oil recovery during multistage waterflooding of experiment IL–8.

The last stage of water injection (0.5 wt% Na_2SO_4 solution) enhanced oil recovery only 1.8%. Sulfate might form a non-specific adsorption through water molecules with carbonate. In summary, the electrostatic forces between the divalent cations and anions with carbonate minerals are slightly affecting oil recovery with a maximum increment of 2.5%.

Fresh water injection was reported to significantly enhance oil recovery in the field, but with unknown reaction mechanisms. For that reason, deionized water was injected in core IL–9 as a secondary mode to determine the impact of free ions water on the interactions. As a result, the highest oil recovery (56.8%) was observed in comparison to the first two tests. This was attributed to the adsorption of hydroxide ions on the limestone, which subsequently increased the electrostatic repulsion forces between crude oil components and rock surface. Seawater injection as a tertiary mode significantly increased oil recovery to 61.3% OOIP, **Figure IX-4**. Based on the water analysis results from OLI software, there is excess of positive ions in seawater (Chapter X). This was further confirmed with zeta potential measurements using limestone particles and seawater (Chapter II). In fact, the electrostatic interactions due to any sudden increase or decrease in salinity can enhance oil recovery. Seawater (without Ca^{2+} and Mg^{2+} ions) and aquifer water (4K mg/L) were injected in the last two stages without any success in sweeping the remaining oil.

We chose seawater for the coreflood tests because it is widely used for water injection as a secondary recovery method in various oil fields. The importance of individual mono and divalent ions, in seawater, on oil production is not clear. To answer this question, more than 3 PV of NaCl at seawater level was injected in core IL–6 as displayed in **Figure IX-5**. Hence, oil recovery stabilized at 50% OOIP. Then, calcium ions were only added to NaCl solution according to seawater composition, **Table II-1**. As a result, 1.7% increment in the oil production was reported. In the last two injection stages, Mg^{2+} and SO_4^{2-} ions were separately added to NaCl-$CaCl_2.2H_2O$ mixture but

with a negligible impact on recovery efficiency. Adsorption studies in various soils showed that SO_4^{2-} had slow reactions with carbonate even at high temperatures (Barrow and Shaw 1977).

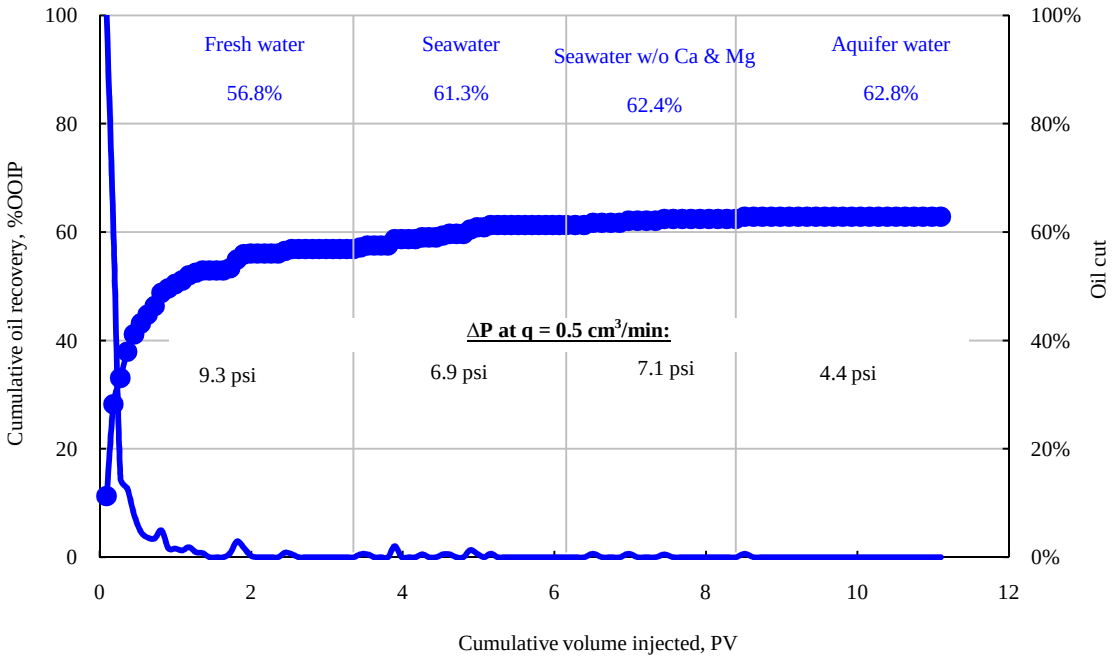

Figure IX-4. Oil recovery during multistage waterflooding of experiment IL–9.

For that reason, the core was left 8 h (overnight) at 90ºC after the last seawater injection stage. The core was re-flooded subsequently with 1.5 PV of seawater, but without any success in decreasing the residual oil saturation. This might be ascribed to the weak adsorption of sulfate ions on the calcite surface (Smallwood 1977).

In test IL–11, seawater injection resulted in 50.8% OOIP during 3.3 PV. The reproducibility of the tests were observed, where seawater injection was always giving oil recovery within 50% of OOIP, except experiment IL–8. Effect of ions combination

on oil production was determined by mixing 0.5 wt% $MgCl_2.6H_20$ and 0.5 wt% Na_2SO_4 with deionized water. More than 3% increase in oil recovery was observed as depicted in **Figure IX-6**.

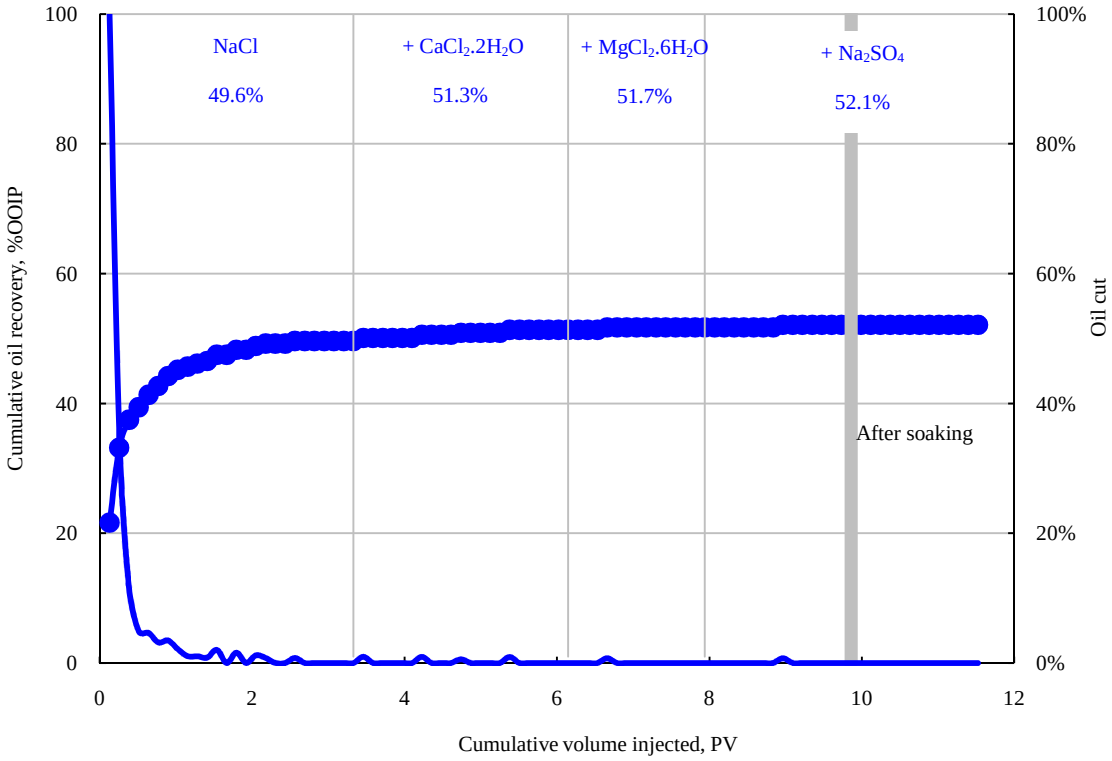

Figure IX-5. Oil recovery during multistage waterflooding of IL–6.

Adding equivalent concentrations of metals and sulfate ions increases sulfate adsorption (Ajwa and Tabatabai 1995). Several mechanisms have been proposed by Ajwa and Tabatabai to explain these phenomena as follow:

1) Specific adsorption of metal ions increases the positive charge on the surface and thereby increases the adsorption of sulfate.

2) Surface complexation reactions by which a metal ion coordinates to two adsorbed SO_4 groups and that enhances the adsorption.

3) Formation of ion pair such as SO_4 that adsorbs to mineral surfaces.

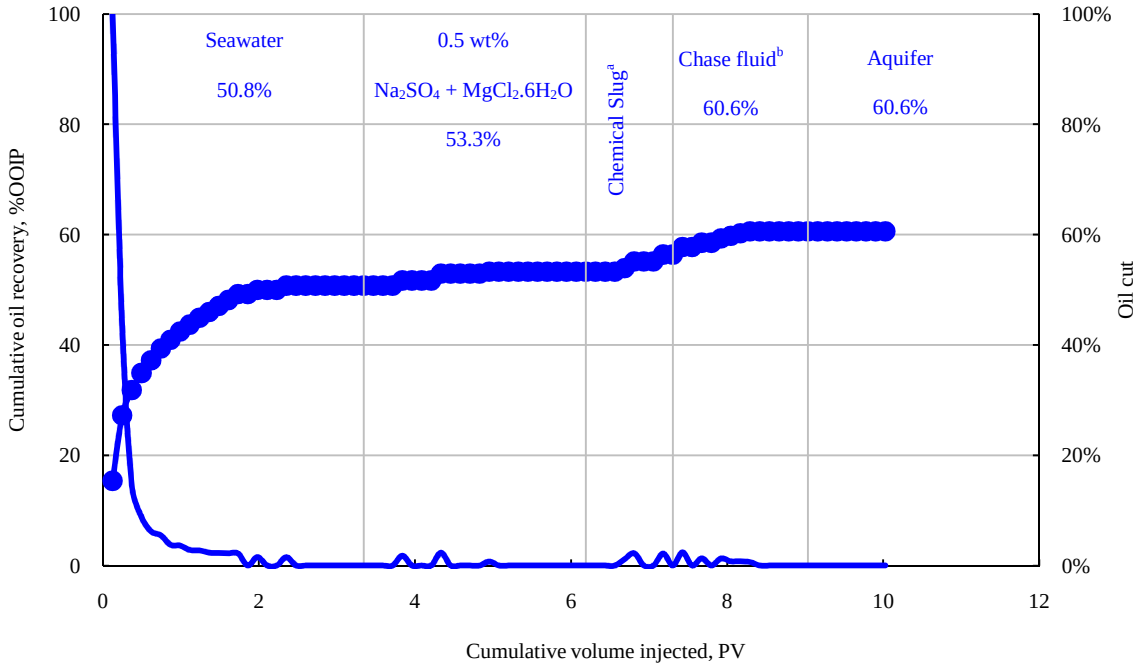

a. Chemical slug: 0.3 wt% surfI + 0.1 wt% polymer in seawater
b. Chase fluid: 0.2 wt% polymer in seawater

Figure IX-6. Oil recovery during multistage waterflooding and surfactant I/polymer injection of experiment IL–11.

Diluted seawater at different ratios increases the concentrations of water molecules (H^+, OH^-) and furthermore decreases the level of cations and anions. After secondary seawater flooding stage in experiment IL–12, dilute seawater (20 vol%) was injected but had no effect on oil recovery (48.7%), **Figure IX-7**.

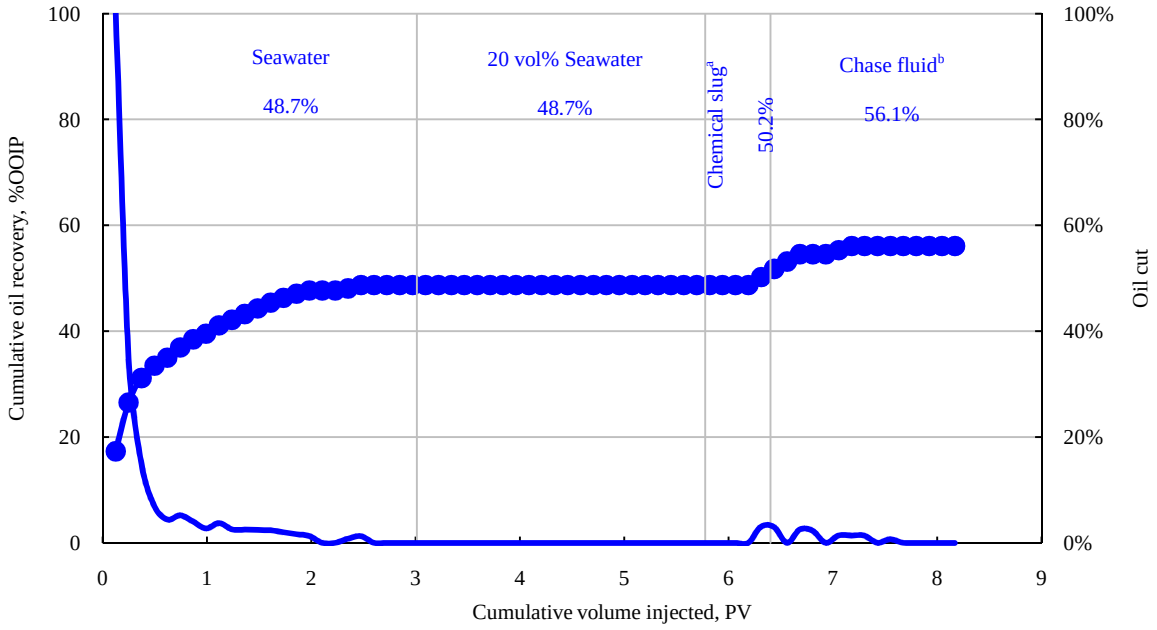

a. Chemical slug: 0.5 wt% surfI + 0.2 wt% polymer in 20 vol% seawater
b. Chase fluid: 0.2 wt% polymer in 20 vol% seawater

Figure IX-7. Oil recovery after multistage water and surfactant I/polymer flooding (IL–12).

This result agrees with similar studies on short chalk cores using diluted North Sea water (Fathi *et al.* 2010). The waterflooding experiments of Indiana limestone cores were summarized in **Figure IX-8**, secondary and tertiary oil recovery trends were plotted against oil recovery.

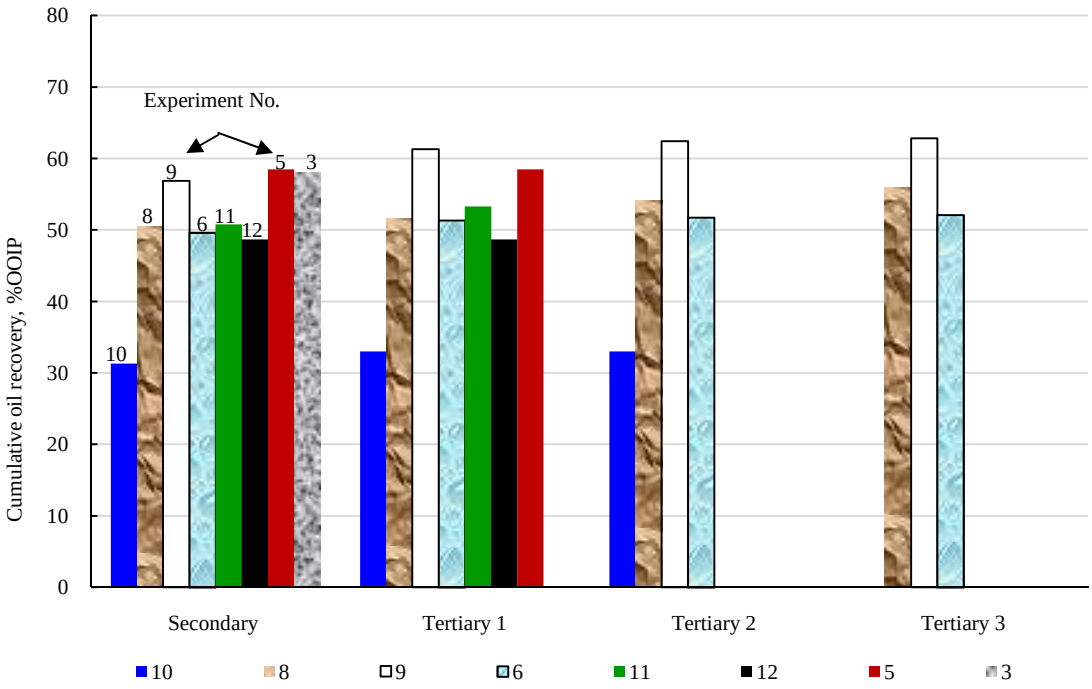

Test No.	Secondary	Tertiary 1	Tertiary 2	Tertiary 3
10	SW	DIW	50 vol% SW	–
8	SW	0.5 wt% $CaCl_2.2H_2O$	0.5 wt% $MgCl_2.6H_2O$	0.5 wt% Na_2SO_4
9	DIW	SW	SW without Ca/Mg	AQ
6 (SW composition)	NaCl	NaCl+$CaCl_2.2H_2O$	NaCl+$CaCl_2.2H_2O$+$MgCl_2.6H_2O$	Regular SW
11	SW	0.5 wt% ($MgCl_2.6H_2O$+ Na_2SO_4)	–	–
12	SW	20 vol% SW	–	–
5	FB	DIW		
3	SW	–	–	–

Figure IX-8. Cumulative oil recovery during secondary and tertiary waterflooding (summary of the waterflooding tests).

Multistage waterflooding (Winterset limestone)

This test was essentially conducted to confirm the previous findings in a different limestone core but with lower permeability and different impurities. The core properties are shown earlier in **Table IX-1**. The next aqueous solutions were injected subsequently at 0.3 cm^3/min.: seawater, seawater without Na, seawater without Ca and Mg, 50% seawater, 10% seawater, seawater (4xMg, Ca~ 0 mg/L) and seawater (2xSO_4, Ca~ 0 mg/L). The core inlet pressure was almost equal the overburden pressure at injection rates higher than 0.5 cm^3/min. Because of pressure limitation, the injection rate was fixed at 0.5 cm^3/min. for all aqueous solutions.

Seawater injection as a secondary mode produced almost 22% of OOIP as shown in **Figure IX-9**. It can be concluded that lowering the rock permeability below 5 md decreased the oil recovery by almost 50%. Excluding the Na ions from the seawater had no effect on oil recovery efficiency. The sodium ions are weakly bonded to the calcite minerals; therefore the contribution of the Na ions in the calcite/brine interactions are expected to be very weak (Chapter III).

Excluding the divalent cations (Mg and Ca) from seawater, on the other hand, surprisingly showed unexpected interactions. The oil recovery slightly increased to 23.8% OOIP, and that was attributed to increasing the complex ions concentration especially the $NaSO_4^{-1}$ and HSO_4^{-1}. It is also matching the previous findings in test IL–9 as the same fluid (seawater without Ca and Mg) showed 1.1% increase in the oil recovery. More discussions on the effect of the complexes and ions pairs on the chemical activities are studied in Chapter X.

Injection of 50 and 10% seawater afterwards did not impact the residual oil saturation as shown in **Figure IX-9**. Similar observations were also reported with increasing the concentrations of Mg and SO_4 ions in seawater without any Ca ions. In summary, the results in test W–1 matched previous conclusions from IL tests as displayed in **Figure IX-8**.

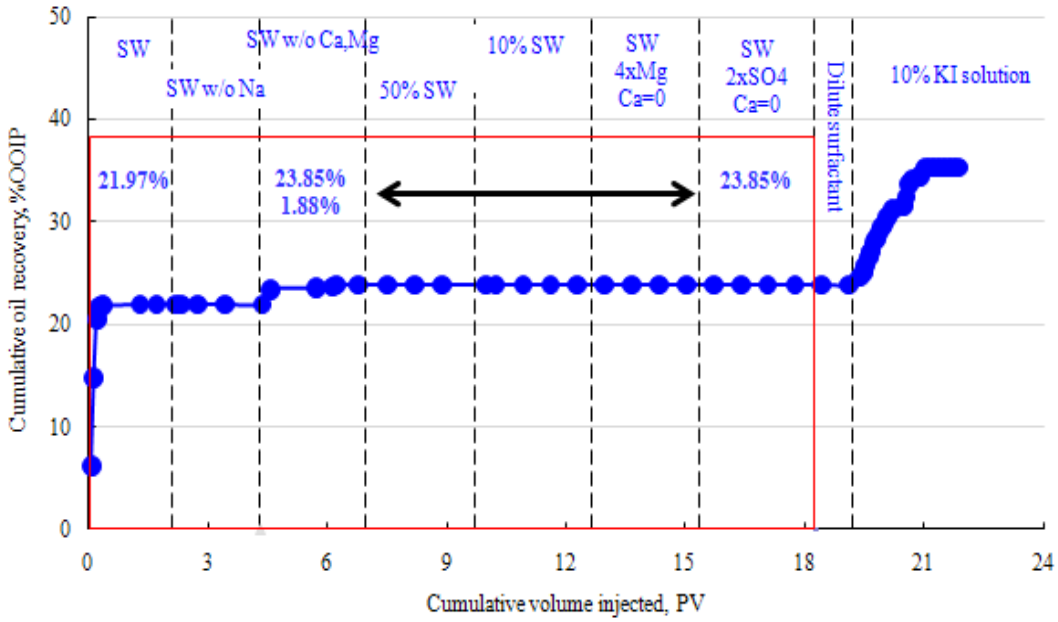

Figure IX-9. Oil recovery after multistage of seawater and dilute surfactant flooding (W–1).

Surfactant/polymer injection

Amphoteric surfactants and AMPS polymers were injected at different ratios in four coreflood experiments. The screening process of the betaine surfactants were previously presented in Chapter VIII. The objective of the coreflood tests was to determine the

effect of new betaine surfactants in combination with AMPS polymers on oil recovery at various salinity conditions. Two surfactants (I and II) were evaluated at 90ºC.

In test IL–10, 2 PV of chemical solution (0.1 wt% surf I and 0.2 wt% polymer in 50 vol% seawater) was injected at injection rate of 0.2 cm^3/min. The oil production started after 0.5 PV of chemicals injection due to decreasing the IFT and increasing the fluids viscosity, **Figure IX-2**. As a result, the oil recovery increased linearly from 32.9 to 41.5%. The polymer concentration in the chase brine was increased further to 0.3 wt% to efficiently displace all mobile oil from core. Hence, 2.3% additional oil was displaced throughout 1.8 PV of chase brine injection.

In test IL–11, the surfactant I and polymer concentrations were prepared in regular seawater solution (0.3 wt% S1 and 0.1 wt% polymer). The chemicals injection resulted in 1.9% increase in oil recovery, while the oil bank started after approximately 0.5 PV, **Figure IX-6**. Chase brine injection (0.2 wt% polymer in seawater) afterward linearly increased the oil recovery by 5.4 %. Overall, the surfactant performance in this test was lower than test IL–10 even after with increasing the surfactant concentration to 0.3 wt%. This could be due to the surfactant partition to the oil phase at such high salinity condition (Winsor 1954).

To avoid the surfactant partition issue, 0.5 wt% surfactant S1 and 0.2 wt% polymer were mixed accordingly with low salinity water (20 vol% seawater) in test IL–12 **(Figure IX-7)**. The surfactant concentration was increased to 0.5 wt% because any adsorption can reduce the remained surfactant concentration in solution especially in

long cores. The increase in oil recovery throughout the chemicals and chase fluids injection were almost matching IL–11 result (7.4%).

The second surfactant II (0.3 wt%) was injected along with 0.2 wt% polymer and 50 vol% seawater in core IL–5 **(Figure IX-10)**. The goal from this test was to determine the impact of different betaine surfactants on ultimate oil recovery results. Chemical and chase fluids injection surprisingly produced the highest oil recovery (17%) in comparisons to the other three coreflood experiments.

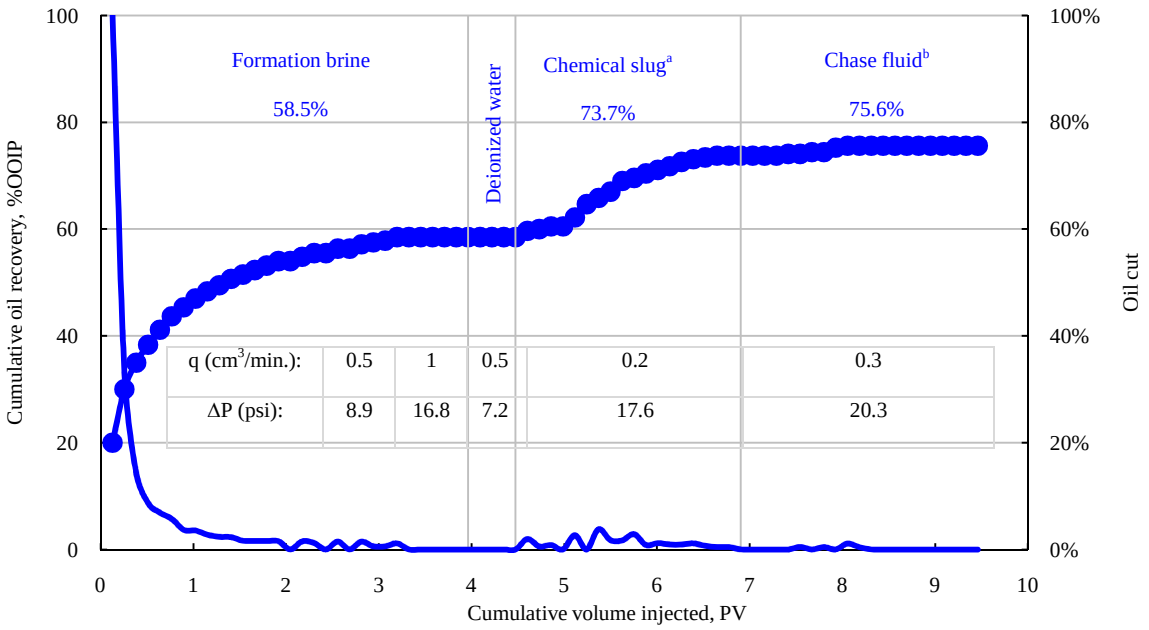

a. Chemical slug: 0.3 wt% surfII+ 0.2 wt% polymer in 50 vol% seawater
b. Chase fluid: 0.2 wt% polymer in 10 wt% KI solution

Figure IX-10. Oil recovery during water and surfactant II/polymer flooding (IL–5).

After the multistage waterflooding, the Winterset limestone test (W–1) was flooded with dilute surfactant I (0.1 wt%) which was prepared in seawater for 0.95 PV.

No polymer was used in this test, because the permeability of the core was very low (< 5md). After that, 10wt% KI (chemical tracer) was injected as a chase fluid to displace the mobile oil from the core. The oil recovery subsequently increased from 23.58 to 35.33% OOIP as a result of reducing the IFT to ultralow values, **Figure IX-9**. We observed a delay in the oil recovery of the low permeability core (Winterset) in comparisons to other Indiana limestone tests.

Pressure behavior

In core IL–10, the highest differential pressure through waterflooding stages was observed for deionized water test. Seawater and dilute seawater (50%) showed a stable pressure drop performance with time, **Figure IX-11**. Chemicals' injection, on the other hand, increased the pressure drop across the core at least three times. The pressure profile was almost steady at various injection rates, which implied that no precipitation or plugging had occurred along the core.

In experiment IL–8, the pressure decreased at the beginning because of the water imbibition into the core. The other injection fluids also showed a steady pressure drop with time at various injection rates, **Figure IX-12**. Similar observations were reported for tests IL–9 and IL–6, **Figures IX-4 and IX-13**.

Pressure profiles in cores IL–5 and IL–12 were steady during waterflooding stages, and then it increased with increasing the fluids viscosity as shown in **Figures IX-10 and IX-14**. The pressure drop in test W–1 fluctuated between 830 and 900 psi throughout water injection because of the low permeability.

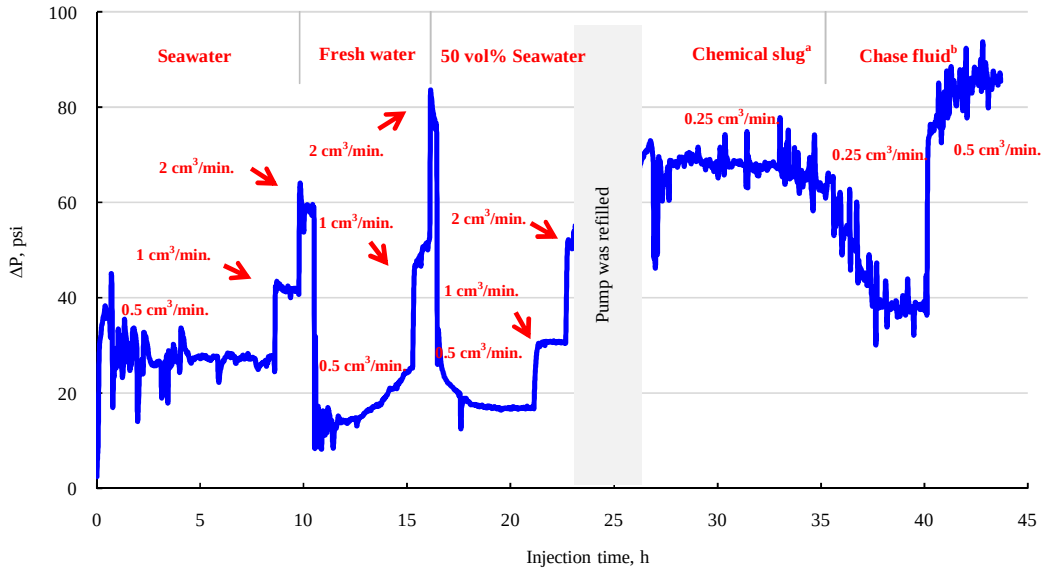

a) Chemical slug: 0.1 wt% surfI + 0.2 wt% AMPS in 50vol% seawater
b) Chase fluid: 0.3 wt% AMPS in 50 vol% seawater

Figure IX-11. Pressure profile during water and surfactant S1/polymer flooding of experiment IL–10.

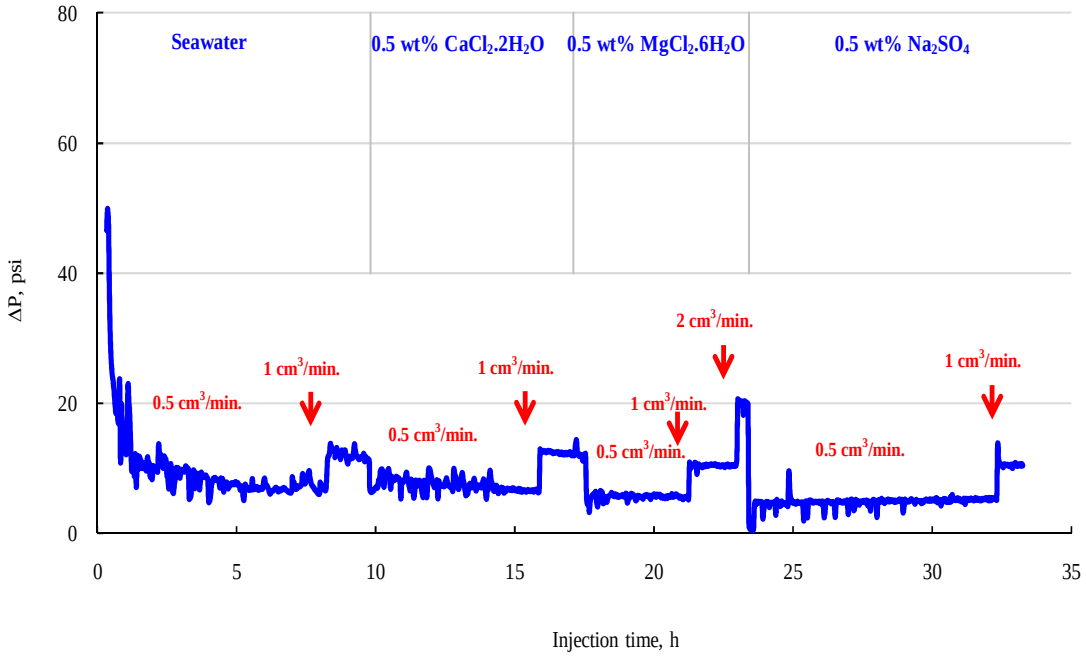

Figure IX-12. Pressure profile during water and chemicals flooding of experiment IL–8.

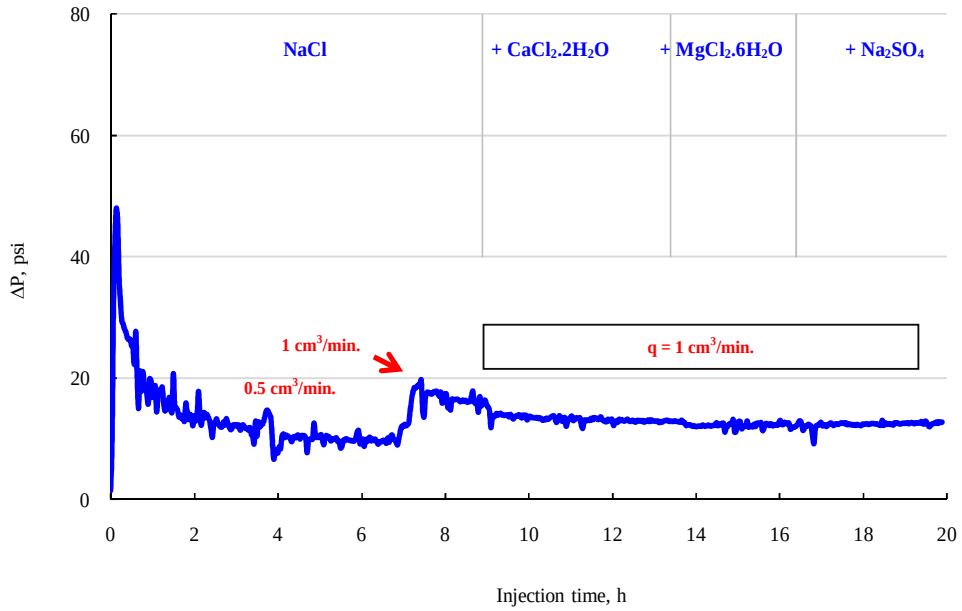

Figure IX-13. Pressure profile during waterflooding of experiment IL–6.

Core effluent analysis

Divalent ions analysis was conducted using inductively coupled plasma optical emission spectroscopy method for experiments IL–10 and IL–9. In addition, turbidity method was utilized to determine the sulfate ion concentration in the collected water samples.

In the two tests, the analysis results showed conclusively that the connate water bank a head of the injection water, **Figures IX-15 and IX-16**. Displacement of connate water in coreflood is not as a piston-like manner but with some degree of mixing with injection water (Russel *et al.* 1947; Brown 1957).

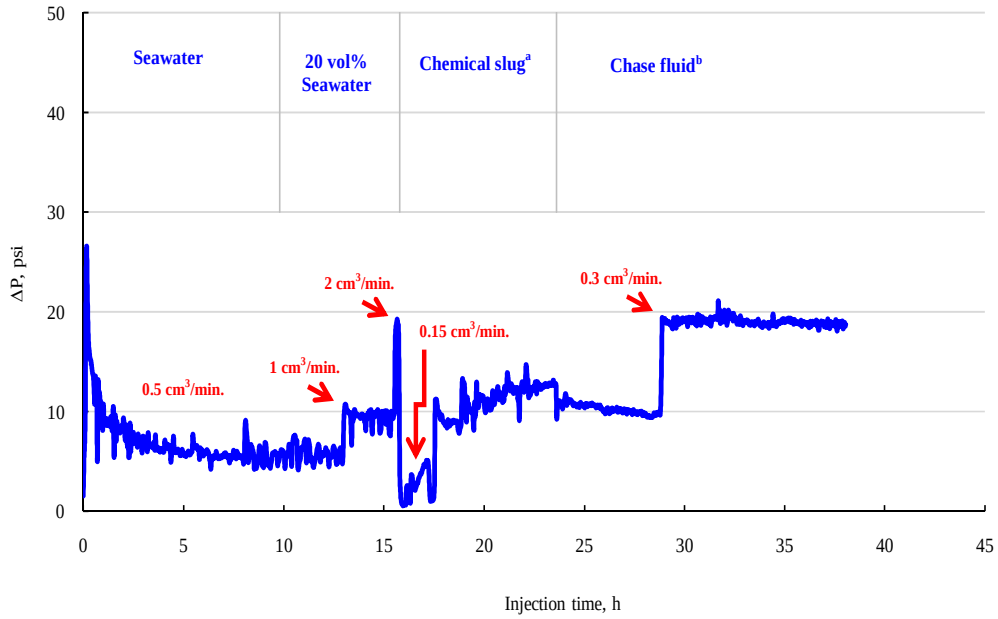

a. Chemical slug: 0.5 wt% surfI+ 0.2 wt% polymer in 20 vol% seawater
b. Chase fluid: 0.2 wt% polymer in 20 vol% seawater

Figure IX-14. Pressure profile during water and chemicals flooding of experiment IL–12.

For that reason, the ion concentrations were a bit lowered than that in the original formation brine, **Table II-1.** The ions profile, in general, was observed to be steady at seawater level after the first PV (IL–10), **Figure IX-15**. On the other hand, the concentration of ions in test IL–9 decreased throughout deionized water injection, **Figure IX-16**.

Various saline solutions were injected as a tertiary recovery for both tests. In the aqueous effluent samples of IL–10, the detected ion concentrations matched that of the original samples after one pore volume of water injection.

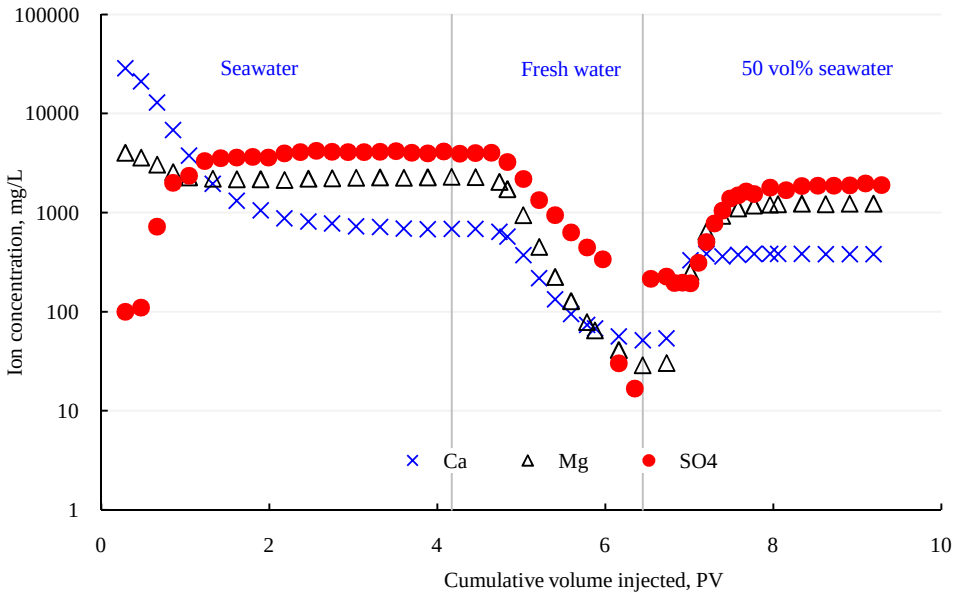

Figure IX-15. Ions analysis of core effluent during waterflooding (IL–10).

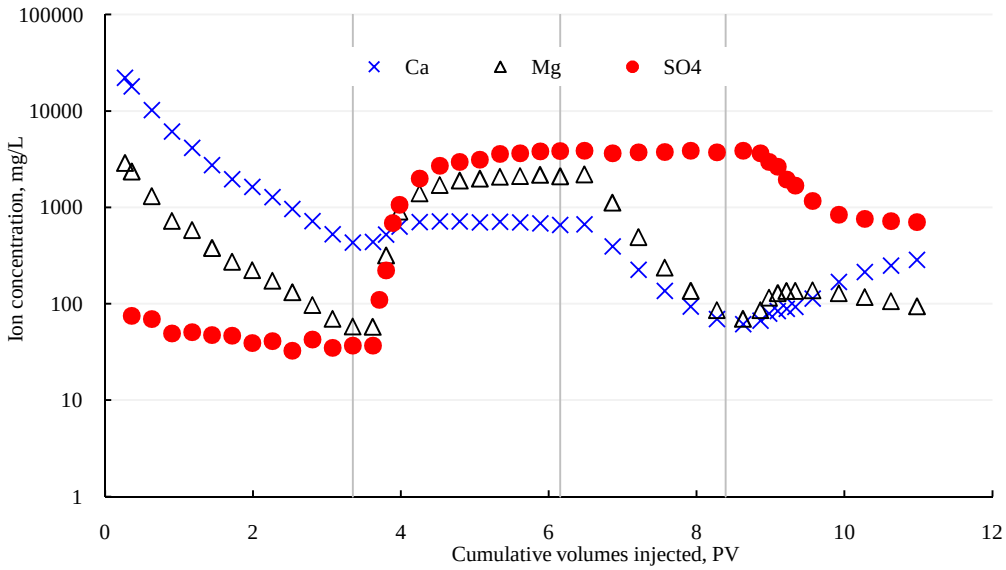

Figure IX-16. Ions analysis of core effluent during waterflooding (IL–9).

Similar observations were also reported in experiment IL-9. These results confirm the rock homogeneity especially no breakthrough to any of the injection fluids was reported. During deionized water injection, the cations and anion concentrations did not reach to a stable value, which might be attributed to the dehydration process. Sulfate profile, in general, was simultaneously matching any change in Ca^{2+} or Mg^{2+} ions. In addition, the three ions were leveling out essentially at the same PV. It can be concluded that no adsorption was observed at 90ºC for various brine systems.

CAT scan

The CAT scan analysis was conducted only for core sample IL–5 and W–1 at different conditions: 1) dry, 2) after water saturation, 3) after oil saturation, and 4) after waterflooding/chemicals injection. The discussion in this section is based on the CAT numbers behavior not the fluids' saturation. **Table IX-2** shows the CAT number for the fluids that were injected in core IL–5.

Table IX-2. CAT numbers for various fluids (experiment IL–5).

Fluid	Formation brine	Crude oil	0.2 wt% AMPS polymer in 10 wt% KI solution
CAT number, Hounsfield	435	-135	2625

The image results indicate the limestone core was homogenous with no vugs or fractures along the core (Appendix E). The trend of the average CAT numbers in core IL–5 at various saturation conditions was shown in **Figure IX-17**. The average porosity

was calculated from the scan core images at dried and after brine saturation (21.9%). The CAT intensity decreased after flooding the core with crude oil, because the displaced formation brine had higher density than the oil phase.

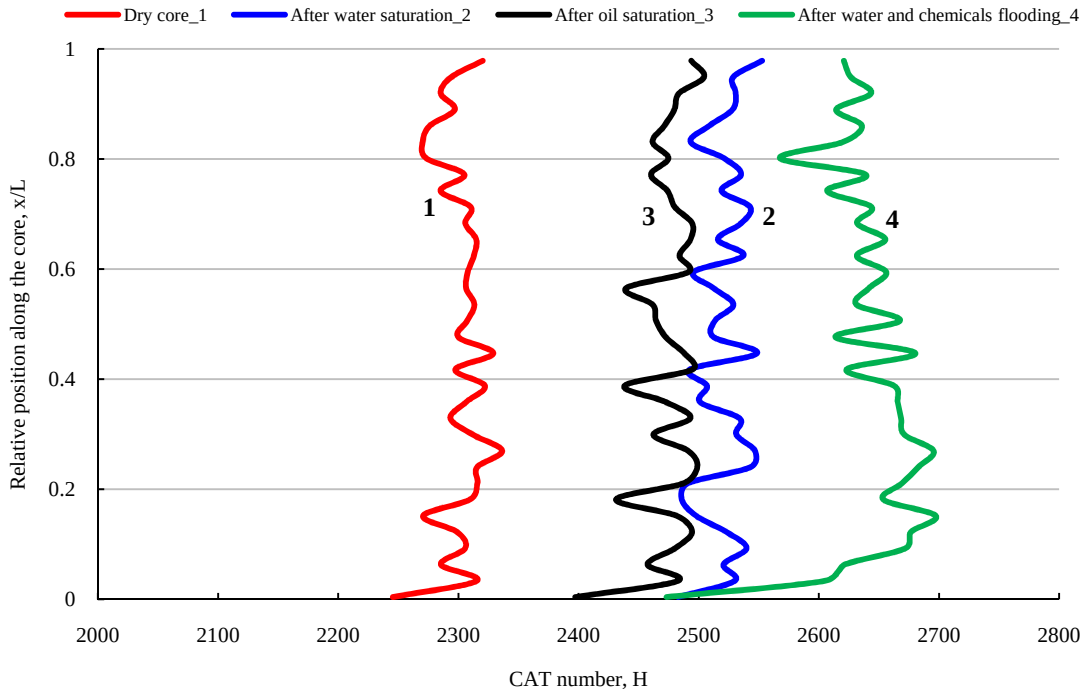

Figure IX-17. CAT number profile for sample IL–5 during different saturation and flooding conditions.

The composition of the chase brine as mentioned earlier was 0.2 wt% polymer in 10 wt% KI solution to differentiate between water and oil phases. There were scattered residual oil along the core as shown in the slice images and tri-planar views (Appendix E). **Figure IX-17** shows advancement in the CAT number after the chase brine injection stage. Also, the injection fluids were clearly bypassed the first two slices which could be due to the capillary ends effect. Since the scan machine measured only the average CAT number for every individual slice, further investigations were performed using advanced scan software (MIPAV).

Three slices were selected at the inlet (1.7 cm), middle (24.2 cm), and end of the limestone core (48.2 cm) for further processing. Selected areas with low and high intensities were analyzed by determining their CAT numbers accordingly. Points A and B in the first slice showed a huge decrease in the CAT number due to remaining crude oil in these areas, **Figure IX-18**. Point C is obviously showed a good sweep area in comparisons to A and B. In addition, similar observations were noticed for the middle slice as shown in **Figure IX-19.**

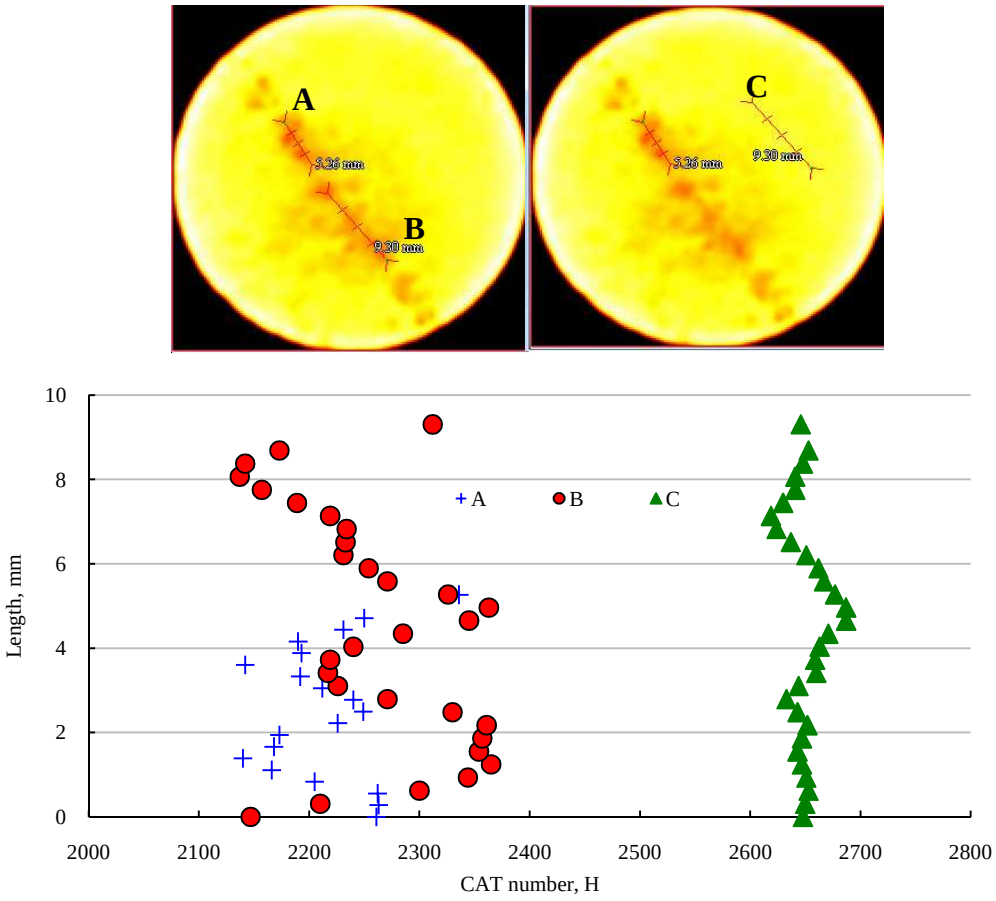

Figure IX-18. CAT scan analysis for slice no. 1 at a core length ratio 0.03 (core IL–5).

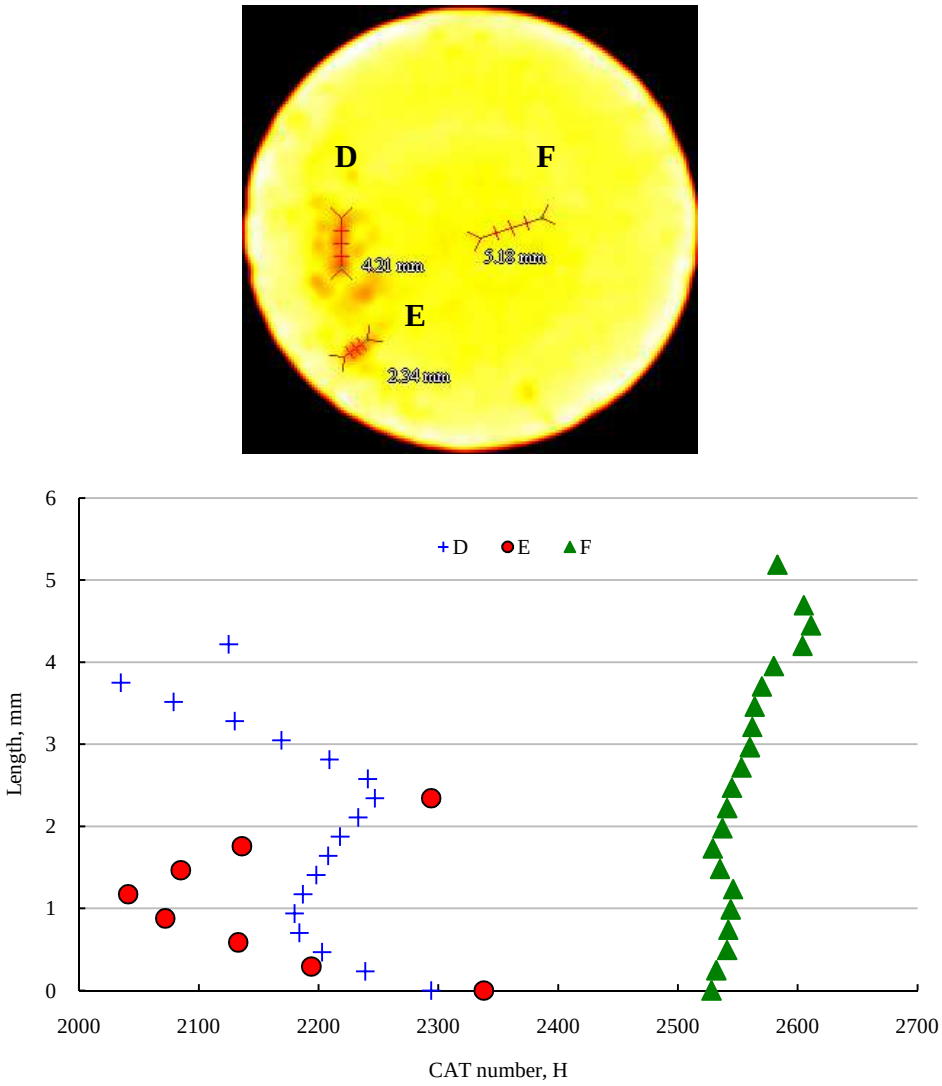

Figure IX-19. CAT scan analysis for slice no. 16 at a core length ratio 0.48 (core IL–5).

The length of the areas that were covered with oil was determined in the slice images as well. To confirm the accuracy of the software, the slice diameter was determined to be 35.85 mm, **Figure IX-20**. It was almost matching the outside diameter of the core (3.7 cm), **Table IX-1**. In summary, 25% of OOIP was not recovered after waterflooding and chemicals injection.

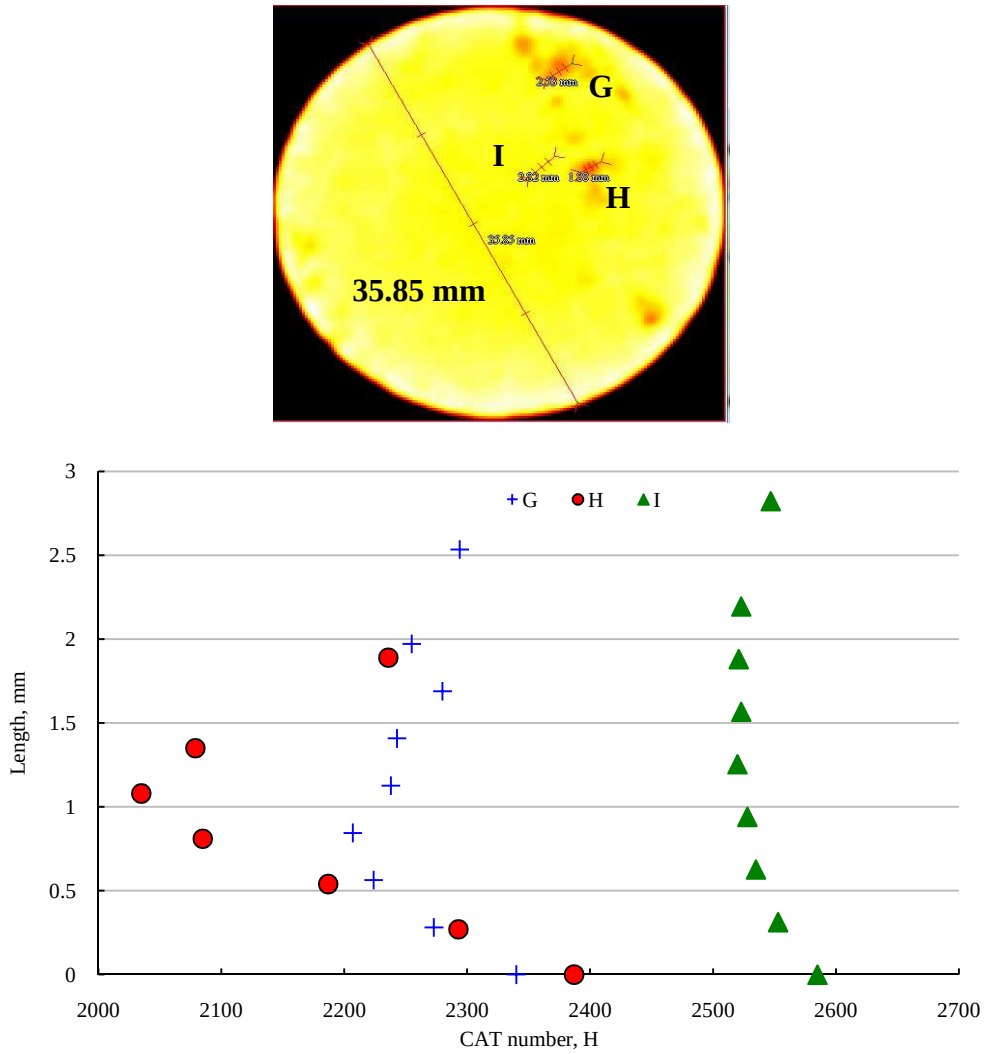

Figure IX-20. CAT scan analysis for slice no. 32 at a core length ratio 0.95 (core IL–5).

The scanning analysis of core W–1 is shown in **Figure IX-21** at different saturation and flooding conditions. As indicated by the CAT number, the middle of the core had some residual oil. The capillary end effects were negligible as the CAT number

at the inlet and the outlet of the core was higher than that of oil saturation. It also indicates the crude oil in the first and last quarters of the core were apparently produced.

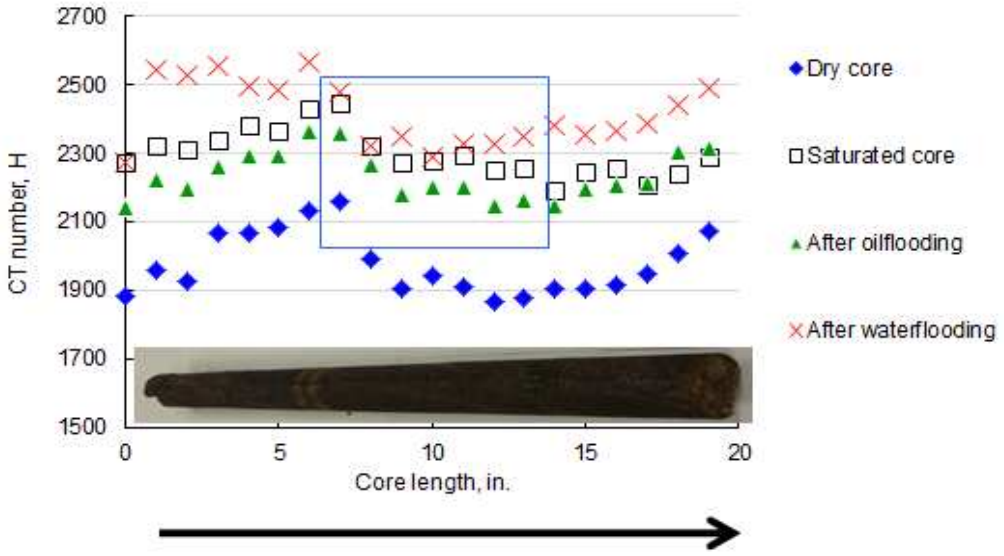

Figure IX-21. CAT number profile for sample W–1 during different saturation and flooding conditions.

Conclusions

Water injection in different carbonate reservoirs was thoroughly examined at different ionic strength. In addition, amphoteric surfactants and acrylamide sulfonate polymer flooding were conducted at 90ºC and harsh environments. The main conclusions from this study are:

1. Seawater injection as a tertiary recovery showed the highest increase in oil recovery (4.4%). The residual oil saturation was substantially reduced by adding equivalent concentrations of magnesium and sulfate ions.

2. Any sudden increase or decrease in injection water salinity slightly increased oil production (up to 1.7%).
3. The surfactants/polymer benefits in four coreflood tests ranged from 7.3 to 17.1% OOIP.
4. After one pore volume of water injection, Ca^{2+}, Mg^{2+}, and SO_4^{2-} ions matched their original concentrations.
5. CAT scan analysis confirmed scattered residual oil near the inlet and along the core. Based on the conclusive results obtained from this study, surfactant/polymer solutions at very low concentrations are more attractive in compare to multistage waterflooding.

CHAPTER X

GEOCHEMICAL SIMULATION OF FLUIDS/ROCK INTERACTIONS

Summary

The subsurface geochemical system consists of solid phase (minerals and organic matter), gas phase, and an aqueous solution (water with its dissolved constituents). The interactions between these three phases depends essentially on various factors such as salt concentrations, temperature and pressure conditions. Such interactions are also affected by the chemical activities of free ions, ion pairs and complexes in the aqueous solution.

In this study, the water/rock interactions were thoroughly investigated at a wide range of temperature, pressure, and salt concentration. Mixing individual streams of seawater and fresh water at various ratios and HTHP conditions showed unpredicted chemical interactions. The calcite/seawater interactions were negligible because of the thermodynamic solubility product of calcite mineral in aqueous solutions is extremely low. Including the crude oil in the interactions was not covered in this chapter because the software had some defects for water/oil/calcite systems.

The results from the geochemical simulation explain the water and brine ions interactions at HTHP with and without calcite minerals. The chemical activities of complexes, ions pairs and free ions in the injection water are affecting the electrostatic charges and interactions. The temperature increased the chemical activities of the ions, while high pressure condition had no effect on the interactions. The negatively ionic

species were apparently impacted by the NaCl and Na_2SO_4 concentrations in seawater. Dilute seawater at different ratios resulted in unexpected activities trends. New findings in this chapter addressed the ions interactions as a function of ionic strength, temperature, and pressures with and without calcite minerals.

Introduction

The chemical activities of the ions and associated complexes are very important in understanding the chemical properties of saline solutions. Such activities are required to estimate the stoichiometric constants for various phenomena such as mineral solubility, dissociation constants, complex formation….etc. In addition, the chemical activities help in categorizing the electrostatic charges between the dissolved species in the interstitial solutions.

The term complex is usually used to describe any association between cations and anions or anionic radicals (when ions are in contact and share electrons). Also, the term “ion pair” is referred to any complexes in which the ratio of the cation to the anion is unity (Garrels and Thompson 1962). Moreover, the ions are separated by water molecules but share their first hydration shell in the “ion pair” case (Murray 2006). In general, the chemical activities must be computed from the concentration before having any interactions with the rock minerals, because the electrostatic forces make the behavior of the solutes to be non-ideal (Fetter 1988).

There are four types of ion pairs: 1) complexes, when the ions are held in contact by covalent bonds, 2) contact ion pairs, when the ions are in contact and linked

electrostatically (with no covalent bonds), 3) solvent-shared ion pair, pairs of ions linked electrostatically and separated by a single water molecule, and 4) solvent-separated ion pairs, pairs of ions linked electrostatically but separated by more than one water molecule (Millero 1974). The important major ion pairs in seawater are the following: $NaSO_4^{-1}$, KSO_4^{-1}, $MgSO_4^{o}$, $CaSO_4^{o}$, SO_4^{o}, $NaCO_3^{-1}$, $MgCO_3^{o}$, $CaCO_3^{o}$, $SrCO_3^{o}$, $NaHCO_3^{o}$, $MgHCO_3^{+1}$, $CaHCO_3^{+1}$, HCO_3^{+1}, MgF^{+1}, CaF^{+1}, and $MgOH^{+1}$.

Chemical Activity

Ions in solution interact with each other as well as with the water molecules. The ions interactions can be ignored at low salt concentrations (C), but the ions behave chemically like they are less concentrated than they really are at high salt concentrations. Chemical activity simply means the actual concentration available for reaction (Deutsch 1997).

Chemical activity (α) = Actual or effective concentration

Infinitely dilute solution, where ionic strength can be ignored ($\alpha = C_i$), is usually called ideal solution (Murray 2006). On the other hand, non-ideal solutions such as seawater have lower effective concentration compare to the real concentration ($\alpha < C_i$)

$\alpha = \gamma * C$

α = chemical activity

γ = activity coefficient

C = molal concentration

Debye-Hückel Model

The activity coefficient of the individual ion can be determined from the Debye-Hückel model (Fetter 1988):

$$-\log \gamma_i = \frac{Az_i^2 \sqrt{I}}{1 + a_i B\sqrt{I}}$$

γ_i = activity coefficient of ionic species i

z_i = charge of ionic species i

I = ionic strength of the solution = $0.5\sum m_i z_i^2$

A&B = constants (temperature and dielectric constant dependent)

a_i = effective diameter of the ion, available in reference (Kielland 1937)

The Debye-Hückel model is applicable for solutions with an ionic strength of 0.1 or less (approximately 5,000 mg/L). For higher ionic strength, the Debye-Hückel model is modified by the addition of a second term which is known as Davies model:

$$-\log \gamma_i = \frac{Az_i^2 \sqrt{I}}{1 + a_i B\sqrt{I}} + 0.3\sqrt{I}$$

Ion Activity Product (K_{iap}) and Scaling Tendency

K_{iap} is the product of the measured activities, and commonly used to determine the saturation condition for aqueous solutions. Saturation index (SI) can be calculated by comparing K_{iap} to the solubility product of the mineral (K_{sp}). The aqueous solutions can be at three different saturation conditions: 1) super saturation at SI>1, 2) saturation at S= 1, and 3) under saturation at S<1.

The scaling tendency is the ratio of real-solution solubility product (K_{iap}) to the thermodynamic limit based on the thermodynamic equilibrium constant (K_{sp}). Saturation

index equal to log (scaling tendency), and the previously discussed saturation conditions can also be applied to the scaling tendency (ST) parameter.

The main objectives of this chapter are to simulate: 1) the geochemical activity of seawater at different conditions of temperature, pressure and composition, 2) the interactions between aqueous solution mixtures including seawater and dilute seawater (50%, 10%, and 1%) and 3) water/calcite interactions at ratios 1:1 and 1:10.

The study is very important in understanding the electrostatic interactions between the ions through determining the effective concentrations (chemical activity). In addition, it brings new insight about the ions interactions of high and low salinity waterflooding in carbonate reservoirs.

Literature Review

Ion association is very important in the molecular structure of solutions, and indeed the ionic and electrostatic interactions. Sulfate ion pairs contain at least one water molecule between the associated ions, which can form a highly dumb-bell type chemical structure (Eigen 1957; Hester and Plane 1964).

The percentages of the major dissolved species present in seawater were determined by Garrels and Thompson (1962). The authors found no evidence of sulfate complexes other than ion pairs. The species that express the total concentration of each cation are:

$Na^{+1}+NaHCO_3^{o}+NaCO_3^{+1}+NaSO_4^{-1} = Na^{+1}$ Total

$Ca^{+1}+CaHCO_3^{+1}+CaCO_3^{o}+CaSO_4^{-1} = Ca^{+2}$ Total

$Mg^{+1}+MgHCO_3^{+1}+MgCO_3^{o}+MgSO_4^{-1} = Mg^{+2}$ Total

The major cations (Na^+, K^+) in seawater exist as uncomplexed species, and only about 10 to 15% of Ca^{+2} and Mg^{+2} are tied up. Magnesium ion is the major cation in terms of the effectiveness in complexing anions. On the other hand, the anions are strongly complexed except the Cl^- ions. Most of the CO_3^{2-}, one third of HCO_3^- and half of SO_4^{2-} are paired with various cations (Garrels and Thompson 1962).

Kester and Pytkowicz (1970) evaluated the effect of temperature and pressure on the major chemical species of sulfate that are presented in seawater. Sulfate-ion pairing in seawater increased as the temperature decreased. The $NaSO_4^{-1}$ ion pairs dissociated with increasing the pressure condition, and thus also increased the concentration of $MgSO_4^{o}$ ion pairs. The effect of the pressure on the ionic speciation is in general agreement, except for $MgSO_4^{o}$ and $CaSO_4^{o}$ (Lafon 1969; Kester and Pytkowicz 1970; Millero 1971). Increasing the pressure increases the percentage of free ions and also decreases the percentage of ion pairs.

The activity coefficients of different ions (H^+, Na^+, K^+, Cl^-, NO_3^-, SO_4^{-2} and Ca^{+2}) in the ground water were calculated using the extended Debye-Hückel equation as shown in **Figure X-1**. The lowest activity coefficient was observed for SO_4^{2-} ions at a wide ionic strength range. The hydrogen ions, on the other hand, had the highest activity coefficient.

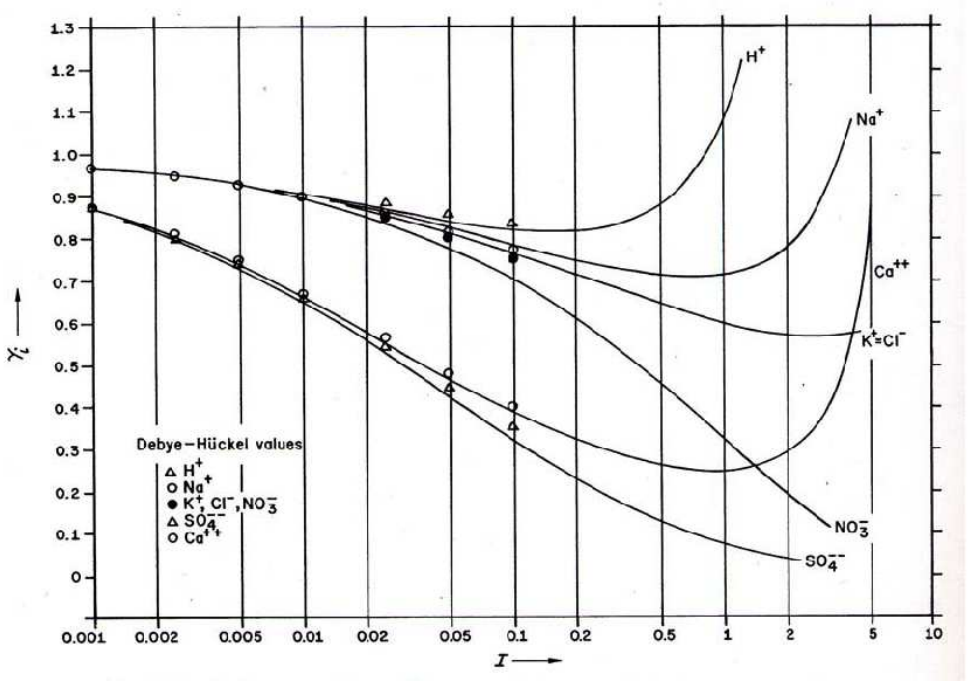

Figure X-1. Single ion activity coefficient versus ionic strength for some common ions (Murray 2006).

OLI Simulation Systems

OLI systems are commonly used to calculate the physical and chemical properties of multi-phase, aqueous-based systems with and without solids. It can be applied to most multi-component solutions, and is predictive over almost any conceivable temperature, pressure and concentration of interest. OLI systems help in understanding and modeling aqueous electrolyte thermodynamics. More attentions are given to the ions species and complexes in terms of their chemical activity with and without calcite mineral. Additional information on OLI software is available on this website www.olisystems.com. It is worth mentioning that the geochemical modeling based on equilibrium and irreversible thermodynamics has become a well recognized tool for understanding water-rock interaction and predicting their consequences. Numerous

computer program codes are available for geochemical modeling including: OLI, PATHI, SOLMNEQ, WATEQ, MINEQL, EQ3/EQ6, PHREEQE, GEOCHEM, SOLVEQ, MINTEQ and DYNAMIX (Kharaka *et al.* 1988).

Approach

The chemical formula for all salt ingredients in seawater was selected and entered to the inflow grids **(Figure X-2**). The geochemical model "aqueous H^+ ions" was used, since it is applicable to most multi-component mixtures of chemicals in water. All calculations were performed at isothermal conditions (90ºC) and constant pressure 500 psi simulating the condition of coreflood experiments in previous chapters. In the single point calculation of seawater, scale tendency and effective concentration (chemical activity) of ions pairs and complexes were only studied.

Multiple point calculations were also evaluated for seawater at various temperatures, pressures and seawater composition. In addition, aqueous streams (seawater and fresh water) and calcite rock were mixed simultaneously at different ratios. The software can predict the behavior of the ions at low salt concentration and in direct contact with calcite rock at high temperature and pressure conditions. Most of the results are presented in terms of the chemical activity versus the complexes and component ions. Since the chemical activity is directly affecting the electrostatic interactions, the other thermodynamic results (Gibbs free energy, entropy, and K-values) are not considered in this study**. Figure X-2** shows the main OLI analyzer window.

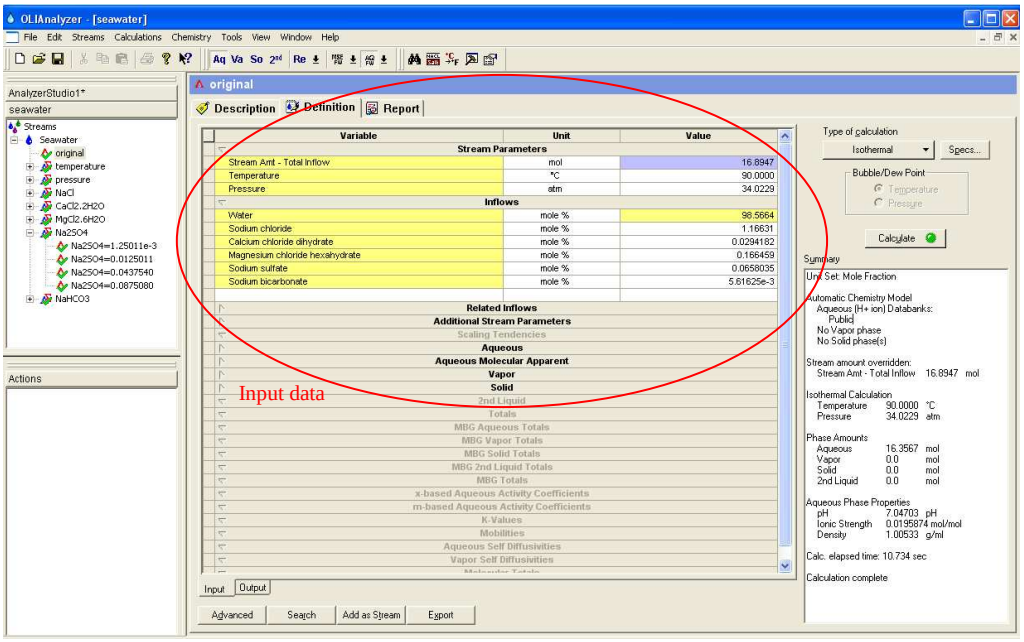

Figure X-2. OLI analyzer window for seawater.

Results and Discussion

Seawater

The chemical activities of the ion-pairs and the ion complexes in seawater are shown in **Figure X-3**. Water molecules apparently had the highest activity result. In addition, the activity of the free Na^{+} and Cl^{-} ions were approximately 0.01. Free Mg^{2+} ions were also expected to be very active in seawater as the Mg concentration in seawater is more than 2,200 mg/L. Surprisingly, the species $NaSO_4^{-}$, $MgSO_4$ and SO_4^{2-} had higher chemical activity than free Ca^{2+}. Therefore, the electrostatic interactions with the reservoirs rocks will be more affected by the complex species in compare to the calcium ions. The activity of the other ion-pairs and complexes were less than 2E-5 as displayed in **Figure X-3**.

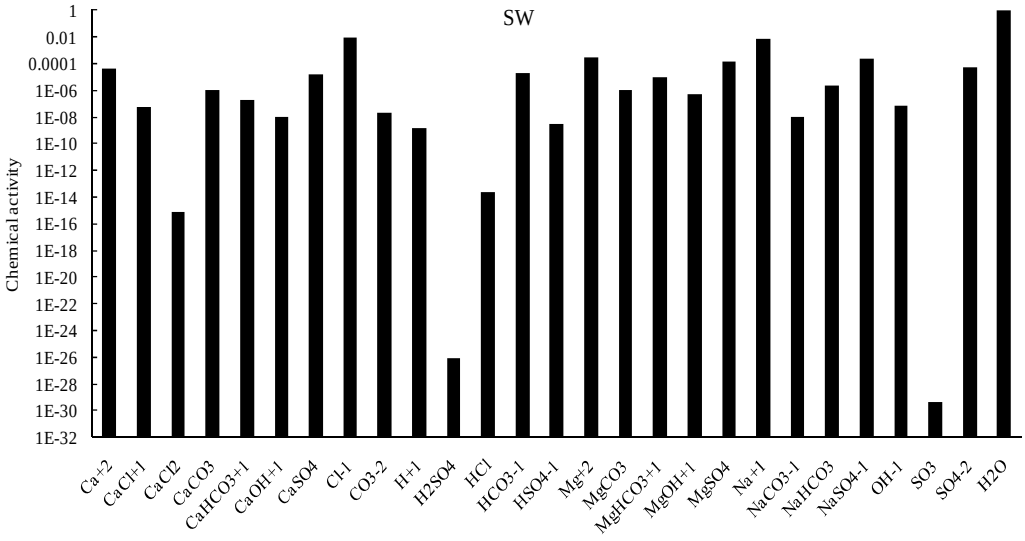

Figure X-3. Chemical activity of ions species in seawater at 90ºC and 500 psi.

The scale tendency (ST) results of various salts in seawater are shown in **Table X-1**. The highest ST (2.97) was observed for $CaCO_{3(s)}$, implying that the seawater was super saturated with $CaCO_3$. On the other hand, the tendency of $CaSO_4$ scale was very minimal as the ST was less than 1 (0.85).

Effect of temperature

The output file of the OLI software has only the concentration of ionic species and activity coefficients. But, in fact, the chemical activity represents the effective concentration rather than the activity coefficient as reported in the introduction part. A sample of the activity coefficient of the positively ion species is shown in **Figure X-4**. The chemical activity can be determined by multiplying the activity coefficient and concentration of ions.

More focus was given to the chemical activity of the positive and negative species as they substantially affect the electrostatic interactions. The activity of water compound in all solutions was observed to be the highest, because the water solvent is the major constituent in seawater and other underground water.

Table X-1. Scaling tendencies of dissolved salts in seawater.

Scaling Tendencies

Row Filter Applied: Only Non Zero Values

Calcium carbonate (calcite)	2.97562
Calcium sulfate	0.855327
Calcium sulfate dihydrate	0.366209
Magnesium carbonate	0.229228
Magnesium hydroxide	0.169640
Magnesium carbonate trihydrate	0.0350389
Sodium chloride	7.82823e-3
Sodium sulfate	3.94882e-3
Magnesium sulfate monohydrate	1.25602e-3
Magnesium sulfate-0.5-(magnesium hydroxide)	8.85280e-4
Magnesium sulfate-0.25-(magnesium hydroxide)-hemihydrate	8.68333e-4
Sodium bicarbonate	5.75367e-4
Sodium carbonate monohydrate	4.93019e-7
Magnesium chloride hexahydrate	1.56744e-7
Magnesium chloride hydroxide	1.15829e-7
Calcium hydroxide	7.44088e-8
Calcium chloride dihydrate	1.31720e-9
Sodium bicarbonate carbonate dihydrate	7.32811e-10
Sodium bisulfate	2.22280e-10
Hexasodium carbonate bissulfate	1.28522e-10

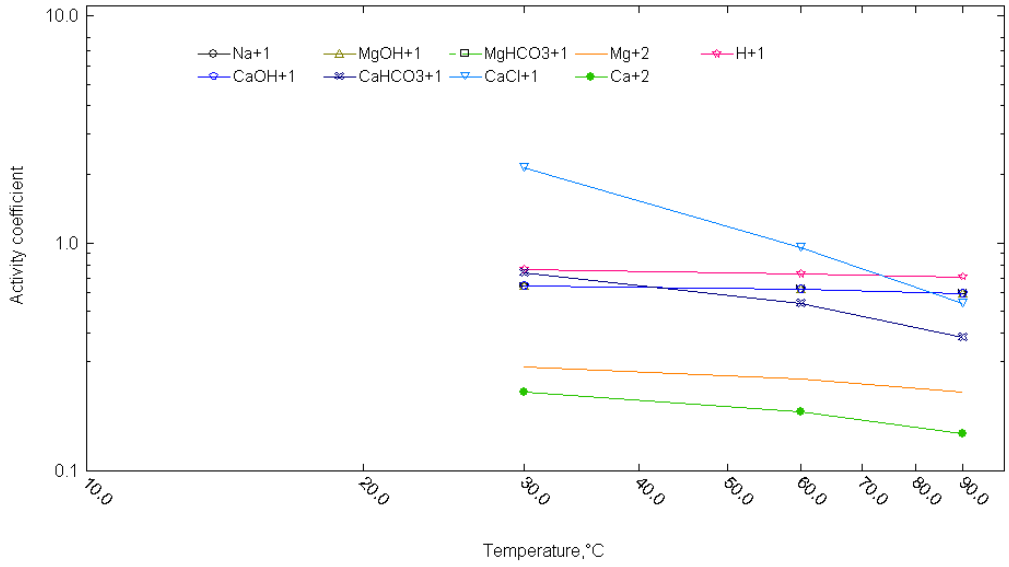

Figure X-4. Activity coefficient of seawater ionic species as a function of temperatures.

Figure X-5 shows the chemical activity of the positive ions versus temperatures. The highest activity was observed for free Na^{+}, Mg^{+2} and Ca^{+2}, respectively. In general, the activity of the ions increased as increasing the temperature, and that was more pronounced at low activity values.

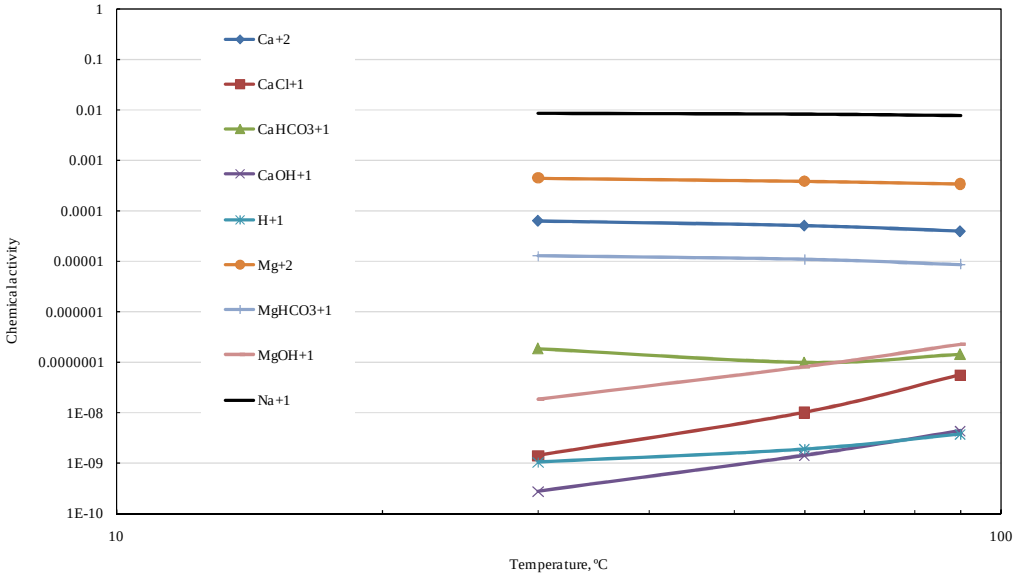

Figure X-5. Chemical activity of positive ionic species versus temperatures.

The highest chemical activities of the negative ionic species were reported for Cl^-, $NaSO_4^{-1}$, SO_4^{2-}, and HCO_3^{2-}, accordingly **(Figure X-6**). Three major trends were observed for the activity of the ions against the temperatures. The ions that had the highest activity were almost independent of the temperature condition. At low activity range, only carbonate and sodium carbonate ions decreased as increasing the temperature condition. The chemical activity does not only depend on the ionic strength but also on other factors such as diameter and valence of the ions. Moreover, there are constants in the activity coefficient equation, which depend on the dielectric constant as well as temperature conditions.

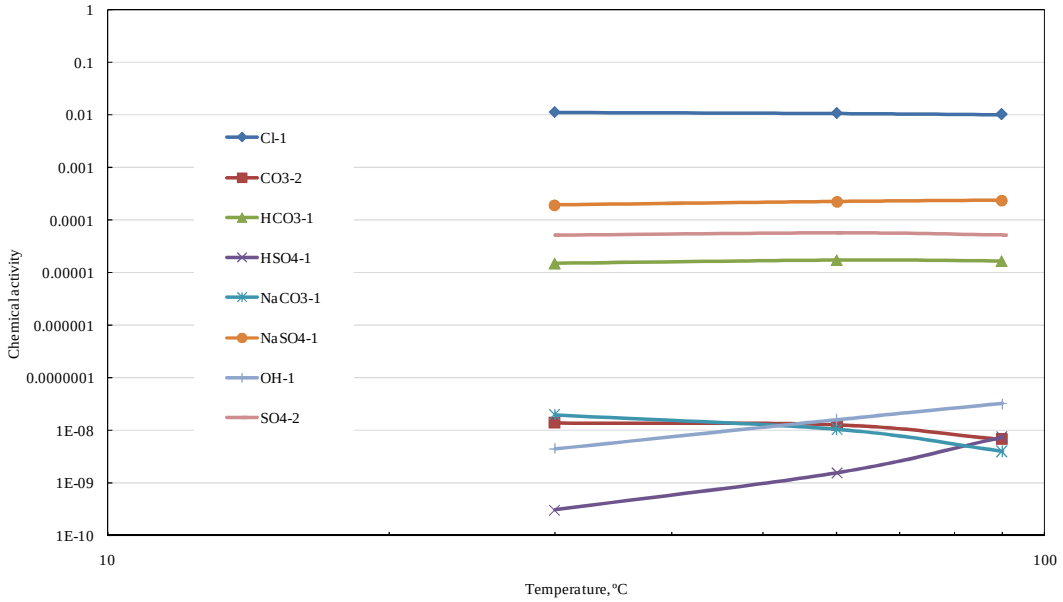

Figure X-6. Chemical activity of negative ionic species versus temperature.

The activity of the chemical compounds in seawater as a function of temperature is shown in Appendix G. H_2O, $MgSO_4$ and $CaSO_4$ had higher chemical activity than the other compounds. This behavior confirmed the additional oil recovery that was previously observed in Chapter IX as a result of Mg and SO_4 combination (experiment IL–11). A direct relationship was observed with temperature at low chemical activity range. On the other hand, the temperature showed no impact on the activity of the salt compounds at higher activity range.

Effect of pressure

The pressure was increased from 100 to 1000 psi, as a result, the chemical activities of positive species were not affected as shown in **Figure X-7**. In contrast, there were slight

changes in the activity of $H_2SO_4^{-1}$ and $NaCO_3^{-1}$ at 1000 psi **(Figure X-8)**. All other ions showed a stable activity at various pressure conditions.

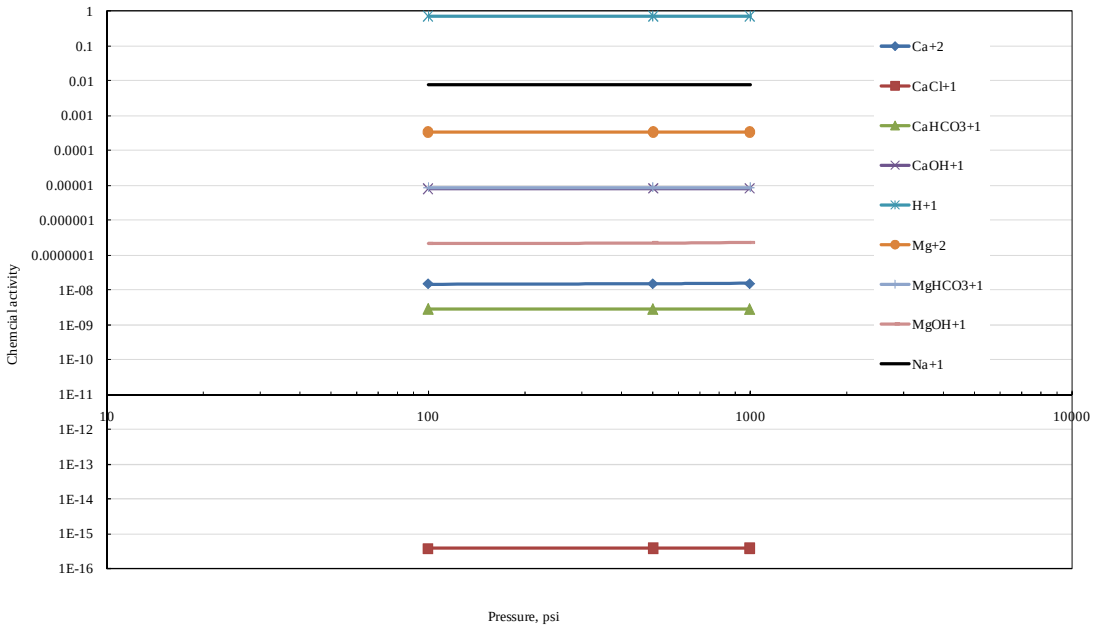

Figure X-7. Effect of pressure on the chemical activity of positive ions in seawater.

Effect of mono and divalent ions concentrations

A sensitivity study was conducted to the seawater composition at wide concentrations ranges of NaCl, $CaCl_2.2H_20$, $MgCl_2.6H_2O$, Na_2SO_4, and $NaHCO_3$. Increasing the NaCl concentration from 1,000 to 40,000 mg/L apparently increased the activity of Na^{+1}, $CaCl^{-1}$, Cl^{-1}, $NaSO_4^{-1}$, and $NaCO_3^{-1}$ **(Figures X-9 and X-10)**. Chloride, in general, does not form ion pairs with the major cations in seawater. In brief, the activities of free ions (Na^{+1}, Cl^{-1}) and also the ion-pairs were affected with increasing the ionic strength. This result matched a study by Millero (1974) which confirmed most of the Na^{+1} are free ions in seawater.

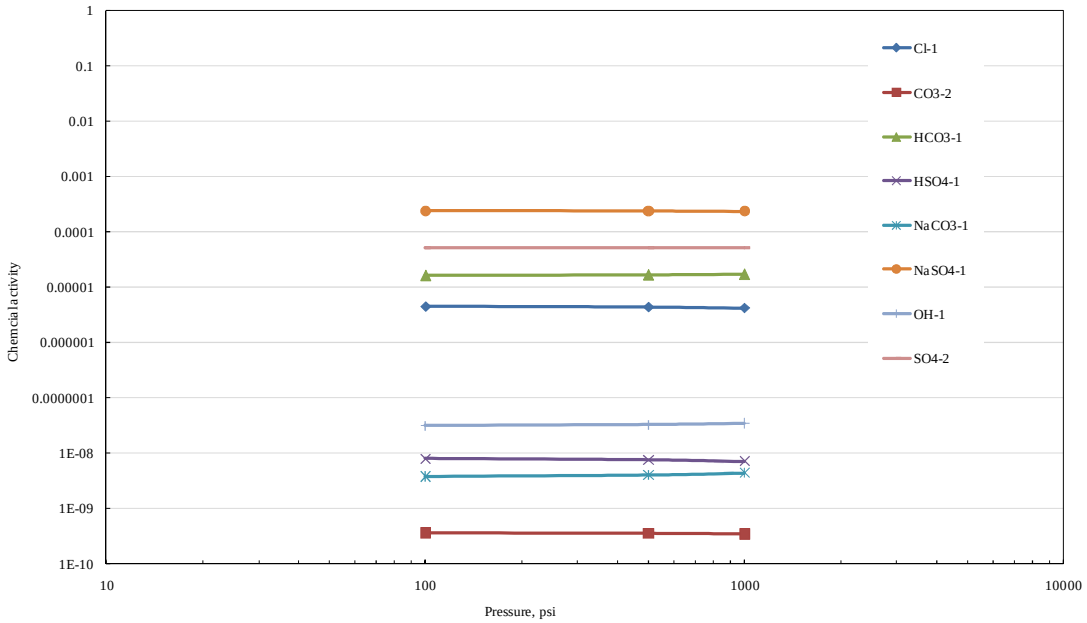

Figure X-8. Effect of pressure on the chemical activity of negative ions in seawater.

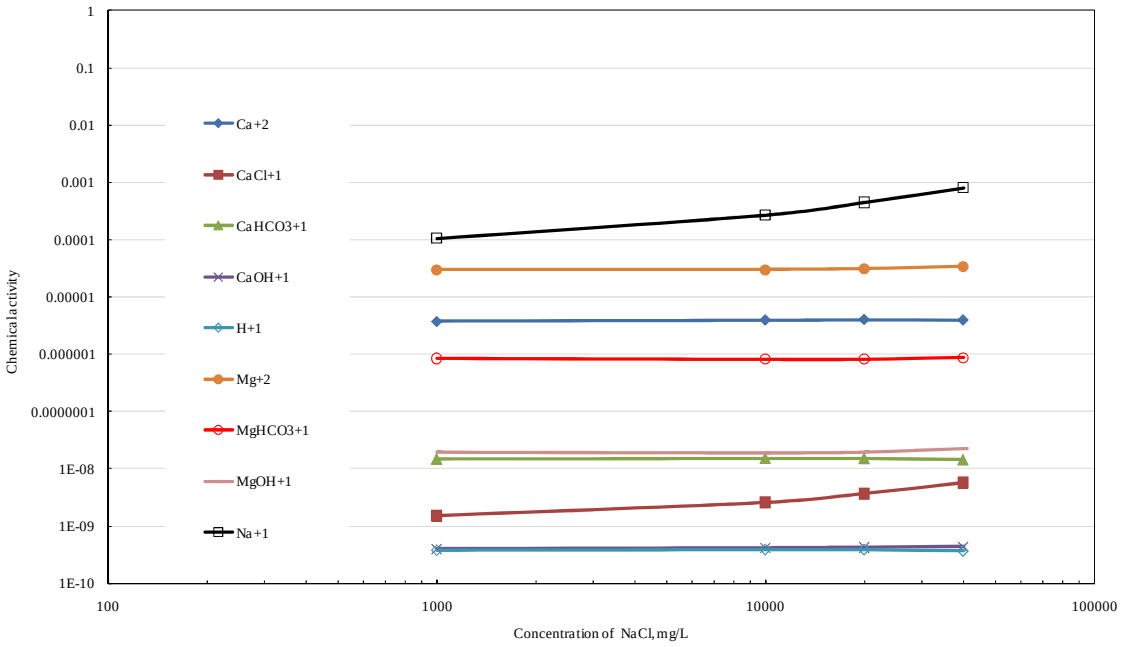

Figure X-9. Effect of NaCl concentration on the chemical activity of positively ionic species in seawater.

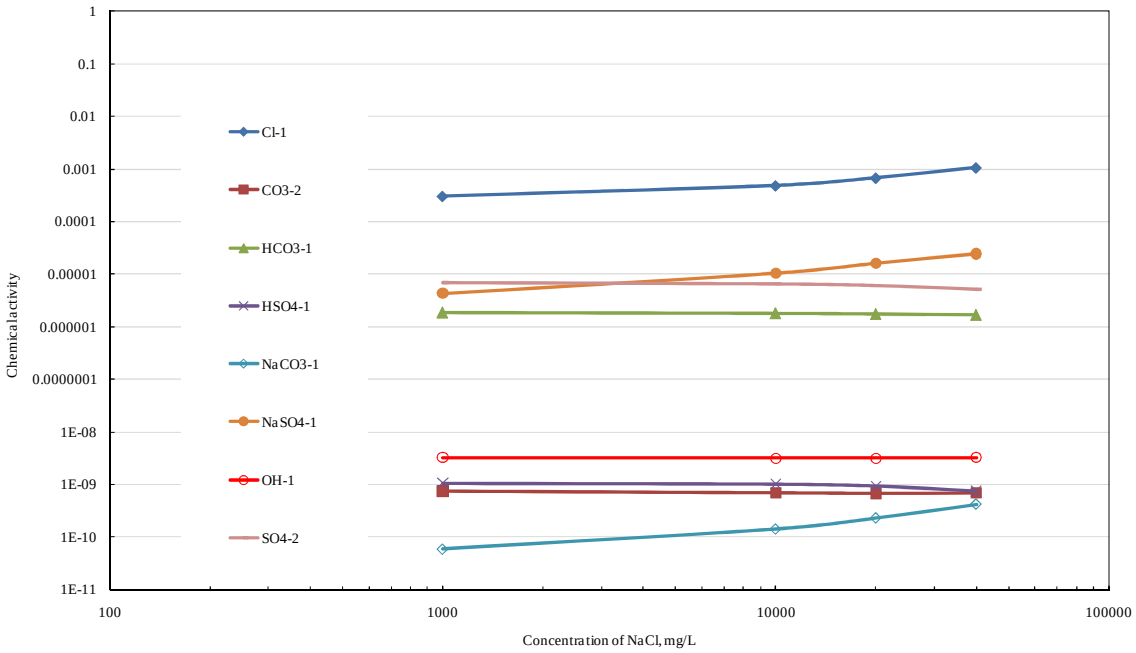

Figure X-10. Effect of NaCl concentration on the chemical activity of negatively ionic species in seawater.

Increasing the $CaCl_2.2H_2O$ concentrations up to 1,000 mg/L significantly increased the activity of the next positive ions: Ca^{2+}, $CaHCO_3^{+1}$, $CaCl^{+1}$, and $CaOH^{+1}$, respectively **(Figure X-11)**. Moreover, the activity of OH^{-1}, CO_3^{-2}, and $NaCO_3^{-1}$ decreased slightly as shown in **Figure X-12**. This decrease in the activity was attributed to the additional complexes that formed with Ca ions at 1,000 mg/L, which accordingly decreased the activity of free negative ions. The effective concentrations of $CaCl_2$, $CaSO_4$, and $CaCO_3$ were gradually increased with increasing the level of Ca ions in seawater. The scale tendency of $CaSO_4$ observed to be 0.34 at Ca concentration 1,000 mg/L. It is worth to mention the concentration range of ions in the sensitivity study was selected based on their original concentrations in seawater **(Table II-1)**.

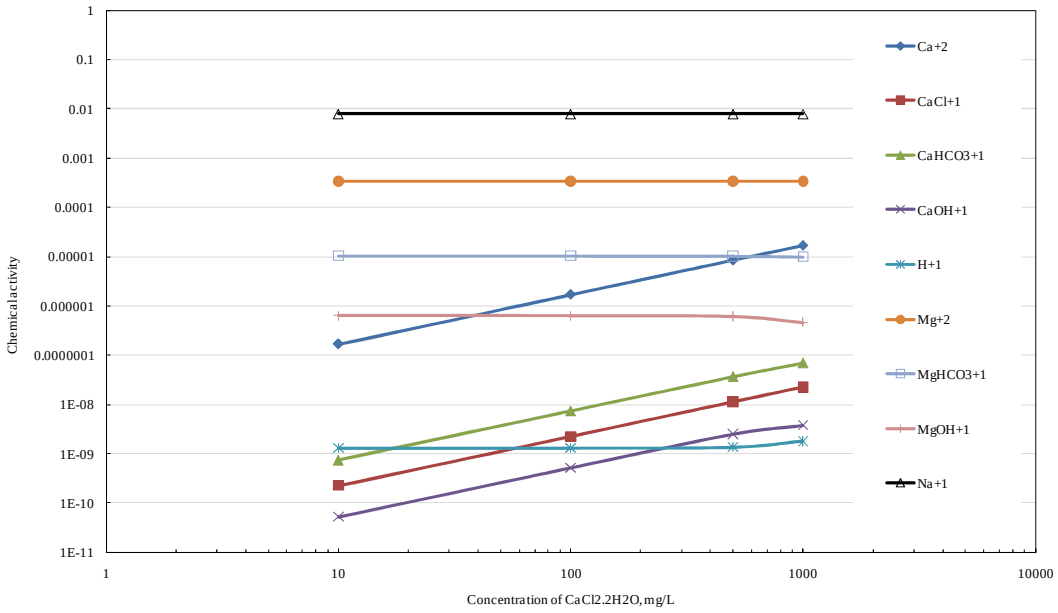

Figure X-11. Effect of $CaCl_2.2H_2O$ concentration on the chemical activity of positively ionic species in seawater.

The effective diameter of the Mg ion (8) is greater than that of Ca ion (6); as a result, the chemical activity of the ions should not be similar. The effect of $MgCl_2.6H_2O$ on the activity of the ions was investigated within the range of 10 to 40,000 mg/L. As expected, the chemical activities of Mg^{+2}, $MgHCO_3^{+1}$, and $MgOH^{+1}$ increased accordingly **(Figure X-13)**. Surprisingly, the negative ionic species was not affected even at higher Mg concentration (40,000 mg/L), **Figure X-14**. $MgCO_3$ and $MgSO_4$ also increased gradually as increasing the Mg concentration in seawater (Appendix G).

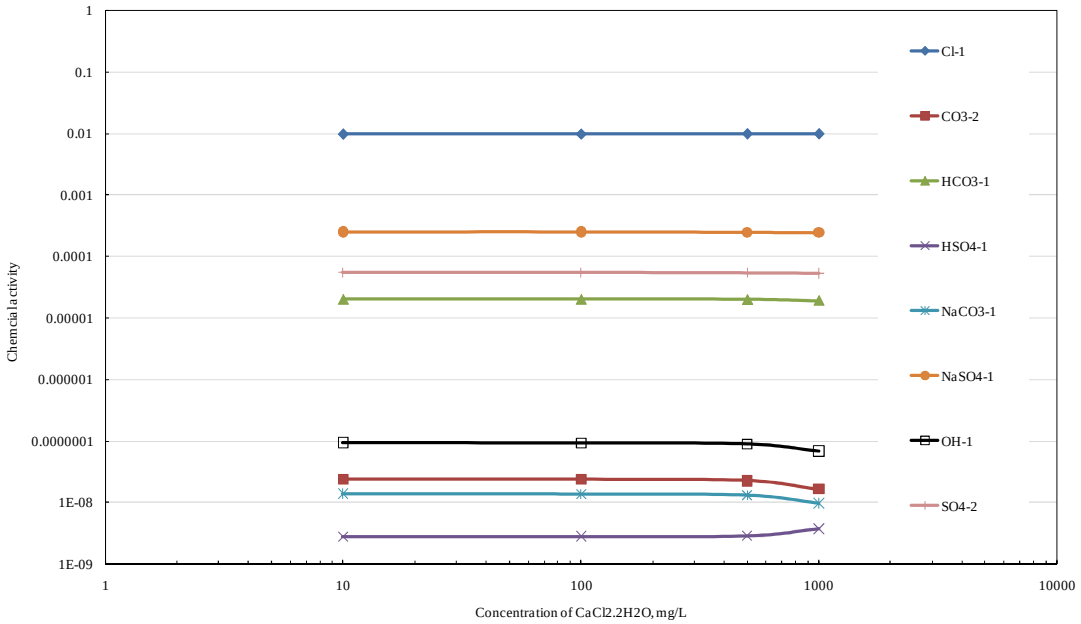

Figure X-12. Effect of $CaCl_2.2H_2O$ concentration on the chemical activity of negatively ionic species in seawater.

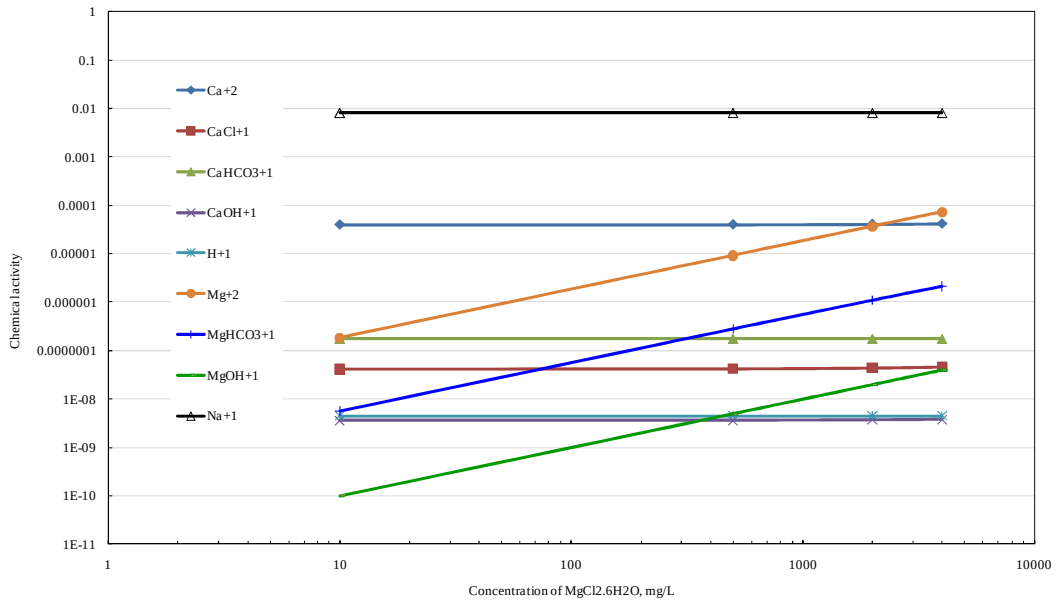

Figure X-13. Effect of $MgCl_2.6H_2O$ concentration on the chemical activity of positively ionic species in seawater.

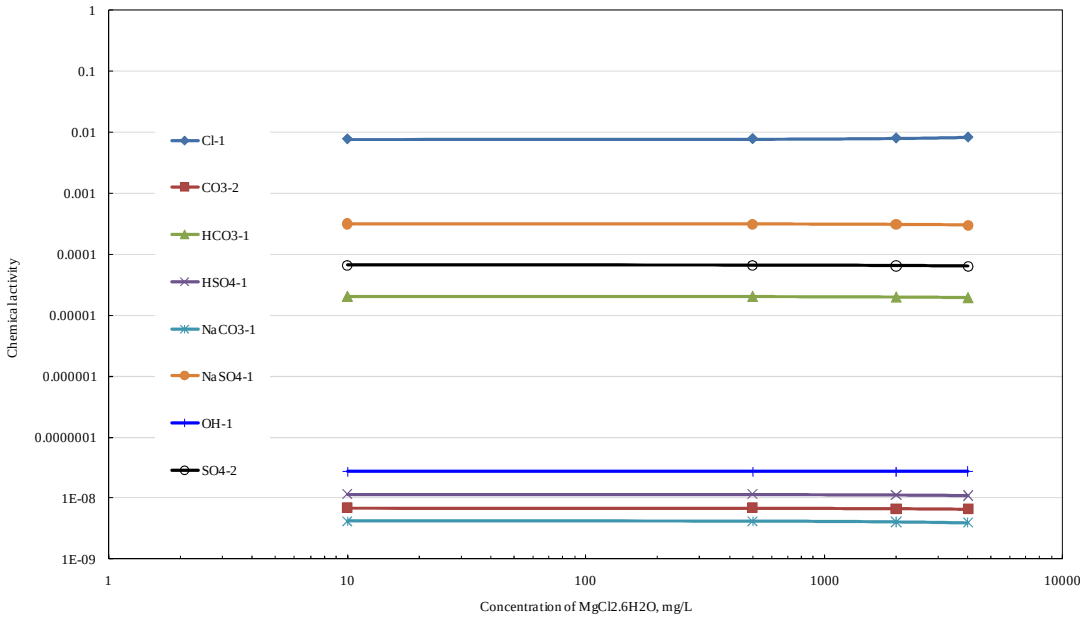

Figure X-14. Effect of $MgCl_2.6H_2O$ concentration on the chemical activity of negatively ionic species in seawater.

The concentrations of sodium sulfate in seawater were also increased from 100 to 7,000 mg/L. The activities of positive ionic species were almost independent on the concentrations of Na_2SO_4 solution **(Figure X-15)**. In contrast, the activity of $NaSO_4^{-1}$, SO_4^{-2}, and HSO_4^{-1} were increased linearly with the concentration of Na_2SO_4 **(Figure X-16)**. The sulfate compounds ($MgSO_4$, $CaSO_4$, H_2SO_4, and SO_3) also became more effective at higher SO_4 concentrations (Appendix G). The free sulfate ion in seawater is usually varied between 39 and 54% (Millero 1974). In short, the activities of sodium species were insignificantly affected compared to sulfate ions, because the Na concentration in seawater was essentially high. Similarly, increasing the concentrations of $NaHCO_3$ in seawater, from 10 to 1,000 mg/L, significantly increased the activities of

the following species and compounds: HCO_3^{-1}, $CaHCO_3^{+1}$, $MgHCO_3^{+1}$, $NaHCO_3$, and $MgCO_3$.

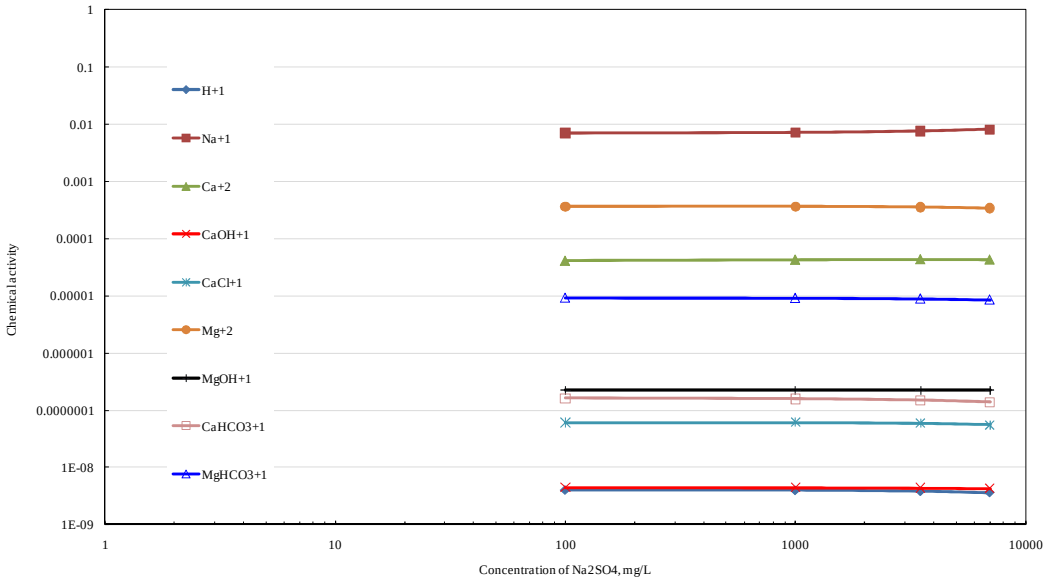

Figure X-15. Effect of Na_2SO_4 concentration on the chemical activity of positively ionic species in seawater.

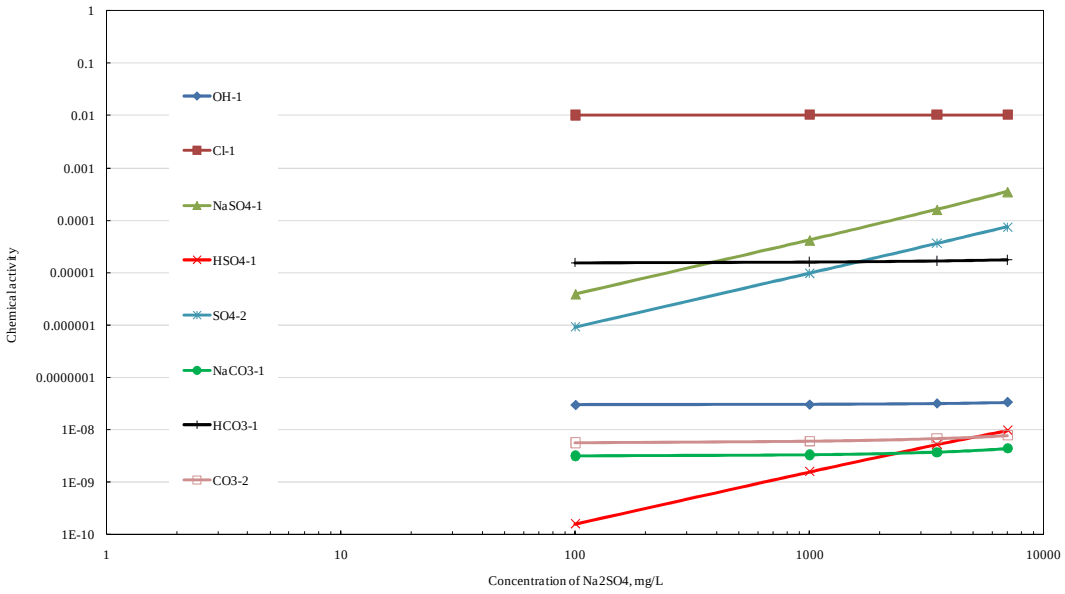

Figure X-16. Effect of Na_2SO_4 concentration on the chemical activity of negatively ionic species in seawater.

Effect of low salinity water

The objective of the next simulation runs was to mix fresh water with seawater streams at different volume ratios, and determine the chemical activities of the new output streams. The ionic strengths of the new streams are certainly decreased but it is still unknown how the concentrations of the ion pairs and the complexes are consequently changing.

Seawater stream was diluted at four different ratios with fresh water: 1, 10, 50 and 90 vol%. The activities of the positive species, in general, decreased gradually as increasing the dilution ratio except the H^{+}. There are three trends for the positive ions as depicted in **Figure X-17**. The free monovalent and divalent cations increased almost linearly with the salinity. Carbonate ions ($MgHCO_3^{+1}$ and $CaHCO_3^{+1}$) and $CaCl^{+1}$ had a steeper decrease in their chemical activities in compare to other positive species. The activities of hydroxide ($CaOH^{+1}$ and $MgOH^{+1}$) and H^{+1} ions were slightly fluctuated at high salinities (50 and 90%). In summary, the activity behavior for low salinity water showed different trends than that of seawater. For example, $MgOH^{+1}$, $MgOH^{+1}$, and H^{+1} ions were very active after using 1 vol% seawater. Also, the activity of $CaHCO_3^{+1}$ ions in seawater was higher compared with 1 vol% seawater. Therefore, it can be concluded that decreasing the seawater salinity changed the chemical activities of the most ionic species.

The activities of the negative species ($NaCO_3^{-1}$, Cl^{-1}, $NaSO4^{-1}$ and $SO4^{-2}$) decreased linearly with decreasing the salinity **(Figure X-18)**. It is very important to observe the steep decrease in the activities of $NaCO_3^{-1}$ in comparison to the other

species. The activity of free OH^{-1} was almost steady except at 90% seawater, because the water is well structure compound and can form molecular cluster together via hydrogen bonding (Deutsch 1997).

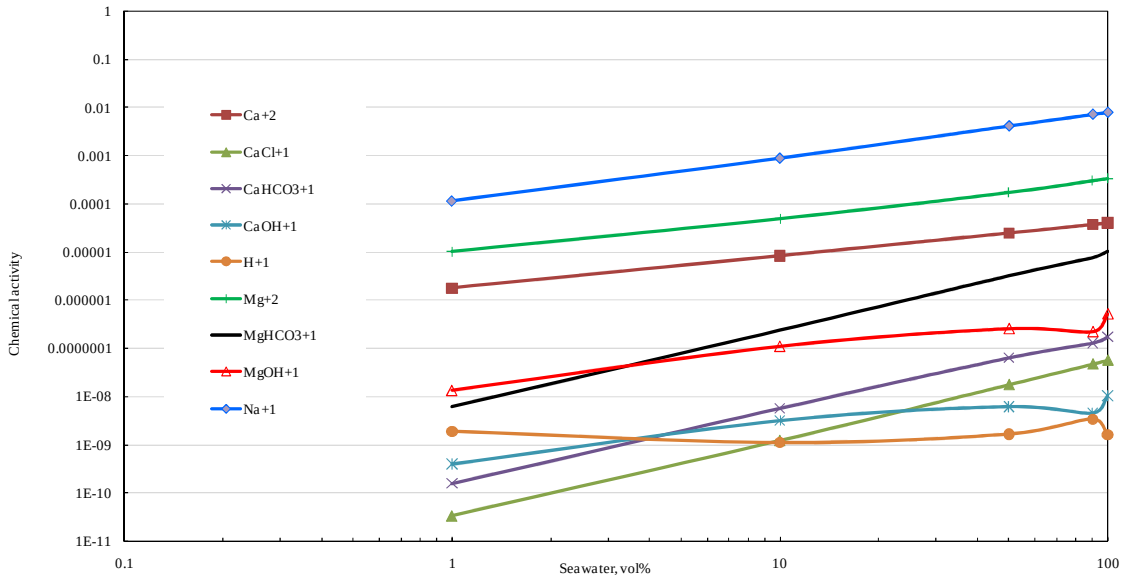

Figure X-17. Effect of salinity on the chemical activity of positively ionic species.

Calcite/water interactions

The equilibrium constant of calcium carbonate in contact with natural water (either surface or ground water) is usually very low (approximately 1E-8.48 at 25ºC and 14.7 psi). The solubility of calcite has inverse and direct relationships with temperature and pressure conditions, respectively (Deutsch 1997). Calcium carbonates (solid phase) were mixed with seawater and 50% seawater at different ratios.

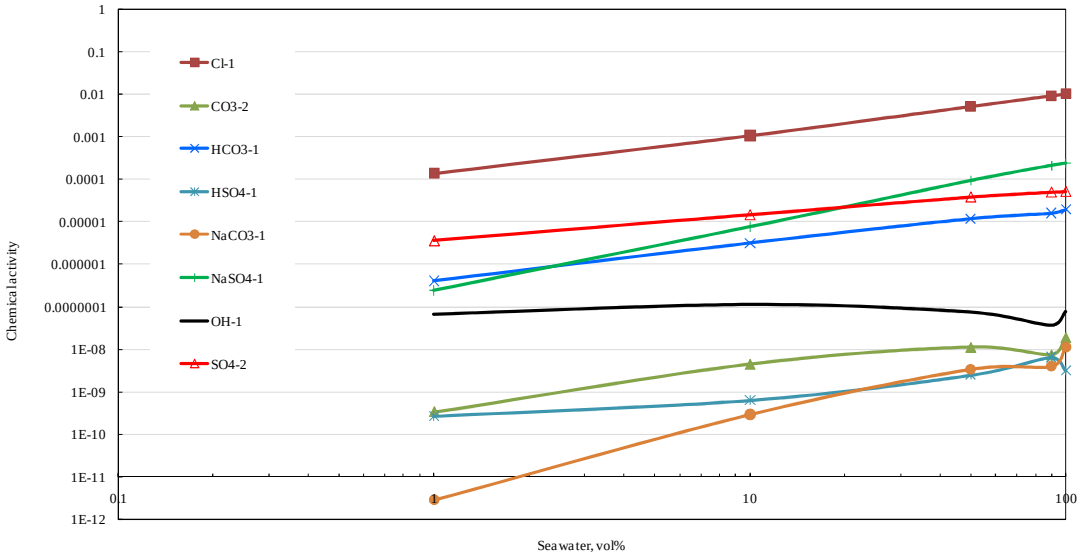

Figure X-18. Effect of salinity on the chemical activity of negatively ionic species.

Presence of calcite in seawater at ratios 1:1 and 1:10 was insignificantly affecting the chemical activities of the positive species. The 50% seawater-$CaCO_3$ system decreased the activities of $CaCl^{+1}$, $CaHCO_3^{+1}$, $MgHCO_3^{+1}$ and Na^{+1} **(Figure X-19)** due to decreasing the seawater salinity which obviously increased the water molecules.

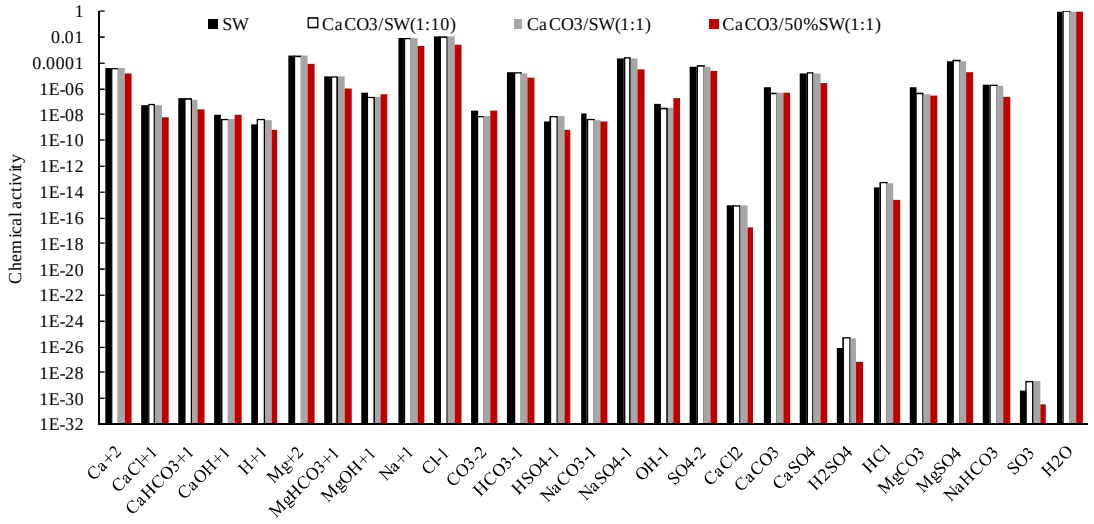

Figure X-19. Chemical activities of calcite/water ionic species at different ratios.

The activities of CO_3^{2-} and OH^{-1} ions in 50% seawater-$CaCO_3$ showed to be higher than other seawater-$CaCO_3$ systems. This was mainly attributed to the ions interactions with calcite mineral. Additionally, the chemical activities of $CaCl_2$, H_2SO_4, and HCl significantly decreased.

Conclusions

The following conclusions were drawn from the geochemical simulation studies using OLI software:

1. The chemical activities of ionic species in seawater and dilute seawater are significantly affecting the positive and negative electrostatic interactions.
2. Temperature increased the activities of the ion pairs and complexes.
3. The pressure had insignificant effect on the interactions of the ions.

4. NaCl and Na_2SO_4 clearly impacted the activities of the negatively ionic species.
5. The negatively ionic components were not affected by the Mg concentration in seawater.
6. Dilute seawater at different ratio produced unexpected activities trends of various positive and negative ionic species.
7. The solubility product of calcite in aqueous solution is known to be low. For that reason, no significant change in the chemical activities of the ions was observed.

CHAPTER XI

CONCLUSIONS

The multistage waterflooding and dilute amphoteric surfactants injection using a wide salinity range were extensively studied from different perspectives in carbonate reservoirs. The major findings were summarized based on surface charge, contact angle, coreflood, CAT scan and simulation results at high temperatures and elevated pressures conditions.

Zeta Potential of Aqueous Phase, Carbonates and Crude Oil

The zeta potential of limestone and dolomite particles were significantly altered to positives values in presence of high salinity brines. This was mainly attributed to the high cations concentrations (Ca and Mg). Decreasing the injection water salinity apparently created negative charges on carbonates' particles by expanding the thickness of the electrical double layer and adsorption of the hydroxide ions. Increasing temperature significantly reduced zeta potential results.

The surface potential of crude oil droplets were affected by 10% diluted seawater (- 24.94 mV), seawater without Ca^{2+} and Mg^{2+} ions (- 17.7 mV), and deionized water (- 26.37 mV) because of hydroxide ions adsorption at the oil/water (O/W) interface. Oil-wet limestone particles behaved differently in water than the intermediate or water-wet particles. The effect of ionic strength was more pronounced in the oil-wet limestone

particles than others. The aqueous layer around oil droplets such as formation brine and seawater played a key role in the generated zeta potential.

Wettability of Carbonates Using Static and Dynamic Contact Angle Methods

Static contact angle results showed major changes in the wettability conditions at higher temperatures. In addition, the contact angle results also were affected by the crude oil composition and aging conditions. Fresh and deionized water altered the calcite wettability to water-wet. It is worth observing the salinity is not changing with time (static). But, in the next paragraph, dynamic contact angle results are summarized.

The partial hydration and dehydration of calcite surface showed no impact on calcite wettability. In addition, contact angle results were not affected by sulfate ions. At high sulfate concentration, $CaSO_4$ precipitation was observed after exceeding the solubility product limitation. Formation brine altered calcite wettability toward oil-wet; however, a subsequent adjustment in salinity did not impact the contact angle. Dilute amphoteric surfactant altered the rock wettability to water-wet at certain concentrations.

Waterflooding and Dilute Surfactants Injection in Vugular Dolomite Reservoirs

Injection of formation brine showed the highest oil recovery in secondary mode tests (dolomite cores). This was mainly attributed to the similarity in the injection and connate brines' compositions. Seawater and shallow aquifer water injection as a tertiary mode insignificantly decreased the residual oil saturation. No ions interactions were reported

between dolomite minerals and saline water ions. Deionized water showed mixed results throughout multistage fluids injection.

Cyclic salinity and dilute seawater injection increased oil recovery by 2 and 4.7% OOIP, respectively. Adsorption of the hydroxide ion at the interface altered the surface charge of the dolomite to negative. As a result, more repulsion forces were created between the carboxylate group in crude oil and the OH^- ions in the adsorbed water later. Dilute amphoteric surfactant with and without HPAM polymer suggested significant enhancement in oil production (up to 21.3%). Polymer flooding did not affect the residual oil saturation, which indicates the capillary forces are more important than the viscous ones. Rotating disk test confirmed no interactions took place between seawater ions and dolomite minerals at 130ºC.

Brine and Surfactant/Polymer Injection in Different Limestone Reservoirs

In limestone tests, seawater injection as a tertiary recovery showed the highest increase in oil recovery (4.4%). The residual oil saturation was substantially reduced by adding equivalent concentrations of magnesium and sulfate ions. In addition, any sudden increase or decrease in the salinity slightly increased oil production (up to 1.7%). The surfactants/polymer benefits in four coreflood tests ranged from 7.3 to 17.1% OOIP. After one pore volume of water injection, Ca^{2+}, Mg^{2+}, and SO_4^{2-} ions matched their original concentrations. CAT scan analysis confirmed scattered residual oil near the inlet and along the core. Based on the conclusive results obtained from this study,

surfactant/AMPS polymer solutions at very low concentrations are more attractive in compare to multistage waterflooding.

Geochemical Simulation of Brine/Rock Interactions

The chemical activities of ionic species in seawater and dilute seawater are significantly affecting the positive and negative electrostatic interactions. Temperature increased the activities of the ion pairs and complexes. NaCl and Na_2SO_4 obviously impacted the activities of the negatively ionic species. Dilute seawater at different ratios produced unexpected activities trends of various positive and negative ionic species. The solubility product of calcite in aqueous solution is extremely low. For that reason, no significant change in the chemical activities of the ions was observed.

REFERENCES

Abriola, L.M. and Bradford, S.A. 1998**.** Experimental Investigations of the Entrapment and Persistence of Organic Liquid Contaminants in the Subsurface Environment. *Environ Health Persp* **106** (Suppl 4): 1083**–**1095.

Access Science. Charged Species. http://www.accessscience.com/index.aspx (accessed 20 December 2010).

Ajwa, H.A. and Tabatabai, M.A. 1995. Metal-induced Sulfate Adsorption by Soils: Effect of pH and Ionic Strength. *Soil Sci* **159** (1): 32–42.

Akin, S. and Kovscek, A.R. 2003. Computed Tomography in Petroleum Research. In *Application of X-ray Computed Tomography in the Geosciences,* ed. Mees, F., Swennen, R., Van Geet, M., and Jacobs, P. 23–38. London: Special Publication No. 215, The Geological Society.

Aksulu, H. 2010. Effect of Core Cleaning Solvents on Wettability Restoration and Oil Recovery by Spontaneous Imbibition in Surface Reactive, Low Permeable Limestone Reservoir Cores. M.Sc. thesis, University of Stavanger, Norway.

Alagic, E. and Skauge, A. 2010. Combined Low Salinity Brine Injection and Surfactant Flooding in Mixed−wet Sandstone Cores, *Energ Fuel* **24** (6): 3551−3559.

Almehaideb, R.A., Ghannam, M.T., and Zekri, A.Y. 2004. Experimental Investigation of Contact Angles of Crude Oil-Microbial Solution on Carbonate Rocks. *Pet Sci Technol* **22** (3**–**4): 423–438.

Alotaibi, M.B., Azmy, R.M., and Nasr-El-Din, H.A. 2010. A Comprehensive EOR Study Using Low Salinity Water in Sandstone Reservoirs. Paper SPE 129976 presented at the SPE Improved Oil Recovery Symposium, Tulsa, Oklahoma, 24–28 April.

Alotaibi, M.B., Nasr-El-Din, H.A., and Fletcher, J.J. 2011. Electrokintics of Limestone and Dolomite Rock Particles. Accepted for Publication in *SPE Reserv Eval Eng.*

Anderson, W.G. 1986. Wettability Literature Survey, Part 1. Rock/oil/brine Interactions and the Effects of Core Handling on Wettability. *J Petrol Technol* **38** (11): 1125–1149.

Andreas, J.M., Hauser, E.A., and Tucker, W.B. 1938. Boundary Tension by Pendant Drops. *J Phys Chem* **42** (8): 1001–1019.

Aoudia, M., Al-Harthi, Z., Al-Maamari, R.S., Lee, C., and Berger, P. 2010a. Novel Alkyl Ether Sulfonates for High Salinity Reservoir: Effect of Concentration on Transient Ultralow Interfacial Tension at the Oil-Water Interface. *J Surfactants Deterg* **13** (3): 233–242.

Aoudia, M., Al-Maamari, R.S., Nabipour, M., Al-Bemani, A.S., and Ayatollahi, S. 2010b. Laboratory Study of Alkyl Ether Sulfonates for Improved Oil Recovery in High-Salinity Carbonate Reservoirs: A Case Study. *Energ Fuel* **24** (6): 3655–3660.

Ashraf, A., Hadia, N.J., Torsæter, O., and Tweheyo, M.T. 2010. Laboratory Investigation of Low Salinity Waterflooding as Secondary Recovery Process: Effect of

Wettability. Paper SPE 129012 presented at the SPE Oil and Gas India Conference and Exhibition, Mumbai, India, 20–22 January.

Attension Company. Surface Tension.. www.attension.com/surface-tension.aspx (accessed 08 June 2009).

Austad, A. and Standnes, D.C. 2003. Wettability and Oil Recovery from Carbonates: Effects of Temperature and Potential Determining Ions, *J Petrol Sci Eng* **39**: 363–376.

Austad, T., Matre, B., Milter, J., Saevareid, A., and Oyno, L. 1997. Chemical Flooding of Oil Reservoirs 8. Spontaneous Oil Expulsion from Oil-and Water-wet Low Permeable Chalk Material by Imbibition of Aqueous Surfactant Solutions. *Colloid Surface A* **137** (1–3): 117–129.

Bagci, S., Kok, M.V., and Turksoy, U. 2001. Effect of Brine Composition on Oil Recovery by Waterflooding. *Petrol Sci Technol* **19** (3-4): 359–372.

Bansal, V.K. and Shah, D.O. 1978. The Effect of Caustic Concentration on Interfacial Charge, Interfacial Tension and Droplet Size: A Sample Test for Optimum Caustic Concentration for Crude Oils. *J Can Petrol Technol* **17** (1): 69–72.

Barrow, N.J. and Shaw, T.C. 1977. The Slow Reactions between Soil and Anions: 7. Effect of Time and Temperature of Contact between an Adsorbed Soil and Sulfate. *Soil Sci* **124** (6): 347–354.

Berger, P.D. and Lee, C.H. 2002. Ultra-low Concentration Surfactants for Sandstone and Limestone Floods. Paper SPE 75186 presented at the SPE/DOE Improved Oil Recovery Symposium, Tulsa, Oklahoma, 13–17 April.

Berger, P.D., and Berger, C.H. 2009. Oil Recovery Method Employing Amphoteric Surfactants. US Patent No. 7,556,098.

Boussour, S., Cissokho, M., Cordier, P., Bertin, H., and Hamon, G. 2009. Oil Recovery by Low Salinity Brine Injection: Laboratory Results on Outcrop and Reservoir Cores. Paper SPE 124277 presented at the Annual Technical Conference and Exhibition, New Orleans, Louisiana, 4–7 October.

Brown, W.O. 1957. The Mobility of Connate Water during a Water Flood. *Trans AIME* **210**: 190–195.

Buckley, J.S. 1994. Chemistry of the Crude Oil/Brine Interface. Paper presented at the 3rd International Symposium on Reservoir Wettability and Its Effect on Oil Recovery, Laramie, Wyoming, 21–23 September.

Buckley, J.S. and Liu, Y. 1998. Some Mechanisms of Crude Oil/brine/solid Interactions. *J Petrol Sci Eng* **20** (3-4): 155–160.

Buckley, J.S., Takamura, K., and Morrow, N.R. 1989. Influence of Electrical Surface Charges on the Wetting Properties of Crude Oils. *SPE Reserv Eval Eng* **4** (3): 332–340.

Cayias, J.L., Schechter, R.S., and Wade, W.H. 1975. The Measurement of Low Interfacial Tension via the Spinning Drop Technique. In *ACS Symposium Ser. No. 8, Adsorption at Interfaces*. 234–247. Washington, D.C.: American Chemical Society.

Chilingarian, G.V. and Yen, T.F. 1983. Some Notes on Wettability and Relative Permeabilities of Carbonate Reservoir Rocks, II, *Energ Source Part A* **7** (1): 67–75.

Chow, R.S., and Takamura, K. 1988. Electrophoretic Mobilities of Bitumen and Conventional Crude-in-Water Emulsions Using the Laser Doppler Apparatus in the Presence of Multivalent Cations. *J Colloid Interf Sci* **125** (1): 212–225**.**

Cicerone, D.S., Regazzoni, A.E., and Blesa, M.A. 1992. Electrokinetic Properties of the Calcite/water Interface in the Presence of Magnesium and Organic Matter. *J Colloid Interf Sci* **154** (2): 423–433.

Dawe, R.A. and Egbogah, E.O. 1978. Recovery of Oil from Petroleum Reservoirs. *J Contemp Phys* **19** (4): 355–376.

Delshad, M., Kim, D.H., Magbagbeola, O.A., Huh, C., Pope, G.A., and Tarahhom, F. 2008. Mechanistic Interpretation and Utilization of Viscoelastic Behavior of Polymer Solutions for Improved Polymer-flood Efficiency. Paper SPE 113620 presented at the SPE/DOE Symposium on Improved Oil Recovery, Tulsa, Oklahoma, 20–23 April.

Deutsch, W.J. 1997. Water/Rock Interactions. In *Groundwater Geochemistry: Fundamentals and Applications to Contamination*, New York: Lewis Publishers.

Dickinson, W. 1941. The Effect of pH upon the Electrophoretic Mobility of Emulsions of Certain Hydrocarbons and Aliphatic Halides. *T Faraday Soc* **37**: 140–148.

Domingo, X. 1996. Betaines. In *Amphoteric Surfactants*, ed. E.G. Lomax, Chap. 3, 75–190, New York, Marcel Dekker.

Dominquez, G.C. and Samaniego V., F. 1992. *Carbonate Reservoir Characterization: A Geologic-Engineering Analysis, Part I*, ed. G.V. Chilingarian, S.J. Mazzullo, and H.H. Rieke. 443–474. New York: Elsevier Science.

Douglas, H.W. 1943. The Electrophoretic Behavior of Certain Hydrocarbons and the Influence of Temperature Thereon. *T Faraday Soc* **39**: 305–311.

Douglas, H.W. and Walker, R.A. 1950. The Electrokinetic Behavior of Iceland Spar against Aqueous Electrolyte Solutions. *T Faraday Soc* **46**: 559–568.

Ehrlich, R. 1971. Relative Permeability Characteristics of Vugular Cores, Their Measurement and Significance. Paper SPE 3553 presented at the Fall Meeting of the Society of Petroleum Engineers of AIME, New Orleans, Louisiana, 3–6 October.

Eigen, M. 1957. Determination of General and Specific Ionic Interactions in Solutions. *Discuss Faraday Soc* **24**: 25–36.

Erbil, Y.H. 2006. Liquid Solution Surfaces. In *Surface Chemistry of Solid and Liquid Interfaces*, Oxford, United Kingdom: Wiley-Blackwell.

Eriksson, R., Merta, J., and Rosenholm, J.B. 2007. The Calcite/water Interface. I. Surface Charge in Indifferent Electrolyte Media and the Influence of Low-molecular-weight Polyelectrolyte. *J Colloid Interf Sci* **313** (1): 184–193.

Farooq, O., Tweheyo, M.T., Sjöblom, J., and Øye, G. 2011. Surface Characterization of Model, Outcrop, and Reservoir Samples in Low Salinity Aqueous Solutions, *J Disper Sci Technol* **32** (4): 519–531.

Fathi, S.J., Austad, T., and Strand, S. 2010. "Smart Water" as a Wettability Modifier in Chalk: The Effect of Salinity and Ionic Composition. *Energ Fuel* **24** (4): 2514–2519.

Fetter, C.W. 1988. Water Chemistry. In *Applied Hydrogeology*, Upper Saddle River, New Jersey: Prentice Hall.

Fogden, A. 2009. Experimental Investigation of Deposition of Crude Oil Compositions in Brine-filled Pores. Paper SCA2009-23 presented at the International Symposium of the Society of Core Analyst, Noordwijk, The Netherlands, 27–30 September.

Francisca, F.M., Rinaldi, V.A., and Santamarina, J.C. 2003. Instability of Hydrocarbon Films over Mineral Surfaces: Microscale Experimental Studies. *J Environ Eng* **129** (12): 1120–1128.

Franks, G.V., Djerdjev, A.M., and Beattie, J.K. 2005. Absence of Specific Cation or Anion Effects at Low Salt Concentrations on the Charge at the Oil/water Interface. *Langmuir* **21** (19): 8670–8674.

Fredd, C.N. and Fogler, H.S. 1998. The Kinetics of Calcite Dissolution in Acetic Acid Solutions, *Chem Eng Sci* **53** (22): 3863–3874.

Gardner, J.E. and Hayes, M.E. 1981. *University of Texas Spinning Drop Interfacial Tensiometer Model 500 Instruction Manual*. Department of Chemistry, University of Texas at Austin, Texas.

Garrels, R. M. and Thompson, M. E., 1962. A Chemical Model for Sea Water at 25°C and One Atmosphere Total Pressure. *Am J Sci* **260**: 57–66.

Garrison, S. 2004. *The Surface Chemistry of Natural Particles*. New York: Oxford University Press.

Green, D.W. and Willhite, G.P. 1998. *Enhanced Oil Recovery*. Textbook Series, Vol. 6, SPE, Richardson, Texas.

Gupta, R. and Mohanty, K.K. 2008. Wettability Alteration of Fractured Carbonate Reservoirs. Paper SPE 113407 presented at the SPE/DOE Symposium on Improved Oil Recovery, Tulsa, Oklahoma, 20–23 April.

Hall, A.C., Collins, S.H., and Melrose, J.C. 1983. Stability of Aqueous Wetting Films in Athabasca Tar Sands. *SPEJ* **23** (2):249–258.

Hammond, P.S. and Unsal, E. 2009. Spontaneous and Forced Imbibition of Aqueous Wettability Altering Surfactant Solution into an Initially Oil-wet Capillary. *Langmuir* **25** (21): 12591–12603.

Hammond, P.S. and Unsal, E. Spontaneous Imbibition of Surfactant Solution into an Oil-wet Capillary: Wettability Restoration by Surfactant-Contaminant Complexation, http://pubs.acs.org/doi/abs/10.1021/la1048503 (accessed 20 May 2011).

Hamouda, A.A. and Karoussi, O. 2008. Effect of Temperature, Wettability and Relative Permeability on Oil Recovery from Oil-wet Chalk. ***Energies*** **1** (1): 19**–**34.

Hanshaw, B.B., Back, W., and Deike, R.G. 1971. A Geochemical Hypothesis for Dolomitization by Ground Water. *Econ Geol* **66** (5): 710–724.

Hester, R.E. and Plane, R.A. 1964. A Raman Spectrometric Comparison of Interionic Association in Aqueous Solutions of Nitrates, Sulfates and Perchlorates. *Inorg Chem* **3**: 769–770.

Hingston, F.J., Atkinson, R.J. Posner, A.M., and Quirk, J.P. 1967. Specific Adsorption of Anions. *Nature* **215**: 1459–1461.

Hiorth, A., Cathles, L.M., and Madland, M.V. 2010. The Impact of Pore Water Chemistry on Carbonate Surface Charge and Oil Wettability. *Transport Porous Med* **85** (1): 1–21.

Hirasaki, G. and Zhang, D.L. 2003. Surface Chemistry of Oil Recovery From Fractured, Oil-wet, Carbonate Formation. Paper SPE 80988 presented at the International Symposium on Oilfield Chemistry, Houston, Texas, 5–7 February.

Hirasaki, G.J., Miller, C.A., and Puerto, M. 2008. Recent Advances in Surfactant EOR. Paper SPE 115386 presented at the International Petroleum Technology Conference, Kuala Lumpur, Malaysia, 3–5 December.

Hjelmeland, O.S. and Larrondo, L.E.1986. Experimental Investigation of the Effects of Temperature, Pressure, and Crude Oil Composition on Interfacial Properties. *SPE Reservoir Eng* **1** (4): 321–328.

Hobson, G.D. 1989. Production from Carbonate Reservoirs. *In Oil Field Development Techniques*: *Proceedings of the Daqing International Meeting*, ed. Mason, J.F. and Dickey, P.A, Chap. 14, 193–207. Tulsa, Oklahoma: American Association of Petroleum Geologists.

Høgnesen, E.J., Strand, S., and Austad, T. 2005. Waterflooding of Preferential Oil-Wet Carbonates: Oil Recovery Related to Reservoir Temperature and Brine Composition. Paper SPE 94166 presented at the SPE Europec/EAGE Annual Conference, Madrid, Spain, 13–16 June.

Huang, Y.C., Fowkes, F.M., Lloyd, T.B., and Sanders, N.D. 1991. Adsorption of Calcium Ions from Calcium Chloride Solutions onto Calcium Carbonate Particles, *Langmuir* **7** (8): 1742–1748.

Issacs, E., Chow, R., and Babchin, A. 1998. On the Significance of Reservoir Wettability on Extraction and Recovery Processes. Paper 1998.021 presented at the 7th UNITAR Heavy Crude and Tar Sands Conference, Beijing, China, 27–30 October.

Jamaloei, B.Y. and Rafiee, M. 2008. Effect of Monovalent and Divalent Ions on Macroscopic Behaviour of Surfactant Flooding. Paper 2008-085 presented at the Canadian International Petroleum Conference, Calgary, Alberta, 17–19 June.

Jirui, H., Zhongchun, Z., Xiang'an, Y., and Huifen, X. 2001. Study of the Effect of ASP Solution Viscoelasticity on Displacement Efficiency. Paper SPE 71492 presented at the SPE Annual Technical Conference and Exhibition, New Orleans, Louisiana, 30 September–3 October.

Kalpakci, B. and Chan, K.S. 1985. Method of Enhanced Oil Recovery Employing Thickened Amphoteric Surfactant Solutions. US Patent No. 4,554,974.

Kaminsky, R. and Radke, C.J. 1997. Water Films, Asphaltenes, and Wettablity Alteration. *SPEJ* **2** (4): 485–493.

Kester, D.R. and Pytkowicz, R.M. 1970. Effect of Temperature and Pressure on Sulfate Ion Association in Sea Water. *Geochim Cosmochim Ac* **34** (10): 1093–1051.

Kharaka, Y.K., Gunter, W.D., Aggarwal, P.K., Perkins, E.H., and DeBraal, J.D. 1988. *SOLIMINEQ 88, a Computer Program for Geochemical Modeling of Water-rock Interactions*. Denver, Colorado: U.S. Geological Survey.

Khilar, K.C. and Fogler, H.S. 1984. The Existence of a Critical Salt Concentration for Particle Release. *J Colloid Interf Sci* **101** (1): 214–224.

Kielland, J. 1937. Individual Activity Coefficient of Ions in Aqueous Solutions. *J Am Chem Soc* **59**: 1676–1678.

Knecht, V., Risselada, H.J., Mark, A.E., and Marrink, S.J. 2007. Electrophoretic Mobility Does Not Always Reflect the Charge on an Oil Droplet. J *Colloid Interf Sci* **318**: 477–486.

Korsnes, R. I., Strand, S., Hoff, Ø., Pedersen T., and Austad, T. 2006. Does the Chemical Interaction between Seawater and Chalk Affect the Mechanical Properties of Chalk? In: *EUROCK 2006 Multiphysics Coupling and Long Term Behaviour in Rock Mechanics*, 427–434. London: Taylor & Francis.

Kossack, C.A. and Gurpinar, O. 2001. A Methodology for Simulation of Vuggy and Fractured Reservoirs. Paper SPE 66366 presented at the SPE Reservoir Simulation Symposium, Houston, Texas, 11–14 February.

Kumar, A. Neale, G., and Hornof, V. 1984. Effects of Connate Water Composition on Interfacial Tension Behaviour of Surfactant Solutions. *J Can Petrol Technol* **23** (1): 37–41.

Kussakov, M.M. and Mekenitskaya, L.I. 1955. On the Thickness of Thin Layers of Connate Water. Paper 6134 presented at the 4th World Petroleum Congress, Rome, Italy, 6−15 June.

Kwok, D. Y. and Neumann, A. W. 1999. Contact Angle Measurement and Contact Angle Interpretation. *Adv Colloid Interface* **81** (3): 167–249.

Lafon, G.M. 1969. *Some Quantitative Aspects of the Chemical Evolution of the Oceans*. Ph.D. dissertation. Northwestern Univ., Evanston, Illinois, USA.

Lake, L. 2010. *Enhanced Oil Recovery*, Richardson, Texas, SPE.

Lebedeca, E., Senden, T, Knackstedt, M., and Morrow, N. 2009. Low Salinity Recovery from Reservoir Sandstone. Paper 4 presented at the 15th European Symposium on Improved Oil Recovery, France, Paris, 27–29 April.

Levine, S., Mingins, J., and Bell, G.M. 1967. The Discrete-ion Effect in Ionic Double-layer Theory. *J Electroanal Chem* **13**: 280–329.

Li, D., Cheng, P., and Neumann, A.W. 1992. Contact Angle Measurement by Axisymmetric Drop Shape Analysis (ADSA). *Adv Colloid Interf Sci* **39**: 347–382.

Lichaa, P.M., Alpustun, H., Abdul, J.H., Nofal, W.A. and Fuseni, A.B. 1992. Wettability Evaluation of a Carbonate Reservoir Rock. In *Advances in Core Evaluation III Reservoir Management, reviewed proceedings of the Society of Core Analysis 3rd European Core Analysis Symposium*, ed. P.W. Worthington and C. Chardaire-Riviere. Paris: Gordon and Breach.

Ligthelm, D.J. 2010. Aqueous Displacement Fluid Injection for Enhancing Oil Recovery from a Limestone or Dolomite Formation. International (PCT) Patent No. WO/2010/092095.

Littmann, W. 1988. *Polymer Flooding*. New York: Elsevier Science.

Machel, H.G. 2004. Concepts and Models of Dolomitization: A Critical Reappraisal, In: *The Geometry and Petrogenesis of Dolomite Hydrocarbon Reservoirs*, ed. Braithwaite, C.J.R., Rizzi, G., and Darke, G, 7–63. London: Geological Society.

Maddox, J. and Tate, J.F. 1977. Surfactant Oil Recovery Process Usable in High Temperature Formations Having High Concentrations of Polyvalent Ions. US Patent No. 4,008,165.

Madsen, L. 2006. Calcite: Surface Charge. In *Encyclopedia of Surface and Colloid Science*, ed. Hubbard, A.T. 1084–1096. New York: Taylor and Francis.

Magbagbeola, O.A. 2008. *Quantification of the Viscoelastic Behavior of High Molecular Weight Polymer Used for Chemical Enhanced Oil Recovery*. M.Sc. thesis, University of Texas, Austin, Texas.

Mannhardt, K., Schramm, L.L., and Novosad, J.J. 1992. Adsorption of Anionic and Amphoteric Foam-forming Surfactants on Different Rock Types. *Colloid Surface* **68** (1–2): 37–53.

Marinova, K.G., Alargova, R.G., Denkov, N.D., Velev, O.D. and Pestsev, D.N. 1996. Charging of Oil-water Interfaces due to Spontaneous Adsorption of Hydroxyl Ions. *Langmuir* **12** (8): 2045–2051.

Millero, F. J. 1974. The Physical Chemistry of Seawater, *Annu Rev Earth Pl Sc* **2**: 101–150.

Millero, F.J. 1971. Effect of Pressure on Sulfate Ion Association in Sea Water. *Geochim Cosmochim Ac* **35**: 1089–1098.

Milter, J. and Austad, T. 1996. Chemical Flooding of Oil Reservoirs 7. Oil Expulsion by Spontaneous Imbibition of Brine with and without Surfactant in Mixed-wet, Low Permeability Chalk Material, *Colloid Surface* A **117** (1–2): 109–115.

Möller, P. and Werr, G. 1972. Influence of Anions on Ca^{2+}- Mg^{2+} Surface Exchange Process on Calcite in Artificial Sea Water. *Radiochim Acta* **18** (3): 144–147.

Morrow, N. and Buckley, J. 2011. Improved Oil Recovery by Low-salinity Waterflooding. *JPT*: 106–110. SPE 129421.

Mott, C.J.B. 1981. Anion and Ligand Exchange. In T*he Chemistry of Soil Processes*, ed. Greenland, D.J. and Hayes. M.H.B., Chap. 5, 179–219. New York: John Wiley & Sons, Ltd.

Mucci, A. and Morse, J.W. 1985. Auger Spectroscopy Determination of the Surface-Most Adsorbed Layer Composition on Aragonite, Calcite, Dolomite and Magnesite in Synthetic Seawater, *Am J Sci* **285**: 306–317.

Murray, J.W. 2006. Chap. 6: Activity Scales and Activity Corrections. Short Course OCN 421 (University of Washington) presented 10 November, Seattle, Washington.

Nasr-El-Din H., Hawkins B. and Green K. 1991. Viscosity Behavior of Alkaline, Surfactant, Polyacrylamide Solutions Used for Enhanced Oil Recovery. Paper SPE 21028 presented at the International Symposium on Oilfield Chemistry, Anaheim, California, 20–22 February.

Nyström, R., Lindén, M., and Rosenholm, J.B. 2001. The Influence of Na^{2+}, Ca^{2+}, Ba^{2+}, and La^{3+} on the ζ Potential and the Yield Stress of Calcite Dispersions. *J Colloid Interf Sci* **242** (1): 259–263.

Okasha, T.M., and Al-Shiwaish, A.A. 2009. Effect of Brine Salinity on Interfacial Tension in Arab-D Carbonate Reservoir, Saudi Arabia. Paper SPE presented

at the SPE Middle East Oil and Gas Show and Conference, Bahrain, Bahrain, 15–18 March.

OLI Systems Incorporated. Analyzer Studio, Version 3.2. http://www.olisystems.com/new-streamanalyzer.shtml (accessed 15 March 2011a).

OLI Systems Incorporated. Electrolyte Thermodynamics Aqueous Model. http://www.olisystems.com/new-chemistry.shtml (accessed 15 March 2011b).

Omotoso, O.E., Munoz, V.A., and Mikula, R.J. 2002. Mechanisms of Crude Oil-Foli systems Mineral Interactions. *Spill Sci Technol B* **8** (1): 45–54.

Parfitt, R.L. 1978. Anion Adsorption by Soils and Soil Materials. Adv Agron **30**: 1–50.

Patel, K. and Greaves M. 1987. Role of Capillary and Viscous Forces in Mobilization of Residual oil. *Can J Chem Eng* **65** (4): 676–679.

Pesret, F. 1972. *Kinetics of Carbonate-seawater Interactions*, M.Sc. Thesis, University of Hawaii, Honolulu, Hawaii.

Pierre, A., Lamarche, J.M., Foissy, A., and Persello, J. 1990. Calcium as Potential Determining Ion in Aqueous Calcite Suspensions. *J Disper Sci Technol* **11** (6): 611–635.

Plank, J. and Bassioni, G. 2007. Adsorption of Carboxylate Anions on a $CaCO_3$ Surface. *Z Naturforsch*, **62b**: 1277–1284.

Pokrovsky, O.S., Mielczarski, J.A., and Schott**,** J. 2000. Surface Speciation Models of Calcite and Dolomite/Aqueous Solution Interfaces and Their Spectroscopic Evaluation. *Langmuir* **16** (6): 2677**–**2688.

Pope, G.A. and Bavière, M. 1991. Reduction of Capillary Forces by Surfactants. In *Basic Concepts in Enhanced Oil Recovery Processes*, ed. Bavière, M. Chap. 3, 89–120. London: Elsevier Science Publishers.

Rashidi, M. 2010. *Physico-chemistry Characterization of Sulfonated Polyacrylamide Polymers for Use in Polymer Flooding*. Ph.D. dissertation, University of Bergen, Norway.

Rashidi, M., Blokhus, A.M., and Skauge, A. 2010. Viscosity and Retention of Sulfonated Polyacrylamide Polymers at High Temperature. *J Appl Polym Sci* **119** (6): 1097–4628.

Rodríguez, K. and Araujo, M. 2006. Temperature and Pressure Effects on Zeta Potential Values of Reservoir Minerals. *J Colloid Interf Sci* **300** (2): 788–794.

Rodríguez-Valverde, M.A., Cabrerizo-Vílchez, M.A.**,** Páez-Dueñas, A., and Hidalgo-Álvarez, R. 2003. Stability of Highly Charged Particles: Bitumen-in-water Dispersions. *Colloid Surface A* **222** (1–3): 233**–**251.

Rosen, M.J. 1978. Characteristic Features of Surfactants. *In Surfactants and Interfacial Phenomena,* Canada: John Wiley & Sons.

Russel, R. G., Morgan, F., Muskat, M. 1947. Some Experiments on the Mobility of Interstitial Waters. *Trans AIME* **170**: 51–61.

Salathiel, R.A. 1973. Oil Recovery by Surface Film Drainage in Mixed-Wettability Rocks. *J Petrol Technol* **25** (10): 1216–1224.

Salehi, M., Johnson, S.J., and Liang, J.T. 2008. Mechanistic Study of Wettability Alteration Using Surfactants with Applications in Naturally Fractured Reservoirs. *Langmuir* **24** (24):14099–14107.

Saner, S., Asar, H.K., Okaygun, H., and Abdul, H.J. 1991. Wettability Study of Saudi-Arabian Carbonate Reservoir Core Samples. *Arab J Sci Eng* **16** (3): 357–371.

Sanz, C.A., Companc, C.N.P, and Pope, G.A. 1995. Alcohol-free Chemical Flooding: From Surfactant Screening to Coreflood Design. Paper SPE 28956 presented at the SPE International Symposium on Oilfield Chemistry, San Antonio, Texas, 14–17 February.

Sanz-Rubio, E., Sánchez-Moral, S., Cañaveras, J.C., Calvo, J.P., and Rouchy, J.M. 2001. Calcitization of Mg–Ca Carbonate and Ca Sulphate Deposits in a Continental Tertiary Basin (Calatayud Basin, NE Spain). *Sediment Geol* **140** (1–2): 123–142.

Schembre, J.M. and Kovscek, A.R. 2005. Mechanism of Formation Damage at Elevated Temperature. *J Energ Resour-ASME* **127** (3): 171–180.

Schramm, L.L and Kutay, S.M. 2000. Emulsions and Foams in the Petroleum Industry. In *Surfactants: Fundamentals and Applications in the Petroleum Industry*, ed. Schramm, L.L, Chap. 3, 94–111. Cambridge, United Kingdom: Cambridge University Press.

Schramm, L.L. ed. 2000. *Surfactants: Fundamentals and Applications in the Petroleum Industry*, Cambridge, United Kingdom: Cambridge University Press.

Schramm, L.L., Mannhardt, K., and Novosad, J.J. 1991. Electrokinetic Properties of Reservoir Rock Particles. *Colloid Surface* **55**: 309–331

Schumacher, M.M. 1978. *Enhanced Oil Recovery: Secondary and Tertiary Methods*. Park Ridge, New Jersey: Noyes Data Corp.

Seethepalli, A., Adibhatla, B., and Mohanty, K.K. 2004. Physicochemical Interactions during Surfactant Flooding of Fractured Carbonate Reservoirs. *SPE J* **9** (4): 411–418.

Shah, D.O. and Schechter, R.S. ed. 1977. *Improved Oil Recovery by Surfactant and Polymer Flooding*, 50–58. New York: Academic Press.

Shah, D.O., Chan, K.S., and Bansal, V.K. 1977. The Importance of Interfacial Charge vs Interfacial Tension in Secondary and Tertiary Oil Recovery Processes. Proc. of AIChE 83rd National Meeting, Houston, Texas, 21–25 March.

Shaw, D.J. 1966. *Introduction to Colloid and Surface Chemistry*. London: Butterworths.

Shupe, R.D. 1981. Chemical Stability of Polyacrylamide Polymers. *J Petrol Technol* **33** (8): 1513–1529.

Siffert, D. and Fimbel, P. 1984. Parameters Affecting the Sign and Magnitude of the Eletrokinetic Potential of Calcite. *Colloid Surf*ace **11** (3–4): 377–389.

Sjöblom, J. ed. 2006. *Emulsions and Emulsion Stability*. New York: Taylor and Francis.

Smallwood, P.V. 1977. Some Aspects of the Surface Chemistry of Calcite and Aragonite, Part I: An Electrokinetic Study. *Colloid Polym Sci* **255** (9): 881–886.

Smani, M.S., Blazy, P., and Cases, J.M. 1975. Beneficiation of Sedimentary Moroccan Phosphate Ores-Part II: Electrochemical Phenomena at the Calcite/Aqueous Interface. *T SME/AIME* **258**: 174–176.

Somasundaran, P. and Agar, G.E. 1967. The Zero Point of Charge of Calcite. *J Colloid Interf Sci* **24** (4): 433–440.

Sorbie, K.S. 1991. *Polymer-improved Oil Recovery*. Glasgow, United Kingdom: Blackie.

Standnes, D.C. and Austad, T. 2000. Wettability Alteration in Chalk 2. Mechanism for Wettability Alteration from Oil-wet to Water-wet Using Surfactants. *J Petrol Sci Eng* **28** (3): 123–143.

Stournas, S. 1984. A Novel Class of Surfactants with Extreme Brine Resistance and Its Potential Application in Enhanced Oil Recovery. Paper SPE 13029 presented at the SPE Annual Technical Conference and Exhibition, Houston, Texas, 16–19 September.

Strand, S., and Austad, T. 2008. Effect of Temperature on Enhanced Oil Recovery from Mixed-wet Chalk Cores by Spontaneous Imbibition and Forced Displacement Using Seawater. *Energ Fuel* **22** (5): 3222–3225.

Strand, S., Austad, T., Puntervold, T., Høgnesen, J., Olsen, M., and Barstad, M.F. 2008. “Smart Water” for Oil Recovery from Fractured Limestone: A Preliminary Study. *Energ Fuel* **22** (5): 3126–3133.

Strand, S., Høgnesen, E.J., and Austad, T. 2006. Wettability Alteration of Carbonates—Effects of Potential Determining Ions (Ca^{2+} and SO_4^{2-}) and Temperature. *Colloid Surface* A **275** (1–3): 1–10.

Strand, S., Standnes, D.C., and Austad, T. 2003. Spontaneous Imbibition of Aqueous Surfactant Solutions into Neutral to Oil-wet Carbonate Cores: Effects of Brine Salinity and Composition. *Energ Fuel* **17** (5): 1133–1144.

Strubbe, F., Beunis, F., Marescaux, M., and Neyts, K. 2007. Charging Mechanism in Colloidal Particles Leading to a Linear Relation between Charge and Size. *Phys Rev E* **75** (3): 0314051–88.

Takamura, K., and Chow, R.S. 1985. The Electric Properties of the Bitumen/water Interface. Part II: Application of the Ionizable Surface-group Model. *Colloid Surface* **15**: 35–48.

Toulhoat, H. and Lecourtier, J. ed. 1991. *Physical Chemistry of Colloids and Interfaces in Oil Production*, 359–360. Paris: Éditions Technip.

Van Cappelen, P., Charlet, L., Stumm, W., and Wersin, P. 1993. A Surface Complexation Model of the Carbonate Mineral-aqueous Solution Interface. *Geochim Cosmochim Ac* **57** (15): 3505–18.

Vdović, N., 2001. Electrokinetic Behaviour of Calcite - The Relationship with Other Calcite Properties, *Chem Geol* **177** (3–4): 241–248.

Walschmidt, W.A., Fitzgerald, P.E., and Lunsdorf, C.L. 1956. Classification of Porosity and Fractures in Reservoir Rocks. *AAPG Bull.* **40** (5): 953–974.

Wang, D., Liu, C., Wu, W., and Wang, G. 2010. Novel Surfactants that Attain Ultra-Low Interfacial Tension between Oil and High Salinity Formation Water without Adding Alkali, Salts, Co-surfactants, Alcohol and Solvents. Paper SPE 127452 presented at the SPE/EOR Conference at Oil & Gas West Asia, Muscat, Oman, 11–13 April.

Wang, W. and Gupta, A. 1995. Investigation of the Effect of Temperature and Pressure on Wettability Using Modified Pendant Drop Method. Paper SPE 30544 presented at the SPE Annual Technical Conference & Exhibition, Dallas, Texas, 22–25 October.

Wardlaw, N.C. 1996. Factors Affecting Oil Recovery from Carbonate Reservoirs and Prediction of Recovery. In *Carbonate Reservoir Characterization: A Geologic-Engineering Analysis, Part II*, ed. G.V. Chilingarian, S.J. Mazzullo, and H.H. Rieke, Chap. 10, 867–903. New York: Elsevier.

Webb, K.J., Black, C.J.J., and Tjetland, G. 2005. A Laboratory Study Investigating Methods for Improving Oil Recovery in Carbonates. Paper IPTC 10506 presented at the International Petroleum Technology Conference, Doha, Qatar, 21–23 November.

Weifeng, L. Bazin, B., Desheng, M., Liu, Q., Han, D., and Wu, K. 2011. Static and Dynamic Adsorption of Anionic and Amphoteric Surfactants with and without the Presence of Alkali. *J Petrol Sci Eng* **77** (2): 209–218.

Wellington, S.L. and Vinegar, H.J. 1987. X-ray Computerized Tomography. J Petrol Technol **39** (8): 885–898.

Wikipedia. Double Layer, http://en.wikipedia.org/wiki/Double_layer_(interfacial) (accessed 20 December 2010a).

Wikipedia. Semi-permeable Membrane, http://en.wikipedia.org/wiki/Semipermeable_membrane (accessed 20 December 2010b).

Winsor, P.A. 1954. *Solvent Properties of Amphiphilic Compounds***.** London: Butterworths.

Xu, W., Ayirala, S.C., and Rao, D.N.2006. Interfacial Behavior of Complex Hydrocarbon Fluids at Elevated Pressures and Temperatures. *Can J Chem Eng* **84** (1): 22–32.

Yang, D., Gu, Y., and Tontiwachwuthikul, P. 2008. Wettability Determination of the Crude Oil−Reservoir Brine−Reservoir Rock System with Dissolution of CO_2 at High Pressures and Elevated Temperatures. *Energ Fuel **22*** (4): 2362–71.

Yarar, B. and Kitchener, J.A. 1970. Selective Flocculation of Minerals: 1- Basic Principles, 2- Experimental Investigation of Quartz, Calcite and Galena, *Inst Min Metall Trans* **79**: 23**–**33.

Yu, L., Strandnes, D.C., and Skjæveland, S.M. 2007. Wettability Alteration of Chalk by Sulphate Containing Water, Monitored by Contact Angle Measurement. Paper SCA2007-01 presented at the International Symposium of the Society of Core Analysts, Calgary, Canada, 10–12 September.

Yunan, M.H, Idris, A.K., and Egbogah, E.O. 1995. Microstructure and Mobilization Mechanism of Residual Oil in Different Wetting Conditions. Paper SPE

29005 presented at the SPE International Symposium on Oilfield Chemistry, San Antonio, Texas, 14–17, February.

Zaitoun, A., Makakou, P., Blin, N., Al-Maamari, R.S., Al-Hashmi, A.R., Abdel-Goad, M., and Al-Sharji, H.H. 2011. Shear Stability of EOR Polymers. Paper SPE 141113 presented at the SPE International Symposium on Oilfield Chemistry, The Woodlands, Texas, 11–13 April.

Zhang, L.D., Liu, S., Puerto, M., Miller, C.A., and Hirasaki, G.J. 2006. Wettability Alteration and Spontaneous Imbibition in Oil-wet Carbonate Formations. *J Petrol Sci Eng* **52** (1–4): 213–226.

Zhang, P., and Austad T. 2006. Wettability and Oil Recovery from Carbonates: Effects of Temperature and Potential Determining Ions. *Colloid Surface* A **279**: 179–187.

Zhang, P., Tweheyo, M.T., and Austad, T. 2007. Wettability Alteration and Improved Oil Recovery by Spontaneous Imbibition of Seawater into Chalk: Impact of the Potential Determining Ions Ca^{2+}, Mg^{2+}, and SO_4^{2-}. *Colloid Surface* A **301** (1–3): 199–208.

Zhang, Y. and Morrow, N.R. 2006. Comparison of Secondary and Tertiary Recovery with Change in Injection Brine Composition for Crude Oil/Sandstone Combinations. Paper SPE 99757 presented at the SPE/DOE Symposium on Improved Oil Recovery, Tulsa, Oklahoma, 22–26 April.

Zhan-Guo, L. and Jun, Y. 2009. The Effect of Vug Density on Fluid Flow. Paper presented at the International Computational Intelligence and Software Engineering Conference, Wuhan, China, 11–13 December.

APPENDIX A

GLOSSARY

Electrical Double Layer (EDL):	EDL is a structure that appears on the surface of an object (solid particle, gas bubble, liquid droplet) after dispersing it into a liquid. Two parallel layers of charge surround the object. The first one represents the surface charge (can be positive or negative), and has cloud of ions adsorbed strongly onto the object. The second layer has free ions that are weakly attracted by the surface charge (Wikipedia, 2010a).
Charged Species:	A chemical entity in which the overall total of electrons is unequal to the overall total of protons (Access Science 2010).
Semi-membrane:	A membrane that allows certain ions or molecules to pass through it by diffusion (Wikipedia, 2010b).
Charging mechanisms:	Measuring the particle's charge for a variety of parameters such as temperature, ionic strength, and pH (Strubbe *et al.*, 2007).

APPENDIX B

CRUDE OIL COMPOSITION

Table B-1. Components of the crude oil A (sweet).

	Target Compound	**% of Total**
1)	Cyclohexane	1.60
2)	Heptane	1.72
3)	Methylene chloride	1.01
4)	Cyclohexane, methyl-	4.99
5)	Toluene	1.79
6)	Cyclohexane, 1,3-dimethyl-	1.31
7)	Octane	3.68
8)	Cyclohexane, ethyl-	2.25
9)	Cyclohexane, 1,1,3-trimethyl-	1.36
10)	p-Xylene	5.05
11)	Nonane	3.66
12)	Cyclohexane, propyl-	2.23
13)	Benzene, 1-ethyl-3-methyl-	1.66
14)	Benzene, 1,2,3-trimethyl-	1.84
15)	Benzene, 1,2,4-trimethyl-	2.81
16)	Decane	4.89
17)	Undecane	5.05
18)	Benzene, 1,2,4,5-tetramethyl-	1.38
19)	Dodecane	6.62
20)	Undecane, 2,6-dimethyl-	1.82
21)	Tridecane	4.68
22)	Naphthalene, 1-methyl-	1.41
23)	Dodecane, 2,6,10-trimethyl	1.91
24)	Tetradecane	4.55
25)	Naphthalene, 1,5-dimethyl-	1.68
26)	Pentadecane	4.11
27)	Hexadecane	7.55
28)	Hexadecane, 7,9-dimethyl-	2.05
29)	Heptadecane	3.02
30)	Pentadecane, 2,6,10,14-tetra	2.10
31)	Octadecane	2.69
32)	Hexadecane, 2,6,10,14-tetra	1.28
33)	Nonadecane	2.27
34)	Eicosane	2.35
35)	Docosane	1.67

Table B-2. Components of the crude oil B (sour).

	Target Compounds	**% of Total**
1)	Cyclopentane, methyl-	4.95
2)	Cyclohexene	1.62
3)	Heptane	2.58
4)	Cyclohexane, methyl-	7.09
5)	Toluene	8.38
6)	Octane	4.15
7)	Cyclohexane, ethyl-	3.3
8)	Ethylbenzene	7.49
9)	p-Xylene	7.43
10)	o-Xylene	2.15
11)	Nonane	3.37
12)	Benzene, 1-ethyl-3-methyl-	2.09
13)	Decane	5.85
14)	Undecane	3.89
15)	Dodecane	3.84
16)	Tridecane	4.07
17)	Dodecane, 2,6,10-trimethyl	2.08
18)	Tetradecane	3.06
19)	Pentadecane	3.5
20)	Hexadecane	4.24
21)	Heptadecane	2.68
22)	Pentadecane, 2,6,10,14-tet	1.64
23)	Octadecane	2.4
24)	Hexadecane, 2,6,10,14-tetr	2.18
25)	Nonadecane	2.13
26)	Eicosane	2.16
27)	Heneicosane	1.67

APPENDIX C

PREPARATION PROCEDURES FOR CONTACT ANGLE TESTS

Used procedure for contact angle tests:

- Cut the rock into small substrates with dimensions of 1.6 cm x 1.8 cm x 0.6 cm.
- Polish the limestone substrates using sand paper (600 meshes and then 300 meshes) to minimize the contact angle hysteresis due to surface roughness.
- Load all substrates into an empty glass flask, and then apply vacuum pressure for at least 2 hrs.
- Introduce formation brine (230K mg/L) to the substrates using vacuum to remove the trapped air for at least 3 hrs. To eliminate the contaminants and surface charges induced by polishing, the substrates left in the brine for at least 24 hrs.
- Place the rocks in crude oil and centrifuge them at 3,000 rpm for 30 min.
- Wait for 30 min. before centrifuging the substrates again at the same speed and time period.
- The centrifuge step was to displace the water droplets on the rock surface to keep only the irreducible water (S_{wi}).
- Some samples were aged in crude oil at 90°C for different aging periods
- The above procedure was followed to simulate the in-situ state of the mineral surface under reservoir condition.
- Dip the substrates into toluene for 2 seconds to remove the external bulk oil from the rock surface.

APPENDIX D

CONTACT ANGLE IMAGES AT DIFFERENT TEMPERATRUES AND SALINITY CONDITIONS

Na_2SO_4 solution (3,560 mg/L)

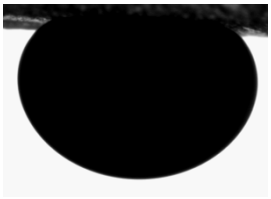
T= 50°C, t= 10 s

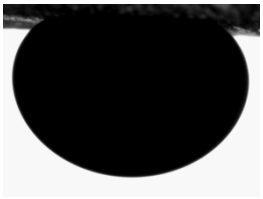
T= 50°C, t = 20.59 min.


T= 90°C, t = 10 s


T= 90°C, t = 22.30 min.

Na_2SO_4 solution (1,780 mg/L)

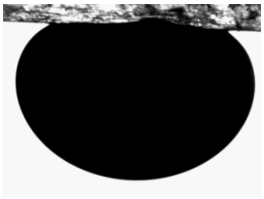
T= 50°C, t= 10 s

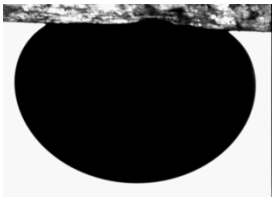
T= 50°C, t = 28.17 min.

Aquifer water (5,436 mg/L)

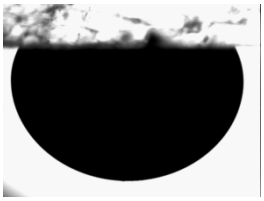
T= 50°C, t= 10 s

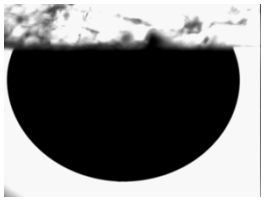
T= 50°C, t= 27.33 min.

Aquifer water (5,436 mg/L)

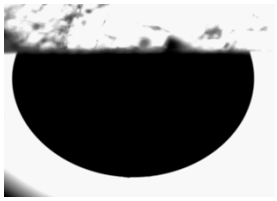
T= 90°C, t = 10 s

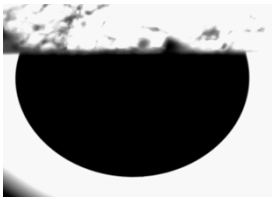
T= 90°C, t = 22.17 min.

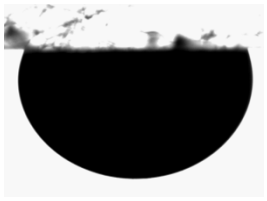
T= 130°C, t = 10 s

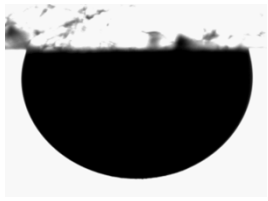
T= 130°C, t = 25.33 h

Formation brine (230K mg/L) [No aging]


T= 90°C, t = 83 h

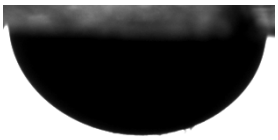
T= 90°C, t = 23.72 h

Seawater (54,680 mg/L)

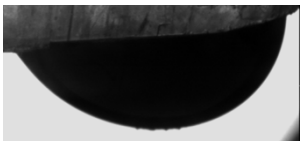
T= 132.2°C , t = 10 s


T= 132.2°C , t = 20.00 h

ı psi).

Formation brine (230K mg/L)			
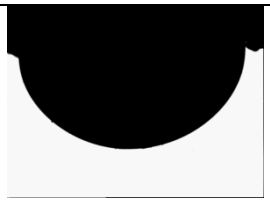	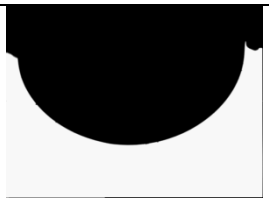	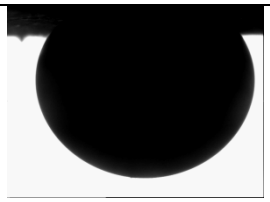	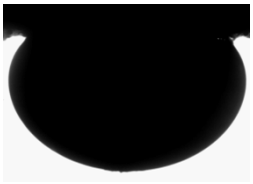
T= 50°C, t = 10 s	T= 50°C, t = 36.16 min.	T= 130°C, t = 10 s	T= 130°C, t = 22.00 h
Aquifer water (5,436 mg/L)			
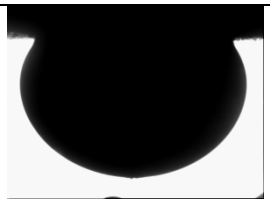	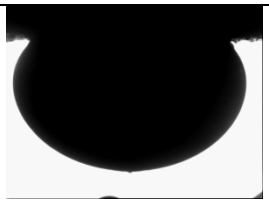	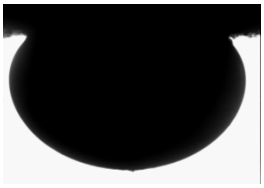	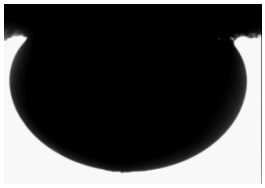
T= 90°C, t = 10 s	T= 90°C, t = 19.50 h	T= 130°C, t = 10 s	T= 130°C, t = 22.00 h

,000 psi).

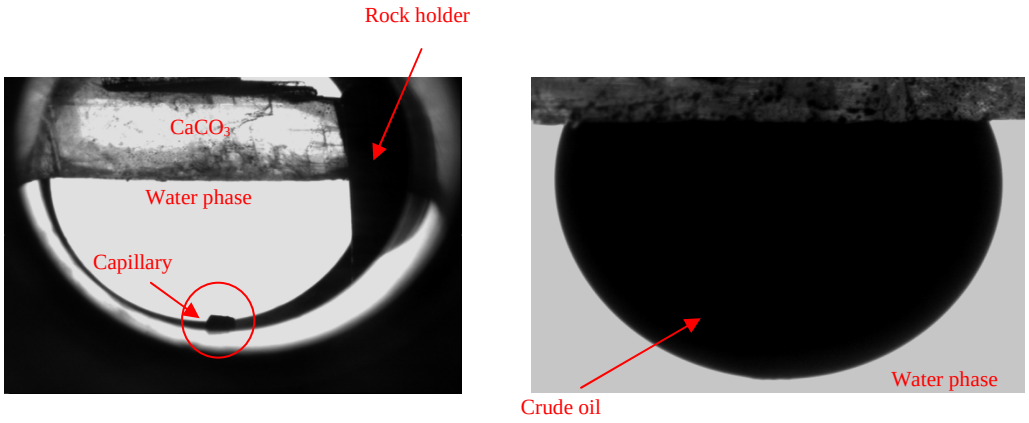

Figure D-3. More details of the rock substrates, capillary, rock holder, and fluids.

APPENDIX E

CAT SCAN IMAGES OF EXPERIMENT IL–5

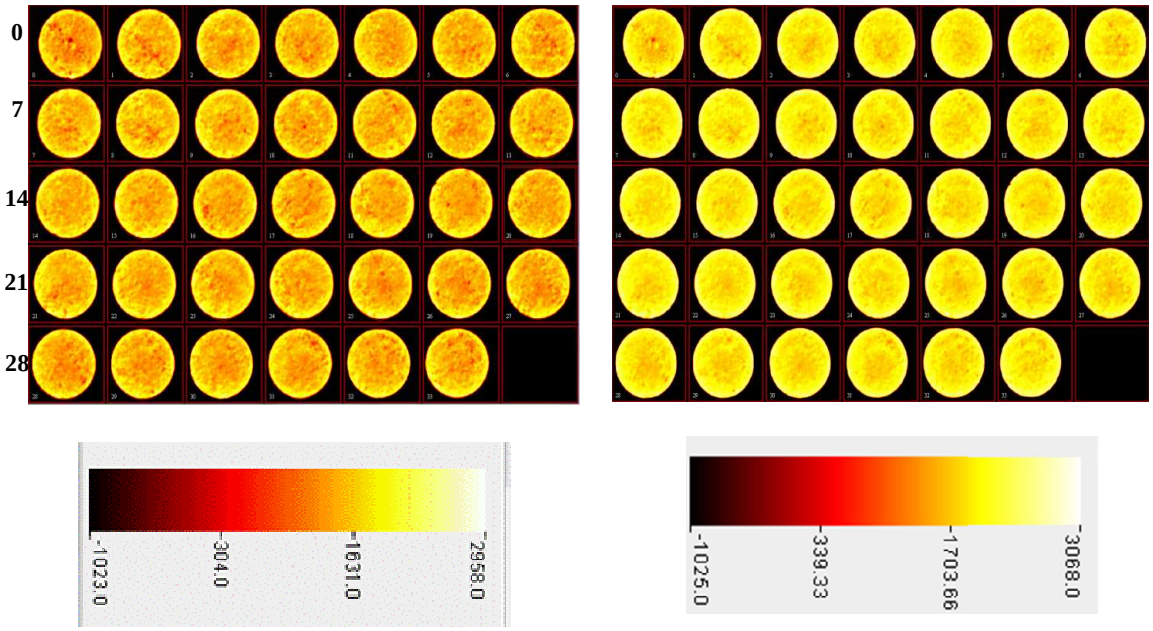

1) Dry core

2) After water saturation

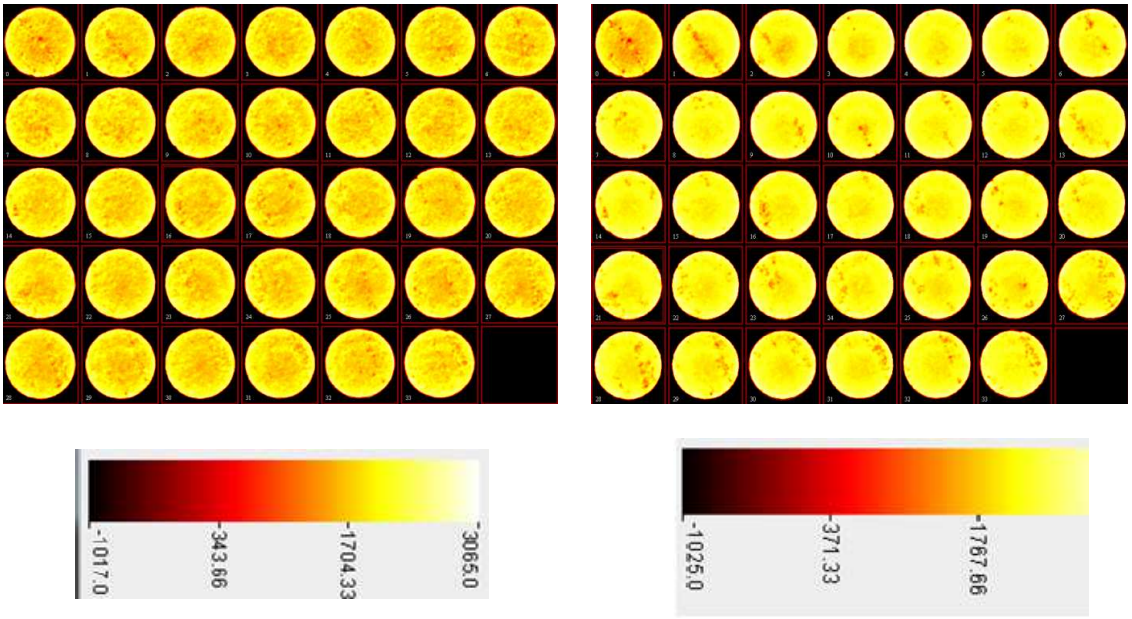

3) After oil saturation

4) After water and chemical flooding

Figure E-1. Core slices at different saturation and flooding conditions (core IL–5).

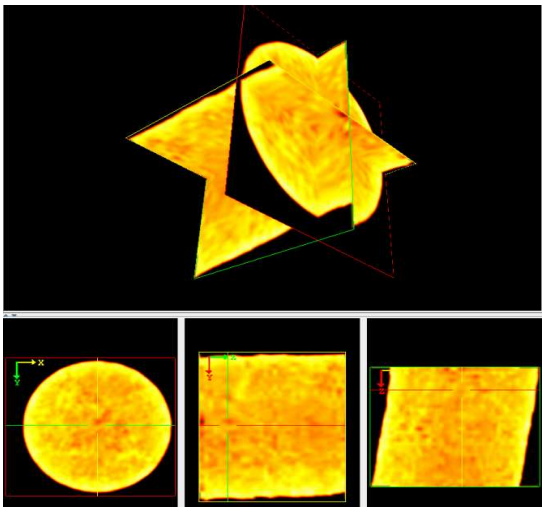

1) Dry core

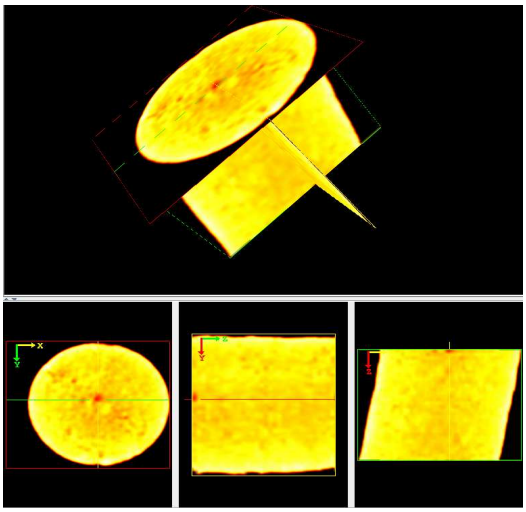

2) After water saturation

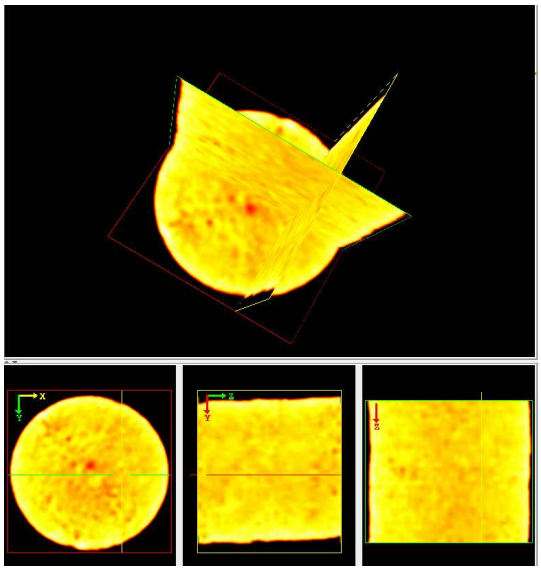

3) After oil saturation

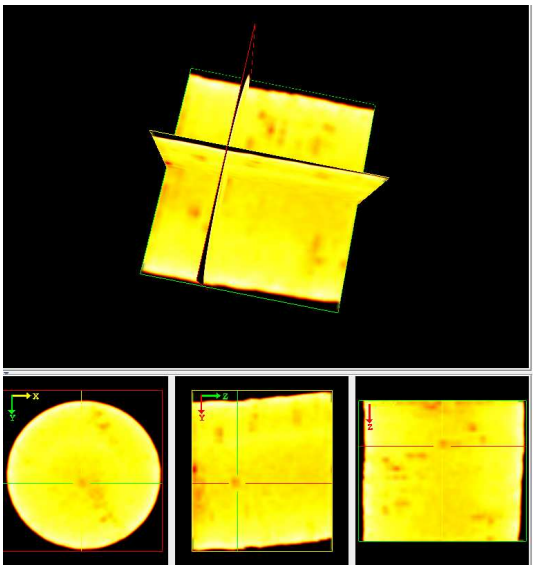

4) After water and chemical flooding

Figure E-2. Tri-planar view (x-y, y-z. x-z) at different saturation and flooding condition (core IL–5).

APPENDIX F

LABORATORY EQUIPMENTS AND INSTRUMENTS

Measuring range	0 – 3 g/cm^3
Temperature	0–90°C
Pressure	145 psi
Accuracy	0.0001 g/cm^3

Figure F-1. Density Meter DMA 4100

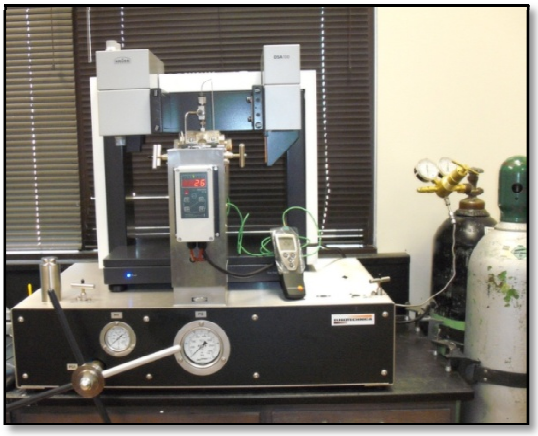

Maximum Temperature	200°C
Maximum Pressure	10,000 psi
Range of contact angle measurements	0 to 180° ± 0.1° accuracy
Range of surface tension measurements	0.01 to 1,000 mN/m 0.01 mN/m resolution

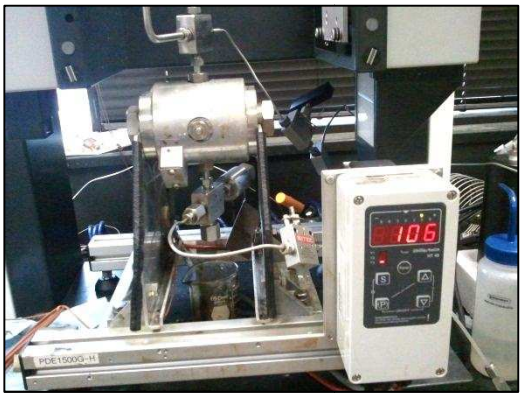

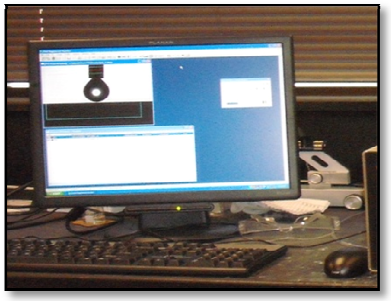

Figure F-2. Digital Tensiometer and Contact Angle Instrument

Figure F-3. Accumulators, oven and core holder setup

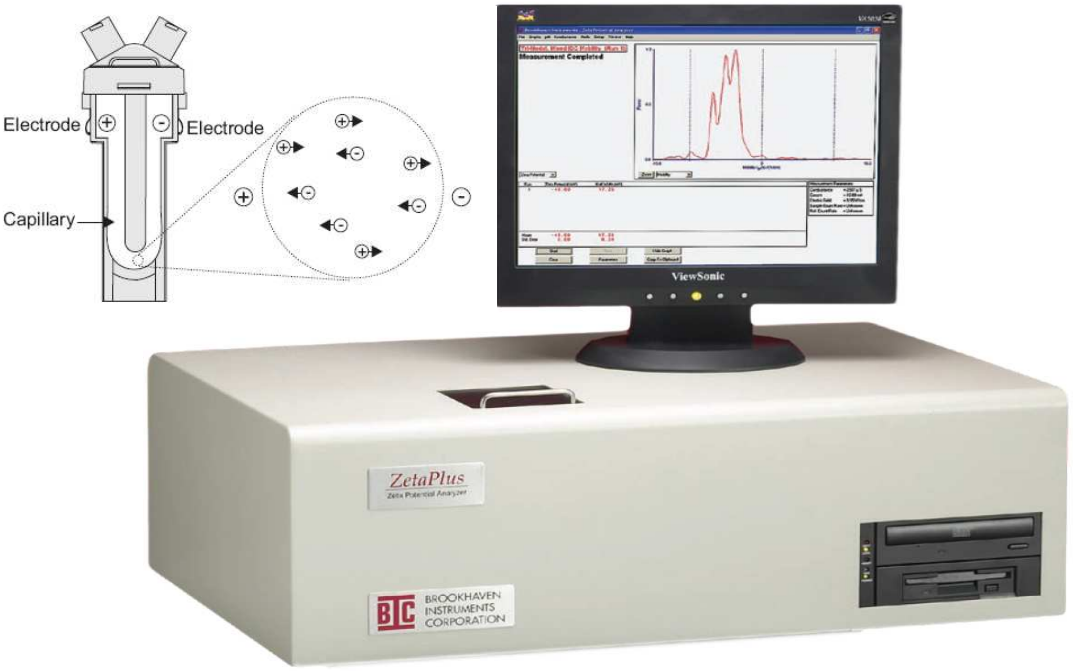

Figure F-6. Zeta Potential Analyzer

Winterset limestone core after water and surfactant flooding

Indiana limestone core IL-10

Vugular Silurian dolomite

Figure F-7.Core samples of carbonates (limestone and dolomite) used throughout this study

Figure F-8. CAT scan instrument

APPENDIX G

CHEMICAL ACTIVITIY OF COMPOUNDS AT DIFFERENT TEMPERATURES AND IONIC STRENGTH

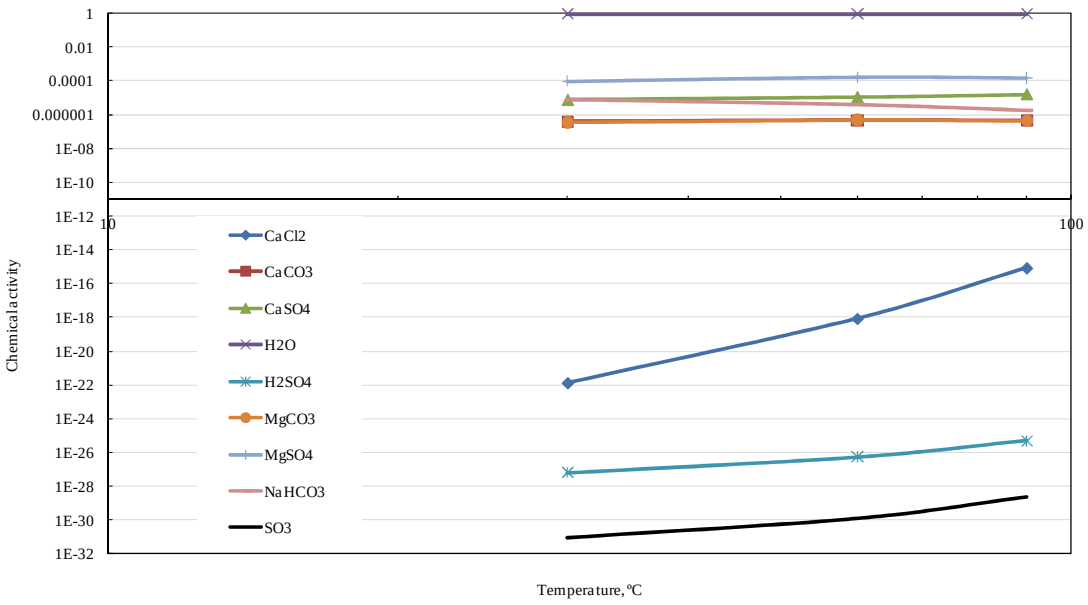

Figure G-1. Effect of temperature on the activity of chemical compounds in seawater.

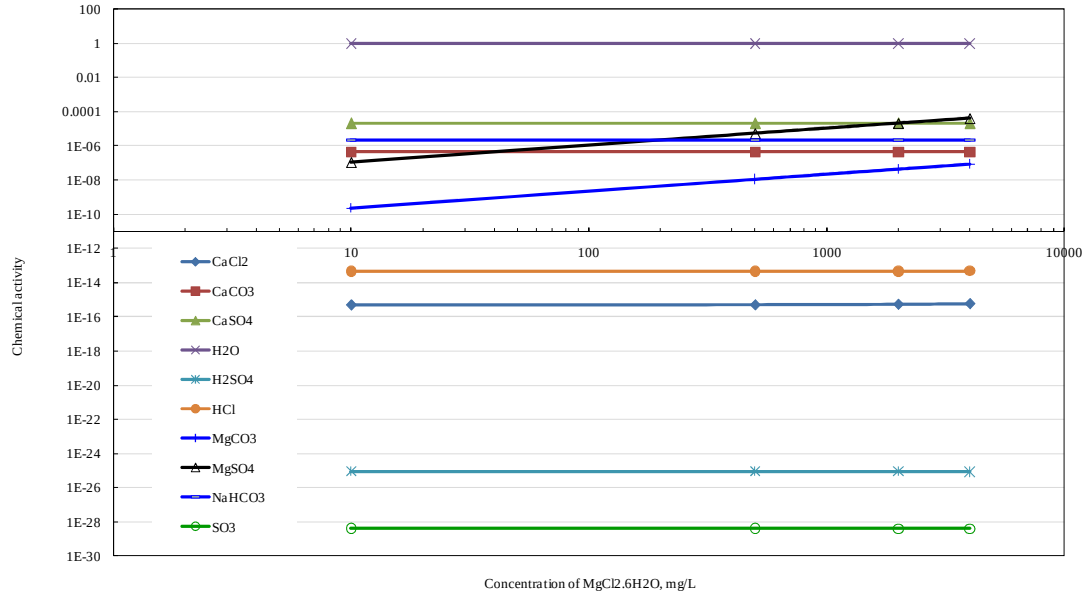

Figure G-2. Effect of $MgCl_2.6H_2O$ concentration on the activity of the chemical compounds in seawater.

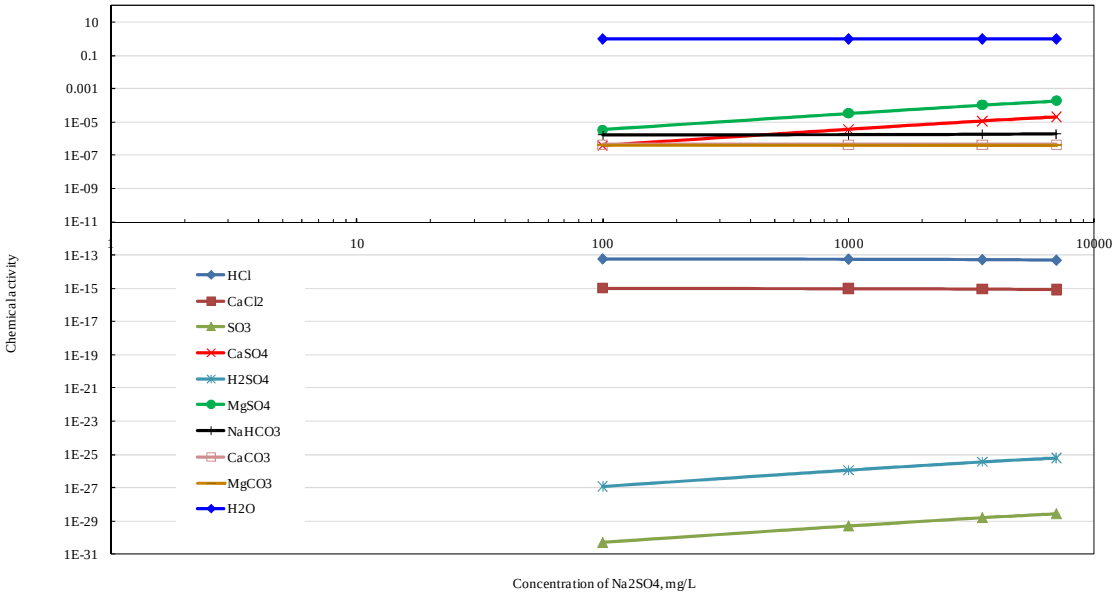

Figure G-3. Effect of Na2SO4 concentration on the activity of the chemical compounds in seawater.

VITA

Name: Mohammed Badri S. Alotaibi

Address: P.O. Box 10311

Saudi Arabia, Dhahran 31311

Email Address: Otaibi03@gmail.com

Education: B.S., Chemical Engineering, King Fahd University of Petroleum & Minerals (Saudi Arabia), 2002.

M.S., Petroleum Engineering, Texas A&M University, 2008.

Ph.D., Petroleum Engineering, Texas A&M University, 2011.